

DISCOVERY AND EVALUATION OF ANTI-CANCER AGENTS

Frankie Fong-Ki Lam, BSc. MSc.

Thesis submitted to the University of Nottingham
for the degree of Doctor of Philosophy

January 2010

Abstract

Cancer is the most common cause of the human death in the UK. Every year 3.2 million Europeans are diagnosed with cancer, and the figure is projected to rise due to the aging population. Although significant advances are being made in the fight against the disease, cancer remains a key public health concern and a tremendous burden on UK society in financial and social terms. This thesis evaluated two classes of compounds that can be potentially developed as anti-cancer agents.

4-(4-Methyl-2-(methylamino)thiazol-5-yl)-2-(4-methyl-3-(morpholin-sulfonyl)phenylamino)pyrimidine-5-carbonitrile (S-134, **5g**) is a novel cyclin-dependent kinase 9 (CDK9) inhibitor showing nano-molar growth inhibitory potentials in established human cell lines. Biochemical assays have confirmed that S-134 primarily inhibits CDK9 at the protein and cellular levels, respectively. The detailed mechanistic investigation demonstrated that the compound caused wild-type p53 stabilisation and cell cycle arrest at the G2/M transition. Cancer cell death induced by S-134 was proven by Annexin-V/PI staining, caspase-3 assay and PARP cleavage. Transcription and expression of anti-apoptotic proteins Mcl-1, Bcl-2 and XIAP were reduced by the inhibitor, as proved by RT-PCR and Western blots respectively.

Compound 2-methoxy-5-(3,4,5-trimethoxyphenethyl)phenyl 2,2,5,5-tetramethyl-2,5-dihydro-1*H*-pyrrole-3-carboxylate-*N*-oxide (ZJU-6, **6g**) a semi-synthetic derivative of the natural medicinal compound Erianin (**6a**) was designed to introduce anti-oxidant property and enhance anti-angiogenic activity of Erianin. The study of ZJU-6 revealed that while the effect of cellular growth inhibition and the transcription of *Bcl-2* were reduced by the structural modification, the suppression of tubulin polymerisation and anti-angiogenic properties were enhanced compared to Erianin.

Compound BI 2536, 4-(8-cyclopentyl-7-ethyl-5-methyl-6-oxo-5,6,7,8-tetrahydropteridin-2-ylamino)-3-methoxy-N-(1-methylpiperidin-4-yl)benzamide (**10**), is one of the most potent and selective inhibitors of Polo-like kinase 1 (Plk1) and is a current experimental candidate for the treatment of cancer. A racemic BI 2536 was synthesised using multiple synthesis routes, which aimed to use as a lead compound for the discovery of novel Plk1 inhibitors.

Acknowledgements

I would like to thank my supervisor, Dr Shudong Wang, for giving me this research project and support during the writing of this thesis. Her ideas led to Cancer Research (UK) and the Royal Society of Chemistry sponsoring part of the work presented here. This thesis has benefited from discussions with the following academic staff within the School of Pharmacy, University of Nottingham: Dr C. de Moor, Dr T. Bradshaw, Dr L. Dekker and Professor P. Fischer. The following chemists, within the Department, provided compounds and advice on the aspect of chemistry presented in this thesis: Mr S. Shi, Dr J. Wilson, Dr A. Zaytsev, Dr E. Merisor, Dr R. Fitzgerald, Dr G. Patwardhan and Dr C. Rochais. The following biologists provided technical support and advice in data presentation: Dr S. Roberts, Mr C. Matthews, Ms. J. Zhang and Dr L. Johnson.

Further thanks go to Dr C. Midgley, Open University, who gave crucial advice on the development of biochemical assays; Dr T. Self and Dr N. Holliday at Institute of Cell Signalling, Nottingham Queens Medical Centre, who provided technical support in the use of Cellomics Array Scan; Professor J. Hewitt, Institute of Genetics, University of Nottingham, who provided valuable advice throughout this research project.

My thanks also go to Dr H. Mao and Professor Y. Pan, Zhejiang University, China, for providing the natural products.

Finally, I would like to pay tribute to my family who supported my decision to participate in this PhD program over the past three years.

List of Abbreviations

Abl	Abelson proto-oncogene
ACS	American cancer society
ADP	Adenosine diphosphate
AGC	PKA, PKG, PKC kinase families
AIDS	Acquired immunodeficiency syndrome
Apaf-1	Apoptotic protease activating factor 1
APC	Adenomatous polyposis of the colon/Anaphase-promoting complex
APC/C	Anaphase-promoting complex/cyclosome
ATM	Ataxia-telangiectasia mutated
ATP	Adenosine triphosphate
ATR	Ataxia-telangiectasia and RAD3-related
BAG-1	Bcl-2-associated athanogene 1
BAK	Bcl-2 antagonist killer
Bax	Bcl-2-associated X
BCG	Bacillus Calmette-Guérin
Bcl-2	B-cell CLL/Lymphoma 2
Bcr	Breakpoint cluster region
BER	Base excision repair

BID	BH3-Interacting Domain death agonist
BIRC5	Baculoviral iap repeat-containing protein 5
BORA	Aurora borealis
bp	Base pair
BRCA 1/2	Breast cancer gene 1/2
BRD4	Bromodomain containing protein 4
BUB3	Budding Uninhibited by Benzimidazoles 3
C.E.	Capping enzyme
CAK	CDK-activating kinase
CAM	Chorioallantoic membrane
CAMK	Calcium/calmodulin-dependent protein kinase
cAMP	Cyclic adenosine monophosphate
CBP-1	Creb-binding protein
Cdc	Cell division cycle
Cdh1	Cadherin 1
CDK	Cyclin-dependent kinase
cDNA	Complementary DNA
cGMP	Cyclin gluanosine monophosphate
Chk	Cell cycle checkpoint kinase
CK1	Casein kinase 1
CLL	Chronic lymphocytic leukaemia
CMGC	CDK, MAPK, GSK3, CLK kinase families
CML	Chronic myelogenous leukaemia
Cnk	Cytokine-inducible kinase
CO ₂	Carbon dioxide

CBP	Creb-binding protein
CTD	C-terminal domain
C-terminal	Carboxyl terminal
DISF	DRB sensitivity inducing factor
DMSO	Dimethyl sulfoxide
DNA	Deoxyribonucleic acid
DNA-PK	DNA-dependent serine/threonine protein kinase
DPPH	1,1-diphenyl-2-picrylhydrazyl
DRB	5,6-dichloro-1- β -d-ribofuranosylbenzimidazole
DSIF	DRB sensitivity inducing factor
EBRT	External beam radiotherapy
EC ₅₀	Half maximal effective concentration
ECL	Enzymatic chemiluminescence
Eg1	Endothelial-derived gene 1
EGCG	Epigallocatechin gallate
EGFR	Epidermal growth factor receptor
EtOH	Ethanol
FACS	Fluorescence activated cell sorting
FADD	Fas-associated death domain
FasL	Fas ligand
FBS	Foetal bovine serum
FGF	Fibroblast growth factor
FITC	Fluorescein isothiocyanate
Fnk	Fibroblast-growth-factor-inducible kinase
G1	Gap phase I

G2	Gap phase II
GI ₅₀	Half growth inhibitory concentration
GTFs	General transcription factors
GTP	Guanosine Triphosphate
H ₂ DCFDA	2',7'-dichlorofluorescein diacetate
H ₂ O ₂	Hydrogen peroxide
HAF	Histone acetyltransferase
HCl	Hydrogen chloride/Hydrochloric acid
HDM-2	Human double minute 2 homolog
Her2	Human Epidermal growth factor Receptor 2
HEXIM	Hexamethylene bis acetamide-inducible Protein
HIV	Human immunodeficiency virus
HPLC	High performance liquid chromatography
HPV	Human papillomavirus
HTS	High-throughput screening
HUVECs	Human umbilical vein endothelial cells
IC ₅₀	Half maximal inhibitory concentration
JNK	C-JUN kinase
K ₂ CO ₃	Potassium carbonate
kD	Kilo Dalton
Leu	Leucine
LiAlH ₄	Lithium aluminium hydride
M	Mitosis
MAD	Mitotic Arrest Deficient
MAP2	Microtubule-associated protein 2

MAPK	Mitogen-activated protein kinase
MAT1	Menage A Trosi 1
MBP	Myelin basic protein
Mcl-1	Myeloid cell leukaemia-1
MEF2	Myocyte enhancer factor 2
MEM	Minimum essential medium eagle
MeOH	Methanol
MLCK	Myosin light chain kinase
MMR	Mismatch repair
MPF	Maturation promoting factor
mRNA	Messenger ribonucleic acid
MS	Mass spectrometry
MTD	Maximum tolerated dose
mTOR	Mammalian target of rapamycin
MTT	3-(4,5-Dimethylthiazol-2-yl)-2,5-diphenyltetrazolium bromide
MYT1	Myelin transcription factor 1
NaOH	Sodium hydroxide
NCI	National Cancer Institute
NELF	Negative elongation factor
NER	Nucleotide excision repair
NFkB	Nuclear factor kappa B
NHEJ	Non-homologous end joining
NMR	Nuclear magnetic resonance
NSCLC	non-small cell lung cancer

<i>N</i> -terminal	Amino terminal
OD	Optical density
PARP	Poly (ADP-ribose) polymerase
PBD	Polo-box domain
PBS	Phosphate Buffered Saline
PCR	Polymerase chain reaction
PDGFR	Platelet-derived growth factor receptor
PDK	Pyruvate dehydrogenase kinase
Pgc-1	PPAR-gamma co-actviator
PI	Propidium iodide
PIC	Pre-initiation complex
PK	Dissociation constant
PI3K	Phosphoinositide-3-kinase
Plk	Polo like kinase
POLR2A	C-terminal domain of RNAP II subunit A
Prk	Proliferation-related kinase
Pro	Proline
PS	phosphatidylserine
P-TEFb	Positive transcription factor b
RAF1	v-RAF-1 murine leukaemia viral oncogene homolog 1
Ran	Ras-related nuclear protein
RB	Retinoblastoma
RCC1	Regulator of chromosome condensation 1
RF	Retardation factor
RhoA	Ras homolog gene family member A

RNA	Ribonucleic acid
RNAi	RNA interference
RNAP	RNA polymerase
RT-PCR	Real time / reverse transcription polymerase chain reaction
S	Synthesis
SAD	Single Ascending Dose
SAPK	Stress-activated protein kinase
SAR	Structure activity relationship
Ser	Serine
SIRT1	Sirtuin 1
Snk	Serum-inducible kinase
snRNA	Single nucleotide RNA
SOCl ₂	Thionyl chloride
SSEs	Secondary-structure elements
STE	Yeast Sterile 7, Sterile 11, Sterile 20 kinases
Tat	Tyrosine aminotransferase
TBS	Tris Buffered Saline
TGF-β	Transforming growth factor beta
THF	Tetrahydrofuran
Thr	Threonine
TK	Tyrosine kinase
TKL	Tyrosine kinase-like
TLC	Thin layer chromatography
TNF	Tumour necrosis factor

TNFR-1	Tumour necrosis factor receptor 1
UV	Ultraviolet
VEGF	Vascular endothelial growth factor
V_{\max}	Maximum rate of velocity
v-onc	Viral-oncogene
XIAP	X-linked inhibitor of apoptosis

Table of Contents

Abstract	i
Acknowledgements	iii
List of Abbreviations	iv
Table of Contents	xii
List of Figures	xvi
List of Tables	xx
Introduction	1
1.1 Cancer	1
1.1.1 Causes of cancers	2
1.1.2 Prevention of cancers	5
1.1.3 Treatments of cancers	8
1.2 Kinases	9
1.2.1 Cyclin-Dependent Kinases	13
1.3 Cell cycle	15
1.3.1 Cell cycle checkpoints and CDKs	18
1.3.1.1 CDK2, 4, 6 and the G1/S checkpoint	19
1.3.1.2 CDK1 and the G2/M checkpoint	21
1.3.1.3 Metaphase checkpoint	23

1.3.2	Cell cycle and cancer	23
1.3.2.1	The RB pathway	24
1.3.2.2	The p53 pathway	26
1.3.3	Apoptosis	28
1.3.4	Anti-apoptotic factors	31
1.4	Eukaryotic transcription and CDKs.....	33
1.5	Natural products	37
1.6	Aims and objectives.....	41
	Mechanism of action of a novel CDK9 inhibitor	42
2.1	Introduction	42
2.1.1	Cyclin-Dependent Kinase 9	42
2.1.2	CDK9 and human pathologies.....	45
2.1.2.1	Virology	45
2.1.2.2	Cardiology	46
2.1.2.3	Oncology	47
2.1.3	Discovery of CDK9 inhibitors.....	49
2.1.3.1	DRB	51
2.1.3.2	Flavopiridol	51
2.1.3.3	Selicielib	52
2.2	Identification of novel CDK inhibitors.....	53
2.3	Cellular growth inhibition of S-134.....	56
2.4	Effect of S-134 on CDK9, CDK2 and CDK7	58
2.5	Effect of S-134 on cell cycle	60

2.6	S-134 induces cell death.....	63
2.7	Cellular CDK inhibition of S-134	69
2.8	S-134 targets anti-apoptotic proteins.....	73
2.9	S-134 induces p53 protein.....	75
2.10	Effect of S-134 on gene transcription.....	79
2.11	Conclusion.....	84
Mechanism of action of a novel natural product derivative		88
3.1	Introduction	88
3.1.1	Erianin	88
3.1.2	Prospective mechanism of action of Erianin	90
3.1.3	Novel derivatives of Erianin.....	91
3.2	Cellular growth inhibition of novel natural product derivatives	91
3.3	Morphological effect of ZJU-6.....	93
3.4	Cell cycle effect of ZJU-6	95
3.5	ZJU-6 induces apoptosis in cancer cells.....	95
3.6	Effect of ZJU-6 on anti-apoptotic proteins.....	98
3.7	p53 induction by ZJU-6.....	99
3.8	Effect of ZJU-6 on transcription.....	101
3.9	Effect of ZJU-6 on polymerisation of tubulin	103
3.10	Effect of ZJU-6 on angiogenesis	105
3.11	Anti-oxidant activity of ZJU-6	106
3.12	Conclusion.....	110
Synthesis of a Plk1 inhibitor – analogue of BI 2536		114

4.1	Introduction	114
4.1.1	Polo-like kinases.....	114
4.1.1.1	Polo-like kinase 2	116
4.1.1.2	Polo-like kinase 3	116
4.1.1.3	Polo-like kinase 4	117
4.1.2	Polo-like kinase 1 (Plk1)	118
4.1.3	Plk1 as a drug target	121
4.1.4	Inhibitors targeting Plk1	122
4.1.5	BI 2536	123
4.2	Synthesis of BI 2536 analogue	125
4.3	Conclusion	132
	General discussion, conclusion and future work	134
5.1	General discussion and conclusion.....	134
5.1.1	Elucidation of the mechanism of action of a novel CDK9 inhibitor	134
5.1.2	Elucidation of the mechanism of action of ZJU-6.....	140
5.1.3	Synthesis of BI 2536 racemate	145
5.2	Future work.....	146
	Materials and Methods	149
	References	163
	Appendix: Publication	182

List of Figures

1.1	The kinase dendrogram (kinase tree)	12
1.2	Functional diversity of cyclin-dependent kinases in human	15
1.3	Schematic diagram of the cell cycle	16
1.4	Molecular pathways involved in the transition of G1 to S phase in the cell cycle	21
1.5	Molecular pathways involved in the transition of G2 to M phase in the cell cycle	22
1.6	The roles of RB in cellular level	25
1.7	The roles of p53 in cellular level	27
1.8	The roles of anti-cancer drugs on apoptosis	30
1.9	Mechanism in the pre-initiation phase of RNA polymerase II dependent transcription	34
1.10	Regulation of transcription initiation and elongation by CDKs	36
2.1	Gene and amino acids sequences of CDK9	43
2.2	Rational of targeting transcription as a potential cancer therapy	48
2.3	Binding between the ATP binding pocket of CDK2 and ATP	49
2.4	Crystal structure of CDK9 (green) bound to cyclin T1 (brown)	50
2.5	Structures of some of the best known CDK inhibitors	50
2.6	The general structures of 2,4-disubstituted pyrimidine 4 and 2,4,5-	

	trisubstituted pyrimidine 5	53
2.7	The proposed binding of 2,4,5-trisubstituted pyrimidine 5 to the ATP binding pocket of CDK9	54
2.8	Chemical structure of S-134 5g	56
2.9	Growth inhibition of S-134 on HCT-116, A2780, MCF-7 and MRC-5 cells	57
2.10	Effect of S-134 on CDK2/cyclin E and CDK9/cyclin T1	58
2.11	Effect of S-134 on the cell cycle of HCT-116 cells	60
2.12	Cell cycle effect of DRB on HCT-116 cells	61
2.13	Cell cycle effect of S-134 and DRB on the synchronised HCT-116 cells	62
2.14	Effect of S-134 on the cell death in HCT-116 cells	64
2.15	Effect of S-134 on the cell death in MRC-5 cells	65
2.16	Effect of S-134 on PARP cleavage in A2780 cells at 24 hours	67
2.17	Effect of S-134 on PARP cleavage in MRC-5 cells at 24 hours	67
2.18	S-134 activates caspase-3	68
2.19	Effect of S-134 on RNA polymerase II at 6 and 24 hours in A2780 cells	70
2.20	Effect of S-134 on RNA polymerase II at 6 and 24 hours in MRC-5 cells	71
2.21	Effect of S-134 on the expression of anti-apoptotic proteins at 6 and 24 hours in A2780 cells	73
2.22	Effect of S-134 on the expression of anti-apoptotic proteins at 6 and 24 hours in MRC-5 cells	75
2.23	Effect of S-134 on the protein expression of p53 and HDM-2 at 6 and 24	

	hours in A2780 cells	76
2.24	Effect of S-134 on p53 and HDM-2 proteins at 6 and 24 hours in MRC-5 cells	77
2.25	Cellomic Array Scan detecting the stabilisation of p53 protein expression in HCT-116 cells	78
2.26	Effect of S-134 on the transcription of anti-apoptotic genes at 6 hours in A2780 cells	80
2.27	Effect of S-134 on the transcription of anti-apoptotic genes at 24 hours in A2780 cells	81
2.28	Effect of S-134 on the transcription of <i>HDM-2</i> in A2780 cells	82
2.29	Quantification of the intensities of cDNA with the presence of S-134 at A) 6 and B) 24 hours	83
3.1	Erianin 6a is a polyphenol identified in a Southeast Asian plant <i>Dendrobium chrysotoxum</i>	89
3.2	Chemical structure of 6a (Erianin) and 6g (ZJU-6)	92
3.3	Imaging studies in MCF-7 cells with Erianin and ZJU-6	94
3.4	Effect of Erianin and ZJU-6 on the cell cycle of MCF-7 cells	95
3.5	Caspase-3 activation in HCT-116 cells with Erianin and ZJU-6	96
3.6	Erianin and ZJU-6 cause PARP cleavage	97
3.7	Effect of Erianin and ZJU-6 on MCF-7 cells' death	98
3.8	Effect of Erianin and ZJU-6 on the protein expression of Mcl-1 and Bcl-2	99
3.9	Effect of Erianin and ZJU-6 on p53 and HDM-2 proteins in MCF-7 cells	100
3.10	Dose dependent effect of compounds on HDM-2 proteins	101

3.11	Effect of Erianin and ZJU-6 on transcription in MCF-7 cells	102
3.12	Effect of compounds on tubulin polymerisation (up to 1 hour)	104
3.13	Effect of Erianin and ZJU-6 on angiogenesis in chick embryo	105
3.14	Molecular structure of DPPH	107
3.15	Effect of compounds on the reduction of DPPH	108
3.16	Effect of compounds in the cellular oxidation state	108
3.17	Effect of compounds in the prevention of cellular oxidation	109
4.1	Structure of human Plk2 polypeptide	116
4.2	Structures of human Plk3 and Plk4 polypeptides	118
4.3	Polypeptide sequence of human Plk1	118
4.4	Multiple roles of Plk1 during Mitosis	120
4.5	Crystal structure of Plk1	122
4.6	Proposed binding model for the selective Plk1 inhibitor BI 2536 in Plk1	124

List of Tables

1.1	Distribution of protein kinases across species	10
1.2	Some of the best known drugs discovered from natural sources	38
2.1	The structure activity relationship (SAR) of a series of novel CDK9 inhibitors based on the GI ₅₀ values	55
2.2	Summary table of GI ₅₀ values of S-134 in the 13 human cell lines	57
2.3	Summary of kinase activities	59
2.4	Summary of the percentage readings from Annexin-V assays	66
3.1	Cellular activity of novel Erianin derivatives on tumour cell lines HCT-116 and MCF-7	91
3.2	Growth inhibition of Erianin and ZJU-6 determined by MTT assay (72 hours)	92
3.3	Percentage of cell death induced by Erianin and ZJU-6	97
3.4	V _{max} values from the tubulin polymerisation assays	104
4.1	Different species show variations in Polo-like kinase diversity	115
4.2	Properties of the four best known Plk1 inhibitors	123
6.1	Sequences of custom designed PCR primers	156

Chapter One

Introduction

1.1 Cancer

Cancer refers to a diversity of diseases characterised by the uncontrolled proliferation of cells into a different form against the normal complement of the organism¹. The continuous proliferation of cancer cells develops into tumour tissues and may spread across to other organs via circulatory systems resulting in metastasis. There are two types of tumours: those demonstrating the properties described above, known as malignant tumours, which result in cancer; and those without malignant properties, which are self-limiting, non-invasive and do not metastasise, known as benign tumours. It is the metastases that are responsible for some 90% of deaths from cancer.

Cancer may affect humans of all ages. According to statistics from the American Cancer Society (ACS), cancer is the third most lethal disease after cardiovascular diseases and infectious and parasitic diseases^{2, 3}. In 2007, 13% of total human death worldwide was caused by cancer. There are 3.2 million Europeans diagnosed with cancer every year⁴. Hence, the medical needs for cancer remain one of the most demanding areas in scientific research.

1.1.1 Causes of cancers

Cancer occurs when genetic mutations accumulate in cells during the replication of genetic material, allowing cells to undergo transformation. The mutations of three major types of genes: oncogenes, tumour suppressor genes and DNA repair genes, play an important role in tumourgenesis.

Oncogenes are genes whose products have the ability to transform eukaryotic cells so that they growth in a manner analogous to tumour cells. This class of genes were initially identified as genes carried by virus that causes transformation of their target cells. A major class of the viral oncogenes have cellular counterparts that are involved in normal cell functions. The cellular counterparts are known as proto-oncogenes, in certain cases their mutation or aberrant activation in the cell to form an oncogene is associated with tumour formation. Oncogenes fall into several groups ranging from transmembrane proteins to transcription factors. The generation of oncogene represents a gain-in-function in which a cellular proto-oncogene is inappropriately activated⁵. This can involve a mutational change in protein, or constitutive activation, over expression, or failure to turn off expression at the appropriate time, which generates a tumourgenic effect in a cell resulting cancer.

Tumour suppressor genes are identified by mutations represent loss-of-function that contributes to cancer formation. These genes usually impose some constraint on cell cycle procession or cell growth, i.e. checkpoint controls. It is necessary for both copies of the gene to be inactivated in cells⁵, the two most important tumour suppressors are retinoblastoma (RB) and p53 (see section 1.3 for details).

DNA damage happens continuously in all living organisms and there are genes acting as a natural defence mechanism to repair these DNA damages (see section 1.1.3). Examples of DNA repairing genes include *BRCA1* and *BRCA2*, which involve in the homologous recombination repair⁶. Although more than 99.9% of mutations are recognised and corrected by self-repairing systems, some cells will escape this monitoring system, thus promoting unlimited growth resulting in cancer.

The genetic mutations may be caused by a number of sources: chemical carcinogens, ionising radiation, viral or bacterial infections, hormone imbalance, immune system dysfunction and heritable factors^{1, 7-9}.

DNA mutations that lead to cell proliferation are not self-driven, often stimulated by external factors or mutagens^{5, 10}. Mutations are usually corrected by the DNA repair systems. Carcinogens, which induce permanent non-repairable DNA damage include tobacco smoke and asbestos fibres, which are respectively associated with 90% of lung cancers and mesothelioma (a rare type of cancer for the outer lining of the lungs and internal chest wall)¹¹. Tobacco smoke may also cause cancers of the lung, larynx, head, neck, stomach, bladder, kidney, oesophagus and pancreas, as it contains over fifty known carcinogens, including nitrosamines and polycyclic aromatic hydrocarbons, and is responsible for about 20% of cancer deaths worldwide. Not all carcinogens (agents that cause cancer) are mutagens (agents which cause DNA mutations); alcohol is an example of this type¹². The carcinogenic effects of alcohol are: an increase in the rate of cell division and a reduction in the period during which DNA repair enzymes can act. Hence, the chances for mutations to be retained are increased.

Ionising radiation consists of subatomic particles or electromagnetic waves that are sufficiently energetic to detach electrons from atoms or molecules, i.e. they cause ionisation. The best known example of ionisation radiation is ultraviolet light (UV)¹³, a natural source of radiation from the sun which can lead to melanoma and other skin malignancies. Radon gas, X-rays and gamma rays are other examples of ionisation radiation which can cause cancer¹⁴.

Some cancers can be caused by infection with pathogens¹⁵. Viral infections are responsible of 15% of all human cancer worldwide, representing the second most important risk factor of cancer after tobacco. The main viruses associated with human cancers are papillomavirus, hepatitis B and hepatitis C, Epstein-Barr and T-lymphotropic virus¹². Viral induction of tumours may be via acute or slow transformation¹⁶. In acute transformation, the virus carries an overactive oncogene or viral-oncogene (v-onc); the infected cell is transformed as soon as v-onc is expressed. In contrast, slowly-transforming viruses insert their genome into the host cell genome at random. This insertion occurs near a proto-oncogene viral promoter (or other transcription regulation element) and induces over-expression of the proto-oncogene, resulting in uncontrolled cell division. Because the insertion is not specific to proto-oncogenes, slowly-transforming viruses require a much longer time to induce over-expression of the proto-oncogene than acutely-transforming viruses. Bacterial infection has also been linked to cancer development, with *Helicobacter pylori* being the best known example, chronic infections of the stomach wall being linked to the development of gastric cancer¹⁷.

Some hormones can act in a similar manner to non-mutagenic carcinogens as they may stimulate excessive cell growth¹⁸. A well-established example is

the role of hyperoestrogenic states in promoting endometrial cancer. Immune system dysfunction also contributes to an increased risk of cancer development. Human immunodeficiency virus (HIV), a lentivirus (a member of the retrovirus family) that leads to acquired immunodeficiency syndrome (AIDS), has been associated with a number of malignancies including Kaposi's sarcoma and non-Hodgkin's lymphoma, both caused by the breakdown of immune surveillance^{15, 19}. Another example, Human papillomavirus (HPV), infects the epidermis and mucous membranes of humans and has been associated with malignancies such as anal and cervical cancer²⁰.

Cancer is sporadic in most cases, with inheritance playing no role in the onset of disease. However, in a number of recognised syndromes, inherited predisposition to cancer due to defects in genes giving protection against tumour formation, such as DNA repair genes and tumour suppressor genes, are passed to the offspring. Examples include the *BRCA1* and *BRCA2* genes, which are associated with increased risks of breast and ovarian cancers, respectively^{21, 22}. Familial adenomatous polyposis, an inherited mutation of the APC gene²³, leading to early onset of colon carcinoma and retinoblastoma in young children, is caused by the inheritance of a mutant retinoblastoma (RB) gene²⁴.

1.1.2 Prevention of cancers

Cancer is caused by genomic instability resulting from mutation. Mutation occurs during gene replication and natural repair mechanisms, which act as the first line of defence against cancer, operate continuously. The DNA repair mechanisms are divided into various types, including direct repair, base

excision repair (BER), nucleotide excision repair (NER), mismatch repair (MMR), non-homologous end joining (NHEJ) and homologous recombination repair⁵. Each of these mechanisms repairs different types of DNA damage.

Direct repair can correct DNA damage without requiring a template; these include UV radiation induced thymine dimers and methylation of the bases guanine, cytosine and adenine.

BER, NER and MMR repair single strand breaks, with the unaffected strand acting as a template for the repair mechanisms. BER repairs damage to a single base caused by oxidation, alkylation, hydrolysis or deamination. The damaged DNA base is removed by a glycosylase before being resynthesised by a polymerase, with ligase performing the nick-sealing step. NER repairs bulky, helix-distorting lesions such as pyrimidine dimers. This type of damage is repaired by a transcription-coupled repair system using a set of NER enzymes while the genes are actively transcribed. Mismatch repair corrects errors arising during DNA replication and recombination which result in mis-paired, but undamaged, nucleotides. This also requires template DNA, the damage being repaired by enzymes in a similar manner to BER and NER.

Non-homologous end joining (NHEJ) and homologous recombination repair correct double strand breaks. NHEJ uses DNA ligase IV to recombine both ends of the broken strands. Recombination repair is also an enzymatic process, but requires the presence of an identical or nearly identical sequence to be used as a template for repair.

The other aspect of cancer prevention involves voluntary actions which, unlike DNA repair, do not occur naturally and automatically. Active measures to reduce the risk of cancer can be achieved by avoiding carcinogens or

altering their metabolism by following a lifestyle or diet that modifies cancer-causing factors and/or medical intervention²⁵. The vast majority of cancer risk factors are environmental or lifestyle-related in nature, including tobacco, alcohol, physical inactivity and obesity²⁶. The use of exogenous hormones, exposure to ionising radiation and ultraviolet radiation as well as certain occupational and chemical exposures are other risk factors for cancer development. These factors can be addressed by changes to life style. Scientific evidence has already shown that avoiding carcinogens can reduce the risk of cancer.

The consensus of opinion on diet and cancer is that obesity increases the risk of developing cancer, although the correlation between reducing obesity and reduced risk of cancer remains to be established²⁷. However, certain types of food are known to increase the risk of certain cancer types. Grilled meat contains high level of heterocyclic amines through the breakdown of proteins under high temperature cooking, these heterocyclic amines act as a source of carcinogen that increase the risk of stomach, colon, breast and pancreatic cancer^{28, 29}. The consumption of vitamins has been correlated to cancer risk. Although for most vitamins the link has not been scientifically proved, deficiency of vitamin D is correlated to the increase risk of cancer³⁰.

A new concept of chemoprevention of cancer has come to light in recent years, supported by a large number of clinical trials. An example of this is the use of Tamoxifen, an oestrogen antagonist³¹. Consumption of Tamoxifen for a period of five years has been found to significantly reduce the risk of breast cancer. Other chemicals such as polyphenols, naturally occurring agents found in green tea and wine, have been suggested to have cancer prevention

properties through the presence of anti-oxidants^{32, 33}. The role of natural products in cancer prevention will be discussed later in more detail.

Since the inheritance of genes such as *BRCA1* and *BRCA2* has been found to increase cancer risk, genetic screening for the existence of these genes is one way to prevent cancer³⁴. There are commercially available products that allow for the rapid screening of clinical specimens to be conducted. Vaccination against viral or bacterial inducers of cancer, such as human papilloma virus (HPV) vaccine, is a new measure to reduce cancer risk. Two vaccines against HPV are currently available, Gardasil and Cervarix, which aim to prevent the development of cervical cancer and genital warts^{35, 36}. There is also a hepatitis B vaccine, which reduces the risk of liver cancer³⁷. A canine melanoma vaccine has also been developed³⁸.

1.1.3 Treatments of cancers

In the unfortunate situation where cancer has been diagnosed, there are a number of treatments available^{39, 40}. As cancer refers to a class of disease, it is unlikely that one single cure for all forms of cancer is possible. The most common methods include surgery, radiation therapy and chemotherapy. There are other methods of treatment such as targeted therapies (monoclonal antibody therapy)⁴¹, immunotherapy⁴² and hormonal therapy⁴³. New methods, immunotherapy in particular, which targets specific antigen solely expressed by tumour cells, only target cancer and not the healthy cell population, hence minimising the adverse effects observed with traditional methods.

Small molecule inhibitors are sometimes classified as targeted therapy as they inhibit specific molecular target(s). Best example of this is Gleevec,

marketed by Novartis, which is the first line treatment of chronic myelogenous leukaemia in America⁴⁴. Gleevec specifically targets the kinase domain of three tyrosine kinases, which are the Abelson proto-oncogene (abl), c-kit and the platelet-derived growth factor receptor (PDGFR). In leukaemia, the translocation between chromosome 9, which contains abl, and chromosome 22, which associates with the breakpoint cluster region (bcr) genes, forms the Philadelphia chromosome, a new form of chromosome 22. The Philadelphia chromosome encoded a fusion protein termed bcr-abl, a tyrosine kinase. Gleevec inhibits the bcr-abl activity in all cell types, however, normal cells have other kinases to substitute this activity and maintain normal cellular activity. Alternatively, some tumour cells depend on bcr-abl activity, the absence of bcr-abl leads to tumour cell death.

1.2 Kinases

Kinases are enzymes which transfer a phosphate group from a high energy donor, such as adenosine triphosphate (ATP), to a specific substrate; a process known as phosphorylation⁴⁵. There are large varieties of kinase across animal and plant species, the largest group being protein kinases. Protein kinases act on and modify the specific activity of a protein, which are used extensively in signal transduction and to control complex metabolic processes in cells. There are three outcomes after a protein is phosphorylated: activation or inhibition of protein activity, enhancement of the binding of a protein to its substrate, initiation or enhancement of degradation through ubiquitination⁷. Thus protein kinases regulate a diverse range of signalling pathways and protein behaviour.

The diversity of protein kinases across species is huge in terms of numbers and types (Table 1.1)⁴⁶. So far, more than 500 protein kinases have been identified in humans, compared to 130 in yeast and 240 in the *Drosophila* fly (*Drosophila melanogaster*).

Group	Families	Subfamilies	Yeast kinases	Worm kinases	Fly kinases	Human kinases
AGC	14	21	17	30	30	63
CAMK	17	33	21	46	32	74
CK1	3	5	4	85	10	12
CMGC	8	24	21	49	33	61
Other	37	39	38	67	45	83
STE	3	13	14	25	18	47
Tyrosine kinase	30	30	0	90	32	90
Tyrosine kinase-like	7	13	0	15	17	43
RGC	1	1	0	27	6	5
Atypical-PDHK	1	1	2	1	1	5
Atypical-Alpha	1	2	0	4	1	6
Atypical-RIO	1	3	2	3	3	3
Atypical-A6	1	1	1	2	1	2
Atypical-Other	7	7	2	1	2	9
Atypical-ABC1	1	1	3	3	3	5
Atypical-BRD	1	1	0	1	1	4
Atypical-PIKK	1	6	5	5	5	6
Total	134	201	130	454	240	518

Table 1.1: Distribution of protein kinases across species⁴⁶. The second and third columns indicate the number of families and subfamilies in general. The numbers of kinases in yeast, worm, fly and human were compared. A general trend exists with more complex organisms having a higher number of kinases. However, it does not affect the variation in each type, all organisms having at least one kinase for each type showing that a minimal function from each kinase type is required for intrinsic signalling cascades common to all species to function properly (Adapted from Manning *et al. Science*. 2002, 298, 1912).

Among the 518 protein kinases in humans, 478 belong to a single super family whose catalytic domains are related in sequence. These can be clustered into groups, families and subfamilies, based on similarity of amino acid sequences and biochemical function. The kinase dendrograms or tree (Figure 1.1) shows the sequence similarity between the catalytic domains of kinases - the distance along the branches between two kinases is proportional to the divergence between their sequences. Using this classification system, the 478 proteins are divided into seven groups. Furthermore, protein kinases can be divided into two groups based on their ability to remove a phosphate

group from ATP and covalently attach it to one of three amino acids of other protein that have a free hydroxyl group, e.g. serine, threonine or tyrosine. Most kinases are able to phosphorylate both serine and threonine, known as serine/threonine specific kinases; while others act on tyrosine, being classified as tyrosine kinases. Dual-specificity kinases are capable of phosphorylating all three amino acids. The relationships shown on the dendrogram can be used to predict protein substrates and biological function for more than 100 uncharacterised kinases presented. A further 40 'atypical' kinases have no sequence similarity to typical kinases, but are known or predicted to have the enzymatic activity of kinases, and some are predicted to have a structural fold similar to typical kinases.

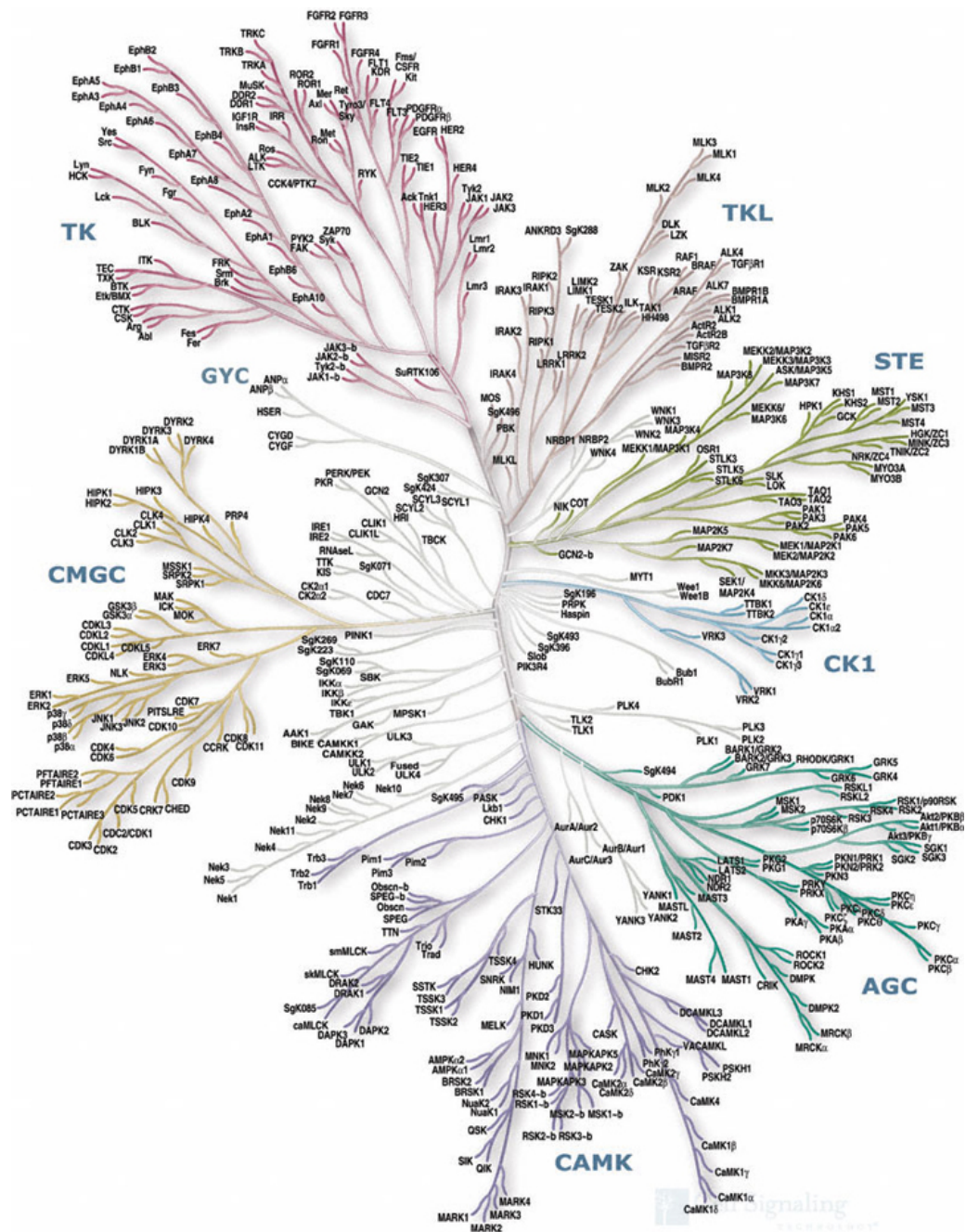


Figure 1.1: The kinase dendrogram (kinase tree)⁴⁶. 478 protein kinases which belong to a single superfamily are divided into seven groups based on similarity of amino acid sequences of the kinases and their biochemical function. These include PKA, PKG, PKC families (AGC); Calcium/calmodulin-dependent protein kinase (CAMK); Casein kinase 1 (CK1); CDK, MAPK, GSK3, CLK families (CMGC); homologs of yeast Sterile 7, Sterile 11, Sterile 20 kinases (STE); Tyrosine kinase (TK) and Tyrosine kinase-like (TKL) family (Adapted from Cell Signalling Technology[®]).

Tyrosine-specific protein kinases are important regulators in signal transduction. They act primarily as growth factor receptors, such as platelet-derived growth factor receptor (PDGFR) and epidermal growth factor receptor

(EGFR), and in downstream signalling from growth factors. Tyrosine kinases consist of a transmembrane receptor with a tyrosine kinase domain projecting into the cytoplasm. These kinases play key roles in regulating cell division, cellular differentiation and morphogenesis. The extracellular part of the kinase serves as a ligand binding domain. Ligand binding triggers the dimerisation of two monomer tyrosine kinase receptors and the cascade of linkage events results in trans-autophosphorylation of the kinase by other members in the kinase complex. This finally leads to the activation of the kinase domain allowing the binding of ATP, hence promoting signal transduction through phosphorylation as enzymatic reactions in most cases.

Serine/threonine-specific protein kinases phosphorylate substrate protein based on residues flanking the phosphor-acceptor site which, together, comprise the consensus sequence. As a result, the catalytic domains of kinases in this group are highly conserved. These kinases are regulated by specific events (e.g. DNA damage), as well as numerous chemical signals, including cAMP/cGMP, diacylglycerol and Ca^{2+} /calmodulin. For clinical interest, serine/threonine kinase expression is altered in many types of cancer. Therefore, these kinases are important targets for cancer therapy⁴⁷. One of the targets is the cyclin-dependent kinases (CDKs).

1.2.1 Cyclin-Dependent Kinases

CDKs are one of the most extensively studied Ser/Thr kinases. Cell division cycle 2 (Cdc2) was the first identified member of the CDKs and was originally isolated from *Saccharomyces cerevisiae*. Initially, Cdc2 was found to regulate the cell cycle of yeast. Later it was found in a range of plants and mammals.

The protein identified in human, homologous to Cdc2, is known as CDK1^{48, 49}. To date, more than 10 types of CDK and 15 types of cyclin genes have been identified in the human genome. Originally, it was thought that CDKs' only role was to regulate the cell cycle. However it has since been discovered that CDKs also play a major role in the regulation of transcription⁴⁶. Other functions operated by CDKs have been indicated in neuronal signalling, cell differentiation, cell death, golgi membrane trafficking, insulin exocytosis by pancreatic β -cells and retinal phosphodiesterase regulation. As mentioned in its name, the functions of CDKs depend on its cyclin counterparts (Figure 1.2); a different cyclin combination to the same CDK may result in changes or affect its function. Using CDK2 as an example, CDK2/cyclin E functions during the cell cycle transition between gap phase I (G1) and DNA synthesis (S) phase, while CDK2/cyclin A is required throughout the progression of S phase⁵⁰. Cyclin binding causes a conformation change within the CDK enzyme, exposing a cleft complementary to ATP, thus enabling ATP binding, which leads to phosphorylation and their activation⁵¹. In the regulation of cell cycle, CDK-activating kinase (CAK) complex is required to phosphorylate CDK1, 2, 4 and 6, which enhances their CDK-cyclin binding^{52, 53}. The CAK complex is composed of the catalytic subunit CDK7, the regulatory subunit cyclin H, and a Menage A Trosi 1 (MAT1) protein subunit, a polypeptide corresponding to residues Met 1 – Asp 65 of RING finger domain⁵⁴. In general, CDKs can be divided into three groups according to their primary function: CDKs involved in cell cycle regulation, which includes CDK1, 2, 3, 4 and 6; CDKs involved in regulation of eukaryotic transcription, which includes CDK7, 8, 9 and 11; CDKs involved in intra-vascular signalling, such as CDK5.

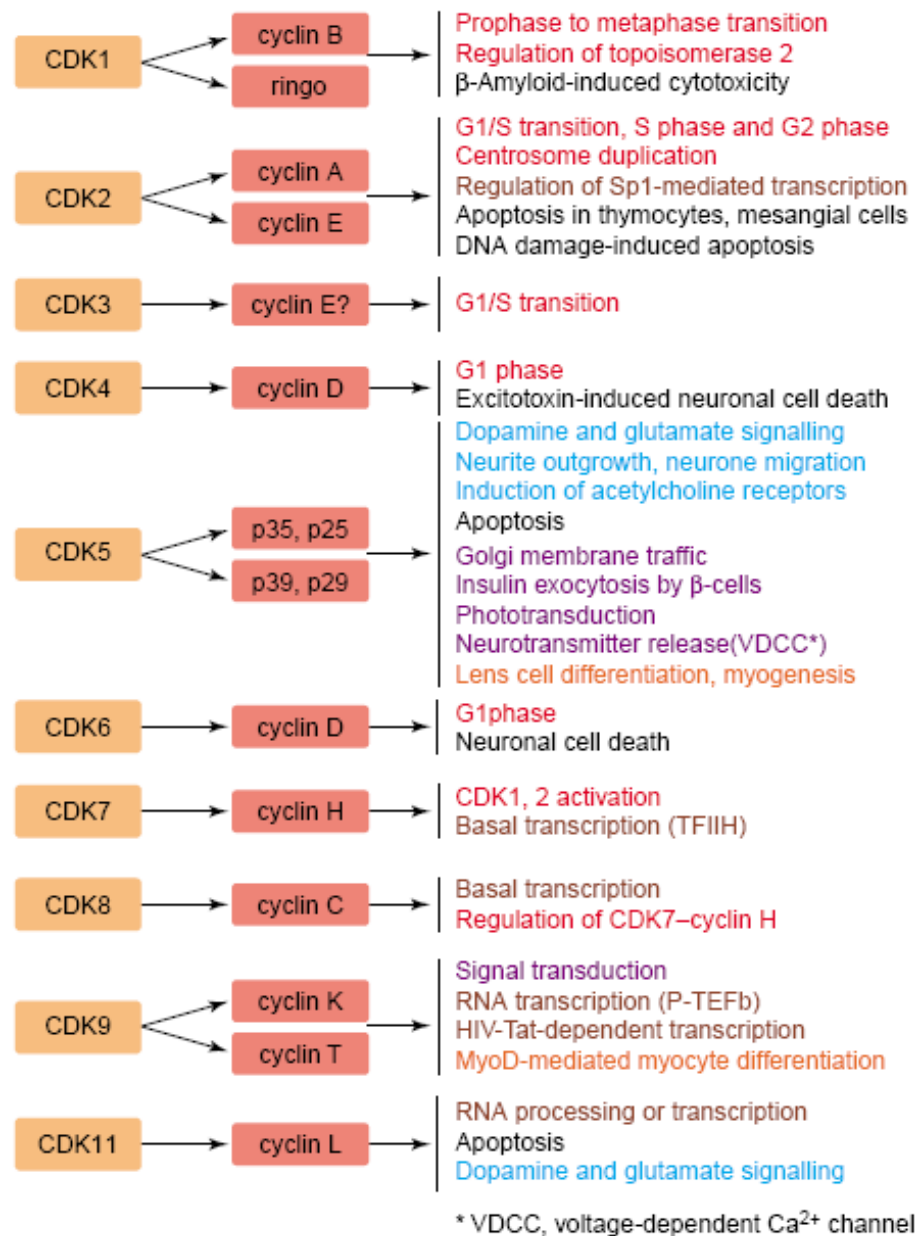


Figure 1.2: Functional diversity of cyclin-dependent kinases in human. The functions of 10 human CDKs have been identified⁵⁰. These CDKs required the association of various cyclin to promote their functions (Adapted from Ferrari. *Cell. Mol. Life. Sci.* 2006, 63, 781)

1.3 Cell cycle

The cell cycle refers to a cascade of cellular events leading to the division and duplication of cells. In eukaryotes, the cell cycle can be divided into two distinct periods: the interphase and the mitotic (M) phase. The interphase

consists of three phases: gap phase I (G1), responsible for synthesis of organelles in most cells; synthesis phase (S), during which DNA is replicated; and gap phase II (G2), which is a period in preparation for cell division. The mitotic phase leads to segregation of chromosomes and results in two daughter cells, which is the end point of cell division. Very often, cells become quiescent or senescent after mitosis; this phase is known as G0.

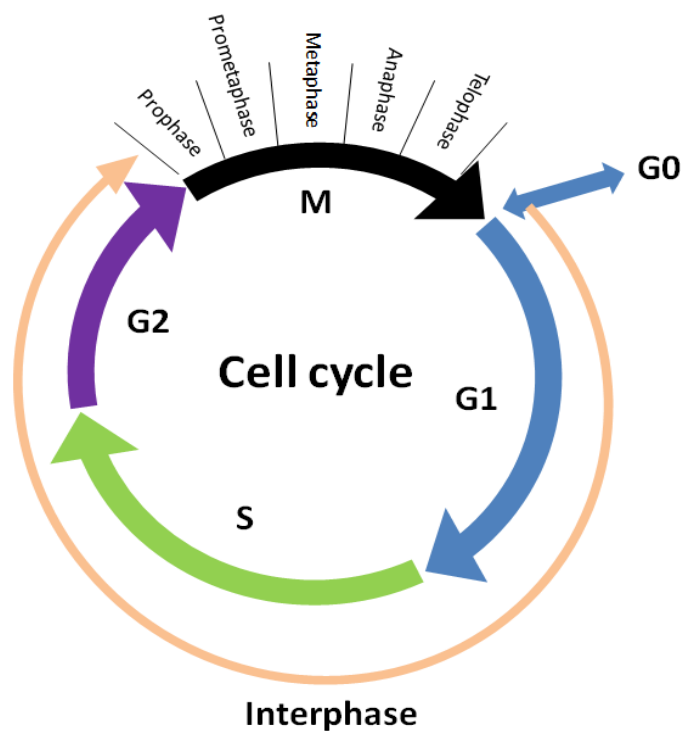


Figure 1.3: Schematic diagram of the cell cycle. Gap phase I (G1), synthesis (S), and gap phase II (G2) are collectively known as interphase. Mitotic (M) phase can be subdivided into further five phases; cytokinesis is the end point of the phase and of cell division.

Activation of each phase of the cell cycle depends on the progression and completion of the previous phase (Figure 1.3). In theory, cells will undergo G1 phase for continuous growth after the completion of mitosis. However, in multi-cellular eukaryotes cells very often enter G0 from G1 if they are non-proliferative. The time span of G0 can be very long, even indefinite in the case of neuron cells and cell types which are fully differentiated. It is also a phase for cellular responses to DNA damage with affected cells becoming senescent,

rendering them at a metabolic active state but unable to divide. It is an alternative to programmed cell death i.e. apoptosis⁵⁵.

G1 phase is the first step in interphase, extending from the end of the previous M phase until the beginning of DNA synthesis. The biosynthetic activity of the cell increases from the previous M phase. The size of the cell increases during G1 phase and the synthesis of enzymes required for DNA synthesis is the most noticeable product of this phase. The duration of this phase varies across cell types, even within the same species. S phase commences with the synthesis of DNA. At the end of the S phase, all chromosomes are replicated, resulting in two chromatids per chromosome. The synthesis of histone is another product in this phase. During the G2 phase, the rate of protein synthesis increases again after falling during the S phase. The main product of the G2 phase is microtubules required for the segregation of chromosomes, together with other components required during mitosis⁵⁶.

Cells enter mitosis after interphase is completed. Mitosis has a relatively short length compared to other phases; it consists of karyokinesis and cytokinesis, the division of nucleus and cytoplasm, respectively. In animal cells, mitosis is divided into five phases: prophase, prometaphase, metaphase, anaphase and telophase. As plant cells contain large vacuoles which shift nuclei to the side of the cells, an extra phase called pre-prophase occurs before prophase. This essential step of moving the nucleus to the middle of a cell before the start of prophase occurs with the formation of phragmosome and the pre-prophase band (a ring of microtubules and actin filaments). During prophase, the centrosomes (a pair of centrioles) appear near the nucleus. The genetic material, normally appearing as chromatin during interphase,

condenses into chromosomes which are lined up with the microtubules formed between the centrioles. Moving into prometaphase, the nuclear membrane is degraded and microtubules invade the nuclear space. These microtubules will then either attach themselves to kinetochores formed by the centromere or interact with opposing microtubules. Metaphase is characterised by chromosomal alignment in the metaphase plate or equatorial plane. During anaphase, sister chromatins are cleaved; each complete set is pulled towards the opposite ends of the cells. At telophase, cells elongate further and microtubules degrade while a new nuclear membrane forms around the chromosomes. Finally, cytokinesis follows, resulting in separation of two daughter cells⁵⁶.

1.3.1 Cell cycle checkpoints and CDKs

In eukaryotic cells, there are three checkpoints operating during the cell cycle: G1/S, G2/M, and the metaphase checkpoint. These checkpoints verify whether the processes at each phase of the cell cycle are completed accurately before progressing to the next phase. An important function of these checkpoints is to detect any DNA damage using an enzymatic sensor system. If damage is detected, a signalling mechanism is used to induce cell cycle arrest until the damage is repaired. Cells with unrepaired damage will undergo apoptosis, which is the effector mechanism of cell cycle control⁵⁷. Cyclin-dependent kinases (CDKs) are key regulators of cell cycle. CDK4 and CDK6 in complex to D-type cyclins together with CDK2/cyclin E1 regulate the transition from G1 to S phase, while CDK1/cyclin B1 controls the cell cycle transition from G2 phase to mitosis⁵⁸. Besides their roles in cell cycle regulation, CDKs are

involved in other functions depending on the way in which they were activated. The failure of these checkpoints leads to diseases such as cancer^{59, 60}.

1.3.1.1 CDK2, 4, 6 and the G1/S checkpoint

The G1/S checkpoint makes the decision whether the cell should divide, delay division, or enter a resting phase (i.e. G0). This restriction point is regulated by CDK inhibitor protein p16⁶¹, a member of INK4 CDK inhibitor family. Other members of the INK4 family including p15, p18 and p19 also play the negative regulatory role to CDK4/6⁶². They inhibit CDK4/6 activity through direct binding to prevent the CDK-cyclin associations. The expression of these CDK inhibitor proteins is induced in response to DNA damage allowing cell cycle arrest and subsequent DNA repair, or continuously expressed throughout the cell cycle providing a threshold level of inhibition which must be overcome.

CDK4 combined with D-type cyclins control the proliferation of cells during G1 phase by altering the phosphorylation state of retinoblastoma (RB) protein⁶³. Three different types of type D cyclins are found in humans: cyclin D1, D2 and D3^{64, 65}. CDK7 has been reported to play a role in cell cycle progression⁶⁶. CDK7 associates with cyclin H and MAT1 to form the CDK-activating kinase (CAK) complex⁵⁴. CAK is a subunit of transcription factor TFIIH, a component of the RNA polymerase II (RNAP II) holoenzyme complex in mammals. Phosphorylation of CDK4 on amino acid residue threonine 172 and the binding of cyclin is triggered by CAK⁶⁷, which leads to the phosphorylation of CDK6 on threonine 177^{68, 69}. CDK4/cyclin D1 or CDK6/cyclin D1 phosphorylates the C-terminal of RB protein^{70, 71}, this phosphorylation leads to the displacement of histone deacetylase and induces

E2F dependent transcription⁷². This activation induces the downstream phosphorylation of CDK2 and disrupts the pocket structure, which activates CDK2 at the end of the G1 phase.

CDK2 is highly homologous to CDK1 in structure⁷³. In growth stimulated normal human fibroblast cells, the mRNA of CDK2 appears in the late G1 or early S phase. In the cell cycle transition, phosphorylation by CAK on threonine 170 and the association of cyclin E is required for the activation of CDK2^{68, 74}. Protein p27 is a member of Cip/Kip CDK inhibitor family that inhibits the activity of CDK2 by associating with the CDK2/cyclin E1 complex⁷⁵. At normal cellular levels of ATP, p27 phosphorylates at Thr 187 modulated by Transforming growth factor beta (TGF- β), which results in the ubiquitination of p27. Another member in the Cip/Kip CDK inhibitor family, p21, functions in a similar manner as with p27 inhibiting the activity of CDK2/cyclin E1⁶².

The cell proceeds from G1 to S phase with CDK2/cyclin E1 maintains the hyper-phosphorylated state of RB and phosphorylates other substrates required for S phase progression such as Histone H1⁷⁶. During S phase, CDK2 binds cyclin A to initiate DNA replication by phosphorylating numerous targets such as the DNA polymerase alpha primase, a key enzyme for DNA synthesis⁷⁷.

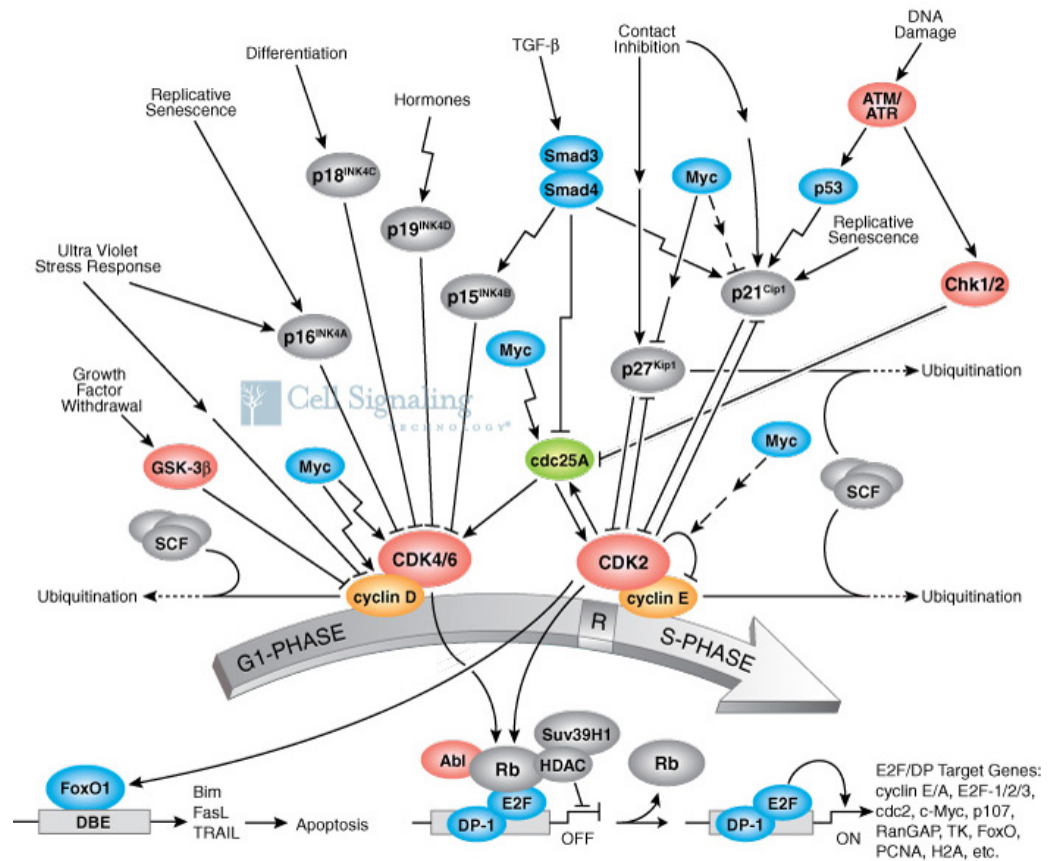


Figure 1.4: Molecular pathways involved in the transition of G1 to S phase in the cell cycle⁷⁸. Environmental stresses induce various negative regulators which suppress the activity of CDK4/6 and CDK2. Removal of these negative regulators and the induction of activators restore the function of the CDKs; phosphorylation of downstream substrates such as RB and E2F leads to the progression of cell cycle from G1 to S phase (Adapted from Cell Signalling Technology[®]).

1.3.1.2 CDK1 and the G2/M checkpoint

The second checkpoint operates at the end of G2 phase. This checkpoint triggers the transition from G2 to M phase. One of the key factors checked is the DNA damage. The main effect protein response to DNA damage is p53. In response to DNA damage, active p53 triggers the direct association of CDK inhibitor proteins, such as p21, with CDK1/cyclin B1 complex, resulting cell cycle arrest⁶².

CDK1 associates with cyclin A and phosphorylates components that are essential for mitosis during late G2 phase of the cell cycle⁷⁷. CDK1 is then

negatively regulated by the phosphorylation of MYT1 kinase at threonine 14 and tyrosine 15⁷⁹. Prior the cell cycle transition from G2 to M phase, CDK1 is dephosphorylated by *cdc25*⁸⁰, which allows the association of CDK1 and cyclin B⁴⁸, also known as the maturation promoting factor (MPF)⁸¹. Phosphorylation of MPF on threonine 161 of CDK1 by CAK triggers the progression of cell cycle from G2 to M phase⁶⁸. CDK1 also plays a role in mitosis by phosphorylating RCC1 (Regulator of Chromosome Condensation 1) protein to coordinate spindle assembly⁸². The activated RCC1 generates RanGTP on mitotic chromosomes, which is essential for spindle assembly and chromosome segregation.

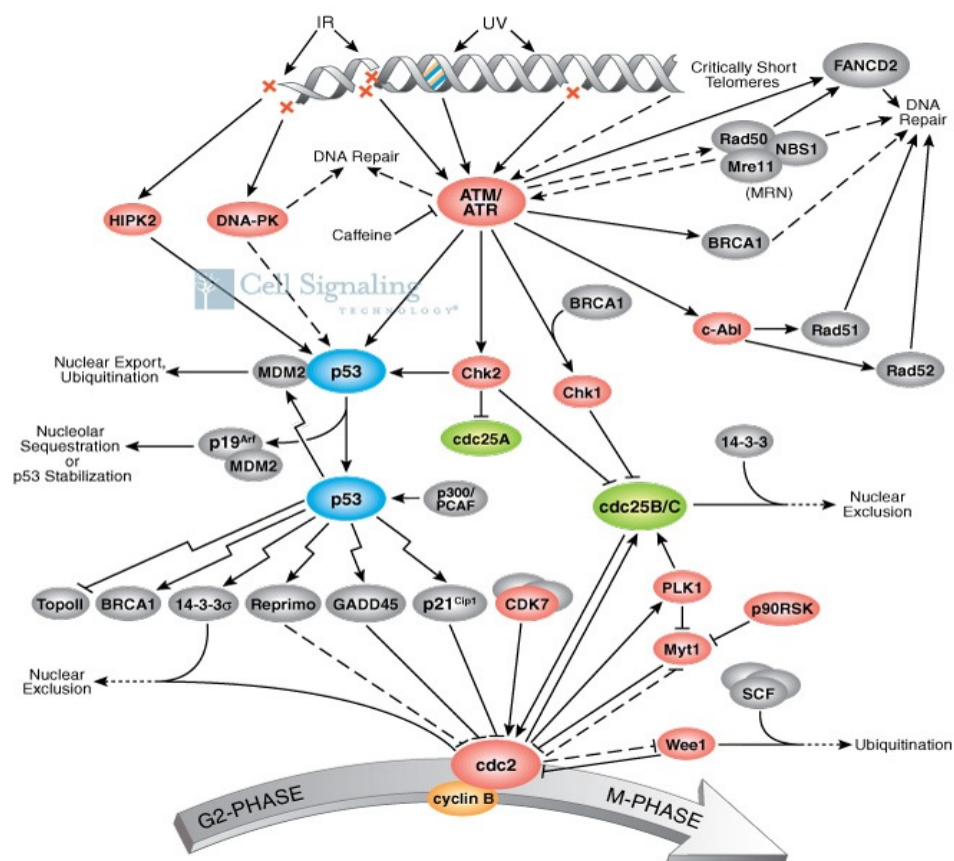


Figure 1.5: Molecular pathways involved in the transition of G2 to M phase in the cell cycle⁷⁸. DNA is the main object checked in this checkpoint. p53 is the main effector protein response to DNA damage. Without DNA damage, majority of Cdc2 negative regulators including p21 will not be induced, which leads the activation of Cdc2 and the progression of cell cycle from G2 to M phase (Adapted from Cell Signalling Technology[®]).

1.3.1.3 Metaphase checkpoint

During mitosis, the metaphase checkpoint monitors the chromosomes alignment during metaphase on microtubules before proceeding to the anaphase. Improper attached kinetochores, a substance that responsible to the attachment of mitotic chromosomes to microtubules and their movements, triggers the arrest of cell cycle at metaphase⁵. The expression of Budding Uninhibited by Benzimidazoles protein 3 (BUB3) is triggered by the improper attachment of kinetochores in eukaryotic cells⁸³. BUB3 forms an inhibitory complex with several proteins, including Mitotic Arrest Deficient proteins (MADs) at the kinetochores, which inhibits the formation of Anaphase-promoting complex (APC). The inhibition APC formation is achieved by MAD2 proteins, which interact directly with Cell Cycle Division protein 20 (Cdc20)⁸⁴, an activator of the APC by promoting ubiquitination of an anaphase inhibitory protein known as securin⁸⁵. Without Cdc20, the centromeres extent the chromosomal microtubules until kinetochores are properly aligned. Once the kinetochores are aligned properly on the mitotic spindle, MAD2 releases Cdc20 which trigger the cascade signalling pathways including the ubiquitination of securin and the cell proceeds to anaphase.

1.3.2 Cell cycle and cancer

Cell cycle abnormalities are a common underlying pathology within human malignancies. These abnormalities are caused by alternations at genetic levels, which lead to the possible transcription alternation and protein dysfunction, resulting uncontrollable cell cycle progression. Vast and diverse alternations

within the cell cycle have been linked with the generation of malignancy in cells^{62, 86}. The two major carcinogenic pathways being commonly altered are the RB and p53 pathways.

1.3.2.1 The RB pathway

Retinoblastoma protein (RB), also known as pRB, was the first proto-oncogene identified, its mutation links to the onset of many cancers including retinoma⁸⁷. It is a key substrate for the CDK-cyclin complexes in the G1/S phase checkpoint. In quiescent cells, or during the first part of G1, RB is bound to the transcription factor E2F⁵. E2F activity is required for transcription of genes which are essential in S phase. The formation of RB-E2F complex is believed to be critical for the arrest of cells at G1 phase. In addition, RB, also interacts with chromatin, it binds histone deacetylases, which may initiate the removal of acetyl groups at the target promoters, thus inactivating the promoters. Components of the chromatin remodelling complex are potential targets of RB. Non-phosphorylated RB forms a complex with D-type CDK4 and CDK6, but it is also a substrate of CDK2/cyclin E⁷². Upon phosphorylation at or close to the restriction point, phosphorylated RB releases E2F allows transcription of genes required for S-phase, and releases suppression of genes suppressed by the RB-E2F complex, which leads to the progression of cell cycle into S phase.

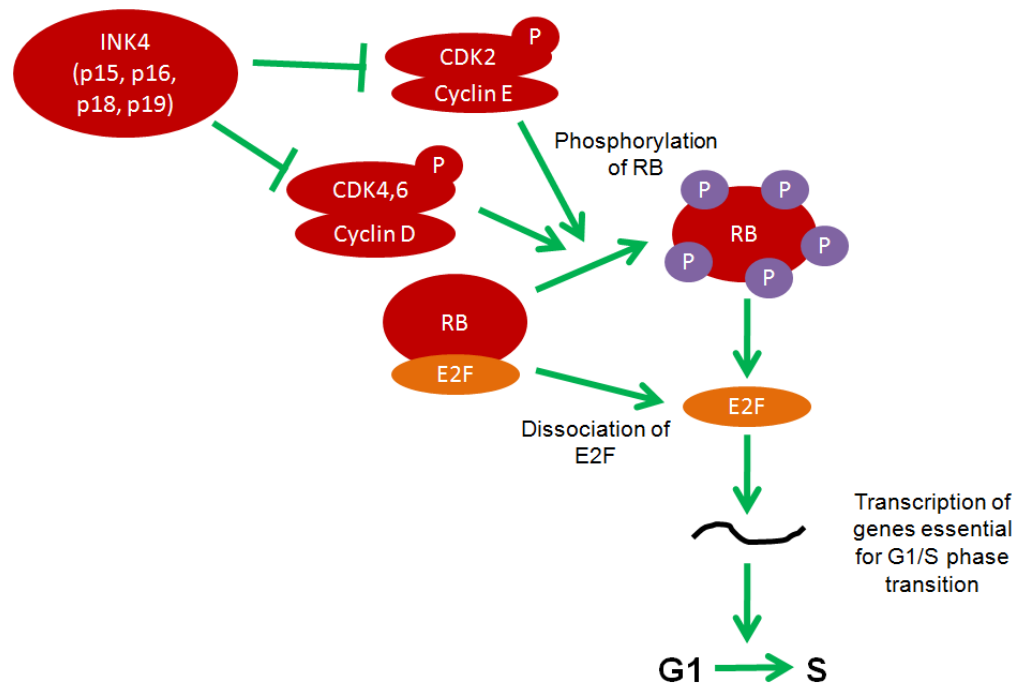


Figure 1.6: The roles of RB in cellular level^{5, 78}. Under normal circumstances, RB is associated with E2F. Members of INK4 family inhibit the activity of CDK2, 4 and 6 to phosphorylate RB. Phosphorylated RB release E2F, which leads to the E2F dependent transcription. The products of E2F dependent transcripts are essential for the G1/S phase transition of the cell cycle to occur. Components in red have been reported to be alternated in cancer, which includes the unregulated CDKs activities and mutation of RB leading to its uncontrolled phosphorylation; over expression of cyclin D leads to hyperactive CDK4/6 and the mutation of INK4 genes leads to unregulated CDKs activities involved in the G1/S checkpoint.

In cancer, a large number of alternations related to abnormalities in RB function. A common alteration in RB results in the unregulated phosphorylation by CDKs operated at the G1/S phase checkpoint (i.e. CDK2, 4 and 6). Direct mutation of RB is also possible; the human papilloma virus (HPV) is able to cause RB mutation via its E7 reading frame. This sort of mutation can be referred to as a loss-of-function mutation⁸⁶; mutated RB loses its ability in binding with E2F, leading to the unregulated E2F transcription and the transcription of proteins required for the cell cycle transition from G1 to S phase.

Over expression of cyclin D is required for oncogenic cells to overcome this checkpoint by competing for the binding of CDK4/6 with their negative

inhibitors⁵. This causes hyper-phosphorylation of RB, release of active E2F and eventually leads to the inappropriate progression of cell cycle.

Mutations within the INK4 genes locus, which encode CDK inhibitor proteins p15, p16, p18 and p19, are other common features within human carcinomas. Depletion or deletion of CDK inhibitor proteins, the most prevalent and relevant to the RB pathway is the mutation of p16⁸⁸. Mutated INK4 genes lead to unregulated activities of CDKs function in cell cycle checkpoints, resulting inappropriate cell cycle progression and carcinogenesis.

1.3.2.2 The p53 pathway

p53, one of the best known tumour suppressors, has a key role in response to DNA damages and other genomic alteration at a cellular level⁸⁹. p53 is negatively regulated by oncoprotein HDM-2. Binding of HDM-2 induces the ubiquitination and proteasomal degradation of p53 to prevent its accumulation in cells⁹⁰. p53 activation requires the phosphorylation by several different protein kinases, including DNA dependent protein kinase, Ataxia-telangiectasia mutated (ATM) - Ataxia-telangiectasia and RAD3-related (ATR) kinases, of Ser 15 and Ser 37 in response to DNA damage⁹¹⁻⁹³, resulting the dissociation of HDM-2 and accumulation of p53. Cell cycle checkpoint kinases, Chk1 and Chk2, enhance p53 tetramerisation, stability and activity by phosphorylating Ser 20 of p53^{94, 95}. Acetylation, which is mediated by p300 and Creb-binding protein (CBP) acetyltransferases, appears to play a positive role in the accumulation of p53 protein in stress response⁹⁶. Since this acetylation effects on p53, it is therefore negatively regulated by HDM-2.

Activated p53 triggers the expression of proteins including p21, which results in cell cycle arrest at the restriction point or G2 phase by inhibiting CDK2/cyclin E or CDK1/cyclin B, respectively. Following DNA damage, p53 is acetylated at Lys 382 in human and Lys 379 in mouse⁹⁷, which promotes direct binding of p53 to the damaged DNA and triggers the DNA repair mechanisms. Deacetylation of p53 occurs through interaction with the Sirtuin 1 (SIRT1) protein following DNA repair⁹⁸. For cells with non-repairable DNA damage or under other circumstances in which programmed cell death is required, p53 can induce a variety of apoptotic pathways including Bcl-2-associated X (Bax) dependent apoptosis⁹⁹ (Figure 1.7). Bax is a pro-apoptotic protein; it binds to mitochondria membrane and triggers caspase-dependent apoptosis.

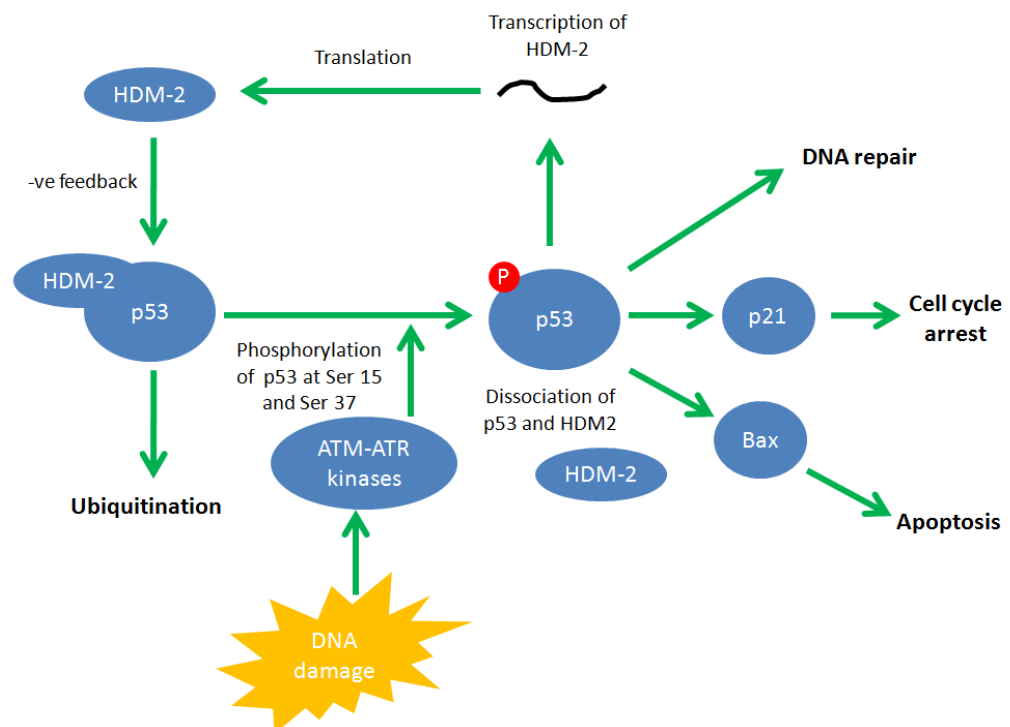


Figure 1.7: The roles of p53 in cellular level⁹⁹. Under normal circumstances, p53 is associated with HDM-2 which leads to the degradation of p53, with ubiquitination as the major pathway. In response to the DNA damage of genomic alteration, p53 is phosphorylated at Ser 15 and Ser 37 which leads to the dissociation of HDM-2 from p53. Activated p53 induces cellular DNA repair, activates p21 which causes cell cycle arrest, or induces Bax dependent apoptosis. The negative feedback loop of p53 increases the translation and expression of HDM-2 which

binds to p53 and regulates its activity. Proteins coloured in blue are reported to be alternated in cancers.

In human tumours, the most common form of p53 alternation is the loss of p53 function. This leads to the reduced or complete loss of p21, resulting in uncontrolled cell cycle progression and cell proliferation⁹⁹. Increased phosphorylation of p53 at Ser 392 has been reported in human tumours to influence the function of growth suppressor, DNA binding and transcriptional activation of p53¹⁰⁰. Bax expression, the potential primary response gene of p53, could be altered by abnormal p53, hence preventing apoptosis⁹⁹. Increased expression of HDM-2 has been noticed in many tumour cell lines as an indirect mechanism of carcinogenesis¹⁰¹. Other regulatory components in the p53 network such as the ATM/ATR kinase may also be altered in malignancy.

1.3.3 Apoptosis

In eukaryotes, some cells must die during development in order to control the number of cells. All cells possess pathways that can cause death, which is known as programmed cell death or apoptosis⁵. Apoptosis requires activation of a pathway that leads to suicide of the cell by a characteristic process in which the cell becomes more compact, blebbing occurs at the cell membranes, chromatin becomes condensed and DNA is fragmented. Ultimately, the dead cells are fragmented and engulfed by cells such as macrophages. However, the pathway is activated only by appropriate stimuli, such as irradiation of cells which triggers p53 activation which induces apoptosis. The ability of p53 to induce apoptosis is a crucial defence against cancer; apoptosis is also a key to

immune defence and elimination of cancerous cells⁵. Apoptosis can be divided into the extrinsic and intrinsic pathways, respectively.

The extrinsic pathway requires extracellular signal transduction from membrane receptor protein across the plasma membrane. One of the best characterised death receptor families is the Tumour Necrosis Factor (TNF) receptors. Other well known death receptors include Fas and CD95¹⁰². The binding of ligands to the appropriate death receptors results in receptor aggregation which triggers recruitment of the adaptor molecule Fas-associated death domain (FADD) and caspase-8.

Caspases are proteases that are involved in multiple stages of the apoptotic pathway and are synthesised as inactive pro-caspases that are activated by auto-cleavage to form the active dimer. ~14 mammalian caspase are identified and divided into two groups. The caspase-1 subfamily is involved in the response to inflammation, while the caspase-3 subfamily (consisting of caspase-3 and caspases-6 to 10) is involved in apoptosis⁵. For extrinsic apoptosis, the cell surface receptor forms a complex with a receptor binding protein, such as TNFR-1/Fas/CD95 with FADD, and caspase-8. Upon interaction between receptors and ligands, caspase-8 is activated through oligomerisation by the receptors, which cleave BH3-Interacting Domain death agonist protein (BID) to release a C-terminal domain that translocates to the mitochondrion, and leads to the release of cytochrome *c* from mitochondria into the cytosol¹⁰³. Cytochrome *c* binds to Apoptotic protease activating factor 1 (Apaf-1) and (pro)-caspase-9 to form the apoptosome. The apoptosome results the activation of caspase-9 by auto-cleavage, which activates other caspases downstream of this cascade with caspase-3 as the main target.

Activation of caspase-3 and other caspases by auto-cleavage triggers the effector phase of apoptosis when cellular structures are destroyed, which includes protein degradation, membrane damage and DNA cleavage, resulting in cell death⁵.

The intrinsic apoptotic pathway is characterised by a change in mitochondrial membrane permeability, which is regulated by members of Bcl-2 family, such as Bax¹⁰². Subsequent release of cytochrome *c* from the mitochondria triggers formation of the apoptosome and results in activation of caspase dependent apoptosis through activation of caspase-9. Hence, both extrinsic and intrinsic apoptotic pathways merge at the mitochondria and subsequently employ the same mechanisms to effect programmed cell death.

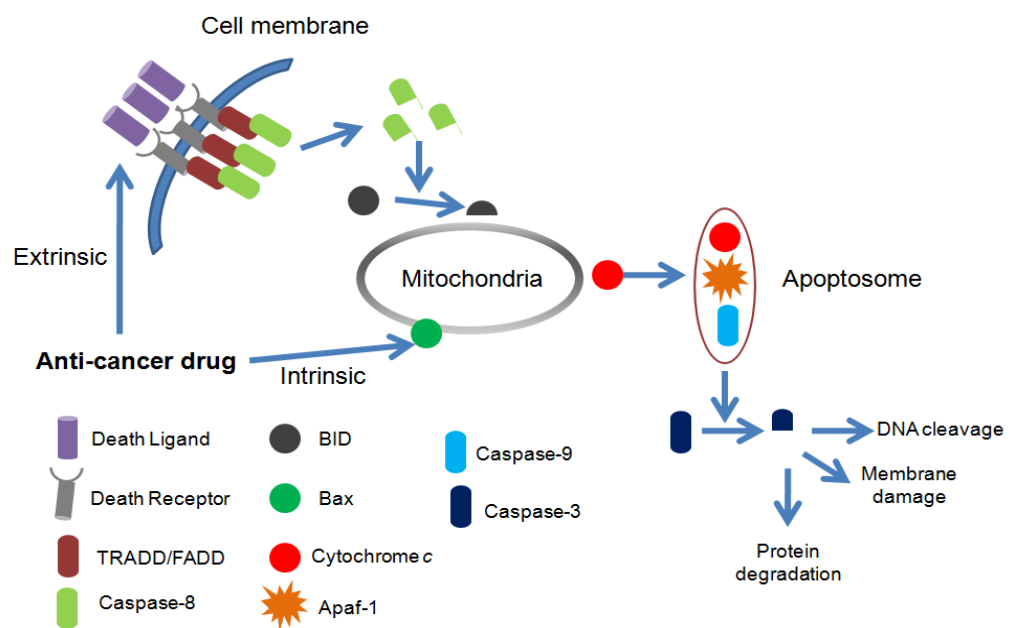


Figure 1.8: The roles of anti-cancer drugs on apoptosis. Anti-cancer drugs employ both extrinsic and intrinsic apoptosis. For extrinsic apoptosis, caspase-8 is activated by auto-cleavage upon the ligand-receptor binding of death ligand (e.g. TNF-TNFR), which cleaves BID protein. The C-terminal domain of cleaved BID induces the expression of cytochrome *c* from mitochondria. Intrinsic apoptosis induced cytochrome *c* expression by changing the permeability of mitochondrial membrane. An example of intrinsic activation is the binding of Bax to mitochondrial membrane triggered by p53 activation. Cytochrome *c* forms a complex known as apoptosome with Apaf-1 and caspase-9. The activated caspase-9 in apoptosome cleaves caspase-3, which leads to the effector phase of apoptosis.

Anti-cancers agents employ both extrinsic and intrinsic apoptosis in order to induce tumour cell death¹⁰². Most of the chemotherapy agents are known to activate extrinsic apoptosis. 5-Fluorouracil, a chemotherapy agent for the treatment of colon carcinomas, is known to activate CD95 for extrinsic apoptosis. Some chemotherapy agents, such as paclitaxel, are known to have an indirect role in activating intrinsic apoptosis by triggering perturbations of intermediate metabolism, or by increasing the concentration of pro-apoptotic second messengers, such as the activation of p53 leading to the expression of Bax (Figure 1.8).

In tumour cells, anti-apoptotic factors are usually expressed to suppress this programmed cell death. There are two stages where anti-apoptotic proteins could suppress this pathway. Bcl-2, one of the best known anti-apoptotic factors, suppresses apoptosis in many cells by inhibiting the release of cytochrome *c* from mitochondria through direct binding to the outer mitochondrion membrane¹⁰⁴. IAPs are another group of anti-apoptotic proteins which inhibit the formation of apoptosome¹⁰⁵. Proteins that antagonise IAPs may be released from the mitochondrion to overturn the effect of these anti-apoptotic proteins.

1.3.4 Anti-apoptotic factors

In tumour cells, transcription of anti-apoptotic factors has been linked to the activity of CDK9. Anti-apoptotic proteins Mcl-1, Bcl-2 and XIAP have been reported to be regulated by CDK9 at transcriptional levels by RNAP II¹⁰⁶.

Mcl-1 (Myeloid cell leukaemia-1) protein is a member of Bcl-2 family which acts as a potent multi-domain anti-apoptotic protein^{107, 108}. Mcl-1 has

been found to be over-expressed in malignant human tumours, including non-small cell lung carcinoma, and cholangiocarcinoma. Mcl-1 localises to the mitochondria and associates with other members of Bcl-2 proteins, such as Bax, which forms a heterodimer to inhibit the activity of these proteins (i.e. apoptotic induction), hence protects cells against apoptosis^{109, 110}. Mcl-1 has also been found to inhibit apoptosis by interfering with the association of p53 and BAK (Bcl-2 antagonist killer)¹¹¹. The formation of the p53/BAK complex has shown to release Mcl-1. This indicates that Mcl-1 works as a negative regulator of p53 by competing with BAK as a binding partner.

Bcl-2 (B-cell CLL/Lymphoma 2) is one of the most extensively studied anti-apoptotic factors and is a cancer survival gene. Bcl-2 was first found to be over-expressed in follicular lymphoma, localised in the inner mitochondrial membrane and suppressing apoptosis of pro-B lymphocytes¹¹². The presence of the RAF1 protein kinase in mitochondria improves Bcl-2 activity in resisting cell death¹¹³. Bcl-2 has also been found in normal human brain tissue, spinal cord tissue, cytotoxic (killer) and memory T cells¹¹⁴⁻¹¹⁶. In addition, Bcl-2 is also involved in a huge number of caspase-dependent / -independent apoptotic pathways¹¹⁷.

XIAP (X-linked inhibitor of apoptosis) gene is located on human chromosome 23 X (Xq25)¹¹⁸. *XIAP* shows high homology with the baculovirus inhibitor of the apoptosis gene which encodes proteins that significantly inhibit apoptotic cell death. XIAP protein inhibits the activation of caspase-3, -7 and -9, all of which are involved in major apoptotic pathways^{119, 120}. XIAP is targeted nuclear factor kappa B (NFkB), which leads to the inhibition of C-JUN kinase (JNK) resulting cell apoptosis¹²¹.

Ubiquitination of XIAPs, a guided degradation, has been suggested as a critical event in apoptosis¹²². XIAP has also been found to associate with other anti-apoptotic proteins, such as BIRC5, and interact with protein kinase A to promote survival in human cancer cells¹²³.

1.4 Eukaryotic transcription and CDKs

Transcription is a process in cells to synthesise messenger ribonucleic acid (mRNA) from genomic DNA; the mRNA is later translated into proteins. In higher eukaryotes including humans, CDK7, CDK8, CDK9 and CDK11 play regulatory roles during the processes of transcription initiation and elongation by RNA polymerase II (RNAP II). There are three types of RNA polymerase - I, II and III⁵. In humans, RNAP II is the most abundant. Ribosomal RNA genes are transcribed by RNAP I ribosomal RNA genes, while RNAP III transcribes small nuclear and transfer RNA genes.

Activator signals, such as growth factor proteins, initiate transcription in eukaryotic cells. The activators bind to the sequences adjacent to the promoter of a particular gene, these sequences, sometimes known as initiator or distal enhancers (Figure 1.9)¹²⁴, can also be located inside the promoter sequence. The binding of an activator to the regulatory sequence leads to the assembly of RNAP II, general transcription factors (GTFs), including TFIIA, TFIIB, TFIID, TFIIE and TFIIH, and a large multi-protein complex mediator which directly communicates with other gene-specific regulators¹²⁵. This assembled protein complex is known as the pre-initiation complex (PIC). PIC assembly is directed to the start site by “core” promoter sequences such as the TATA

box¹²⁶, a tandem repeated DNA sequence consisting of 5'-TATAAA-3', which is recognised primarily by TFIID and other GTFs.

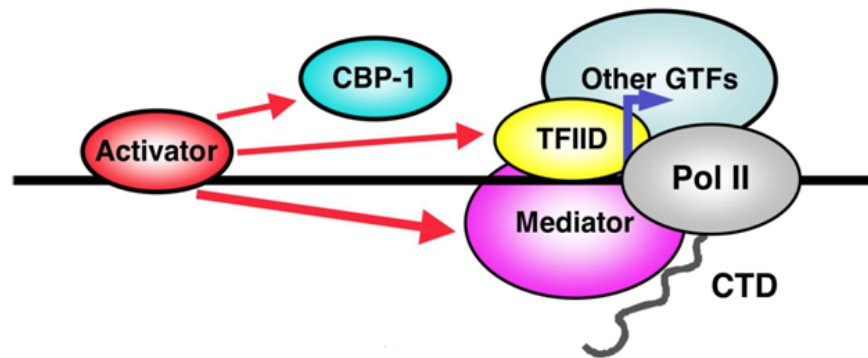


Figure 1.9: Mechanism in the pre-initiation phase of RNA polymerase II dependent transcription¹²⁴. Activator binds to upstream promoter region to initiate the formation of pre-initiation complex (PIC), which includes RNA polymerase II, general transcription factors (GTFs) and the Mediator. TFIID is the predominant GTF involved in PIC. In some genes, chromatin modifying co-factors such as histone acetyltransferase (HAT). Creb-binding protein 1 (CBP-1) will also be recruited if histone modification is involved in the regulation of that particular gene (Adapted from Blackwell & Walker. Transcription mechanism. *WormBook*. 2006).

The most fundamental mechanism of PIC recruitment is gene specific activation to induce transcription, but PIC assembly is also influenced by histone modification and its positioning¹²⁷. Histones are the basic protein building blocks of chromatin, which acts as a reel for DNA coiling and regulate gene expression. At the promoter region of a gene, specific gene activators or repressors affect the configuration of chromatin by recruitment of chromatin modification or remodelling factors. Transcription regulation by histone modification is a hugely complicated process involving many other signalling pathways. The process of binding of activators to the PIC assembly in the core promoter region is known as the 'pre-initiation' phase of transcription.

From early studies in *C. elegans* and human cells, it has been shown that the process of transcription occurs dominantly through the phosphorylation of RNAP II at its large subunit (RPB1) C-terminal domain (CTD) after the assembly of PIC. RNAP II CTD consists of tandem repeats (38 in *C. elegans*,

52 in humans) of a seven amino acids sequence (5'-Tyr-Ser-Pro-Thr-Ser-Pro-Ser-3')¹²⁴. RNAP II is recruited to the PIC with the CTD in an unphosphorylated state¹²⁸. The CTD repeat is phosphorylated on Ser 5 by CDK7 at the promoter region of the gene. This phosphorylation is regulated by CDK8, which is associated with cyclin C (another component of RNAP II holoenzyme complex)¹²⁹ and regulates the activity of CDK7 through the phosphorylation of cyclin H1 at Ser 5 and Ser 304, resulted in suppression of transcriptional activation by TFIIF^{125, 130}. The phosphorylation of RNAPII by CDK8 prevents the RNAP II assembly on to the promoters, therefore prevents the initiation of transcription. The phosphorylation at the Ser 5 of RNAP II in the PIC complex by the CDK7 subunit of TFIIF promotes RNAP II to proceed from the promoter region to the downstream sequence, a process known as promoter clearance. The RNAP II complex is then arrested at the 5,6-dichloro-1-β-d-ribofuranosylbenzimidazole (DRB) sensitivity inducing factor (DSIF) - negative elongation factor (NELF) complex¹³¹, which acts as a checkpoint allowing and ensuring the association of mRNA capping enzyme (C.E.) to RNAP II, which add the 5'cap to the nascent pre-mRNA transcript.

The RNAP II CTD is subsequently phosphorylated on Ser 2 by CDK9 (Figure 1.10) which initiates transcription elongation and allows mRNA termination and processing factors to be recruited directly to the CTD. At this stage, RNA nucleotides assemble at their complementary base on the coding DNA through RNAP II. CDK11/cyclin L is involved in this stage of transcription with one of its two isoforms in humans, p110, functioning in transcriptional related activity and RNA splicing¹³². Reduction of p110 *in vitro* has shown a reduction in transcriptional activity, while the re-addition of p110

rescued transcriptional activity. Similarly, immunodepletion of p110 from splicing extracts shows profound reduction in the amount of spliced RNA transcript produced *in vitro*¹³³.

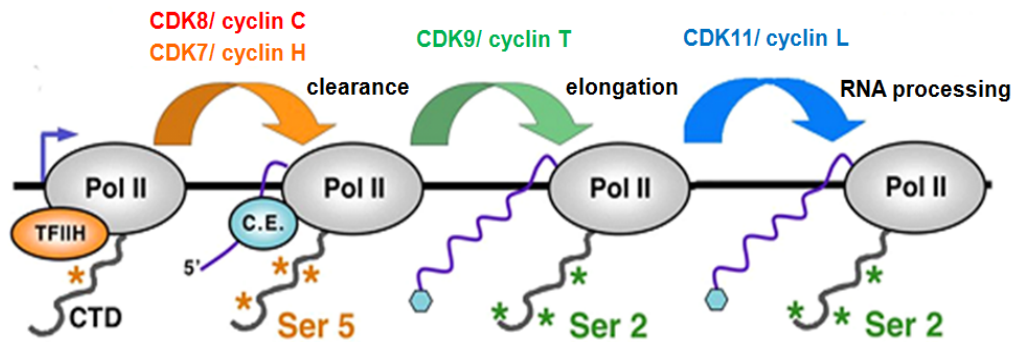


Figure 1.10: Regulation of transcription initiation and elongation by CDKs¹²⁴. CDK7/cyclin H, which is regulated by CDK8/cyclin C, phosphorylate RNAP II CTD at Ser 5, which allows dissociation of TFIID from RNAP II and promotes clearance of RNAP II from the core promoter. Capping enzyme (C.E.) binds to RNAP II to generate a 5' cap for the mRNA. Phosphorylation of CTD Ser 2 by CDK9 follows and transcription elongation begins. CDK11 regulates the transcriptional activity and the mRNA splicing (Adapted from Blackwell & Walker. Transcription mechanism. *WormBook*. 2006).

Once RNAP II reaches the terminator sequences on the DNA template, RNAP II detaches from the template DNA, proteins recognise the terminator sequences cause the cleavage of the nascent RNA from the DNA template following the polyadenylation signal⁵. The addition of a poly-A tail stabilises the mRNA which exports outside the nucleus for post-transcriptional processing.

The phosphorylation of the CTD of RNAP II is a key regulatory event of the process from transcription initiation to downstream nuclear events which include mRNA processing, termination and nuclear export¹²⁸. CDK7 and CDK9 are essential for the initiation and synthesis of mRNA, which leads to the nuclear export and translation of mRNA to the synthesis of protein in the ribosome.

1.5 Natural products

Natural products refer to chemical compounds or substances naturally synthesised by living organisms¹³³. Sometimes, these natural products have biological activity against disease and may therefore have potential for use in drug discovery and design. Chemicals that may be synthesised in the laboratory, but are found naturally occurring in organisms, are also considered as natural products.

Natural products may be extracted from terrestrial plants, marine organisms or micro-organism fermentation broths. A crude extract from any one of these sources typically contains a vast range of novel, structurally diverse chemical compounds. The degree of diversity comes from the geographic and environmental diversity of the species' habitats, coupled with variation in the species themselves.

The plant kingdom is the most common source of natural products; plants having been used for medicinal purposes since the beginning of human civilisation and have been successfully exploited in Chinese medicine. The simplicity of plant organisation increases their ability to adapt to the environmental changes through variation¹³⁴. Plants represent a rich source of compounds with therapeutic properties, such as morphine, cocaine, digitalis, quinine, tubocurarine, nicotine and muscarine. These compounds very often have complex structures and are unlikely to be easily synthesised in laboratories.

Micro-organisms, such as bacteria and fungi, have been invaluable in drug discovery. The most famous example is the discovery of penicillin¹³⁵. After its discovery, water and soil samples were studied intensively to obtain new

strains of antibiotic producing microbes, leading to the discovery of antibacterial agents such as cephalosporins, tetracyclines, aminoglycosides, rifamycins and chloramphenicol.

Marine organisms have recently received significant attention in natural product discovery. Coral, sponges, fish and other marine microorganisms contain potent chemicals with anti-inflammatory, antiviral and anticancer activities. Curacin A is a compound obtained from marine cyanobacterium with anti-tumour activity¹³⁶. Animals, their venoms and toxins are other sources which have yielded new medicines¹³⁷.

Sources	Drugs being discovered
Plant	morphine, cocaine, digitalis, quinine, tubocurarine, nicotine, muscarine, paclitaxel, artemisinin
Microbes	penicillin, cephalosporins, tetracyclines, aminoglycosides, rifamycins, asperlicin, lovastatin, ciclosporin, chloramphenicol
Marine	curacin A, eleutherobin, discodermolide, bryostatins, dolostatins, cephalostatins
Animal, venoms and toxins	epibatidine, teprotide

Table 1.2: Some of the best known drugs discovered from natural sources¹³⁵⁻¹³⁸. Plants contribute the most drugs of all natural sources, their compounds treating a wide range of diseases. Microbes are the second most abundant source for natural product discovery, the majority being anti-microbial agents. There are some exceptions such as asperlicin and lovastatin which reduce anxiety and cholesterol levels respectively. Animals, venoms and toxins contribute to drug discovery occasionally, examples being epibatidine and teprotid, an extract from the Ecuadorian poison frog and a peptide isolated from the venom of the Brazilian viper, which are analgesic and antihypertensive agents respectively.

The complexity of many natural products poses a problem to their study, making them far too expensive to synthesise in the laboratory. Drugs such as penicillin, morphine and paclitaxel (Taxol) can only be obtained from natural sources¹³⁸.

In the developed world, almost all clinically used chemotherapeutics have been produced by semi- or total chemical synthesis as this is a most efficient way to obtain medicine. However, many non-natural, synthetic drugs induce

severe adverse effects unacceptable except in last resort treatments for terminal diseases. Although most natural medicinal products, particular those with anti-cancer properties, are highly toxic, the use of metabolites discovered in medicinal plants and other natural sources still have the possibility avoid the adverse effects of synthetic drugs as these compounds may accumulate within living cells in the species itself without adverse effects.

Semi-synthetic procedures often involve harvesting a biosynthetic intermediate from the natural source, which can then be converted to the final product by conventional synthesis. There are two advantages in using this approach. Firstly, the intermediate may be more easily extracted in higher yield than the final product, an abundant supply being available for conversion into the active compound within the species itself. Secondly, it may allow the possibility of synthesising analogues of the final product to generate chemical diversity. Production of penicillins is an illustration of this approach; semisynthetic penicillins, which have similar functions to natural penicillins, are currently used as medicines¹³⁹.

The use of natural products is one of the major approaches in drug discovery. A large number of natural products and derivatives were approved as registered drugs and contributing currently approximately 50% of marketed drugs. More importantly, there is still enormous scope for the development of natural products as, despite their long history of medicinal use, the potential for most plant species remains unexplored.

In recent years, natural products are believed to have an effect on the prevention of disease. Compounds with polyphenolic functions are often identified in natural sources, such as grapes and tea¹⁴⁰. These polyphenols

possess anti-oxidant properties, which are believed to prevent or slow down the occurrence of diseases such as cancer. Among these compounds, the most extensively studied polyphenol is Epigallocatechin gallate (EGCG)³².

EGCG is the most abundant catechin (polyphenolic anti-oxidant plant metabolite) found in green tea and may have therapeutic properties for many disorders, including cancer and AIDS¹⁴¹. Although oxidation is an essential process in living organisms, free oxygen radicals are mutagens which cause DNA damage and are associated with certain forms of cancer; hence oxidative stress may induce cell damage and death¹⁴². Therefore, dietary intake of anti-oxidants, including polyphenols and vitamins, are implicated in the prevention of disease. In the case of EGCG, experimental data have proven that it could reduce oxidative stress and may be beneficial in HIV treatment¹⁴³. However, the quantity required to achieve such an effect cannot be achieved through normal dietary intake. Nevertheless, extensive research has been carried out to investigate the medicinal use of polyphenols.

1.6 Aims and objectives

The project is divided into three parts:

- Evaluation of CDK9 inhibition as an anti-cancer strategy using chemical biology approaches. A class of rationally designed inhibitors were tested for their anti-proliferative activity against human cancer cells. A lead inhibitor was further selected and used to study the detailed cellular mode of action and anti-cancer property.
- The study of natural product derivatives. The cellular growth inhibitory effect of the product will be investigated. This includes its effect on cell cycle and cell death induction, expression and transcription of anti-apoptotic, and tumour suppressor proteins, suppression of tubulin polymerisation as well as its anti-angiogenic and anti-oxidant properties
- The synthesis of BI 2536, a known Polo-like kinase 1 (Plk-1) inhibitor, was attempted in order to use this compound as a biologic tool for the validation of Plk-1 as a pharmacologic target for cancer.

Drug discovery is a multi-step process; this project involves the synthesis phase and *in vitro* biological evaluation and mechanistic study of small molecule inhibitors. A wide range of biological and chemical techniques are also employed. These techniques are critical at the early stages of drug discovery, which determines whether a compound has the potential to become a successful drug.

Chapter Two

Mechanism of action of a novel CDK9 inhibitor

2.1 Introduction

Protein kinases are fundamental regulators of essential molecular pathways in live cells. One of most extensively studied kinase groups is the serine/threonine (Ser/Thr) protein kinases. Some of the best known Ser/Thr protein kinase family members include cyclin-dependent kinases (CDKs), Polo-like kinase (Plks) and Aurora kinases. These kinases are involved in the progression of the cell cycle and are altered in several diseases including cancers.

2.1.1 Cyclin-Dependent Kinase 9

Cyclin-dependent Kinase 9 (CDK9) was initially identified in mice in 1994. It was first isolated by performing PCR on a mouse embryonic cDNA library, using oligonucleotide primers based on regions conserved over CDK1 related proteins¹⁴⁴. The CDK9 gene was isolated by comparing the PCR product to a cDNA library from humans. The human CDK9 gene was later mapped to be

on chromosome 9 (9q34.1). By performing a northern blot analysis, which separates the RNA by size, it was found that the mRNA of CDK9 was expressed with a length of 2.8 and 3.2 kb in human. The highest levels of mRNA expression were found in the liver and placenta. Real time PCR (RT-PCR) of total RNA from HeLa cells led to the identification of two isoforms of CDK9; these were CDK9-55 and CDK9-42 with a calculated molecular weight of 55 and 42 kD, respectively. CDK9-55 contains a 117 amino acids *N*-terminal extension with a proline-rich region and a glycine-rich region in addition to the 372 amino acids of CDK9-42 (Figure 2.1). The ratio between the two CDK9 isoproteins varies between different tissues, with CDK9-42 generally a more dominant form over CDK9-55 in most tissues¹⁴⁵. Human macrophages activated by lipopolysaccharide or infected with HIV are an exception with CDK9-55 expressed dominantly.

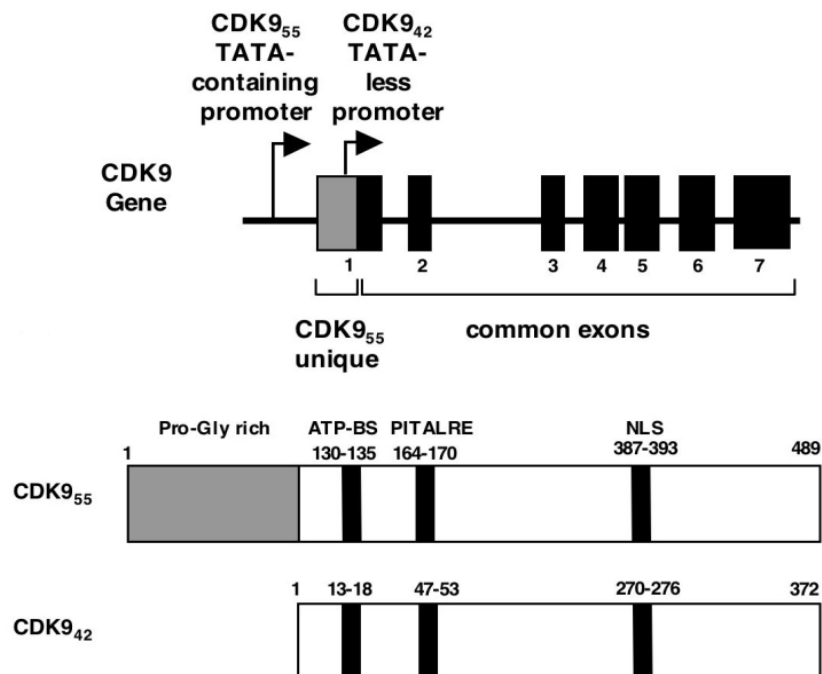


Figure 2.1: Gene and amino acids sequences of CDK9¹⁴⁵. The genes sequence of CDK9 encoded both CDK9-55 and CDK9-42. The gene sequence of CDK9-55 has an extended exon 1 sequence over CDK9-42. Hence the amino acid sequence of CDK9-55 has an additional 117 amino acids at the *N*-terminal of the protein compared to CDK9-42.

Comparing the amino acid sequences to other CDKs, CDK9 has shown 41 - 43% sequence conservation with CDK1, CDK2, CDK4 and CDK5 with CDK2 most homologous to CDK9¹⁴⁶. CDK9 binds to cyclin T1, T2a, T2b or cyclin K to become an active unit known as positive transcription factor b (P-TEFb)¹⁴⁷. The association between CDK9 and cyclin T requires the interaction of bromodomain containing protein 4 (BRD4)¹⁴⁸, a transcriptional co-activator. Increased expression of BRD4 causes increased phosphorylation of RNAP II CTD¹⁴⁹. The recruitment of P-TEFb to a promoter is BRD4 dependent and is enhanced by the increase of chromatin acetylation. At the cellular level, half of the P-TEFb was negatively regulated by 7SK small nuclear RNA (snRNA) and Hexamethylene bis-acetamide-inducible (HEXIM1 or HEXIM2) protein^{148, 150}. Various stimuli, including stress and hypertrophic signals, induce release of P-TEFb from the inhibitory complex, which allows the binding of transcription factors, such as nuclear factor kappa B (NFkB). Following the binding of co-activators (e.g. BRD4), P-TEFb is recruited to the transcription initiation complex.

The function of P-TEFb is to regulate transcription elongation by RNAP II through phosphorylation. P-TEFb phosphorylates the DSIF-NELF complex which allows the removal of promoter-proximal pausing on the transcription initiation complex. Subsequent phosphorylation of RNAP II CTD at Ser 2 of the tandem repeats (5'-Tyr-Ser-Pro-Thr-Ser-Pro-Ser-3') promotes active transcription elongation. The phosphorylation of Ser 2 also has an indirect role in the regulation of RNA splicing, termination and polyadenylation of nascent mRNA¹⁵¹.

2.1.2 CDK9 and human pathologies

Since CDK9 is involved in transcription, an essential process that occurs in almost all living cells at some stage, therefore CDK9 has been linked to many disease areas, including virology, cardiology and oncology¹⁵¹.

2.1.2.1 Virology

Many viruses require their host transcription system to synthesise proteins essential for their replication, particularly the human immunodeficiency virus (HIV). CDK9 was found to be linked to acquired immunodeficiency syndrome (AIDS), with its prospective role in (HIV)-1 related to transcription through 7SK RNA¹⁵¹. In humans, 7SK is an abundant snRNA transcribed by RNA polymerase III. 7SK RNA inhibits the activities of P-TEFb and HIV-1 tyrosine aminotransferase (Tat)-specific transcription by suppressing the activity of CDK9 and preventing recruitment of P-TEFb to the HIV-1 promoter¹⁵². Treating cells with agents that enhance HIV-1 transcription and RNAP II phosphorylation such as actinomycin D shows 7SK RNA dissociate from P-TEFb, enhancing CDK9 activity and transcription. P-TEFb and 7SK RNA association is a specific and reversible interaction. As CDK9 is crucial for HIV-1 transcription, the activity of 7SK snRNA is suppressed in HIV-1. The role of BRD4 in P-TEFb is replaced by Tat in HIV-1; therefore Tat is required for the formation of P-TEFb in HIV-1. Another component of P-TEFb, cyclin T1, its C-terminal domain helix shows flexibility that might be critical for HIV-1 Tat and HEXIM association that regulates the activity of P-TEFb.

2.1.2.2 Cardiology

Over-expression of CDK9 is also linked to cardiac hypertrophy¹⁵³, a syndrome with an increase in the size of terminally differentiated cardiomyocytes. Increased CDK9 activity against the C-terminal domain of RNAP II subunit A (POLR2A) was found in ventricle samples from patients with heart failure caused by dilated cardiomyopathy¹⁵⁴. Studies from cyclin T1 deficient mice have shown that the induction of cyclin T1 expression in cardiomyocytes maintained CDK9 activity in mouse hearts, resulting in myocyte enlargement and selective suppression of PPAR-gamma co-activator (Pgc1), a master regulator of several metabolic processes, including mitochondrial biogenesis and respiration. The ultimate effects of such CDK9 activity induction in defective mice were mitochondrial defects, enhanced myocyte apoptosis, predisposition to heart failure and early death¹⁵⁵.

Another known function of CDK9 is its involvement in myogenesis, the generation of muscle cells¹⁵⁶, including the pacemaker of the heart. Over-expression of CDK9/cyclin T2a induced the expression of MyoD and enhanced myocyte differentiation. MyoD also acts as a transcription factor which binds to P-TEFb promoting transcription elongation. Cyclin T2a has also been found to induce the expression of other myogenic differentiation factors such as myogenin and myosin heavy chain. P-TEFb was found to selectively activate transcription mediated by the myocyte enhancer factor 2 (MEF2) in murine C2C12 cells¹⁵⁷. Knockdown of endogenous cyclin T1 by siRNA was found to reduce the expression of MEF2 dependent reporter genes, which may underlie the potential transcription mechanisms in muscle cells.

2.1.2.3 Oncology

The alteration of cell cycle has been linked to the onset of cancer. As described in section 1.3, the unregulated cell cycle CDKs activity leads to the alteration and dysfunction of tumour suppressors, such as RB and p53. Tumour suppressors' dysfunction lead to the unregulated transcription of components required for cell cycle progression, or anti-apoptotic factors which suppress programmed cell death in oncogenic cells. CDK9 has been linked to the transcription of components in the RB and p53 pathways, such as p21 in the INK4 CDK inhibitor family. CDK9 is also associated with the transcription of anti-apoptotic factors Mcl-1 (Myeloid cell leukaemia-1), Bcl-2 (B-cell CLL/Lymphoma 2), XIAP (X-linked inhibitor of apoptosis) and BAG-1 (Bcl-2-associated athanogene 1)¹⁰⁶.

One of the major applications of CDK9 inhibitors is for the treatment of chronic lymphocytic leukaemia (CLL) in B-lymphocytes¹⁰⁶, a type of cancer characterised by combination of blocks in apoptosis, such as the expression of Mcl-1 and Bcl-2 (see section 1.3.4). An inhibitor targeting CDK9 may suppress transcription in cancers; this suppression of transcription could reduce the synthesis of anti-apoptotic proteins required for the survival of cancer cells, which will lead to cell death.

In normal healthy cells, apoptotic factors such as the Fas ligand (FasL), a member of tumour necrosis factor (TNF)^{158, 159}, are expressed at low levels. Oncogenic transformation refers to the process where normal cells are transformed into tumour cells *via* carcinogenic induction. After oncogenic transformation, a number of apoptotic factors such as TNFs is released, triggers a cascade of signalling pathways and the activates caspase-dependent

apoptosis¹⁶⁰. Tumour cells are highly mutated cells that may escape programmed cell death by expressing anti-apoptotic genes and proteins including Bcl-2, Mcl-1, IAPs and survivin^{108, 161}. CDK transcriptional inhibition can suppress the transcription and expression of anti-apoptotic proteins and causes cancer cell death¹⁶² (Figure 2.2).

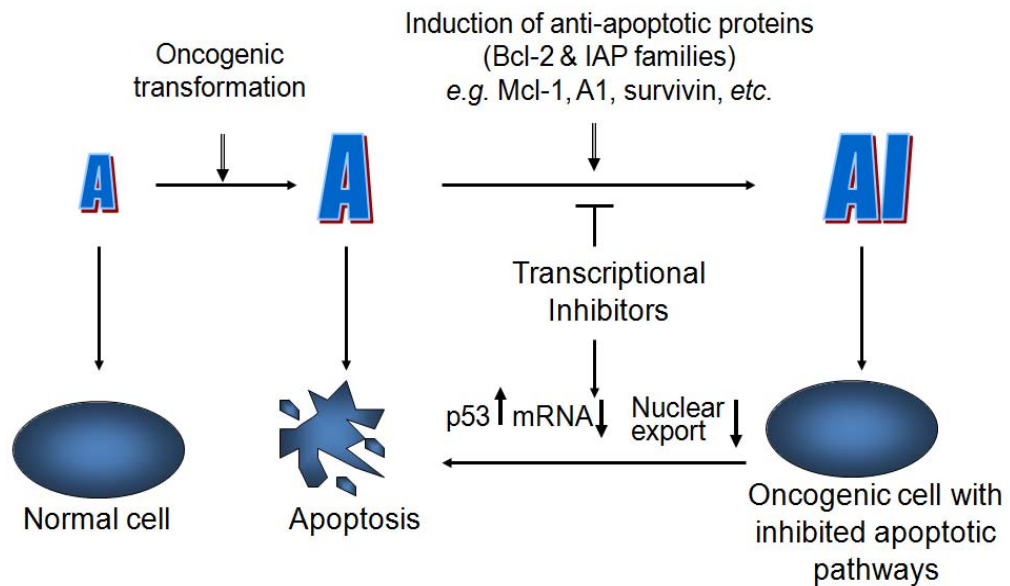


Figure 2.2: Rational of targeting transcription as a potential cancer therapy¹⁶². The oncogenic transformation should increase the sensitivity of cells to apoptotic signals (A). However, tumour cells' expression anti-apoptotic factors (I) suppress the function of apoptotic factors (AI) and reduce the sensitivity of tumour cells to apoptosis, hence enable tumour cell survival. Transcriptional inhibitors should suppress the production of anti-apoptotic factors (I) which would lead to tumour cell death. Normal cells however, do not affected by transcriptional inhibition, as majority of normal cells are in G₀, i.e. quiescent and do not required transcription (Adapted from Koumenis *et al. Mol. Cell. Biol.* 1997, 17, 7306).

In tumour cells, transcription of anti-apoptotic factors has been linked to the activity of CDK9. Anti-apoptotic proteins Mcl-1, Bcl-2 and XIAP have been reported to be regulated by CDK9 at transcription by RNAP II¹⁰⁶. The use of CDK9 inhibitors for cancer treatment hopes to suppress the expression of these anti-apoptotic proteins transcribed in tumours cells¹⁶³, which results in tumour cell death.

2.1.3 Discovery of CDK9 inhibitors

CDK9 inhibition has presented as one of the most effective targets for the treatment of proliferative diseases. To identify inhibitor compounds, two strategies are frequently used, e.g. kinase structure-based design, or inhibitor compound analogue design and modification. Most kinase inhibitors, including Gleevec⁴⁴, are designed as ATP antagonists. Based on the x-ray crystal structure of CDK2, three regions in the ATP-active binding domains are crucial for design of the ATP mimetics: the hinge region, the ribose binding domain and the hydrophobic binding pocket. The latter is crucial for designing inhibitors with specificity for individual CDKs¹⁶⁴. The structure of ATP binding domain is conserved among the CDKs, in particular between CDK2 and CDK9¹⁶⁵.

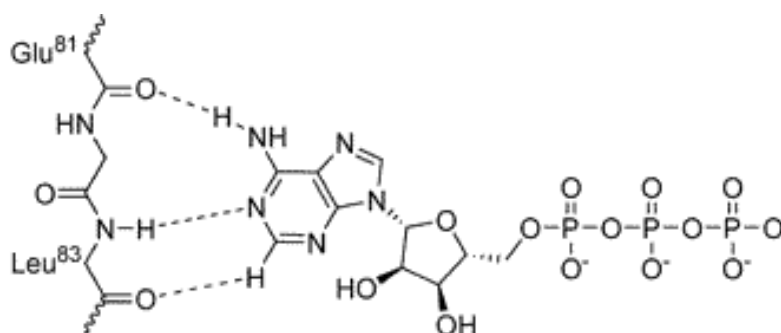


Figure 2.3: Binding between the ATP binding pocket of CDK2 and ATP¹⁶⁴. Three hydrogen bonds are crucial for this binding in this ATP-CDK complex: NH₂: Glu 81 CO; pyrimidine N1: Leu 83 NH; pyrimidine H6: Leu 83 CO, respectively. Most kinase inhibitor-CDK complexes have replicated and conserved binding in this form (Adapted from Wang *et al. J. Med. Chem.* 2004, 47, 1662).

The crystal structure of CDK9 in complex with cyclin T1 has recently been solved (Figure 2.4)¹⁴⁷. Docking studies show that ATP antagonists bind to the ATP binding site of CDK9 inducing unanticipated structural changes that possibly inhibit kinase activity.

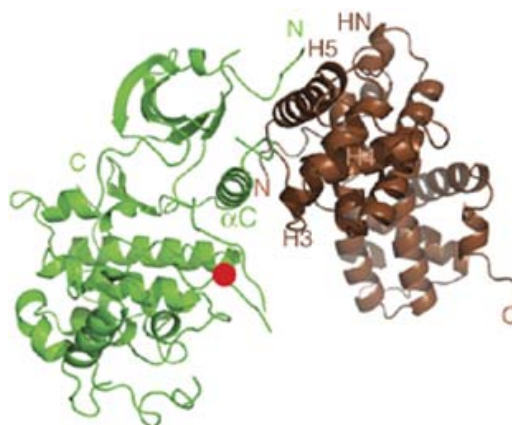


Figure 2.4: Crystal structure of CDK9 (green) bound to cyclin T1 (brown)¹⁴⁷. The red dot is the phospho-threonine residue in the activation segment. Cyclin T1 consists of 5 helices (H) and short *N*- (NH) and *C*- terminal (Adapted from Hirose & Ohkuma. *J. Biochem.* 2007, 141, 601).

Our novel CDK9 inhibitors are designed as the ATP antagonists against the ATP binding pocket of the kinase domain. The potency and selectivity were optimised based on our advanced medicinal chemistry and structural biology techniques.

A number of CDK9 inhibitors have been reported in the literature, some of which are currently undergoing clinical trials⁵⁰ (Figure 2.5). As they target the ATP active binding site, many of these known inhibitors are pan-CDK inhibitors^{151, 166}.

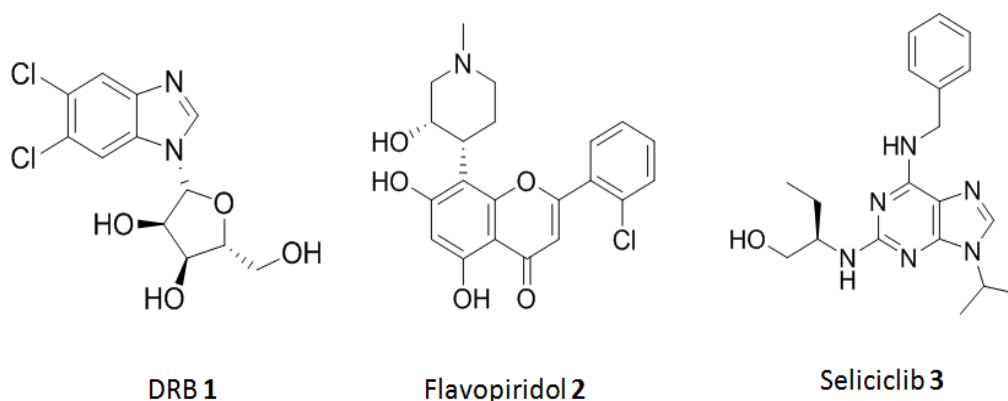


Figure 2.5: Structures of some of the best known CDK inhibitors. DRB is regarded as the prototype of CDK9 inhibitor, as it is a substance naturally found in eukaryotic transcription. DRB is the most selective CDK9 inhibitor. Flavopiridol and Seliciclib inhibit multiple kinases and are currently under clinical evaluation.

2.1.3.1 DRB

5,6-dichloro-1- β -d-ribofuranosylbenzimidazole (DRB) **1** is a substance originally identified in the DRB sensitivity inducing factor (DISF) - negative elongation factor (NELF) checkpoint, this checkpoint appeared shortly after the elongation of pre-mRNA to ensure the addition of 5'cap during transcription¹³¹. DRB can be regarded as the prototype due to its close association with the original identification of CDK9 P-TEFb kinase. DRB had long been known to suppress the transcription of long mRNA; this property was then related to the inhibition of a number of cellular kinases. To date, DRB is still the most selective inhibitor against CDK9 possibly due to its role in nature. DRB had been evaluated as a possible therapy for cancers and HIV^{167, 168}. However due to the poor cellular activity and unfavourable pharmaceutical properties (such as its inhibition over a large range of human kinases resulting in the lack of selectivity), DRB was unable to proceed to clinical trials.

2.1.3.2 Flavopiridol

Flavopiridol **2**, also known as Alvocidib or HMR-1275, is a semi-synthetic flavonoid of a natural product Rohitukine, which is isolated from *Dysoxylum binectariferum*¹⁶⁹. Flavopiridol works by competing with ATP for binding to the active site, thereby inhibiting the activities of CDKs. *In vitro* data revealed Flavopiridol inhibited the phosphorylation of RNAP II CTD and led to a significant reduction in Mcl-1 and XIAP expression, resulting in caspase-3 dependent apoptosis. Flavopiridol is most potent CDK9 inhibitor with a *Ki* value of 3 nM in kinase assay; it also inhibits CDK2 and CDK7 but at lower

potencies. Flavopiridol has also shown to inhibition the transcription of HIV¹⁷⁰.

Flavopiridol is currently undergoing clinical trials for the treatment of solid tumours and chronic lymphocytic leukaemia (CLL)¹⁷¹. However, differential protein binding of flavopiridol in humans was observed¹⁷². In addition, pro-inflammatory side effects have been observed within phase I and II clinical trials¹⁷³. In terms of efficiency, Flavopiridol as a monotherapy agent for solid tumours has shown partial tumour resolution or reduced tumour progression. Combination therapy with traditional cytotoxic agents was shown to increase tumour cell death¹⁷⁴. From *in vivo* studies treating tumour cells with anti-neoplastic agents, such as paclitaxel, followed by flavopiridol, it is thought that flavopiridol enhances the anti-tumour activity of anti-neoplastic agents by reducing the apoptotic threshold¹⁷⁵.

2.1.3.3 Seliciclib

Seliciclib **3**, also known as *R*-roscovitine or CYC202, was developed by Cyclacel Ltd. It was developed from the separation of the two optical isomers from Roscovitine, which was originally found to prevent cell division of sea urchin embryos¹⁷⁶. Seliciclib was developed as a potential treatment for non-small cell lung cancer (NSCLC), leukaemia, HIV-1 infection, herpes simplex infection and chronic inflammation disorders. Seliciclib inhibits the activity of most CDKs, preferably against CDK2/cyclin E, CDK7/cyclin H and CDK9/cyclin T1 (see section 2.4). CDK2 activity is most affected by this compound, hence, inducing cell cycle arrest at S phase and G2/M transition in treated cells.

Seliciclib is currently undergoing Phase IIb clinical trials. However, a number of adverse effects were reported during the Phase I trials, including vomiting, transient elevations in serum creatinine and transient hypokalaemia. Seliciclib is also undergoing clinical trials for treating B-cell lymphomas, relating to its inhibition of CDK9 activity in B-lymphocytes. The possibility of using Seliciclib in the treatment of AIDS and chronic inflammatory diseases, such as cystic fibrosis, are currently under evaluation.

The work described in this chapter investigates the properties of a series of novel inhibitors designed to inhibit CDK9 activity in hope of identifying a novel selective CDK9 inhibitor which is also a potent inhibitor of cancer cell growth.

2.2 Identification of novel CDK inhibitors

A class of small molecule inhibitors were designed based on the structure of 2,4-disubstituted pyrimidine **4** CDK inhibitor series¹⁶⁴ (Figure 2.6).

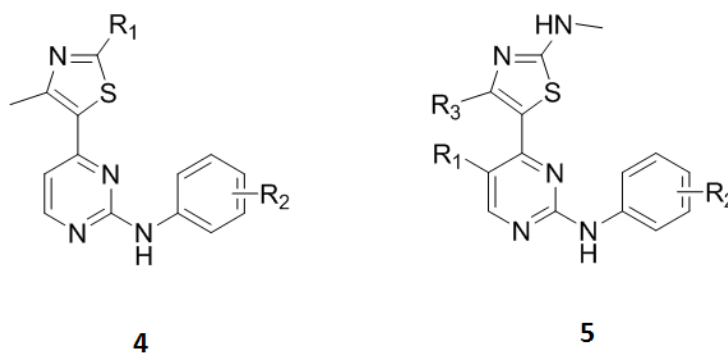


Figure 2.6: The general structures of 2,4-disubstituted pyrimidine **4** and 2,4,5-trisubstituted pyrimidine **5**.

Both compound series **4** and **5** were designed to work as ATP antagonists of CDK9. Inspection of the binding mode of compound **4** in the ATP binding pocket of CDK2 revealed that this compound bind similarly to natural ATP¹⁶⁴.

2.2. Identification of novel CDK9 inhibitors

In both cases, a group of three H-bonds between the ligand and the backbone of CDK2 residues Glu 81 and Leu 83 was observed. The three hydrogen bonds formed between **4** and the CDK2 ATP binding pocket were: pyrimidine H6: Glu 81 CO; pyrimidine N1: Leu 83 NH; aniline NH: Leu 83 CO, respectively.

To improve the potency and selectivity for CDK9, a novel class of 2,4,5-trisubstituted pyrimidines **5** with R₁ at the 5C-position of the pyrimidine ring was designed, which was expected to interact with the gatekeeper residue Glu 81 CO (Figure 2.7). The extension of the heterocyclic system of the molecule can also be achieved by introduction of a hydrophobic group, including phenyl, tert-butyl or isobutyl groups, in the thiazole ring (R₃).

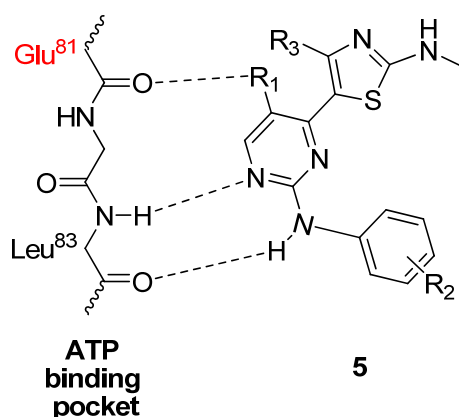


Figure 2.7: The proposed binding of 2,4,5-trisubstituted pyrimidine **5** to the ATP binding pocket of CDK9. Glu 81 (in red) CO represents the gate keeper residue which should be covalently bound with the R₁ residue of **5**. Another two H-bonds should be formed between pyrimidine N1: Leu 83 NH; aniline NH: Leu 83 CO, respectively.

A number of compounds were tested against MTT proliferation assays with 72 hours exposure to the compounds, as described in section 6.3, were used to estimate the concentration of molecules required to inhibit cell growth by 50% (GI₅₀). Two human cancer cell lines and a human fibroblast cell line were used for the screening; the human cancer cell lines used to estimate the effect of our molecules on inhibiting cancer cell growth were HCT-116 human colon carcinomas cells and MCF-7 human breast adeno-carcinomas cells. A human

2.2. Identification of novel CDK9 inhibitors

embryonic lung fibroblast cell line MRC-5 was used to indicate selectivity of compounds between cancer and normal cells. Many compounds demonstrated potent anti-proliferative activity in cancer cells.

Compounds	R ₁	R ₂	R ₃	GI ₅₀ (μM/L)		
				HCT-116	MCF-7	MRC-5
5a	H	m-SO ₂ -N-morpholine	CH ₃	0.32	0.70	N/A
5b	H	m-SO ₂ -N-morpholine, <i>p</i> -Me	CH ₃	0.39	0.46	3.14
5c	H	m-CO-N-morpholine	CH ₃	0.52	0.55	4.16
5d	H	m-CO-N-methylpiperazin	CH ₃	0.71	0.75	6.10
5e	H	m-CO-N-acetylpiperazin	CH ₃	0.62	0.66	6.60
5f	H	m-4-Piperidoneethyleneketal, <i>p</i> -Me	CH ₃	0.49	0.61	N/A
5g	CN	m-SO ₂ -N-morpholine, <i>p</i> -Me	CH ₃	0.07	0.39	0.64
5h	CN	<i>p</i> -OH	CH ₃	0.40	0.23	1.05
5i	CN	<i>m</i> -OH	CH ₃	0.03	0.07	0.54
5j	CN	m-CO-N-morpholine	CH ₃	0.59	0.06	4.43
5k	CN	m-CO-N-acetylpiperazin	CH ₃	5.88	4.96	79.92
5l	CN	<i>m</i> -COOH	CH ₃	47.25	47.41	>100
5m	H	<i>m</i> -NO ₂	Phenyl	0.06	0.61	0.65
5n	H	<i>m</i> -Br	Phenyl	0.08	0.83	4.60
5o	H	m-SO ₂ -N-morpholine, <i>p</i> -Me	Phenyl	0.48	0.64	4.10
5p	H	m-CO-N-acetylpiperazin	phenyl	0.53	2.14	8.12
5q	CN	<i>m</i> -SO ₂ NH ₂	CH ₃	0.03	1.87	>100
5r	CN	<i>p</i> -SO ₂ NH ₂	CH ₃	0.20	1.64	4.51
5s	CN	<i>m</i> -NO ₂	CH ₃	0.04	0.22	0.08
5t	CN	m-CO-N-methylpiperazin	CH ₃	0.75	5.02	6.28
5u	CN	<i>p</i> -morpholine	CH ₃	0.62	0.47	2.16
5v	CN	m-SO ₂ -N-morpholine	CH ₃	0.30	0.70	4.17
5w	CN	<i>p</i> -SO ₂ -N-morpholine	CH ₃	0.47	0.69	0.35

Table 2.1: The structure activity relationship (SAR) of a series of novel CDK9 inhibitors based on the GI₅₀ values. MTT assays were performed following 72 hours exposure to agents against HCT-116, MCF-7 can MRC-5 cells.

From Table 2.1, compound **5a** to **5g** generally demonstrate a 10 times selective between cancer cells (HCT-116 and MCF-7) and Fibroblast cell (MRC-5) lines. Although some of these compounds, such as **5b**, show a better selectivity than **5g**, however, their chemical structures are lack of novelty.

2.2. Identification of novel CDK9 inhibitors

Other compounds in Table 2.1 (i.e. **5h** to **5w**) which show better potency and selectivity were synthesised almost a year after **5g**, therefore, for the interest of this project, **5g** was selected for further mechanistic studies; we named this compound S-134.

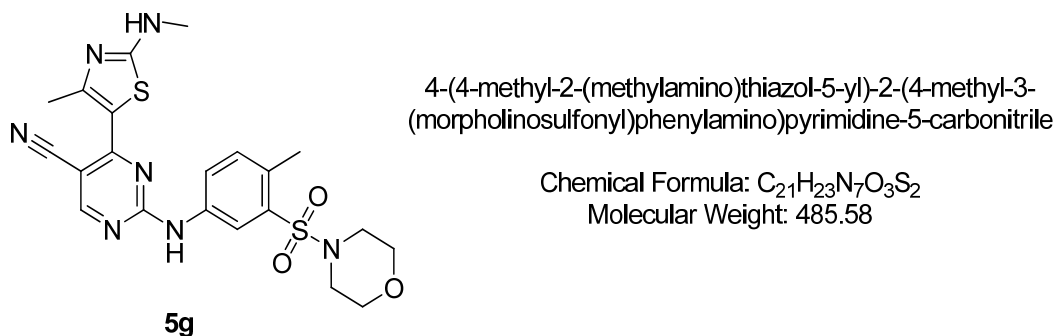


Figure 2.8: Chemical structure of S-134 **5g**.

2.3 Cellular growth inhibition of S-134

HCT-116 and MCF-7 was used for the initial screening. The GI₅₀ of S-134 **5g** were in a range of 0.07 to 0.39 μ M. The compound was also active against MRC-5 with a GI₅₀ values of 0.64 μ M. There was approximately 7.5 fold selectivity between HCT-116 human colon carcinomas cells and MRC-5 human embryonic fibroblast cells. A total of 13 human cell lines were then used to further investigate the effect of S-134 on cancer cell lines derived from a wider spectrum of organ sites (Table 2.2). S-134 was shown to be most effective against HCT-116 and A2780 ovarian carcinoma cells (Figure 2.9).

2.3. Cellular growth inhibition of S-134

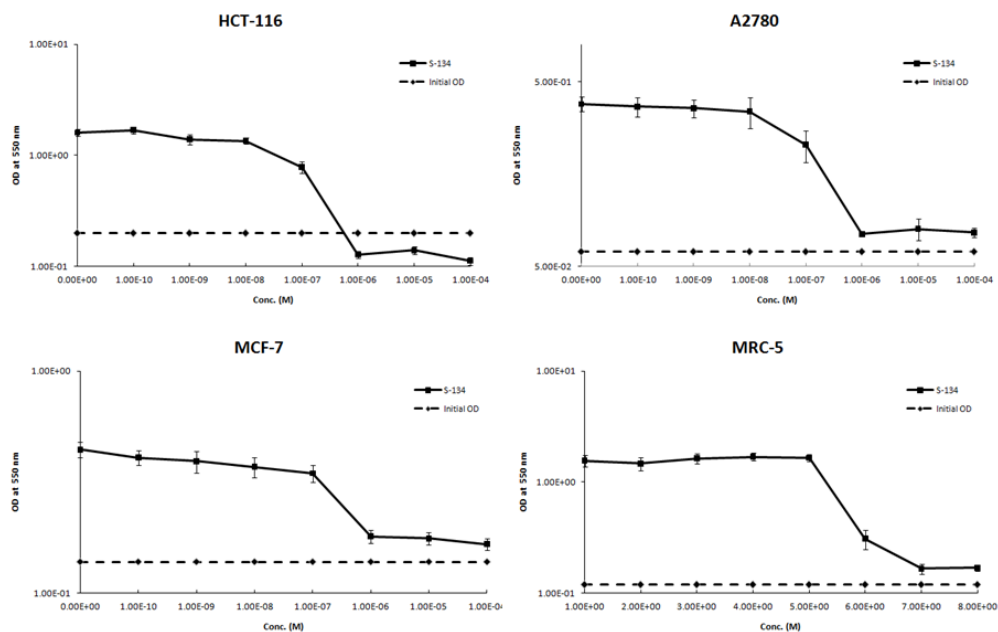


Figure 2.9: Growth inhibition of S-134 on HCT-116, A2780, MCF-7 and MRC-5 cells. OD reading indicates the viability of cells. Among the 13 cell line tested, S-134 was most potent in HCT-116 and A2780 cells indicated with the rapid decrease of OD. There was selectivity between tumour cells HCT-116 and A2780 cells to MRC-5 fibroblast cells in between 4-8 fold. In addition, high concentration of S-134 kills HCT-116 cells as indicated by the OD reading, which dropped below initial OD.

S-134 was a nano-molar inhibitor in most of the cell lines tested. However, two cancer cells - U373 and SNB19 which are human astrocytoma and malignant glioma cell lines, respectively - were less sensitive to S-134.

Cell line	Origin	GI ₅₀ (μmol/L)
HCT-116	Human colon carcinoma	0.07
MCF-7	Human breast adeno-carcinoma	0.39
MRC-5	Human embryonic lung fibroblast	0.64
WI 38	Human Caucasian foetal lung fibroblast	0.78
A2780	Human ovarian carcinoma	0.15
U373	Human astrocytoma	7.71
A549	Human carcinomic alveolar basal epithelial	0.53
SNB19	Human malignant glioma	5.38
HMEC-1	Human microvascular	0.77
HELA	Human cervical carcinoma	0.66
MDA-MB-231	Human breast carcinoma	0.92
PANC W1	Human pancreatic carcinoma	0.37
MIA PaCa-2	Human pancreatic carcinoma	0.47

Table 2.2: Summary table of GI₅₀ values of S-134 in the 13 human cell lines.

DRB was used as a positive control in this assay; the GI_{50} of DRB in HCT-116, A2780, MCF-7 and MRC-5 cells were in a range of 5 to 30 μ M, respectively. From the supplier information (Calbiochem), DRB has an IC_{50} of 6 μ M in cells. Our MTT assay data has shown similar results to reported data, proving that our data is comparable to the literature.

2.4 Effect of S-134 on CDK9, CDK2 and CDK7

CDK inhibition by S-134 was initially tested by *in vitro* CDK2 and CDK9 kinase assays. Among the CDK cyclin combination of the two CDKs, CDK2/cyclin E and CDK9/cyclin T1 were our objective for investigation, as both are widely screened with CDK inhibitors.

This kinase assay was initially done in-house to estimate the effect of S-134 on CDK9/cyclin T1. As CDK2 and CDK7, which later became of interest, were not available in-house, all kinase assays were eventually done externally by Millipore (Billerica, MA, USA).

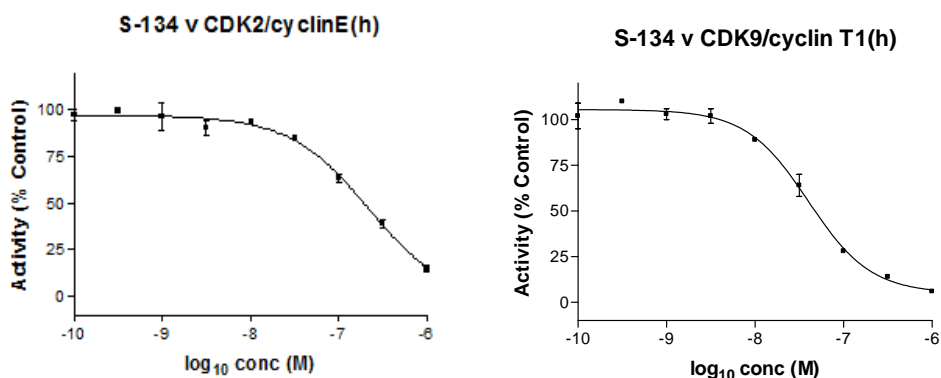


Figure 2.10: Effect of S-134 on CDK2/cyclin E and CDK9/cyclin T1. The data were given by Millipore (Billerica, MA, USA). For optimal reaction conditions, ATP (120 and 45 μ M) was used with the CDK2/cyclin E and CDK9/cyclin T1 assay, respectively. The IC_{50} values are 0.23 μ M against CDK2/cyclin E and 0.04 μ M against CDK9/cyclin T1.

2.4. Effect of S-134 on CDK9, CDK2 and CDK7

The initial kinase assay against CDK9/cyclin T1 carried out in-house with 100 nM ATP showed that S-134 had an estimated IC₅₀ value of 0.02 μM. E-29 **5b**, a 2,4-disubstitute pyrimidine analogue of S-134, has an IC₅₀ of 0.06 μM. The external assay indicated that S-134 has an IC₅₀ of 0.23 μM against CDK2/cyclin E and 0.04 μM against CDK9/cyclin T1 (Figure 2.10), using 120 and 45 μM ATP in the respective kinase assays. E-29 showed an IC₅₀ of 0.55 μM against CDK2/cyclin E and 0.05 μM against CDK9/cyclin T1, in the external kinase assays. These results indicated that S-134 has a relatively potent effect on CDK9 with E-29 being two times more selective than S-134 between CDK9/cyclin T1 and CDK2/cyclin E.

Gathering all our kinase assay and literature data¹⁵¹ (Table 2.3), clinical compounds such as Seliciclib and Flavopiridol were unable to provide the potency for CDK9 inhibition and the selectivity for CDK2 as shown by our compounds. DRB, the most selective CDK9 inhibitor to date, has shown huge selectivity against other CDKs, but it is much less potent than S-134 and other clinical candidates in inhibiting the activity of CDK9. Nevertheless, because of its selectivity, DRB was used as a positive control in some of our cellular assays to directly compare its activity with S-134.

Compounds	CDKs IC ₅₀ or Ki (μmol/L)		
	CDK2/cyclin E	CDK7/cyclin H	CDK9/cyclin T1
DRB	>1	>1	0.34
Flavopiridol (alvocidib)	0.19	0.30	0.003
Seliciclib	0.25	0.25	0.79
S-134 5g	0.23	0.81	0.04
E-29 5b	0.55	N/A	0.05

Table 2.3: Summary of kinase activity¹⁵¹.

2.5 Effect of S-134 on cell cycle

Transcription occurs throughout the cell cycle; during S phase, the rate of RNA transcription and protein synthesis are reduced. An exception is the synthesis of histone, which is essential for the replication of chromosomes during S phase⁵. Since CDK9 functions as a transcription regulator, S-134 is expected to induce cell cycle accumulation at either G1 phase or G2/M transition, where transcription is highly active¹⁷⁷.

To investigate the effect of S-134 on cell cycle, treated cells were stained with propidium iodide (PI). PI is a fluorescent molecule which passes through the cell membrane and intercalates into cellular DNA, which is detectable and quantifiable by Fluorescent-activated cell sorting (FACS) using flow cytometry. Hence, the quantity of PI in a cell represents the amount of DNA and the cell cycle status of a cell can be determined.

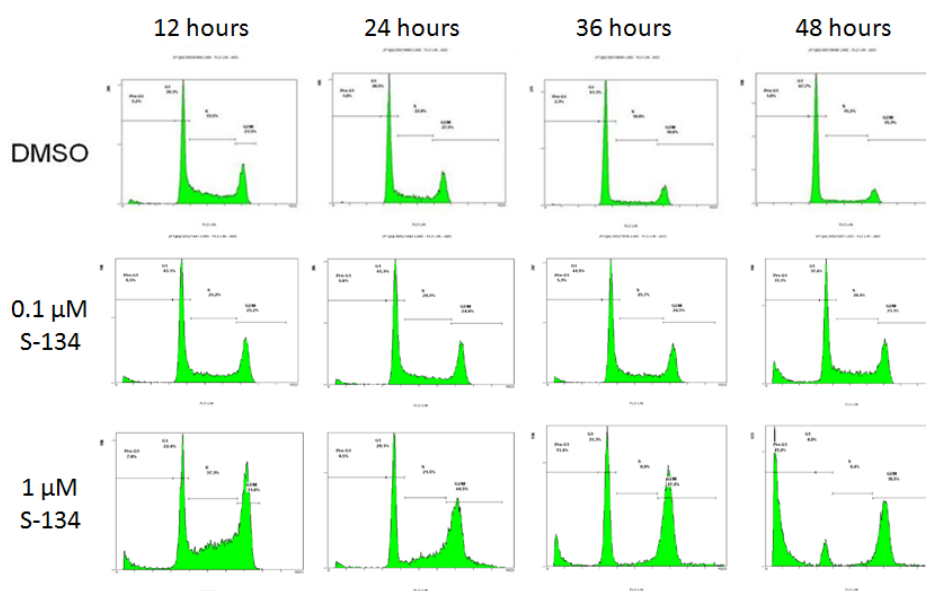


Figure 2.11: Effect of S-134 on the cell cycle of HCT-116 cells. No effect on the cell cycle was observed at the GI_{50} concentration during a 48 hour time period. With the compound concentration increased to ~ 10 times GI_{50} concentration, a G2/M blockage was observed.

2.5. Effect of S-134 on cell cycle

HCT-116 cells were treated with 0.1 or 1 μM S-134; i.e. ~ 1 time and ~ 10 times GI_{50} concentration respectively (Figure 2.11). Samples were harvested at 4 time points: 12, 24, 36 and 48 hours. Without the treatment of agents, the majority of cells are at G1 phase. The treatment of S-134 resulted in a G2/M transition blockage, indicated by the massive increase in G2/M population under 1 μM S-134. To prove that the G2/M cell cycle arrest was caused by CDK9 inhibition, DRB was tested in similar manner to S-134, but at 6 or 60 μM concentration, corresponding to 1 time GI_{50} and 10 times GI_{50} concentrations (Figure 2.12).

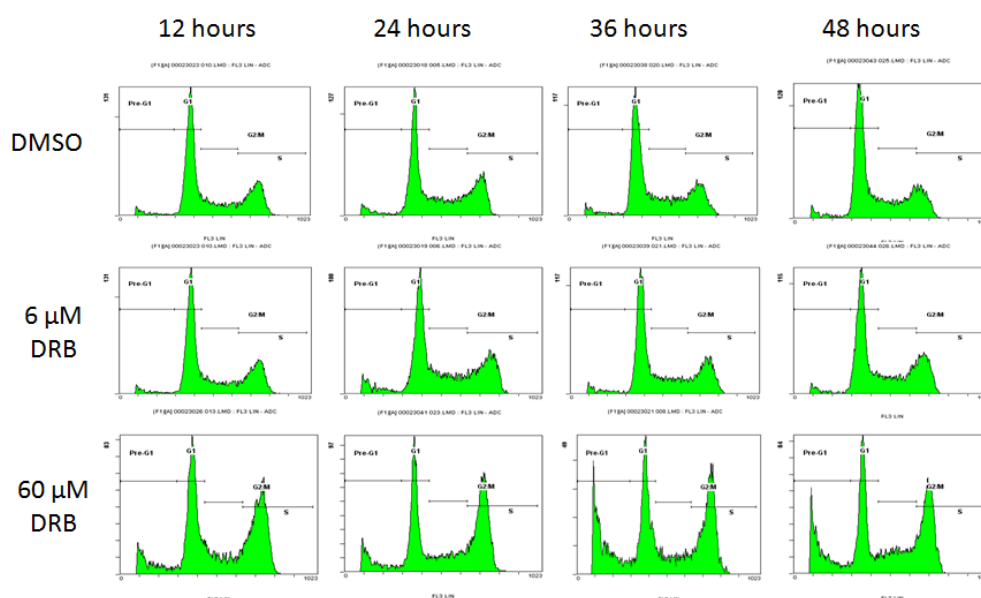


Figure 2.12: Cell cycle effect of DRB on HCT-116 cells. Treating cells with GI_{50} concentration in the 48 hour time period showed DRB has no effect on the cell cycle. A G2/M transition blockage in the cell cycle was observed when the compound concentration increased to ~ 10 times GI_{50} value. The results show that CDK9 inhibitors induced G2/M transition block in the cell cycle of HCT-116 cells, which also proved S-134 affected the cell cycle in the same manner as a CDK9 inhibitor.

The cell cycle data of DRB proved that CDK9 inhibitors induced G2/M cell cycle transition blockage in HCT-116 cells. It also proved that S-134 performed in the same way as a CDK9 inhibitor. To make a definite conclusion that the G2/M cell cycle transition blockage was caused by S-134,

2.5. Effect of S-134 on cell cycle

the experiment was repeated with HCT-116 cells with double thymidine block, which inhibits the synthesis of DNA and causes synchronisation of cells in G1/S phase, before the addition of compound. HCT-116 cells were treated with 1 μ M S-134 or 60 μ M DRB and harvested at 3, 6, 8, 12 and 24 hours (Figure 2.13). The results again showed that S-134 and DRB act in a similar way on the cell cycle of HCT-116 cells. At 6 hours, cells with DMSO vehicle control had moved on to the G2/M transition, while cells with either S-134 or DRB were still in transition from S phase to M phase. This indicated both S-134 and DRB inhibited cell growth at ~ 10 times GI_{50} concentration. At 8 hours, cells in all samples entered the G2/M transition phase. At 12 hours, cells with DMSO control moved back to G1, while cells treated with the compounds had accumulated at the G2/M transition phase of the cell cycle. The cell cycle state of HCT-116 cells at 24 hours was the same as in cells without synchronisation - a G2/M transition block had resulted with the presence of the compounds.

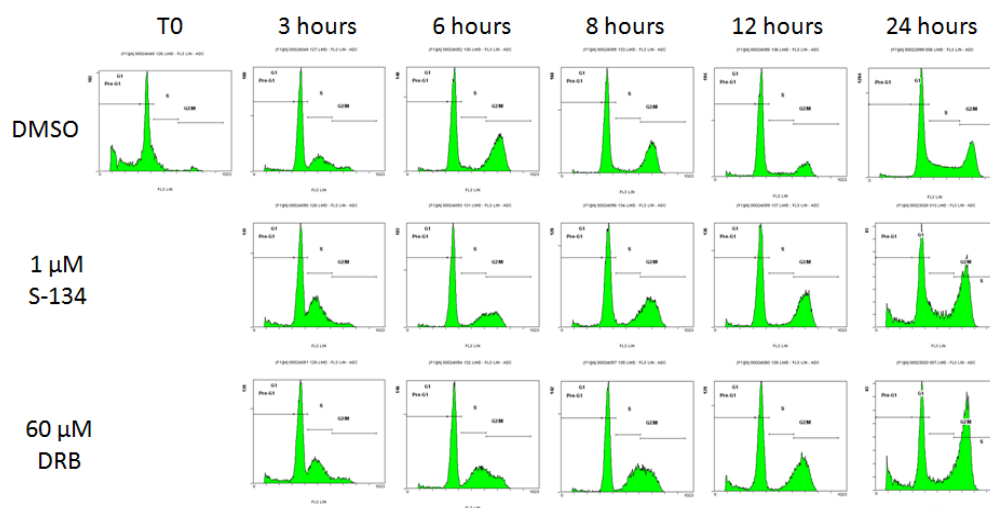


Figure 2.13: Cell cycle effect of S-134 and DRB on the synchronised HCT-116 cells. With 10 times GI_{50} concentration of S-134 or DRB, the cell cycle slowed down in the entry of G2/M transition as seen in 6 hours. G2/M transition blockage was observed from 12 hours onwards with the presences of compounds. Cells without compounds managed to return to G1 phase at 12 hours and continue cell growth.

A simple explanation of this G2/M transition accumulation is that S-134 and DRB may target other proteins such as CDK7/cyclin H, which phosphorylate CDK1 in order to bypass the G2/M checkpoint. 1 μ M S-134 is higher than the IC₅₀ of CDK7/cyclin H inhibition as determined by kinase assays. Alternatively, S-134 inhibits CDK9 only, but cells may manage to complete G1 and S phase without CDK9 dependent transcription; however, the production of proteins without the ‘natural enzyme’ are inaccurate. These proteins could not perform normal function and cells arrest at the G2/M transition checkpoint, resulting in accumulation and cell death. This cell cycle arrest also suggests p53 may be induced by the compounds, which leads to the cell cycle arrest at G2 phase for the repair of DNA (see section 2.9).

2.6 S-134 induces cell death

With the inhibition of CDK9 activity, the transcription of anti-apoptotic proteins such as Mcl-1 and Bcl-2 should be reduced. This increases the sensitivity of cancer cells to the apoptotic signals which leads to programmed cell death. An Annexin-V assay was adopted to observe cell populations undergoing early apoptosis and cell death. HCT-116 cells were treated with 0.5 or 1 μ M S-134 and harvested at 24, 36 and 48 hours (Figure 2.14). Cells were stained with Annexin-V labelled with fluorescein isothiocyanate (FITC) and propidium iodide (PI) then analysed by flow cytometry. Cells undergoing cell death externalise phosphatidylserine (PS) on the cell membrane. FACS detects the PS-mediated binding of Annexin-V-FITC to cells and the cellular concentration of PI. Hence, healthy cells are negative for Annexin-V and PI, while cells undergoing early apoptosis are Annexin-V positive and PI negative.

PI is only able to enter cells through holes on cell membranes. Therefore, late apoptotic or dead cells will have PI inside the cell and Annexin-V expression. The graphs generated by FACS represent concentration of Annexin-V (X axis) and the PI (Y axis).

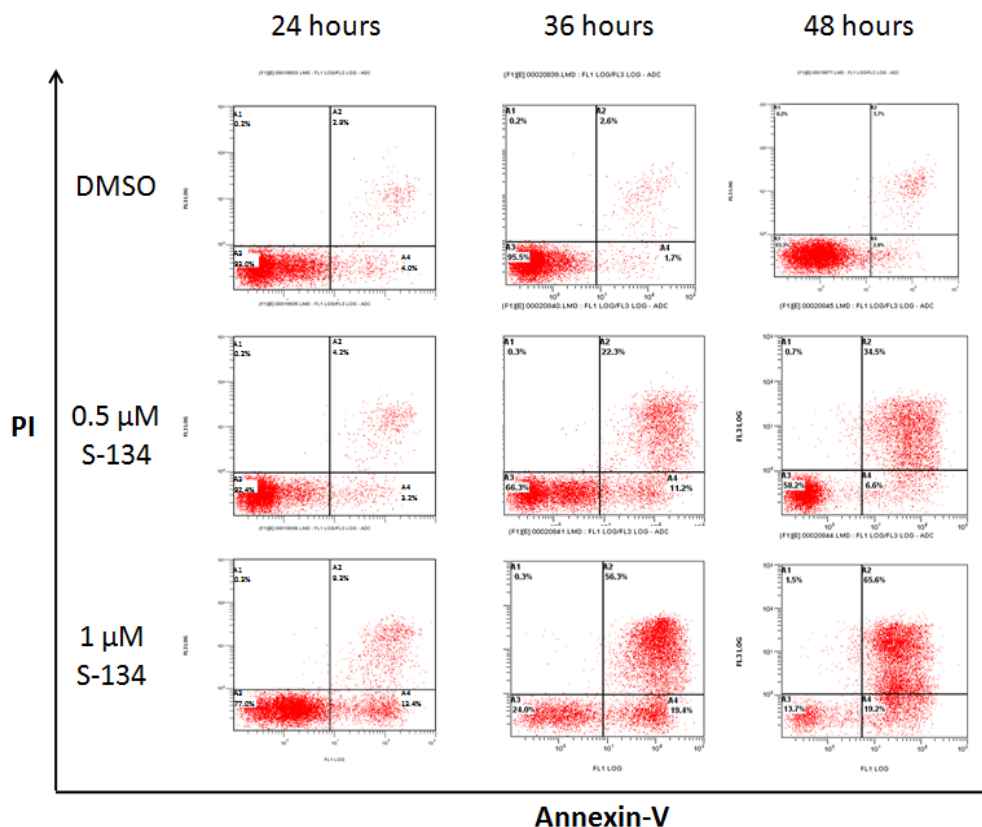


Figure 2.14: Effect of S-134 on the cell death in HCT-116 cells. From the graphs illustrating the presence of PI, induction of early apoptosis is shown at 24 hours with 1 μM S-134. A significant cell death was observed from 36 hours with 1 μM S-134. For percentage readings of graphs, see Table 2.4.

The results of Annexin-V assay with HCT-116 cells indicated that 1 μM S-134 (~10 times GI_{50} concentration) induced early apoptosis by 24 hours. This is indicated by the significant increase of PI in the bottom right quadrant (A4) of the graph indicating PI leaks into cells. From 36 hours, 1 μM S-134 also induced a significant increase in cell population containing PI and expressing Annexin-V, as indicated by the increase of PI in the top right quadrant (A2) of the graph. This indicates cells were in definite cell death. The appearance of

PI in A4 followed by A2 during the time course indicates that cell death was caused by apoptosis.

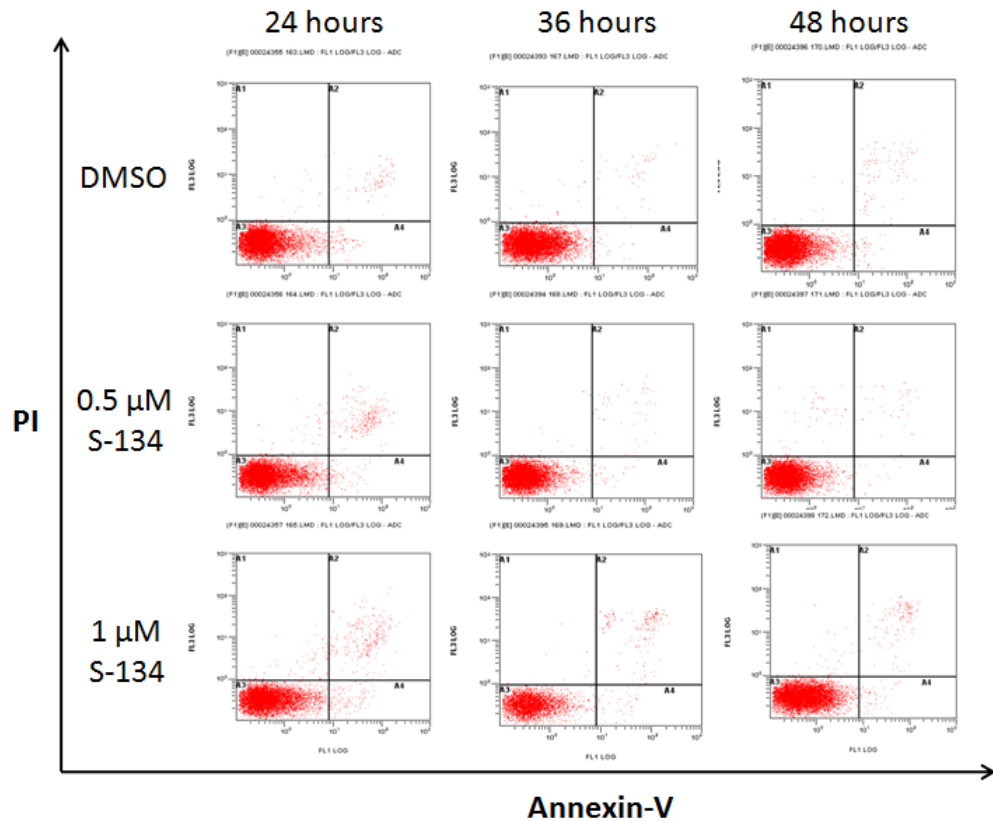


Figure 2.15: Effect of S-134 on the cell death in MRC-5 cells. S-134 showed no sign of causing cell death during the 48 hour time period as the PI was kept in the bottom left quadrant (A3) only, which represented healthy cell population. For percentage readings of graphs, see Table 2.4

To investigate whether S-134 induces apoptosis selectively in cancer cells, Annexin-V assay was performed with MRC-5 fibroblast cells and the result is shown in Figure 2.15. Modest effect on MRC-5 cells was observed by S-134 treatment at the same concentration used with HCT-116 cells.

2.6. S-134 induces cell death

A) HCT-116									
Time point	DMSO			0.5 μ M S-134			1 μ M S-134		
	A2	A3	A4	A2	A3	A4	A2	A3	A4
24 hours	2.9%	93.0%	4.0%	2.6%	95.5%	1.7%	3.7%	93.3%	2.8%
36 hours	4.2%	92.4%	3.2%	22.3%	66.3%	11.2%	34.5%	58.2%	6.6%
48 hours	9.3%	77.0%	13.4%	56.3%	24.0%	19.4%	65.6%	13.7%	19.2%

B) MRC-5									
Time point	DMSO			0.5 μ M S-134			1 μ M S-134		
	A2	A3	A4	A2	A3	A4	A2	A3	A4
24 hours	1.5%	97.5%	0.3%	0.3%	99.4%	0.1%	0.3%	99.4%	0.1%
36 hours	0.5%	98.3%	0.8%	0.5%	98.0%	1.0%	0.0%	99.4%	0.0%
48 hours	1.5%	95.1%	0.6%	1.3%	96.3%	0.2%	1.8%	95.7%	0.9%

Table 2.4: Summary of the percentage readings from Annexin-V assays. Table A) are readings from samples of HCT-116 cells, while table B) are readings from samples of MRC-5 cells. Quadrant A2 represents the population of death cells, while quadrant A3 represents healthy cells population and A4 represents the percentage of cells undergoing apoptosis.

Poly (ADP-ribose) polymerase (PARP), a protein appears to be involved in DNA repair in response to environmental stress, hence maintains cell viability¹⁷⁸. PARP can be cleaved by many caspases *in vivo*, including caspase-3¹⁷⁹. The cleavage of PARP facilitates cellular disassembly and serves as a marker of cells undergoing apoptosis¹⁸⁰. Initially, PARP cleavage was detected with HCT-116 cells; however, there were some difficulties in observing a detectable signal. Therefore, for the interest of other experiments, A2780 cells were used instead. Cells were treated with 0.5, 1, 2.5 or 5 μ M S-134 (~4, ~8, ~20 and ~40 times GI_{50} respectively) for 24 hours. Cells were also treated with 30, 60 or 135 μ M DRB (~5, ~10 and ~22 times GI_{50} concentration respectively, Figure 2.16). Western blots were used to detect the presence of PARP cleavage from the cell lysates.

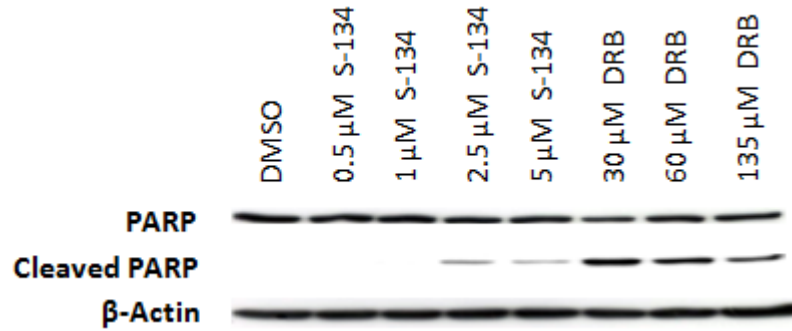


Figure 2.16: Effect of S-134 on PARP cleavage in A2780 cells at 24 hours. PARP cleavage was induced at 24 hours by S-134 from 2.5 μ M. DRB induced PARP cleavage from 30 μ M.

PARP cleavage was observed with S-134 at 2.5 μ M and above. DRB generated cleaved PARP at all concentrations tested. To investigate the selectivity on apoptotic induction by S-134 between cancer cells and normal cells, the experiment was repeated using MRC-5 cells under the same conditions (Figure 2.17). The result showed PARP cleavage was induced by 5 μ M S-134. DRB cleaved PARP at 60 and 135 μ M.

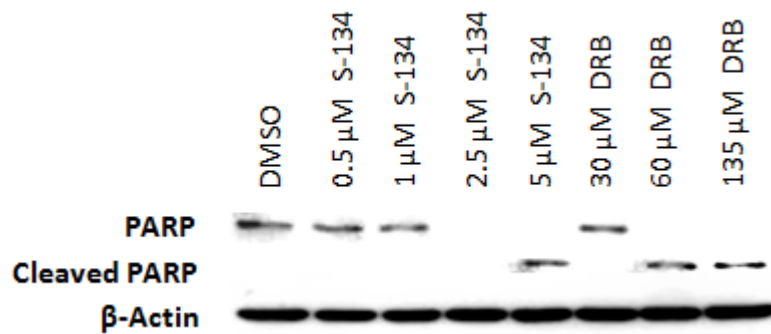


Figure 2.17: Effect of S-134 on PARP cleavage in MRC-5 cells at 24 hours. PARP cleavage was induced at 24 hours by S-134 at 5 μ M only. DRB induced PARP cleavage from 60 μ M.

Apoptosis is caused by the activation of various factors; the major cellular apoptotic pathway is the activation of caspase-3. Other known pathways include the activation of pro-caspase-6 and caspase-7. To investigate which apoptotic pathway is activated by S-134, caspase-3 assay was performed on

HCT-116 cells to detect the activation of caspase-3 and the result is shown in Figure 2.18.

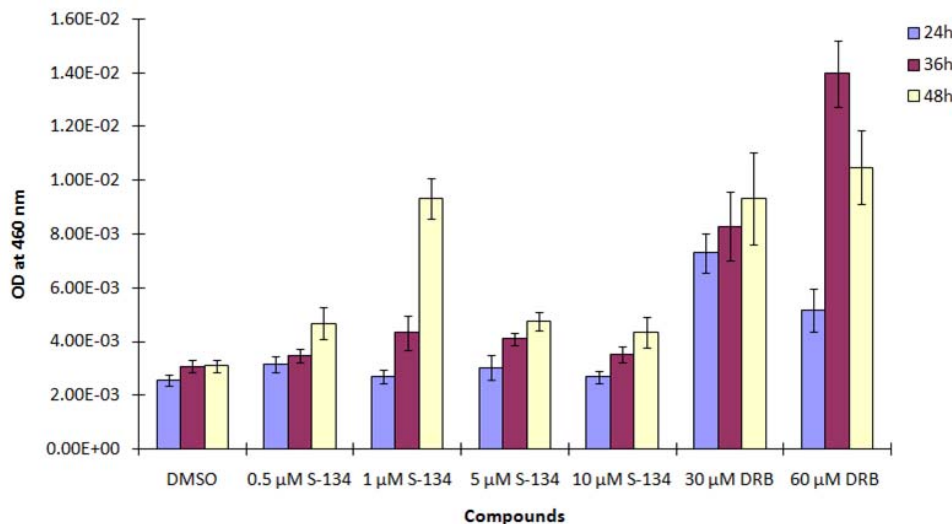


Figure 2.18: S-134 activates caspase-3. There is a sharp rise of caspase-3 activation in HCT-116 cell at 48 hours with 1 μM S-134. The low level of caspase-3 activation at 5 and 10 μM S-134 was possibly due the reduction in cell number caused by the compound, hence the signals were reduced. Alternatively, other apoptotic pathways may be employed by S-134.

This fluorimetric caspase-3 assay indicated a significant increase in activated caspase-3 at 48 hours with 1 μM S-134 in HCT-116 cells. Western blot detection of PARP cleavage indicated significant apoptosis induced at 24 hours with 2.5 μM S-134 and above. Cells treated with 1 μM have shown a rise in caspase-3 activation. As the counting of cell number was not involved before the analysis of samples, the reduction of signal at a higher concentration possibly due to the reduction in cell number caused by S-134 at these time points, which is one of the limitation of this assay. DRB at concentrations of 30 μM and above resulted in significant caspase-3 activation in a time dependent manner.

2.7 Cellular CDK inhibition of S-134

CDK9 regulates transcription elongation by phosphorylating serine 2 (Ser 2) on the C-terminal domain (CTD) of RNA polymerase II (RNAP II). CDK7 phosphorylates serine 5 (Ser 5) during transcription initiation, the phosphorylation of Ser 5 by CDK9 has been observed from HIV-1 related transcription¹⁸¹. A selective CDK9 inhibitor should therefore dominantly suppress the phosphorylation of Ser 2, with lesser effect on Ser 5. Selectivity between CDK7 and CDK9 is difficult to achieve as both kinases have similar amino acid sequences in their kinase domain and operate at the same time. Therefore, most of the known CDK9 inhibitors suppress the phosphorylation of both Ser 2 and Ser 5 at similar level.

To verify whether CDK9 is the primary target of S-134 at the cellular level, Western blot is the only available method which detects against the expression levels of phosphorylated Ser 2 and Ser 5 in the CTD of RNAP II. A2780 ovarian carcinoma cells were treated with 0.5, 1, 2.5 or 5 μ M S-134. 30, 60 or 135 μ M DRB treatments were used as positive control in this experiment. Cells were treated with the compounds for 6 and 24 hours. Cell lysates were subjected to Western blot and antibodies used to detect phosphorylated Ser 2, Ser 5 and total level of RNAP II.

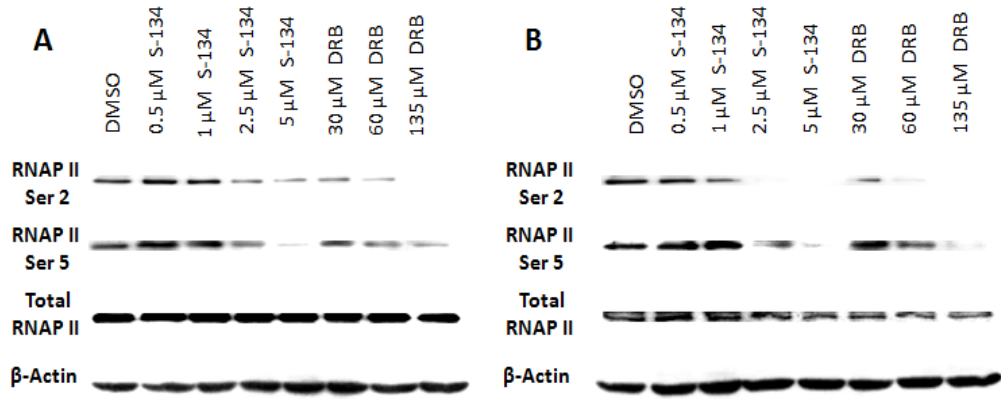


Figure 2.19: Effect of S-134 on RNA polymerase II at 6 and 24 hours in A2780 cells. A) At 6 hours, both S-134 and DRB reduced the phosphorylation of serine 2 (Ser 2) and serine 5 (Ser 5) in a dose dependent manner. S-134 reduced phosphorylation of both Ser from 2.5 μM , while DRB reduced the phosphorylation of Ser 2 at all concentration and Ser 5 from 60 μM . The expression level of RNAP II was not affected by either compound. B) At 24 hours, both compounds reduced the phosphorylation of both Ser dose dependently. S-134 reduced the phosphorylation of Ser 2 and Ser 5 from 1 μM and 2.5 μM respectively. DRB reduces the phosphorylation of both Ser in the same manner as at 6 hours. Again, no effect on the RNAP II expression was found with either compound.

At 6 hours (Figure 2.19), a dose dependent reduction in phosphorylation of Ser 2 by S-134 was observed starting from 2.5 μM . The same effect was observed with DRB from 30 μM . The reduction pattern of Ser 2 induced by both compounds was also observed with the phosphorylation of Ser 5. Comparing the intensity of the bands between Ser 2 and Ser 5, both S-134 and DRB have a more profound effect in inhibiting Ser 2 phosphorylation. This indicated that S-134 and DRB primarily targeted CDK9 rather than CDK7 at 6 hours in A2780 cells. With 5 μM S-134, with the phosphorylation of Ser 5 more significantly suppressed than Ser 2, which indicates 5 μM S-134 may inhibit both CDK7 and CDK9. The effect on CDK7 is more significant could be due to the order of their phosphorylation during transcription. There was no effect on the expression of RNAP II by both compounds.

For the 24 hour time point, a dose dependent reduction in phosphorylation of Ser 2 by S-134 started from 1 μM treatment, with the Ser 2 phosphorylation

completely suppressed with 2.5 and 5 μM S-134. 30 μM DRB reduced phosphorylation of Ser 2 with a complete suppression with 60 and 135 μM . Reduction in phosphorylation of Ser 5 was observed with S-134, starting from a concentration of 2.5 μM with 5 μM completely suppressing phosphorylation. 60 μM DRB reduced Ser 5 phosphorylation with a complete suppression observed at 135 μM . Similar to the observation at 6 hours, both S-134 and DRB have a major effect in suppressing phosphorylation of Ser 2 over Ser 5. No effect on the expression of RNAP II was induced by the compounds.

From these observations, S-134 inhibits CDK9 followed by CDK7 in transformed cellular environment. To investigate whether the selectivity for cell death induction between cancer cells and normal cells observed earlier were due to the effect of compounds on CDKs, hence phosphorylation of RNAP II, the above Western blot experiments were repeated with MRC-5 cells.

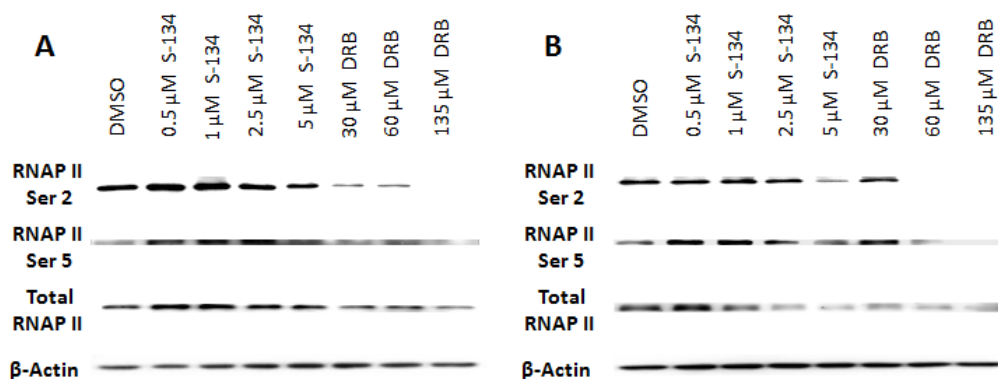


Figure 2.20: Effect of S-134 on RNA polymerase II at 6 and 24 hours in MRC-5 cells. A) At 6 hours, S-134 reduced the phosphorylation of both Ser at 5 μM treatment, while DRB reduced phosphorylation of both Ser at all concentrations. S-134 induced no effect on the expression level of RNAP II, but DRB suppressed RNAP II. B) At 24 hours, 5 μM S-134 reduced the phosphorylation of both Ser, as observed at 6 hours. DRB inhibited phosphorylation of Ser 2 and reduced phosphorylation of Ser 5 from 60 μM treatment. Both compounds showed a more profound effect on the phosphorylation of Ser 2 over Ser 5. In addition, both affected the expression levels of RNAP II, with S-134 reducing the expression from 2.5 μM treatment and DRB across all concentrations.

At the 6 hour time point (Figure 2.20), reduction in the phosphorylation of both Ser by S-134 was observed with 5 μ M treatment. DRB suppressed Ser 2 phosphorylation at all concentrations tested. Phosphorylation of Ser 5 was observed with 5 μ M S-134. In DRB treated samples, a dose dependent reduction of phosphorylated Ser 5 started from 30 μ M. S-134 was observed to have no effect on the expression of RNAP II, but DRB suppressed the expression of RNAP II. This indicates that the reduction of RNAP II phosphorylation by DRB could be due to its effect on the expression level of RNAP II in MRC-5 cells, rather than inhibiting the activity of CDKs.

At the 24 hour time point, phosphorylation of Ser 2 was reduced by S-134 with 5 μ M treatment and with 60 and 135 μ M DRB. For Ser 5, phosphorylation was reduced by 5 μ M S-134. DRB reduced Ser 5 phosphorylation with 60 μ M treatment, a complete suppression observed with 135 μ M. Similar to the observation at 6 hours, both S-134 and DRB affected Ser 2 more severely than Ser 5. This once again indicates that S-134 and DRB primarily target CDK9. However, in MRC-5 cells, both compounds affected the expression of RNAP II at 24 hours. S-134 reduced RNAP II expression at 2.5 μ M, with DRB affecting RNAP II expression at all concentrations tested. This indicates that not only DRB affects the expression of RNAP II, S-134, in a lesser extent, if also affects the expression level of RNAP II which may lead to the reduction in phosphorylation, rather than CDKs in MRC-5 cells.

The reduced phosphorylation of Ser 2 was corresponding to the induction of PARP cleavage in both cell lines. Hence, apoptosis of cells could be due to the inhibition of CDK9.

2.8 S-134 targets anti-apoptotic proteins

Anti-apoptotic proteins inhibit apoptosis through their interactions with cellular components, such as the interaction between Bcl-2 and mitochondria (see section 1.3.3), or by inhibiting the function of proteins that induce apoptosis through direct binding, such as the relationship between Mcl-1 and Bax (see section 1.3.4). The expression of several anti-apoptotic proteins, including Mcl-1, Bcl-2 and XIAP, were found to be regulated by CDK9¹⁰⁶. Since S-134 is a CDK9 inhibitor, the cellular expression of these anti-apoptotic proteins is expected to be reduced with the treatment of S-134.

To prove this hypothesis, Western blots were used to examine the expression levels of these anti-apoptotic proteins. A2780 cells were treated with S-134, using DRB as positive control, at the same concentrations used in previous experiments (see section 2.7 for details). Samples were harvested at 6 and 24 hours. Cell lysates were detected with antibodies against Mcl-1, Bcl-2 and XIAP.

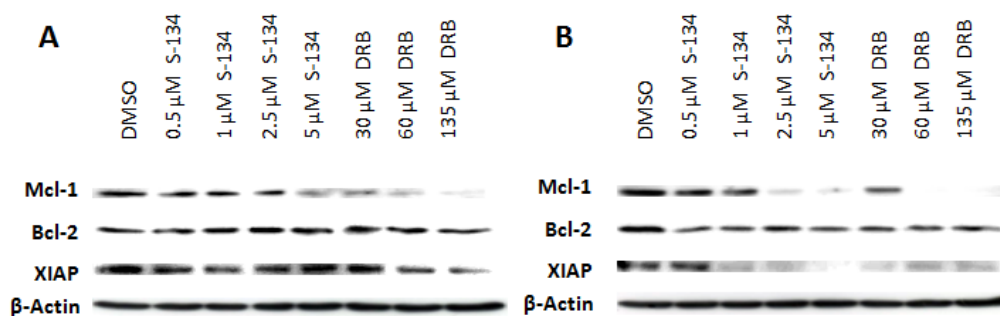


Figure 2.21: Effect of S-134 on the expression of anti-apoptotic proteins at 6 and 24 hours in A2780 cells. A) At 6 hours, S-134 reduced the expression of Mcl-1 at 5 μM with DRB affecting the expression of Mcl-1 at all concentrations tested in a dose dependent manner. No effect on Bcl-2 was observed with compounds. A reduction in XIAP was detected only from 60 μM DRB. B) At 24 hours, S-134 reduced the expression of Mcl-1 protein in a dose dependent manner from the concentration of 1 μM. In comparison to the DMSO control, the expression of Bcl-2 was reduced by both compounds. S-134 reduced the expression of XIAP from 1 μM with DRB reducing XIAP expression at all concentration. The half life of Mcl-1 is much short that that of Bcl-2, 1-2 hours and 18 hours, respectively. Therefore, the effect of S-134 on Bcl-2 was not as profound as Mcl-1 at both time points.

2.8. S-134 targets anti-apoptotic proteins

At 6 hours (Figure 2.21), the expression of Mcl-1 protein was suppressed with 5 μ M S-134 while DRB reduced Mcl-1 expression at all tested concentrations in a dose dependent manner. The reduction of Mcl-1 by both compounds corresponds to the reduction pattern of Ser 2 phosphorylation (see section 2.7), hence the activity of CDK9. S-134 had no effect on the protein expression of Bcl-2 and XIAP. Although DRB also has no effect on Bcl-2, a reduction of XIAP by DRB started from 60 μ M.

At the 24 hour time point, the expression of Mcl-1 was reduced by both S-134 and DRB. S-134 showed a dose dependent reduction on the expression of Mcl-1 from 1 μ M with a complete suppression observed at 5 μ M. DRB reduced Mcl-1 expression dose dependently with a total suppression from 60 μ M. A low level of reduction in the expression of Bcl-2 by both compounds was observed at all concentrations compared to the DMSO vehicle control. The expression of XIAP was reduced dose dependently at 24 hours from 1 μ M S-134 with a total suppression observed at 5 μ M. DRB also reduced the expression of XIAP at this time point. Considering this data together with the observation on the effect of compounds on RNAP II phosphorylation; the inhibition of CDK9 by S-134 could lead to the reduction of Mcl-1, followed by Bcl-2 and finally XIAP.

To verify the effect of S-134 in normal cells as before, Western blot experiments were repeated in MRC-5 cells. However, the expression of XIAP could not be detected in MRC-5 cells. Although the same total protein concentration was used as with A2780 cells, the expression signals of Mcl-1 and Bcl-2 detected were much weaker than those from A2780 cells. The weak Mcl-1 and Bcl-2 and absence of XIAP signals may be explained by the non-

essential expression of anti-apoptotic proteins in maintaining the survival of normal cells.

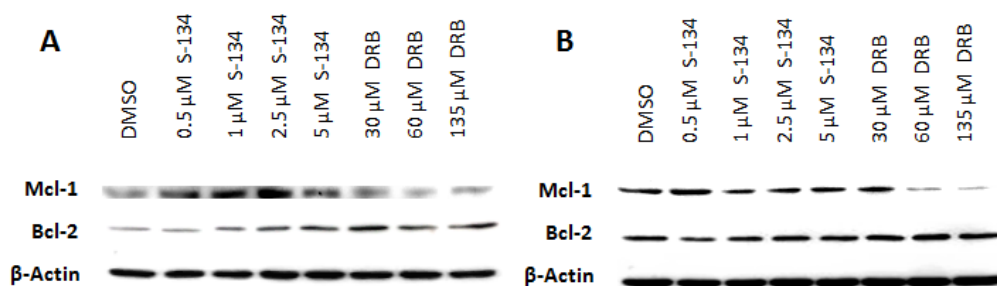


Figure 2.22: Effect of S-134 on the expression of anti-apoptotic proteins at 6 and 24 hours in MRC-5 cells. A) No change in the protein expression levels of Mcl-1 and Bcl-2 was induced by compounds at 6 hours. B) Except that the expression of Mcl-1 was suppressed by DRB starting from 60 μM, there was no alteration on the protein expression of Mcl-1 and Bcl-2 by the inhibitors at 24 hours.

Reduced phosphorylation of RNAP II Ser 2 in MRC-5 cells with 5 μM S-134 and 60 μM DRB was observed at 6 hours (see section 2.7). However, no change in the expression levels of Mcl-1 or Bcl-2 proteins was induced by the compounds at this time point (Figure 2.22). At 24 hours, no change in expression of Mcl-1 and Bcl-2 was induced by S-134. The protein expression of Mcl-1 was reduced starting from 60 μM DRB, with the expression of Bcl-2 not affected.

2.9 S-134 induces p53 protein

Anti-apoptotic proteins reduce the sensitivity of cancer cells to apoptotic signals. The loss of anti-apoptotic protein expression would initially allow the expression of tumour suppressor proteins to be re-induced, leading to cancer cell death. One of the best known tumour suppressors is p53, which has a key role in the cellular response to DNA damages and other genomic alteration at a cellular level⁸⁹. It is important to investigate whether S-134 stabilises p53 (i.e.

increases the presence of p53 proteins) and induces p53 activation in cancer cells.

To investigate the effect of S-134 on p53 at the protein level, Western blot was carried out on A2780 cells, a cell line expressing wild-type p53. Cells were treated with S-134 and the positive control, DRB, at the same conditions as in previous experiments (see section 2.7). Samples at 6 and 24 hours were detected with antibodies against p53 and HDM-2.

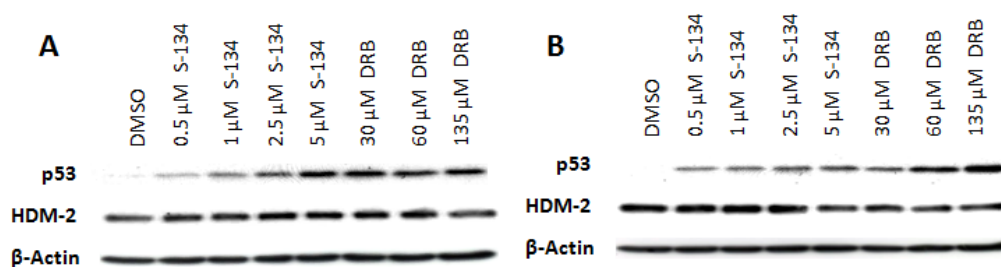


Figure 2.23: Effect of S-134 on the protein expression of p53 and HDM-2 at 6 and 24 hours in A2780 cells. A) S-134 and DRB caused a dose dependent increase in the protein expression level of p53 at 6 hours. The level of HDM-2 protein also increased with the exception of 135 μM DRB. This indicates that the compounds induced the stabilisation of p53. B) Both compound caused an increase in p53 protein again in a dose dependent manner at 24 hours. Compared to the DMSO control, the protein level of HDM-2 had no change until 5 μM S-134 which reduced the protein expression. The expression of HDM-2 reduced at all concentrations of DRB tested

The results showed the level of p53 protein increased dose dependently by the inhibitors at 6 hours (Figure 2.23). However, the level of HDM-2 increased as a negative feedback of p53. We observed a suppression of HDM-2 expression only with 135 μM DRB. Hence S-134 and DRB only stabilised p53 at 6 hours. At 24 hours, the level of p53 protein was increased dose dependently by the inhibitors. The expression of HDM-2 remained constant with the DMSO vehicle control and a reduction was observed with 5 μM S-134. DRB reduced the expression of HDM-2 at all concentrations. The results indicate that the negative feedback loop of p53 was suppressed. Hence, the p53 expressed at this time point should be functionally active. As in previous

experiments, the effect of compounds on p53 and HDM-2 in normal fibroblast cells were investigated.

Western blot experiments were repeated with MRC-5 cells under the same conditions as with A2780 cells. At 6 hours, the expression level of p53 remained constant in all samples (Figure 2.24). Compared to the DMSO vehicle control, an increase in the expression of HDM-2 was observed with 0.5 and 1 μ M S-134 with a reduction in the expression of HDM-2 observed with 5 μ M S-134 and 135 μ M DRB. In all other samples, the expression level of HDM-2 was the same as in the DMSO control.

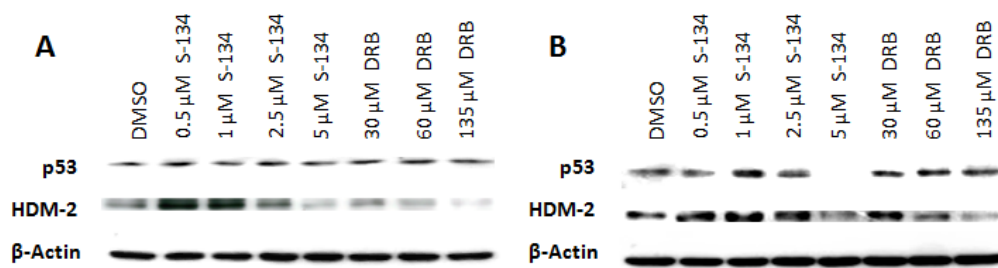


Figure 2.24: Effect of S-134 on p53 and HDM-2 proteins at 6 and 24 hours in MRC-5 cells. A) At 6 hours, S-134 and DRB have no effect on the protein level of p53. Compared to DMSO vehicle control, the level of HDM-2 protein increased with 0.5 and 1 μ M S-134. There was no change in the expression level of HDM-2 with 2.5 μ M S-134 as well as 30 and 60 μ M DRB. A reduction in the HDM-2 protein was observed with 5 μ M S-134 and 135 μ M DRB. B) Except the observation of a complete suppression of p53 with 5 μ M S-134, both inhibitors have no effect on p53 at 24 hours. The level of HDM-2 protein reduced with 5 μ M S-134 and dose dependently from 60 μ M DRB.

The observation in the expression level of HDM-2 in MRC-5 cells was similar to that in A2780 cells at 6 hours. However, both inhibitors have no effect on p53. Since normal cells should have relatively less genomic alteration compared to cancer cells, the results may indicate that MRC-5 cells do not require p53 proteins in its growing environment (i.e. p53 surveillance).

At the 24 hour time point, the expression of p53 was suppressed by 5 μ M S-134. Compared to DMSO control, no other changes was detected with other

samples (Figure 2.24). The effect of the inhibitors on HDM-2 was similar to that in A2780 cells. The expression of HDM-2 protein had no change with a reduction observed with 5 μM S-134 and a dose dependent reduction was observed with 60 and 135 μM DRB.

The reduction of p53 by S-134 at 24 hours reveals that p53 has no role in the apoptosis detected by PARP cleavage in MRC-5 cells (see section 2.6). Instead, this observation may indicate that S-134 generates p53 independent toxicity to normal cells at higher concentrations.

Since it is clear that S-134 induced the stabilisation of p53 and possibly activation at later time points with high concentration in cancer cells, the next stage was to compare the effect of S-134 on p53 stabilisation to other novel analogues in our CDK9 inhibitor series. A Cellomic Array Scan was carried out to estimate the expression level of p53 proteins by observing the percentage of cells in a population having positive stain in cell nucleus with p53 antibodies. HCT-116 cells were treated with a serial dilution of compounds for 8 hours (Figure 2.25).

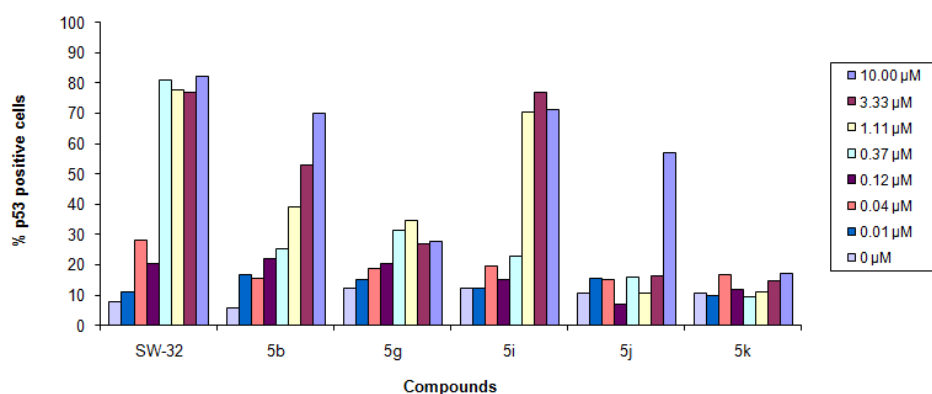


Figure 2.25: Cellomic Array Scan detecting the stabilisation of p53 protein expression in HCT-116 cells. The lead compounds SW-32 and E-29 **5b** induced >40% cells with p53 positive stains at the concentration of 0.37 and 1.11 μM , respectively. S-134 **5g** stabilised p53 at 0.37 μM , but the effect was not as profound as the other analogues, such as **5i** and **5j** at higher concentrations.

The effect of S-134 **5g** in stabilising p53 was clearly not as effective as the lead compound, SW-32. S-134 induced a higher percentage of p53 positive cells at low concentration, with other analogues (**5i** and **5j**) inducing better effect at higher concentration, which is likely due to their potency in cells (Table 2.1).

2.10 Effect of S-134 on gene transcription

Since CDK9 operates at transcription elongation, the inhibition of CDK9 by S-134 should suppress the synthesis of messenger RNA (mRNA) from genes regulated by CDK9. These genes include anti-apoptotic factors *Mcl-1*, *Bcl-2* and *XIAP*. To prove this hypothesis, reverse transcription polymerase chain reaction (RT-PCR) was carried out by extracting RNA from cells treated with compounds and synthesising complementary DNA (cDNA) through reverse transcription. The cDNA were amplified by normal PCR with primers designed for amplifying specific genes of interest; changes in the intensity of the desired cDNA between samples were observed using electrophoresis. Since the effect of compounds in the mRNA is our interest, the primers were designed based on the available mRNA sequences of the target genes in human. These primers amplify a 125 bp region on the gene between the end of exon 1 and the beginning of exon 2; this should solely amplify the mature mRNA rather than pre-mature RNA in nucleus.

A2780 cells were used in this experiment and treated with S-134 or DRB at the concentrations used in previous experiments (see section 2.7). Cells were

2.10. Effect of S-134 on gene transcription

harvested at 6 and 24 hours. RNA was extracted from cells for appropriate PCR amplification.

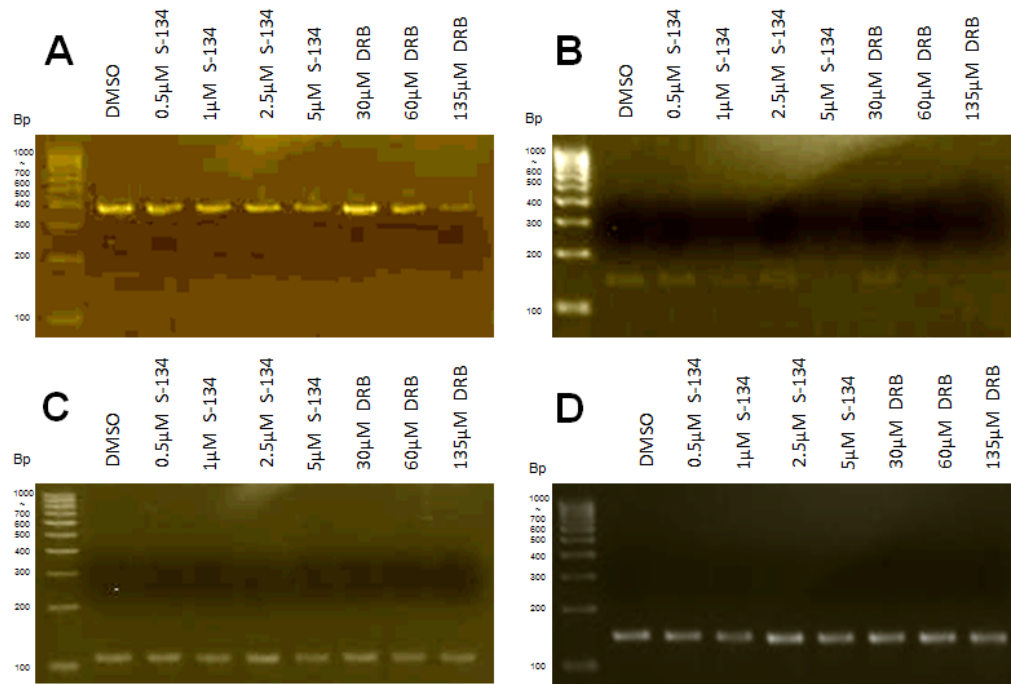


Figure 2.26: Effect of S-134 on the transcription of anti-apoptotic genes at 6 hours in A2780 cells. A) The amount of cDNA of *Mcl-1* was reduced with 5 μM S-134 and 135 μM DRB. B) The amount cDNA of *Bcl-2* was reduced dose dependently from 1 μM S-134 and 60 μM DRB. C) The level of cDNA of *XIAP* remained constant with the addition of compounds. D) The mRNA level of *β -Actin* was constant across all samples.

The changes in the mRNA level of *Mcl-1*, *Bcl-2* and *XIAP* were investigated (Figure 2.26). In A2780 cells, the cDNA of *Mcl-1*, synthesised by RT-PCR from the mRNA, was reduced by 5 μM S-134 and 135 μM DRB. Although the PCR products are approximately 380 bp, it should only represent our target mature mRNA fragment (i.e. exon). Since the length of intron 1 in the mRNA of *Mcl-1* is 350 bp, if intron 1 was included in the PCR product, the total size of the PCR fragment should be between 450 to 500 bp. For the transcription of *Bcl-2*, a significant dose dependent reduction was observed from 1 μM S-134 and 60 μM DRB. No alteration in the mRNA level of *XIAP* was induced by the compounds.

2.10. Effect of S-134 on gene transcription

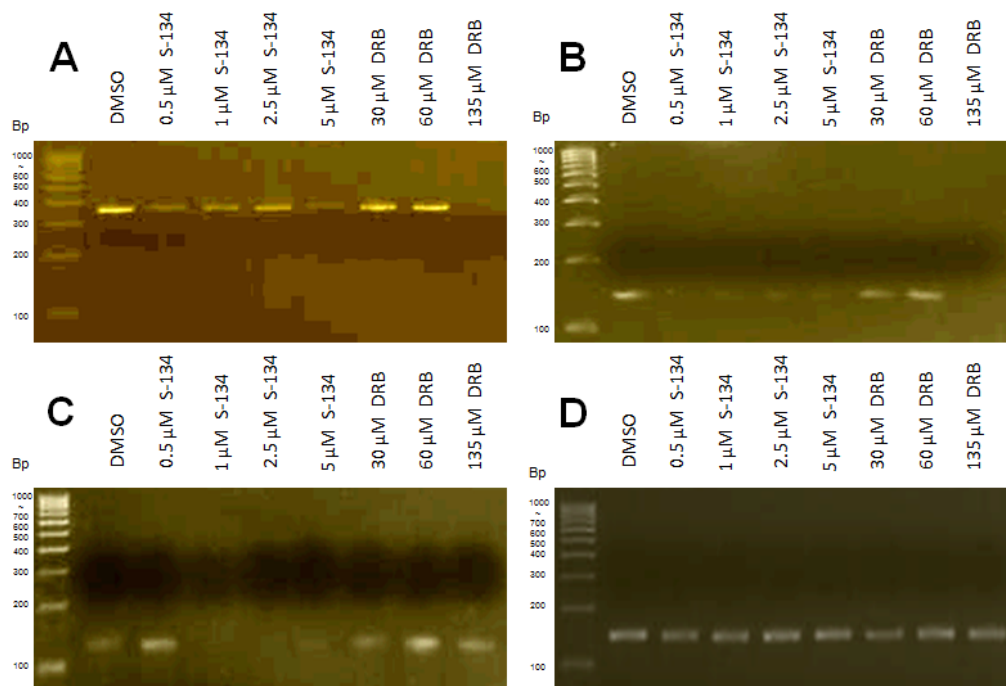


Figure 2.27: Effect of S-134 on the transcription of anti-apoptotic genes at 24 hours in A2780 cells. A) A reduction in the amount of cDNA of *Mcl-1* was observed with S-134 at all concentrations and with 135 μM DRB. B) The amount cDNA of *Bcl-2* was significantly suppressed by S-134 from 0.5 μM and 135 μM DRB. C) For *XIAP*, the cDNA was reduced from 1 μM S-134, which was also observed with DRB. D) The mRNA level of β -*Actin* was constant across all samples.

At 24 hours (Figure 2.27), the RT-PCR has indicated an alteration in the mRNA level of *Mcl-1*, induced with S-134 at all concentrations. A complete suppression of the transcription of *Mcl-1* was caused by 135 μM DRB. S-134 inhibited the transcription of *Bcl-2* completely from 0.5 μM . DRB also affected the transcription of *Bcl-2*, a complete suppression was observed with 135 μM . The transcription of *XIAP* was affected by S-134 with a total transcription inhibition from 1 μM . A reduction in the amount of mRNA for *XIAP* was induced by DRB. The results of RT-PCR at 24 hours matched the observation with the Western blot, hence the observation in mRNA links to the changes in protein expression. The effect of compounds on mRNAs was more profound than on proteins as CDK9 operates at transcription. This RT-PCR

2.10. Effect of S-134 on gene transcription

data also explains the reduction of anti-apoptotic proteins, caused by the suppression of their transcription by inhibiting CDK9.

The effects of compounds on the expression of p53 and HDM-2 proteins were investigated in the previous section (see section 2.9). As a negative feedback, the expression of HDM-2 protein increased at 6 hours and reduced at 24 hours with high concentration of S-134. The effect of S-134 on the transcription of *HDM-2* was investigated here and compared with the results from Western blot (Figure 2.28).

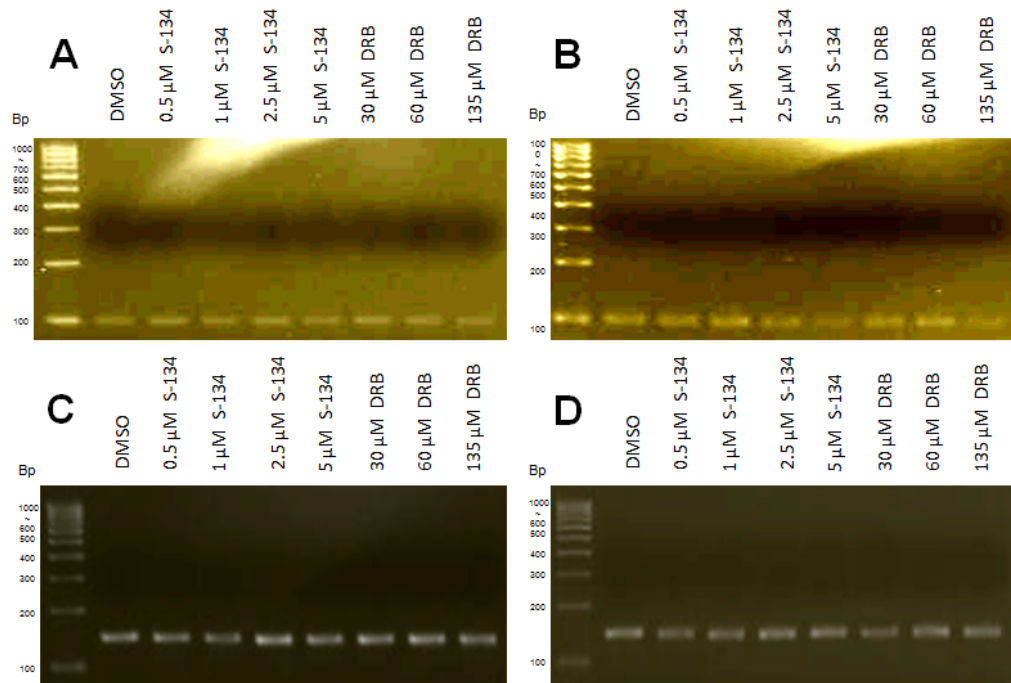


Figure 2.28: Effect of S-134 on the transcription of *HDM-2* in A2780 cells. A) At 6 hours, the transcription of *HDM-2* remained unchanged. B) A dose dependent reduction on the transcription of *HDM-2* by S-134 was detected from 2.5 μM at 24 hours. DRB reduced *HDM-2* transcription with 135 μM . The mRNA level of $\beta\text{-Actin}$ was constant in all samples during C) 6 hours and D) 24 hours.

According to the RT-PCR data, both inhibitors have no effect on the mRNA of *HDM-2* at 6 hours. At 24 hours, a dose dependent reduction in the transcription of *HDM-2* was detected with 2.5 and 5 μM S-134. DRB (135 μM) also affected the transcription of *HDM-2*. The effect of DRB on transcription and protein expression are similar. S-134 showed a more

2.10. Effect of S-134 on gene transcription

profound effect on mRNA than the protein of HDM-2. In other words, S-134 suppresses the negative feedback loop of p53 activation by inhibiting the transcription of *HDM-2* which leads to the reduction in protein expression.

To compare the effect of S-134 on the transcription between the genes, the intensity of the cDNA bands from each set of genes were quantified, which represents the trends in the changes of mRNA levels (Figure 2.29). By comparing the gradient of the trend lines, S-134 is most effective in suppressing the transcription of *Mcl-1*, followed by *Bcl-2* and *XIAP*. This quantification further confirms that S-134 affects *Mcl-1* and *Bcl-2* at both time points with *XIAP* and *HDM-2* being affected at 24 hours only.

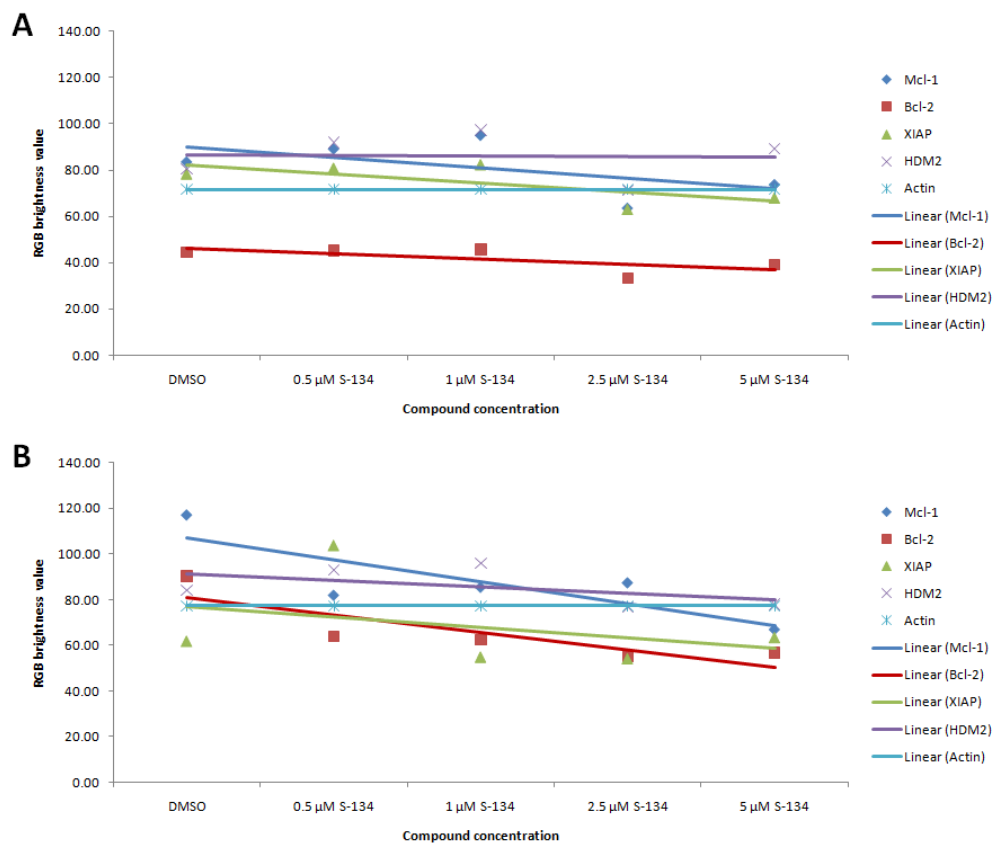


Figure 2.29: Quantification of the intensities of cDNA with the presence of S-134 at A) 6 and B) 24 hours. The calculated trends assume S-134 induced a linear dose dependent effect on transcription.

2.11 Conclusion

To a certain extent, cancer cells should be sensitive to apoptotic signals due to their genomic abnormalities. However, anti-apoptotic genes are constantly transcribed and translated into anti-apoptotic proteins which provide cancer cells with resistance to apoptotic signals and cell death. Anti-cancer drugs which target transcription should inhibit the expression of anti-apoptotic proteins and re-induce the expression of tumour suppressors, forcing cancer cells to undergo cell death. For this reason, CDK9, a kinase which regulates transcription elongation, is an effective anti-cancer drug target.

A series of novel inhibitors which were designed to suppress the activity of CDK9 were synthesised and growth inhibitory properties tested. To generate SAR data, the compounds were screened against two tumour cell lines, HCT-116 and MCF-7. Compounds were tested also against the fibroblast cell line MRC-5 to estimate compound selectivity between tumour and normal cells. The majority of these novel inhibitors showed high potency in and selectivity for cancer cells. S-134 provided ~10 fold selectivity between HCT-116 and MRC-5 cells and was selected for further *in vitro* mechanism studies. S-134 was screened against 13 human cell lines using the MTT assay; this compound was particularly potent against HCT-116 colon and A2780 ovarian carcinomas cells.

S-134 was tested in kinase assays for activity against CDK9/cyclin T1, CDK2/cyclin E and CDK7/cyclin H, with the IC₅₀ of 0.04 µM, 0.23 µM and 0.801 µM, respectively. The result indicated that S-134 was not only effective in inhibiting the activity of CDK9, it was also selective against CDK2, the closest homologue protein to CDK9, and against CDK7, a kinase which

functions in the regulation of transcription as with CDK9. The selectivity between these three CDKs as demonstrated by S-134 was wider than other CDK9 inhibitors in clinical trials, such as Seliciclib and Flavopiridol.

Although CDK9 was not directly involved in the cell cycle, S-134 induced a G2/M transition arrest in the cell cycle of HCT-116 cells. This cell cycle arrest was also observed with DRB, another CDK9 inhibitor. The cell cycle arrest could be due to the fact that cells cannot synthesis some key proteins required for G2 phase in the absence of CDK9, leading to the inability of the cells to bypass the cell cycle checkpoint that regulates mitotic entry. In addition, CDK7 functions during the G2/M cell cycle transition and the concentration of S-134 resulted in this cell cycle arrest exceed the IC_{50} of CDK7/cyclin H inhibition in kinase assay, therefore the compounds could inhibit CDK2 at higher concentrations resulting in the observed cell cycle arrest.

The Annexin-V assay shows that apoptosis in HCT-116 cells was induced by 1 μ M S-134 at 24 hours with a peak level observed at 36 hours. MRC-5 cells were treated with S-134 under the same condition as with HCT-116 cells; there was no apoptosis detected by the Annexin-V assay. From the Western blots, PARP cleavage was observed in A2780 and MRC-5 cells at 2.5 and 5 μ M S-134, respectively at 24 hours. The Annexin-V assays and Western blots show a therapeutic window can be obtained with S-134, which induced cell death in cancer, but not normal cells.

The effect of S-134 on the phosphorylation of RNA polymerase II (RNAP II) was observed by Western blots. CDK9 and CDK7 phosphorylated Ser 2 and Ser 5 on the C-terminal domain (CTD) of RNAP II, respectively. In A2780 cells, low concentrations of S-134 reduced the phosphorylation of Ser

2, but not Ser 5, at 6 hours. With higher concentrations of S-134, the phosphorylation of Ser 2 was suppressed profoundly at 24 hours by the inhibitor, compared to the phosphorylation of Ser 5. These observations indicate that S-134 primarily inhibits the activity of CDK9 followed by CDK7.

Transcriptional CDKs regulate the level of anti-apoptotic proteins including Mcl-1, Bcl-2 and XIAP. Western blot was carried out to examine the expression levels of these anti-apoptotic proteins in cells treated with S-134. In A2780 cells, the expression of Mcl-1 was reduced under the same conditions as the inhibition of RNAP II Ser 2 phosphorylation. The expression of Bcl-2 and XIAP were reduced at 24 hours only. In MRC-5 cells, S-134 affected the expression of the three anti-apoptotic proteins at 24 hours only; reduction of Mcl-1 and XIAP were observed with high concentration of the inhibitor (5 μ M).

p53 protein was stabilised by S-134 at all concentrations and time points tested in Western blot with A2780 cells, but not in the fibroblast cells. The expression of HDM-2 protein is reduced at 24 hours with 2.5 and 5 μ M S-134, which is the condition for a definitely active p53. This activated p53 corresponds to the induction of PARP cleavage detected in Western blot which indicates apoptosis. HCT-116 cells were used to compare the effect of S-134 and other novel analogues within the series of inhibitors in stabilising p53 using a Cellomic Array Scan. In this assay, S-134 only showed a moderate effect in stabilising p53 compared to other analogues.

The effect of S-134 on the transcription of *Mcl-1*, *Bcl-2* and *XIAP* in A2780 cells was examined using reverse transcription PCR. The transcription of *Mcl-1* was most profoundly suppressed by S-134, followed by the transcription of

Bcl-2 and *XIAP*. The transcription of *HDM-2* was suppressed at 24 hours with high doses of S-134, which corresponds to the observation in Western blot.

Combining all the data, S-134 has been demonstrated to be a promising, potent and selective CDK9 inhibitor. A therapeutic window has been indicated for the treatment of cancers.

Chapter Three

Mechanism of action of a novel natural product derivative

3.1 Introduction

Natural products have a key role in drug discovery; a large number of current drugs are natural products or inspired by nature. In the last few decades, a more dominant role for synthetic compounds in anti-cancer drug discovery has emerged. However, since natural products have been found to have cancer prevention properties during the last decade, the investigation of natural products which possess anti-cancer activity has once again become a favoured topic.

3.1.1 Erianin

Erianin **6a** is isolated from the extract of *Dendrobium chrysotoxum*, a plant species found in Southeast Asia¹⁸². Erianin (Figure 3.1) shows high cellular potency in a range of 0.013 to 0.082 μM . Literature data has shown that Erianin suppresses the growth of Bel7402 human hepatoma and A375 melanoma xenografts, inducing observable vascular shutdown within 4 hours

of administering 100 mg/kg of the compound. Erianin also demonstrated potent anti-angiogenic activities *in vitro*; it reversed spontaneous or basic fibroblast growth factor (FGF) induced neovascularisation in chick embryo. The molecule suppressed proliferation of human umbilical vein endothelial cells (HUVECs) with an EC_{50} of $0.034 \pm 0.0013 \mu\text{M}$, which interrupted the formation of endothelial tubules and abolished both migration across collagen and adhesion to fibronectin. In addition, Erianin showed selectivity between endothelial cells; quiescent endothelium being less sensitive to Erianin when compared with proliferative endothelium and transformed endothelial cells. From cytoskeletal studies using fluorescent microscopes with HUVECs, both F-actin and β -tubulin were depolymerised by Erianin; the effect of the compound was more profound in proliferating than in confluent HUVECs¹⁸².

Erianin induced tumour cell death, growth suppression and significant vascular shutdown in tumour xenografts; angiogenesis was inhibited *in vivo* and *in vitro* and disorganisation of endothelial cytoskeletal was found to occur. These observations indicate that Erianin has therapeutic potential against cancer by inhibiting growth and angiogenesis of tumour tissues¹⁸².

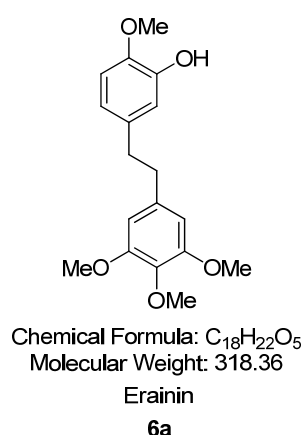


Figure 3.1: Erianin **6a** is a polyphenol identified in a Southeast Asian plant *Dendrobium chrysotoxum*.

3.1.2 Prospective mechanism of action of Erianin

The mechanism of action of Erianin in inducing tumour cell death was investigated. Using HUVECs, Erianin has shown a dose dependent metabolic inhibition which was indicated by reduced acidification rate and viability of HUVECs¹⁸². There is selectivity against endothelial cells. In addition, Erianin reduced lactate production, glucose consumption and intracellular ATP level in HUVECs. Most importantly, Erianin induced a dose and time dependent phosphorylation of JNK/SAPK as indicated by Western blot¹⁸³. This mechanism may be involved in the potential anti-tumour and anti-angiogenic actions of Erianin¹⁸².

From other studies with human HL-60 leukaemia cells, Erianin induced cellular DNA fragmentation, this morphological change was observed by fluorescence and electron microscopy¹⁸⁴. Immunohistochemical analysis established that Erianin suppressed *Bcl-2* gene and increased *Bax* gene expression. A cell cycle block at the G2/M transition was also observed. As mentioned in the previous chapter, Bcl-2 is a key anti-apoptotic protein - the loss of function in Bcl-2 caused an increased sensitivity of tumour cells to apoptotic signals, resulting in tumour cell death.

Cumulative literature data inferred that Erianin has excellent anti-tumour and anti-angiogenic properties. This compound affected cell cycle by targeting pathways and proteins essential for tumour cell survival; the molecular targets of Erianin were cell type dependent. However, Erianin induces severe toxicity to patients in clinical trials, which has hampered its clinic development (S. Wang personal communication).

3.1.3 Novel derivatives of Erianin

In an attempt to reduce the toxicity and improve the drug-like properties of Erianin, various chemical modifications have been made. However, as Erianin is a natural product, the limited availability of the compound for organic syntheses and the resulting yield availability for biological testing are major challenges. In this chapter, we demonstrate a series of studies to review the mechanism of action of Erianin, and compare its properties to novel synthetic derivatives.

3.2 Cellular growth inhibition of novel natural product derivatives

In this section, we review the anti-tumour / growth inhibitory activity of Erianin and its novel derivatives. Six novel compounds were derived following modification of Erianin. Activity was tested using the MTT assay following 72 hours exposure, as described in section 6.3, against tumour cell lines HCT-116 and MCF-7. Their activities are summarised below (Table 3.1).

Compounds	GI ₅₀ (μ mol/L)	
	HCT-116	MCF-7
Erianin 6a	0.06 \pm 0.00	0.06 \pm 0.01
ZJU-1 6b	6.57 \pm 1.03	5.22 \pm 0.20
ZJU-2 6c	53.47 \pm 0.52	8.54 \pm 0.08
ZJU-3 6d	39.81 \pm 7.45	41.18 \pm 1.09
ZJU-4 6e	36.98 \pm 2.72	20.97 \pm 3.95
ZJU-5 6f	>100	44.89 \pm 0.14
ZJU-6 6g	2.79 \pm 0.31	1.21 \pm 0.35

Table 3.1: Cellular activity of novel Erianin derivatives on tumour cell lines HCT-116 and MCF-7. The synthetic analogues demonstrated reduced activity compared with Erianin with the GI₅₀ shifted from nano-molar to micro-molar values. Among these compounds, ZJU-6 **6g** was the most potent molecule and was selected for further screening.

3.2. Cellular growth inhibition of novel natural product derivatives

The chemical modifications of Erianin reduced the activity of resultant analogues from inhibition at nano-molar to micro-molar values. The most potent compound in this group was ZJU-6 **6g** (Figure 3.2), followed by ZJU-1 **6b**.

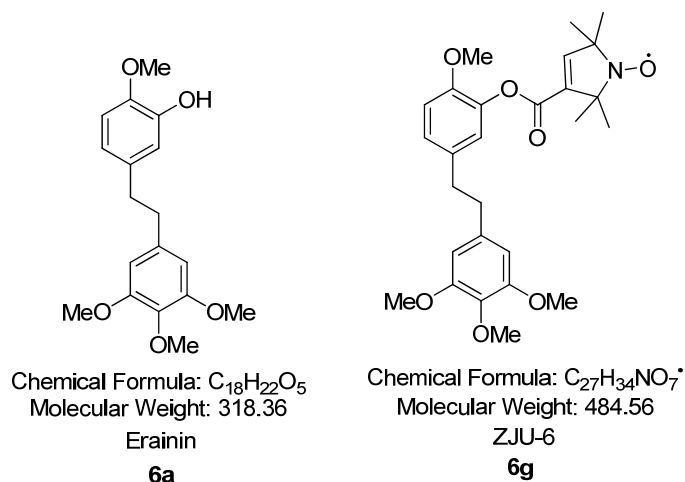


Figure 3.2: Chemical structure of **6a** (Erianin) and **6g** (ZJU-6).

The purpose of ZJU-6 having an oxygen anion is to enhance the anti-oxidant property of Erianin. It is proposed that the molecule could protect lipids from per-oxidation by free radicals or reactive oxygen species by donating its electron without becoming reactive itself¹⁸⁵

Cell line	Origin	GI_{50} (μ mol/L)	
		Erianin	ZJU-6
HCT-116	Human colon carcinoma	0.06 ± 0.00	2.79 ± 0.31
MCF-7	Human breast adeno-carcinoma	0.06 ± 0.01	1.21 ± 0.35
MRC-5	Human embryonic lung fibroblast	0.07 ± 0.01	1.18 ± 0.51
TK10	Human renal cell carcinoma	0.77 ± 0.17	5.89 ± 0.67
HCC-2998	Human colon carcinoma	0.07 ± 0.03	0.07 ± 0.01
U373M	Human astrocytoma	0.02 ± 0.01	0.25 ± 0.08
A549	Human carcinomic alveolar basal epithelial	0.07 ± 0.00	0.64 ± 0.04
SNB 1evR	Human malignant glioma	0.08 ± 0.02	0.68 ± 0.10
MDA-468	Human breast carcinoma	0.04 ± 0.01	0.07 ± 0.01
MIA PaCa-2	Human pancreatic carcinoma	0.01 ± 0.00	0.05 ± 0.01

Table 3.2: Growth inhibition of Erianin and ZJU-6 determined by MTT assay (72 hours). After 72 hours incubation with compounds, the GI_{50} of ZJU-6 was reduced between two to 47 times compared to Erianin in all cell lines tested except HCC-2998.

3.2. Cellular growth inhibition of novel natural product derivatives

ZJU-6 was selected for further screening against a total of 10 cell lines for cellular growth inhibition in parallel with Erianin (Table 3.2). With the exception in HCC-2998, ZJU-6 shows a reduced activity between two to 47 times compared to Erianin. Both Erianin and ZJU-6 were most potent in human pancreatic carcinoma cell line MIA PaCa-2, with a GI₅₀ value of 0.006 μ M and 0.054 μ M, respectively. ZJU-6 showed similar potency in MDA-468 cells, a human breast cancer cell line.

Erianin and ZJU-6 have similar potency on HCC-2998 cells. Although both compounds are potent to this cell line, however, HCC-2998 has been reported in the literature to be unpredictable during culture¹⁸⁶; hence this result may not be reliable. In order to carry out the imaging experiment (section 3.3), a cell type with large size is required. Hence, MCF-7 cells were selected to carry out most of the cellular assays for the mechanism studies of ZJU-6 despite the lesser potency of the molecule in this cell line.

3.3 Morphological effect of ZJU-6

Imaging studies were carried out to examine whether ZJU-6 performed in the same way as Erianin before proceeding with further specific experiments. Erianin has been reported to affect cell cycle by arresting the formation of micro-tubulin¹⁸², therefore, this property is expected to be found with ZJU-6. MCF-7 cells were treated with compounds at approximately the four times GI₅₀ concentration. Images were taken in short intervals at specific regions of the plate. The results are shown below (Figure 3.3).

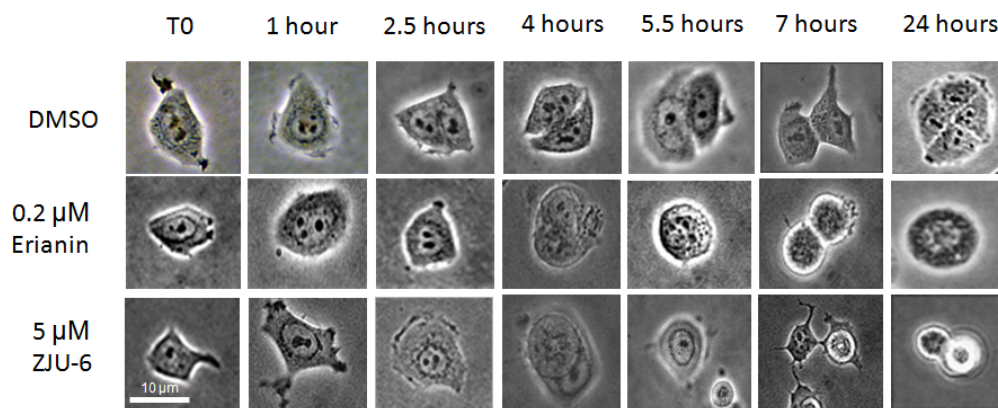


Figure 3.3: Imaging studies in MCF-7 cells with Erianin and ZJU-6. With four times GI_{50} concentration of either compound, cells were unable to divide as shown at 4 hours. As a consequence, genetic material in cells became disarrayed; cells detached from wells and rounded up, followed by cell death. The scale bar represents 10 μm .

The compound induced no effect during the first few hours of observation. At 4 hours, the size of the cells increased, but the cells were unable to divide. In vehicle-treated cells, genetic material was observed clearly in nuclear regions. In contrast, a loss of genetic material from nuclei was observed in cells treated with either Erianin or ZJU-6. At 5.5 hours, cells began to round up and genetic material was lost. At 7 hours, cells detached from the culture plate indicating cell death. In contrast, cells exposed to DMSO vehicle grew normally and continued to divide during this 24 hour time period.

From these observations, we can conclude that at four times GI_{50} concentration, Erianin and ZJU-6 function in a similar way in causing mitotic arrest in MCF-7 cells, followed by the possible disruption of microtubule polymerisation resulting in disarray of chromosomes in treated cells, and eventually leading to cell death. Therefore we were now able to carry out further experiments to examine cell cycle and tubulin polymerisation and so confirm mitotic arrest.

3.4 Cell cycle effect of ZJU-6

MCF-7 cells were treated with either Erianin or ZJU-6 at two or four times GI_{50} concentrations for 24 or 48 hours. The cell cycle effects were analysed by FACS which is shown in Figure 3.4.

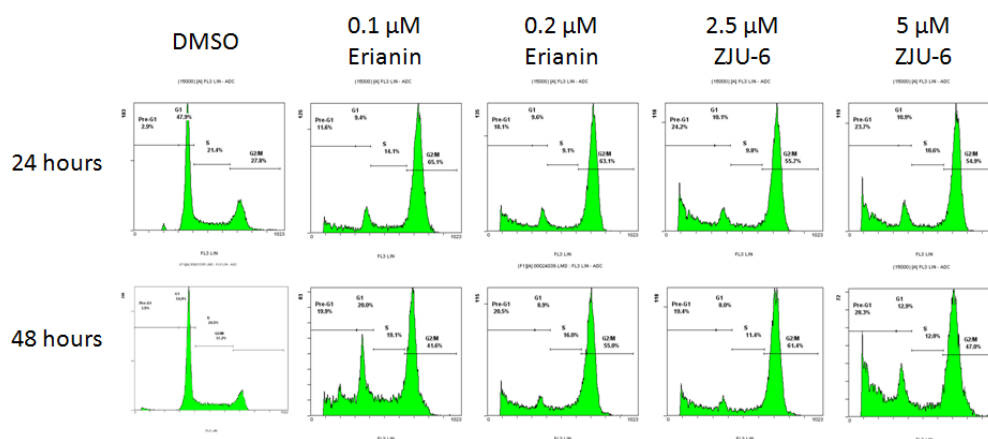


Figure 3.4: Effect of Erianin and ZJU-6 on the cell cycle of MCF-7 cells. Cells were treated with compounds for 24 or 48 hours. Significant G2/M transition block was observed with both compounds. However the effect of Erianin was reduced at 48 hours with 0.1 μ M, while the effect of ZJU-6 at 2.5 μ M was the same at both time points.

The G2/M blockage was observed by Erianin or ZJU-6 treatment at all concentrations tested. For 0.1 μ M Erianin, cells were predominantly arrested at G2/M transition at 24 hours with the G1 population being reintroduced at 48 hours, while at 0.2 μ M the percentage of G2/M cell population at both time points remained the same. In the case of ZJU-6, its effect at 2.5 μ M remained the same at both time points.

3.5 ZJU-6 induces apoptosis in cancer cells

From the pre-G1 population indicated in cell cycle analysis, we may hypothesise that ZJU-6 is more effective in inducing cell death. To further test this hypothesis, caspase-3 assays were carried out in HCT-116 cells (Figure

3.5. ZJU-6 induces apoptosis in cancer cells

3.5); MCF-7 cells are inappropriate for caspase-3 assay as the cells do not express caspase-3¹⁸⁷. HCT-116 cells were treated with either Erianin or ZJU-6 for 24, 36 or 48 hours. The level of caspase-3 activation, as an indication of apoptotic induction, was measured by optical density (OD).

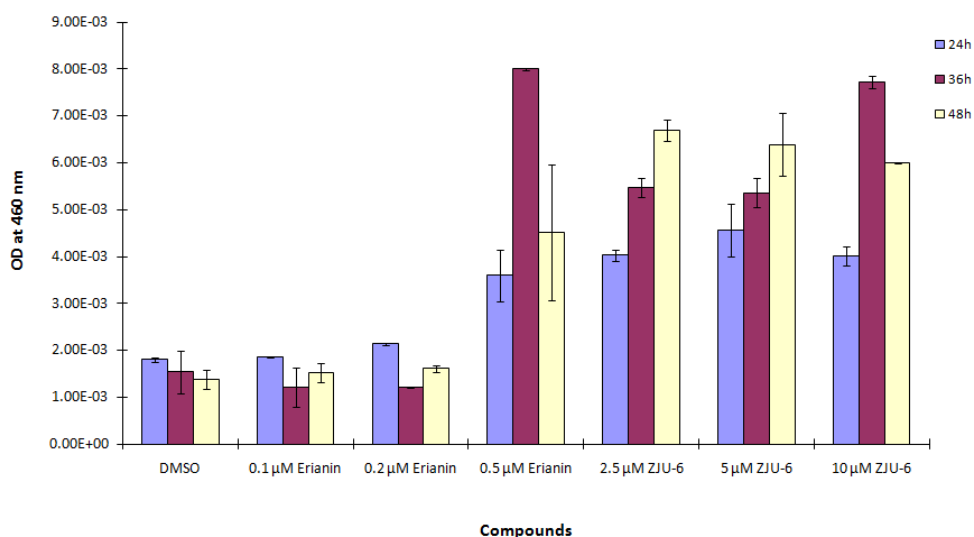


Figure 3.5: Caspase-3 activation in HCT-116 cells with Erianin and ZJU-6. Approximately 10 times GI_{50} concentration of Erianin was required for significant caspase-3 activation. Significant caspase-3 activation was observed with two times GI_{50} ZJU-6 concentration.

By comparison with the DMSO samples, Erianin only induced a significant level of caspase-3 activation at 0.5 μ M, with the peak effect observed at 36 hours. In the case of ZJU-6, significant caspase-3 activation was induced with all concentrations tested and at all time points. This activation increased in a time dependent manner. The peak activation level was at 36 hours with 10 times GI_{50} concentration for both compounds. The caspase-3 assay indicated that Erianin was not toxic to cells as it only induced significant apoptosis at approximately 10 times GI_{50} concentration while ZJU-6 induced significant apoptosis at all concentrations. The results further confirmed that ZJU-6 was more toxic to cells.

3.5. ZJU-6 induces apoptosis in cancer cells

To verify the apoptotic effect caused by the compounds in MCF-7 cells, we performed Western blot to observe their effect on PARP cleavage (Figure 3.6).

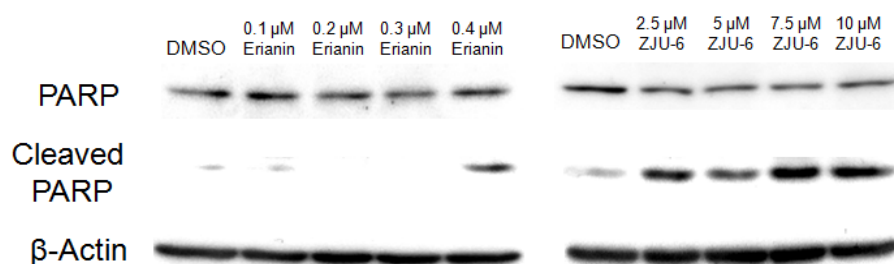


Figure 3.6: Erianin and ZJU-6 cause PARP cleavage. At 24 hours, PARP cleavage was induced at 0.4 μM Erianin in MCF-7 cells. ZJU-6 induced PARP cleavage from 2.5 to 10 μM . This result shows similarity to the caspase-3 assay with HCF-116 cells.

As carried out in the previous chapter, PARP protein was used here, as a marker for the detection of apoptosis caused by Erianin and ZJU-6 (see section 2.6). MCF-7 cells were treated with either Erianin or ZJU-6 for 24 hours. Significant levels of PARP cleavage were caused by 0.4 μM Erianin compared to cells treated with DMSO only. A low level of PARP cleavage was found in samples treated with DMSO and 0.1 μM Erianin, possibly due to the over growth of cells. With ZJU-6, although the DMSO sample also revealed cleaved PARP as a result of over population, higher levels of PARP cleavage were shown in all samples treated with compound ranging from two to eight times GI_{50} concentration. This observation once again indicates that ZJU-6 is more toxic once it has entered the cells, corroborating the results of the caspase-3 assays in HCT-116 cells.

Sample	Average total cell death (%)
DMSO	4.20 \pm 2.51
0.2 μM Erianin	13.40 \pm 2.19
0.4 μM Erianin	15.43 \pm 3.47
1 μM Erianin	18.23 \pm 3.90
5 μM ZJU-6	14.80 \pm 2.89
10 μM ZJU-6	13.97 \pm 3.46

Table 3.3: Percentage of cell death induced by Erianin and ZJU-6.

3.5. ZJU-6 induces apoptosis in cancer cells

A further experiment to verify cell death is the Annexin-V assay preformed in caspase-3 negative MCF-7 cells. Cells were treated with 0.2, 0.4 or 1 μM Erianin and 5 or 10 μM ZJU-6 for 24 hours. Both compounds induced apoptosis between 3- to 5- fold compared to the control (Figure 3.7).

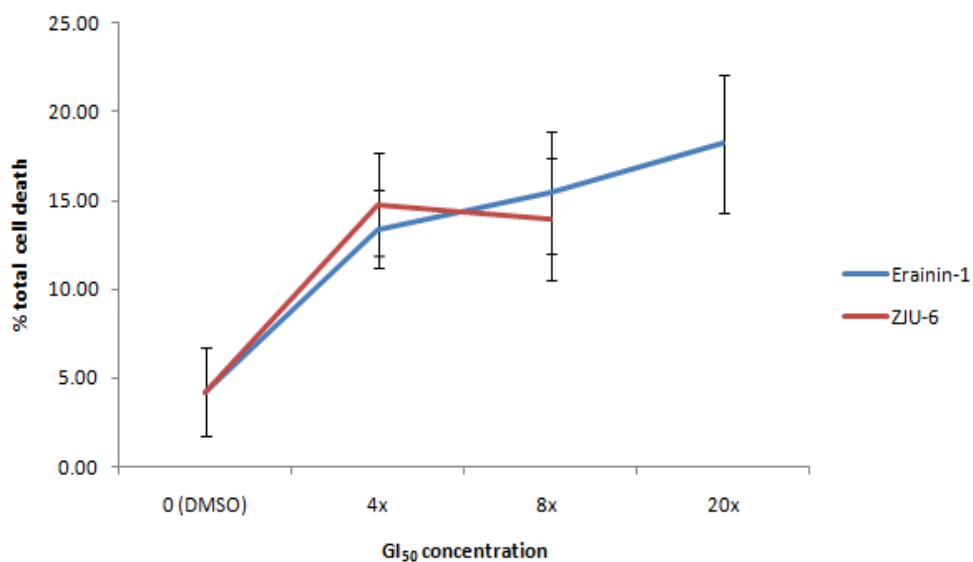


Figure 3.7: Effect of Erianin and ZJU-6 on MCF-7 cells' death. Cells were treated with compounds based on their GI₅₀ values. Both compounds induced similar levels of cell death. Erianin induced cell death in a dose dependent manner. ZJU-6 induced a slightly higher level of cell death at four times GI₅₀ concentration. However the difference in cell death between four times and eight times GI₅₀ was 0.83%, which is a region within the standard deviation and therefore insignificant.

3.6 Effect of ZJU-6 on anti-apoptotic proteins

ZJU-6 has been shown to be less toxic than Erianin. However, once cells were treated with both compounds at the same GI₅₀ equivalents, which could represent the same amount of compounds have entered the cells, the effect of ZJU-6 was more profound than Erianin (indicated by the apoptotic assays). It has been reported that Erianin suppresses the transcription of *Bcl-2*, resulting in reduced *Bcl-2* mRNA level¹⁸⁴. Western blots were used to detect the protein expression level of anti-apoptotic proteins Mcl-1 and Bcl-2 (Figure 3.8).

3.6. Effect of ZJU-6 on anti-apoptotic proteins

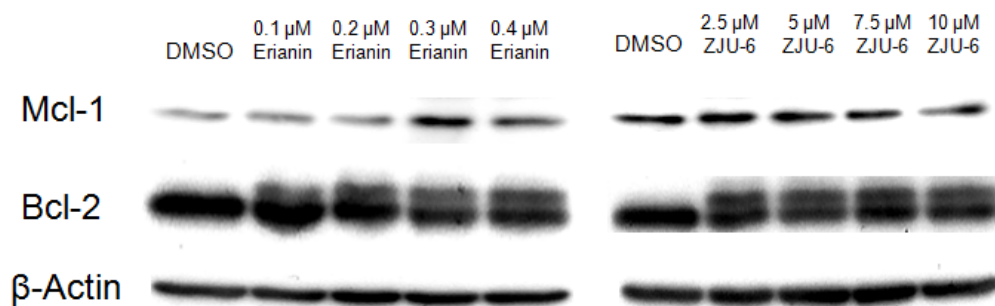


Figure 3.8: Effect of Erianin and ZJU-6 on the protein expression of Mcl-1 and Bcl-2. No effect on Mcl-1 was observed by either compound. Both compounds affect Bcl-2 by inducing the expression of an isoform protein with a higher molecular weight, possibly by altering the original transcription or translation mechanisms. Phosphorylation of Bcl-2 resulting in an increase in size is another possibility.

MCF-7 cells were treated with either Erianin or ZJU-6 for 24 hours. Neither compound suppressed the expression of Mcl-1. For Bcl-2 expression, however, an extra, higher molecular weight band was shown. This may indicate that both compounds induced an alternative isoform of Bcl-2 with a larger molecular weight, through alternation of transcription or translation mechanisms, which has been observed in lymphoma¹⁸⁸. Phosphorylation of Bcl-2 is another possibility as the addition of phosphate could increase the molecular weight of Bcl-2. No further clues for the exact mechanism of Bcl-2 alteration could be obtained by Western blot; further experiments are required to understand the mechanisms in detail.

3.7 p53 induction by ZJU-6

Protein *p53* is one of the most important tumour suppressor genes. The effect of Erianin on stabilisation of p53 has not been reported directly; however, since Erianin inhibits tubulin polymerisation in cells, which affects the chromosome segregation, it could induce the expression of p53. Here, Western blots were

used to determine the effect of Erianin and ZJU-6 on p53 protein, and its negative regulator, HDM-2, in MCF-7 cells (Figure 3.9).

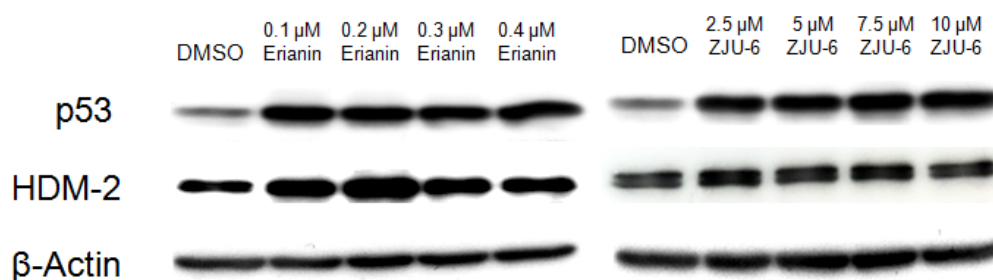


Figure 3.9: Effect of Erianin and ZJU-6 on p53 and HDM-2 proteins in MCF-7 cells. At 24 hours, both compounds enhanced the expression of p53. However, a biphasic change on HDM-2 expression, with an increase expression at low concentration followed by a decrease expression at high concentration was observed in the presence of both compounds.

MCF-7 cells were treated with both compounds for 24 hours in a range between two to eight times GI_{50} concentrations. In the presence of either compound, p53 protein concentration was increased compared to cells treated with DMSO only. However, the level of HDM-2 protein showed a biphasic change with the presence of both compounds. An increase of HDM-2 expression was observed with 0.1 and 0.2 μ M Erianin, with a decrease emerging at higher concentrations (Figure 3.10). For ZJU-6, a similar trend to Erianin was observed. The result indicated that both Erianin and ZJU-6 enhanced the synthesis of p53 proteins. However, they did not suppress the negative feedback by HDM-2; hence, we could not confirm whether the p53 proteins here were active. Higher concentration of compounds may suppress this negative feedback, but for the highest compound concentration here, the protein level of HDM-2 was still relatively higher than samples treated with DMSO vehicle. Hence, in this particular experiment, we could only conclude that Erianin and ZJU-6 help to stabilise p53.

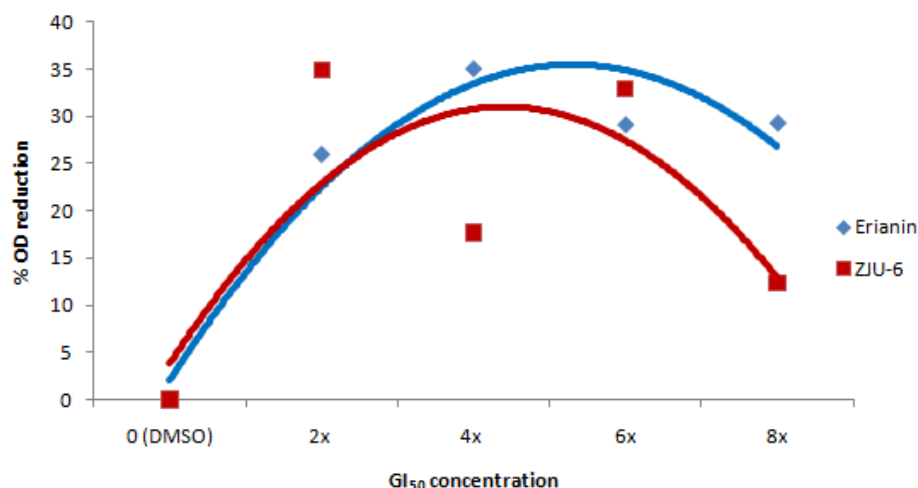


Figure 3.10: Dose dependent effect of compounds on HDM-2 proteins. Western blot results on the effect of HDM-2 expression caused by Eriain-1 and ZJU-6 were used in Image JTM to measure the relative grey intensity. The calculated readings from the measurements of samples were calibrated with the readings from the DMSO sample on the corresponding blot. Both compounds have shown a trend to initially increase the expression HDM-2 protein, with a suppression observed dose dependently at higher concentration. ZJU-6 promoted a relatively better effect than Erianin in suppressing HDM-2 expression. However, the expression levels still exceed that of DMSO even at the highest compound concentration tested here.

3.8 Effect of ZJU-6 on transcription

We detected the effect of ZJU-6 on anti-apoptotic proteins Mcl-1 and Bcl-2, together with p53 negative regulator HDM-2 through Western blots. Although significant reduction was not found in any of these proteins, Bcl-2 protein modification was observed in the presence of these compounds. Consequently, we investigated the effect of Erianin and ZJU-6 on the transcription of these proteins using RT-PCR (Figure 3.11). As in Western blot, MCF-7 cells were treated with either compound for 24 hours at a range of concentrations based on the GI₅₀ values.

3.8. Effect of ZJU-6 on transcription

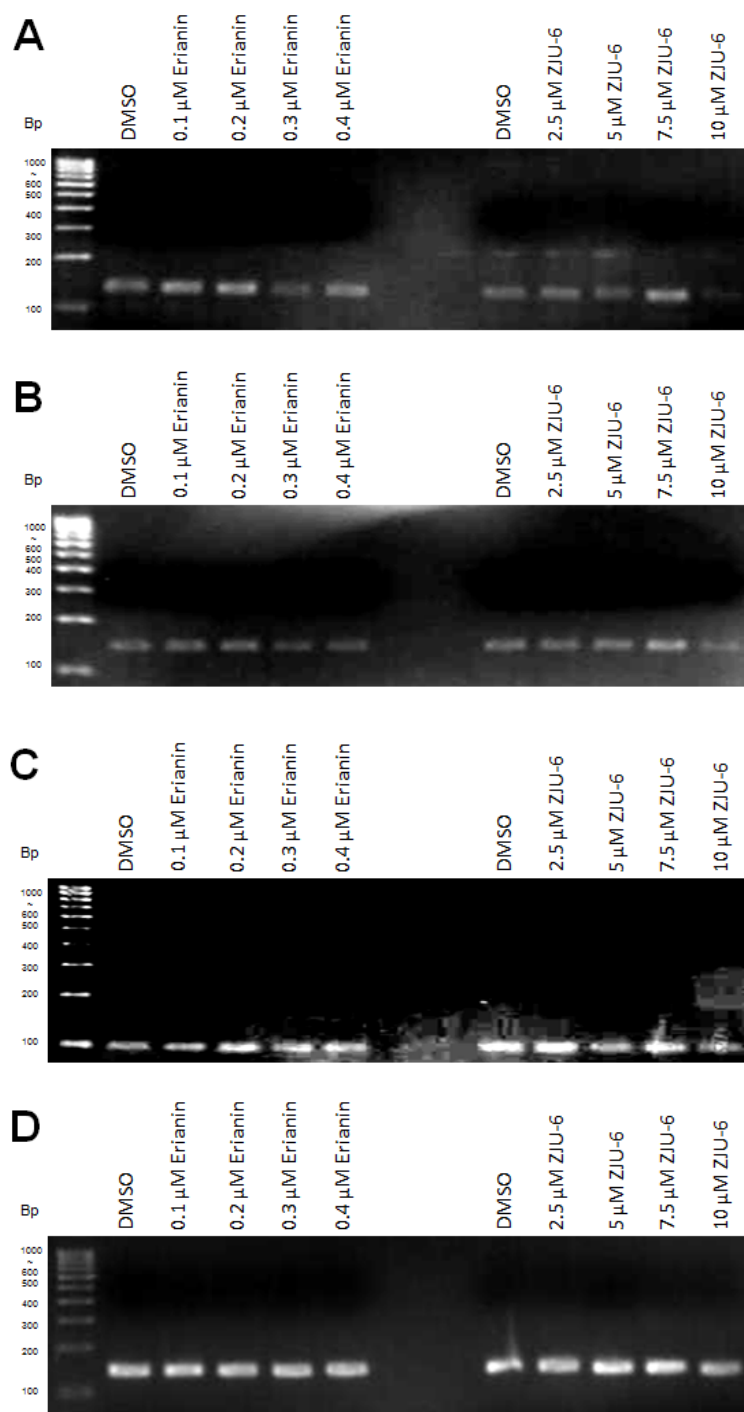


Figure 3.11: Effect of Erianin and ZJU-6 on transcription in MCF-7 cells. After 24 hours treatment with compounds, A) mRNA of *Mcl-1* was affected by ZJU-6 at 10 μM only; Erianin had no effect on *Mcl-1* transcription. B) Erianin reduced the transcription of *Bcl-2* from concentrations of 0.3 μM . ZJU-6 reduced *Bcl-2* mRNA level at 10 μM only. C) No significant effect on transcription of *HDM-2* was shown by either compound. D) Transcription of β -Actin remains constant.

The results from RT-PCR have shown that ZJU-6 affected the transcription of *Mcl-1* at 10 μM concentration. However, from previous experiments, 10 μM

ZJU-6 caused significant cell death. Therefore, this reduction could be a consequence of cell death, rather than ZJU-6 specifically targeting *Mcl-1* to induce cell death. No effect on the mRNA synthesis of *Mcl-1* was induced by Erianin. The transcription of *Bcl-2* was reduced by Erianin from concentrations of 0.3 μ M, matching observations reported in the literature¹⁸⁴. ZJU-6 induced a similar effect on *Bcl-2* mRNA as with *Mcl-1*, reducing mRNA levels at 10 μ M. Therefore, Erianin, but not ZJU-6, could induce tumour cell death by affecting *Bcl-2* transcription. Both compounds had no effect on the transcription of *HDM-2*, matching Western blot observation.

3.9 Effect of ZJU-6 on polymerisation of tubulin

Tubulin is involved in the formation of mitotic spindles in the mitotic phase of the cell cycle. Microtubule formation is essential for the segregation of sister chromatids and the formation of two daughter cells as the end product of the cell cycle. It has been reported that Erianin is capable of inhibiting tubulin polymerisation¹⁸². Our cell cycle analysis showed that both ZJU-6 and Erianin induced a G2/M transition block in MCF-7 cells, indicating that the compounds alter components essential for this phase of the cell cycle. This cell cycle block was suspected to be caused by alteration of tubulin. Therefore, an *in vitro* biochemical assay which determines the rate of tubulin polymerisation by measuring OD was performed to examine the effect of tubulin polymerisation induced by Erianin and ZJU-6 (Figure 3.12). Since ZJU-6 has shown to be the more effective compound in the induction of cell cycle arrest, ZJU-6 was expected to be more potent than Erianin in inhibiting tubulin polymerisation.

3.9. Effect of ZJU-6 on polymerisation of tubulin

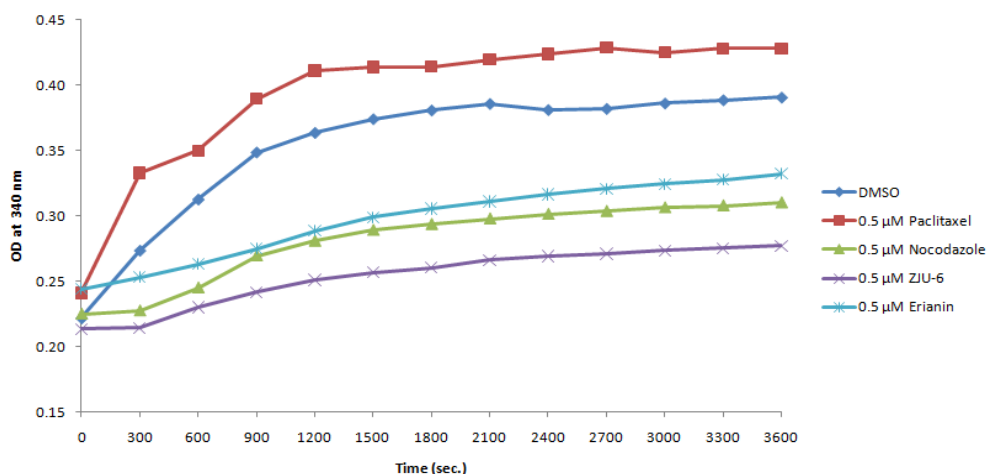


Figure 3.12: Effect of compounds on tubulin polymerisation (up to 1 hour). All compounds were used at 0.5 μ M. Paclitaxel and Nocodazole were used as additional controls known to enhance tubulin polymerisation and depolymerisation, respectively.

The effect of compounds was compared at 0.5 μ M and polymerisation of tubulin was allowed to occur for 1 hour. In this assay, Paclitaxel and Nocodazole were the positive and negative controls, respectively. Paclitaxel, a mitotic inhibitor used in cancer chemotherapy, was discovered in 1967 from the extract of pacific yew, *Taxus brevifolia*. It is well known that Paclitaxel binds to tubulin to suppress dissociation of microtubules¹⁸⁹. Nocodazole functions in a manner opposite to Paclitaxel; it interferes with the polymerisation of microtubules by binding to β -tubulin and preventing formation of one of the two interchain disulfide linkages between tubulins. After three experimental repeats (Table 3.4), the results indicated that ZJU-6 has a more potent effect than Erianin in suppressing the polymerisation of tubulin.

Compound	DMSO	0.5 μ M Paclitaxel	0.5 μ M Nocodazole	0.5 μ M ZJU-6	0.5 μ M Erianin
V_{\max} (OD = 340 nm)	0.37 \pm 0.10	0.40 \pm 0.12	0.31 \pm 0.02	0.29 \pm 0.06	0.33 \pm 0.04

Table 3.4: V_{\max} values from the tubulin polymerisation assays. The results show Paclitaxel induced tubulin polymerisation while the other 3 compounds suppressed polymerisation of tubulin. ZJU-6 has a more potent effect than positive control Nocodazole in suppressing the polymerisation reaction, while Erianin was less potent.

3.10 Effect of ZJU-6 on angiogenesis

After clonal expansion of tumour cells *in vivo*, formation of blood vessels is essential for further growth of tumours and metastasis. Oxygen and required nutrients are supplied to tumours, and waste removed *via* the blood. Compounds with anti-angiogenic properties suppress new blood vessel formation within tumours, hence blocking their oxygen and nutrient supply and halting their further development. It has already been reported that Erianin has anti-angiogenic properties based on 48 hours treatment of the compound on chick chorioallantoic membrane¹⁸², we hypothesised that ZJU-6 may also possess anti-angiogenic properties. An *ex vivo* experiment, the chorioallantoic membrane (CAM) assay, was used to test the effect of compounds on neovascularisation in fertilised chicken eggs. The CAM assay allows observation of blood vessel formation in the chick embryo over a six day incubation period (Figure 3.13). The effects of vehicle alone, 0.2 μM Erianin and 5 μM ZJU-6 on blood vessel formation in chick embryos were compared. The concentrations used were four times GI_{50} concentration in MCF-7 cells.



Figure 3.13: Effect of Erianin and ZJU-6 on angiogenesis in chick embryo. Based on four times GI_{50} concentration, ZJU-6 has shown a relatively potent anti-angiogenic effect in this CAM assay compared to Erianin, almost completely suppressing the formation of blood vessels. The scale bar represents 1 mm.

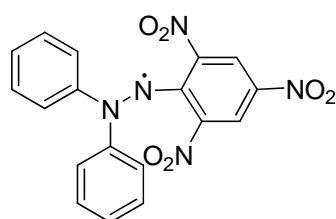
The CAM assay was performed at least three times; all repeats showing similar effects. The results indicated that both Erianin and ZJU-6 have anti-angiogenic effects on blood vessel formation in chick embryos. At four times GI_{50} concentration, ZJU-6 demonstrated a more profound anti-angiogenic effect than Erianin.

A number of limitations are associated with the CAM assay, one of which is a possible genetic variation between each chick embryo; hence, the time required for blood vessel formation may vary between embryos. In addition, anti-infectious agents such as antibiotics could not be used to prevent infection, as the embryos would be killed by these agents. The embryo may become infected within a six day period which leads to the low success rate of the assays. The position of the filter paper carrying the compounds may also affect the result. As angiogenesis starts from within the embryo, placing the filter paper closer to the embryo may induce a more profound effect. Another challenge is the concentration of compounds used in this assay; four times GI_{50} concentration was used to overcome the question of compound delivery while being the highest concentration which would not kill the embryo as indicated by the earlier assays. Finally, the mode of compound delivery to the embryo was by filter paper followed by diffusion. The actual concentration of compounds in the tissue may be less than the concentration stated. Hence, the effect of compounds may be more profound than reported here.

3.11 Anti-oxidant activity of ZJU-6

Natural products, particularly polyphenols, are understood to have anti-oxidant properties, a possible factor contributing to cancer prevention properties of

natural products. Part of the principles behind the modification of Erianin to ZJU-6 with a free radical was to introduce the anti-oxidant effect to the molecule. To examine this hypothesis, we carried out an *in vitro* biochemical assay using 1,1-diphenyl-2-picrylhydrazyl (DPPH) **21**. DPPH (Figure 3.14) is a molecule with a free radical in the central nitrogen atom which is readily reduced by compounds. Such reduction is accompanied by a colour change which can be monitored spectrophotometrically.



1,1-diphenyl-2-picrylhydrazyl (DPPH)

7

Figure 3.14: Molecular structure of DPPH. Free radical in the central nitrogen atom allows reduction by anti-oxidant agents. DPPH reduction results in a colour change from deep violet to yellow.

The DPPH assay is commonly used to estimate the anti-oxidant/reducing properties of natural products. From the OD measurements, the estimated IC_{50} values of compounds can be determined. After three assay repeats (each in triplicate), the anti-oxidant activities of Erianin and ZJU-6 were plotted (Figure 3.15) with the IC_{50} values of 43.69 μM and $>100 \mu\text{M}$ were estimated for the two compounds respectively. The positive controls in this assay were ascorbic acid and Epigallocatechin gallate (EGCG), the active ingredient in green tea with cancer prevention and anti-oxidant properties. Their IC_{50} values in this assay were 23.58 μM and 3.72 μM , respectively. Literature data indicated that ascorbic acid should have an IC_{50} value of 19.90 μM in this assay¹⁹⁰, hence our results are comparable.

3.11. Anti-oxidant activity of ZJU-6

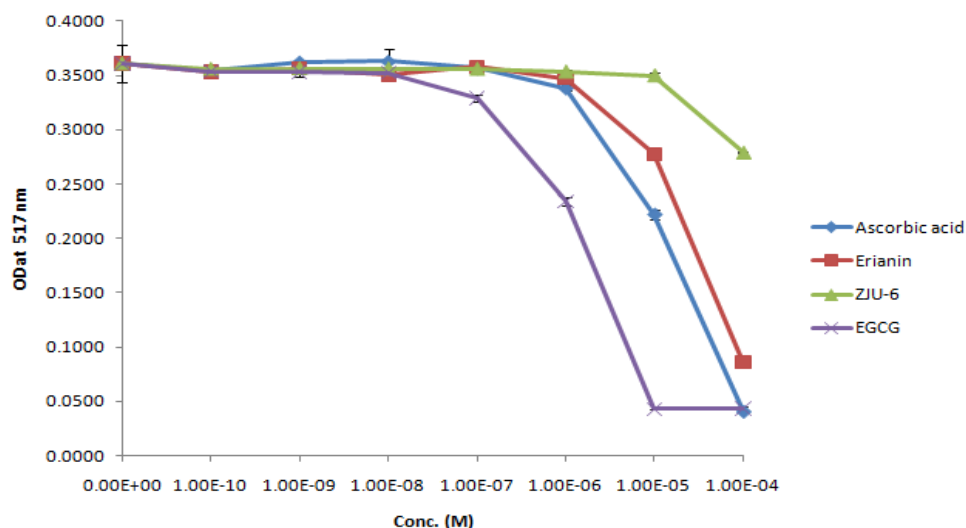


Figure 3.15: Effect of compounds on the reduction of DPPH. Results of DPPH assay measuring the anti-oxidant effects of Erianin and ZJU-6. EGCG from green tea and ascorbic acid were used as positive controls. The IC_{50} values of ascorbic acid, EGCG and Erianin in this assay were 23.58, 2.58 and 46.23 μ M, respectively. ZJU-6 had an estimated IC_{50} of >100 μ M.

Further experiments were carried out to investigate whether anti-oxidant properties can be demonstrated at a cellular level. 2',7'-dichlorofluorescein diacetate (H_2DCFDA) was used to detect the oxidation states of cells. H_2DCFDA de-esterifies in the presence of intracellular oxidative species and turns to highly fluorescent 2',7'-dichlorofluorescein. Cellular fluorescence was quantified by FACS which estimates the oxidation states of cells.

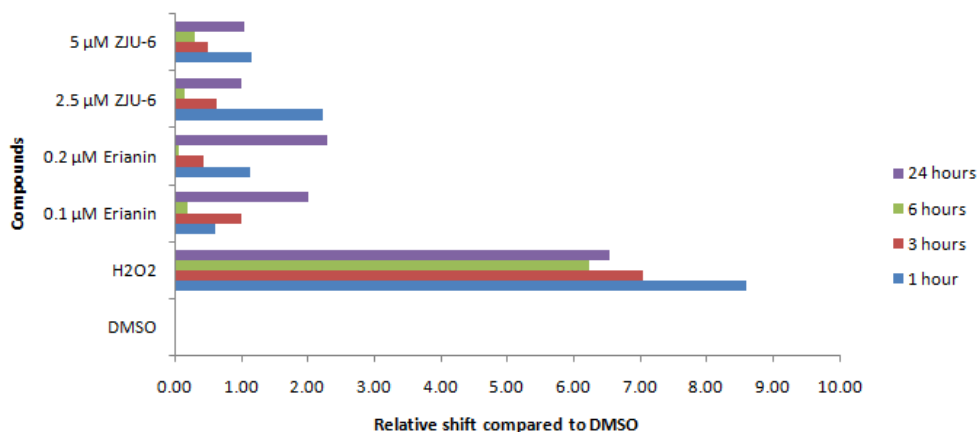


Figure 3.16: Effect of compounds in the cellular oxidation state. H_2DCFDA detection has shown that Erianin and ZJU-6 had pro-oxidant effect at cellular level with Erianin is more potent than ZJU-6. Although the pro-oxidant effect was reduced between 1 to 6 hours, the effect could not be concluded as being anti-oxidant as the fluorescent level was higher than the DMSO sample.

HCT-116 cells were incubated with Erianin or ZJU-6 for 1, 3, 6 or 24 hours. 5 μM hydrogen peroxide (H_2O_2) was used as positive control. The results showed a relative increase in cellular fluorescence in all Erianin and ZJU-6 treated samples compared to DMSO treated samples (Figure 3.16), indicating a pro-oxidant effect in cells. Erianin had a more profound effect than ZJU-6, increasing the cellular oxidation state up to 3-fold during the 24 hours period. ZJU-6 had a less significant effect, inducing a maximum ~ 2 -fold increase in cellular oxidation level compared to DMSO controls.

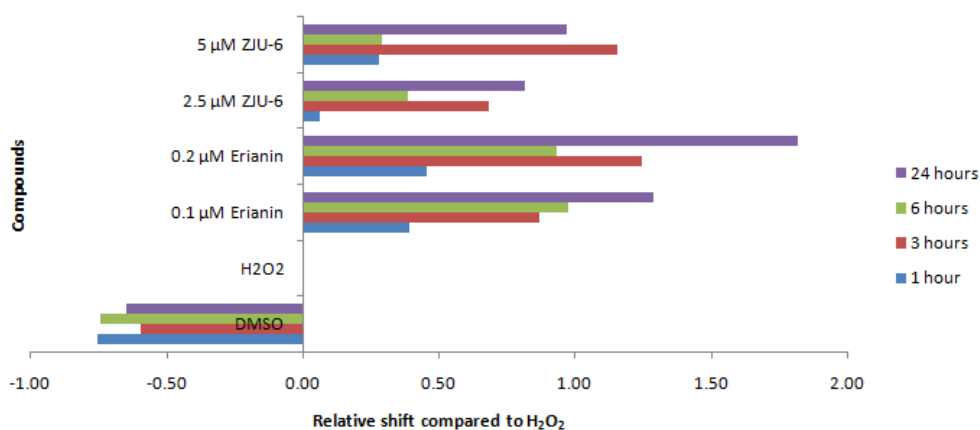


Figure 3.17: Effect of compounds in the prevention of cellular oxidation. After pre-treating cells with hydrogen peroxide, except in the DMSO control, H_2DCFDA detection has shown that Erianin and ZJU-6 had pro-oxidant effects at cellular level compared to H_2O_2 treated samples. The results were similar to previous experiments, indicating that Erianin and ZJU-6 enhanced cellular oxidation states of HCT-116 cells up to 3-fold and around 2-fold, respectively.

Since an unexpected result was observed from the H_2DCFDA assay, the assay method was altered, and all samples (except DMSO control) were pre-treated with 5 μM H_2O_2 for 30 minutes before harvesting and FACS analysis. This should have allowed us to observe the effect of test compounds in preventing cellular oxidation induced by H_2O_2 (Figure 3.17). However, results were similar to those obtained in the previous experiment, indicating that both

compounds induced pro-oxidant effects. Since the DPPH assay is a biochemical assay, while the H₂DCFDA assay is a cellular assay, the results of these two assays could suggest that Erianin and ZJU-6 could have anti-oxidant properties, but not at cellular levels.

3.12 Conclusion

Erianin, a natural product obtained from the Southeast Asian plant *Dendrobium chrysotoxum*, is already in phase II clinical trials for treatment of leukaemia (S. Wang personal communication). It inhibits cell growth with GI₅₀ value between 12.5 to 81.9 nM in a range of cell lines. The known properties of Erianin include prevention of angiogenesis, disruption of endothelial tube formation, abolition of cell migration across collagen and adhesion to fibronectin, and depolymerisation of F-actin and β -tubulin. ZJU-6, a novel analogue of Erianin has shown a reduced potency in some cell lines, except HCC2998, by at least 20-fold. The GI₅₀ values of ZJU-6 in the cell lines tested were ranging from 0.06 to 2.79 μ M (as shown in Table 3.2).

Both Erianin and ZJU-6 were able to block the segregation of chromosomes in MCF-7 cell nuclei following 4 hours treatment with compounds at concentration of four times GI₅₀. The shape of the genetic material inside the cell nucleus gave us an early indication that microtubule, possibly tubulin, was disrupted by the compounds. As a consequence, cells become enlarged in size and rounded up, followed by detachment from the tissue culture plate and cell death.

The observation of cell enlargement indicated that ZJU-6 possibly induced a G2/M phase block in cell cycle. Cell cycle analysis by FACS confirmed that

both Erianin and ZJU-6 induced arrest at G2/M transition, at similar levels correlated to their GI₅₀ concentrations. Profound G2/M cell cycle transition arrest has also been observed in other cell lines (HCT 116, A549, MDA-468) exposed to Erianin (100 nM, 200 nM, 24 - 48 hours; T.D. Bradshaw personal communication).

ZJU-6 induces tumour cells to undergo apoptosis. ZJU-6 caused caspase-3 activation in HCT-116 cells from two times GI₅₀ concentration, while Erianin induced caspase-3 activation only at eight times GI₅₀ value. The peak effect of the two compounds was found at 36 hours with eight times their GI₅₀ concentrations. PARP cleavage was detected by Western blot using MCF-7 cells treated with compounds; a similar result to the caspase-3 assay was observed. PARP cleavage was detected with ZJU-6 from two times GI₅₀ concentration, while Erianin only induced PARP cleavage at eight times GI₅₀ concentration. These apoptotic assays indicated that ZJU-6 was more effective at apoptosis induction, correlating to their GI₅₀ concentrations.

Since Erianin has been reported in affecting the transcription of Bcl-2, expression of anti-apoptotic proteins Mcl-1 and Bcl-2 were examined by Western blot in MCF-7 cells treated with the two compounds. No effect on Mcl-1 was induced by either compound. An isoform of Bcl-2 with a higher molecular weight was detected, which suggests the compounds might affect transcription or translation of Bcl-2. The effect of compounds on p53 has also been investigated. Erianin and ZJU-6 stabilising p53 increasing the protein level of both p53 and its negative regulator HDM-2 consequently. Since HDM-2 remains its negative regulatory effect on p53, therefore p53 induced by the compounds may not be active.

The effect of compounds on transcription of *Mcl-1*, *Bcl-2* and *HDM-2* in MCF-7 cells was detected by RT-PCR. Erianin was a better compound for inhibiting *Bcl-2* transcription, while ZJU-6 was more effective in inhibiting the transcription of *Mcl-1*. Both compounds have no effect on the transcription of *HDM-2*, which further confirm that p53 expression by the compounds observed in Western blot may not be active. The protein and PCR observations suggest ZJU-6 function in similar way as Erianin on *Bcl-2*, but not *Mcl-1*. The result also indicated that p53 was not responsible for the cell death, given that it may not be active as interpreted from the unchanged *HDM-2* levels.

Tubulin is essential for mitotic spindle formation which is required for chromosome segregation during mitosis. Since literature data reports that Erianin arrested tubulin polymerisation¹⁸², together with our observation on the G2/M cell cycle transition arrest with both compounds, ZJU-6 should also suppress polymerisation of tubulin. A biochemical assay was used to estimate the effects of Erianin and ZJU-6 on tubulin polymerisation. Using 0.5 μM compounds, ZJU-6 showed a more profound effect than Erianin in suppressing tubulin polymerisation. Furthermore, the ZJU-6 concentration used below its GI_{50} in most of the cell lines tested, it also suggests that inhibition of microtubule polymerisation could be the primary action of ZJU-6, but not Erianin.

Erianin has been reported to possess anti-angiogenic properties. The *ex vivo* chorioallantoic membrane (CAM) using four times GI_{50} compound concentrations on MCF-7 cells proved ZJU-6 to be a more effective anti-angiogenic compound than Erianin. However, the sensitivity of chick embryo to the compounds is likely to be different to MCF-7 cells. Perhaps the better

anti-angiogenic effect of ZJU-6 was induced by the high concentration of compound, i.e. 5 μ M ZJU-6 vs. 0.2 μ M Erianin.

Anti-oxidant properties contribute to cancer prevention. The free radical on ZJU-6 was intended to introduce anti-oxidant property. The *in vitro* biochemical assay using DPPH surprisingly revealed Erianin, which is not a polyphenol and do not contain free radicals, to be the more effective anti-oxidant. FACS analysis was used to investigate the anti-oxidant effect of both compounds in HCT-116 cells; the results, however, indicated that neither compound possesses anti-oxidant properties nor low levels of pro-oxidant activity were revealed. Erianin, again, was proven to be more effective than ZJU-6 in the possible anti-oxidant property at biochemical level and its pro-oxidant property at cellular level.

Gathering all our data, Erianin itself is a potential anti-tumour agent. As mentioned at the beginning of the chapter, Erianin has been found to have severe toxicity to patients in clinical trials. The development of semi-synthetic compounds using Erianin as a skeleton could generate a range of novel anti-tumour agents, such as ZJU-6, to improve the compound property as a clinical candidate by reducing its toxicity and possibly its adverse effects.

Chapter Four

Synthesis of a Plk1 inhibitor – analogue of BI 2536

4.1 Introduction

Since the discovery of CDKs, many other kinases, which show evolutionary conservation with CDKs in terms of genetic sequence and protein structure, have been found to be functionally related to CDKs, such as their roles in cell cycle progression. Examples of these are the Polo-like kinases (Plks). These kinases have also been investigated as potential drug targets in various diseases including cancer.

4.1.1 Polo-like kinases

Polo-like kinases (Plks) are enzymes first discovered in *Drosophila melanogaster* (polo) and *Saccharomyces cerevisiae* (cdc5) mutant cells that failed to undergo normal mitosis¹⁹¹. Subsequently, Plks have been found in many eukaryotes¹⁹². Human Plk was first cloned in 1993. This gene encodes a polypeptide containing 603 amino acids. Several nucleotide sequence differences were noted among the published sequences, but later these

differences were proved to be conservative changes in the amino acid sequence and were likely to be polymorphisms. The molecular weight of the Plk protein is 66 kD. This first identified form of Plk was later denoted as Plk1. The expression of Plk1 was found at a low level during G1 phase of the cell cycle, the expression level starting to accumulate during G2/M phase transition.¹⁹³ Lately discovered members of the Plk family were expressed primarily during mitosis. Hence, Plks are involved in key roles such as cell entry into mitosis, bipolar spindle formation, chromosome segregation and cytokinesis¹⁹⁴.

There are several different types of Plks, all of which show structural similarity, i.e. a canonical serine/threonine kinase domain at the amino terminus and a regulatory domain containing two signature motifs, known as polo boxes, at the carboxyl terminus. The genomes of *Drosophila melanogaster*, *Saccharomyces cerevisiae* and *Schizosaccharomyces pombe* have only one Plk (Polo, Cdc5 and Plo1, respectively), whereas vertebrate species have several Plks¹⁹⁴.

Organism	Plk	Proposed primary functions
Mammals	Plk1	Multiple roles during mitosis and cytokineses
	Plk2 (Snk)	DNA-damage response, regulation of synaptic plasticity, G1/S function
	Plk3 (Fnk, Prk)	DNA-damage response, regulation of synaptic plasticity, G2/M function
	Sak (Plk4)	Mitotic exit
<i>Xenopus laevis</i>	Plx1	Mitotic entry and exit
	Plx2	No specific function determined
	Plx3	No specific function determined
<i>Drosophila melanogaster</i>	Polo	Egulation of mitosis and cytokinesis
<i>Caenorhabditis elegans</i>	Plc1, Plc2, Plc3	Nuclear-envelope breakdown
<i>Schizosaccharomyces pombe</i>	Plo1p	Regulation of mitosis and cytokinesis
<i>Saccharomyces cerevisiae</i>	Cdc5	Regulation of meiosis, mitosis and mitotic exit

Table 4.1: Different species show variations in Polo-like kinase diversity^{194, 195}. *X. laevis*, *C. elegans* and mammals have multiple Plk members. *D. melanogaster*, *S. pombe* and *S. cerevisiae* have only one Plk. All Plks commonly function during mitosis.

In mammals, there are four Plk family members (Table 4.1)¹⁹⁵. The function of Plk1 will be discussed in detail in section 4.1.2.

4.1.1.1 Polo-like kinase 2

Plk2 also known as serum-inducible kinase (Snk), is a 685 amino acids protein (Figure 4.1) with a calculated molecular mass of about 78 kD. It also contains an ATP-binding motif within the kinase domain and a conserved polo box¹⁹⁶. Plk2 was found to be highly expressed in rat organs including adult testis, spleen and the occipital lobe, as well as in foetal lung, spleen, kidney and heart tissues. In humans, Plk2 was found to function in normal lung fibroblast cell division. The proposed functions of Plk2 include: DNA damage response, synaptic plasticity regulation and regulation of the G1/S cell cycle transition.

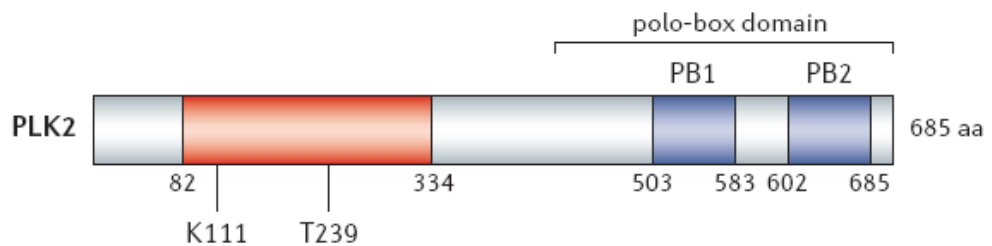


Figure 4.1: Structure of human Plk2 polypeptide¹⁹⁶. The red coloured region is the kinase domain with a T-loop (T239) which is critical for the regulation of its activity. There are two functional polo-box domains (PBDs) shown here in blue which phosphorylate downstream substrate proteins. This PBD is conserved across the Plk family (Adapted from Strebhardt & Ullrich. *Nat. Rev. Cancer*. 2006, 6, 321).

4.1.1.2 Polo-like kinase 3

Plk3 has various names including fibroblast-growth-factor-inducible kinase (fnk), cytokine-inducible kinase (cnk) and proliferation-related kinase (Prk). Plk3 protein has a 646 amino acid sequence containing an *N*-terminal catalytic domain which consists of an ATP-binding site (kinase domain), a central putative nuclear targeting signal motif and the polo-box domain (PBD) at the *C*-terminal regulatory domain (Figure 4.2). It has a conserved sequence with other Plk family members, with 91% homology to mouse Fnk, 50% homology

to human Plk, 48% homology to *D. melanogaster* polo and 38% homology to *S. cerevisiae* Cdc5. Plk3 expression has been found in a limited number of human tissues; a moderate level of Plk3 being found in placenta and low levels in ovary, lung, and peripheral blood leukocytes¹⁹⁷. Reduced expression has been found within tumour tissues, significantly in primary lung carcinoma. Plk3 regulates the G2/M transition by phosphorylating the C-terminal domain of cdc25c, a phosphoprotein found activated in the G2 phase of the cell cycle which is critical for the onset of mitosis. Plk3 is also known to associate with centrosomes in several human cell lines which regulate microtubule dynamics and centrosomal function. Other reported functions of Plk3 are similar to those of Plk2, which include DNA damage responses and synaptic plasticity regulation.

4.1.1.3 Polo-like kinase 4

The sequence of Plk4 is highly homologous to the mouse Sak gene; therefore, it is also referred to as Sak, a kinase consisting of 970 amino acids (Figure 4.2). There is suggestion that the lack of Plk4 may be implicated in mitotic infidelity tumour development¹⁹⁸. It also functions as an upstream regulator for centriole formation¹⁹⁹. Centrioles are important parts of centrosomes which are involved in the organisation of the mitotic spindle and in the completion of cytokinesis. Plk4 therefore also has a critical role in the regulation of mitosis and mitotic exit. Abundant Plk4 transcription has been detected in testis and thymus, but not in other tissues.

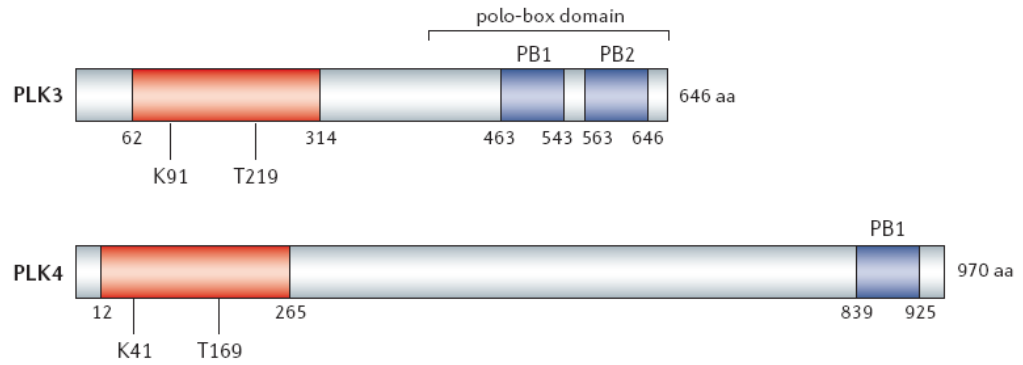


Figure 4.2: Structures of human Plk3 and Plk4 polypeptides¹⁹⁶. The structure of Plk3 is similar to Plk2 in length, position of T-loop and number of PBDs. Plk4 is distinguished from other members of Plk family by a much longer length, a slightly up front T-loop and only one PBD (Adapted from Strebhardt & Ullrich. *Nat. Rev. Cancer*. 2006, 6, 321).

4.1.2 Polo-like kinase 1 (Plk1)

Polo-like kinase 1 (Plk1) is the most investigated member of the Plk family. Plk1 protein consists of a kinase domain in the *N*-terminal region and a PBD in the *C*-terminal region^{200, 201}. The kinase domain is responsible for phosphorylation; while the PBD is involved in localisation^{202, 203} (Figure 4.3). The activity of Plk1 is tightly regulated by cells via phosphorylation within a short region of the catalytic kinase domain, known as the T-loop, together with the nearby D-box motif²⁰⁴.

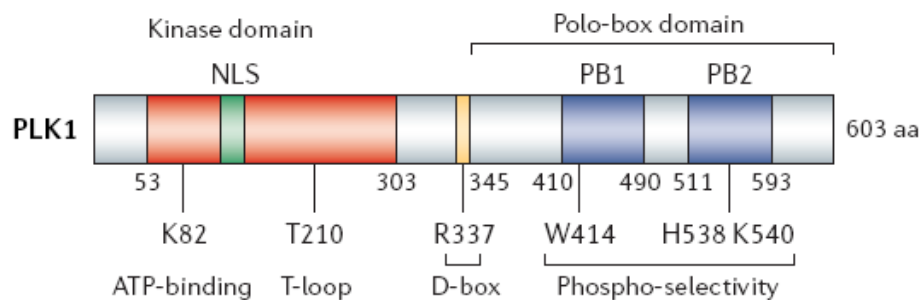


Figure 4.3: Polypeptide sequence of human Plk1¹⁹⁶. The *Plk1* gene encodes a polypeptide sequences with 603 amino acids. Plk1 consists of 2 parts: the *N*-terminal kinase domain and the *C*-terminal polo box domain (PBD). Three key residues at PBD: Trp414, His538 and Lys540, are responsible for phosphor-peptide binding. T-loop (Thr210) and the D-box motif are required for degradation by, for example the APC/C - Cdh1 system²⁰⁵, through phosphorylation, which are conserved in all members of Plks (Adapted from Strebhardt & Ullrich. *Nat. Rev. Cancer*. 2006, 6, 321).

In mouse, expression of Plk1 is observed in adult thymus tissues, ovaries and in foetuses. In humans, the expression of Plk1 was detected in the placenta, but high levels are also found in tumours of various origins. Studies with established growing cell lines show Plk1 transcript level to be low during the G1 phase of the cell cycle; accumulating during S phase and reaching maximal levels during the G2/M transition^{206, 207}.

To further examine the role of Plk1 during mitosis, recombinant human Plk1 expressed in insect cells phosphorylates casein on serine and threonine residues. It also phosphorylates myelin basic protein (MBP) and microtubule associated protein 2 (MAP2), but to a lesser extent. Confocal microscopy studies found that Plk1 binds to components of the mitotic spindle at all stages of mitosis^{208, 209}, but was redistributed as cells progressed from metaphase to anaphase. Specifically, Plk1 is associated with spindle poles up to metaphase, before relocating to the equatorial plane, where the spindle microtubules overlap, as cells progress through anaphase²¹⁰. These observations led to the conclusion that Plk1 functions in mitotic cells to control spindle dynamics and chromosome segregation (Figure 4.4).

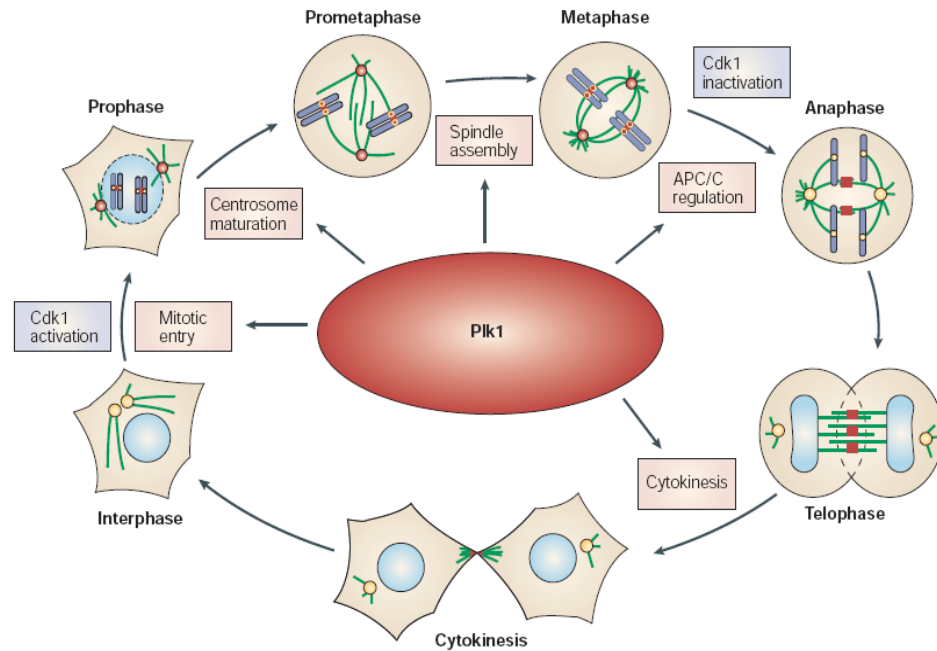


Figure 4.4: Multiple roles of Plk1 during Mitosis¹⁹⁴. Mammalian Plk1 is believed to regulate multiple processes during mitosis. These include the regulation of mitotic entry by association to components of the mitotic spindle; the control of centrosome maturation between prophase and prometaphase²¹¹; regulation of spindle assembly between prometaphase and metaphase; control of the APC/C complex between metaphase and anaphase where a multi-component ubiquitin ligase targets proteins for degradation by the proteasome; finally, the control over cytokinesis for daughter cell segregation (Adapted from Dai. *Oncogene*. 2005, 24, 214).

The activity of Plk1 was found to be regulated by Aurora kinase A and its co-factor Aurora borealis (BORA) which is also known to control G2/M phase cell cycle transition²¹². BORA accumulates in the G2 phase and promotes Aurora A-mediated activation of Plk1 through phosphorylation of T-loop Thr210, resulting in the activation of cyclin-dependent kinase 1 (CDK1) and mitotic entry.

During anaphase, Plk1 regulates cytokinesis by localising to the central spindle^{208, 213}. This promotes the local activation of RhoA GTPase, which induces assembly and ingression of the contractile ring leading to the initiation of cytokinesis²¹⁴.

4.1.3 Plk1 as a drug target

In an early study, Plk1 was found to induce mitosis in quiescent NIH 3T3 mouse embryonic fibroblast cells and caused proliferation in low serum media. Microinjection of Plk1 mRNA was later found to produce tumours in nude mice²¹⁵. Plk1 is not expressed in most normal mammalian tissues. However, as expression of Plk1 occurs in many different types of cancer²¹⁶. Therefore, Plk1 has been linked to the promotion or progression of cancer and proposed as a diagnostic marker for several tumours.

As Plk1 is activated during mitosis of dividing tumour cells, it has been suggested that inhibiting Plk1 functions may arrest cell proliferation in all human cancers regardless of their organ of origin, or oncogene and tumour suppressor gene status. A vector-based RNA interference (RNAi) study showed that normal cells can survive with depletion of Plk1²¹⁷, but Plk1 depleted carcinomas showed inhibition of cell proliferation, decreased viability and cell cycle arrest during G2/M transition, eventually leading to apoptosis^{47, 218}. Caspase-3 activation and the formation of fragmented nuclei which led to activation of p53 as a result of DNA damage were all involved in causing tumour cell apoptosis by Plk1 depletion²¹⁹.

In addition to normal quiescent cells do not necessarily require the activity of Plk1 to maintain their survival, Plk family has shown no homology to other known human kinase families to date. Therefore, compounds targeting Plk1 hold potential as effective anticancer agents, as Plk1 inhibitors should have a much improved specificity and selectivity compared to chemotherapeutic agents²²⁰.

4.1.4 Inhibitors targeting Plk1

Approximately one dozen compounds targeting Plk1 have entered clinical trials for treatment of cancers, but none have been approved to date. With the crystal structure of the kinase domain only recently becoming available²²¹ (Figure 4.5), the design of early Plk1 inhibitors relied on compound screening and ATP antagonism.

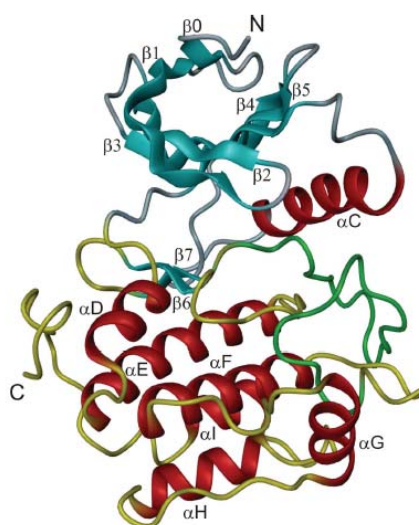


Figure 4.5: Crystal structure of Plk1²²¹. The C^α chains of the N-terminal and C-terminal lobes are coloured grey and yellow, respectively. The secondary-structure elements (SSEs) are highlighted (cyan for β-strands, red for α-helices). The activation segment, which is located in the C-terminal domain, is shown in green (Adapted from Cheng *et al. The EMBO journal*. 2003, 22, 5757).

The four best known Plk1 inhibitors are Wortmannin, Scytonemin, BI 2536 and ON01910 (Table 4.2). Wortmannin **9** is one of the earliest Plk1 inhibitors to enter clinical trials; it is a competitive ATP inhibitor. The disadvantage of Wortmannin is poor specificity; in addition to inhibiting Plk1, it also inhibits mTOR, DNA-PK, Phosphoinositide-3-kinase (PI3K), some phosphatidylinositol 4-kinases, myosin light chain kinase (MLCK) and mitogen-activated protein kinase (MAPK). Scytonemin **8** has the lowest potency against Plk1 compared to the others and inhibits other kinases.

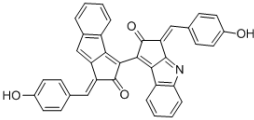
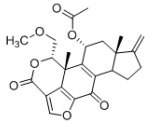
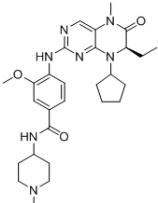
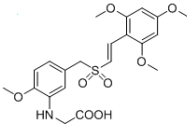
Compound	Chemical class	Potency	IC ₅₀ value against Plk1	Selectivity
 Scytonemin 8	Condensation of Tryptophan- and phenylpropanoid-derived subunits	Inhibits recombinant Plk; might be a mixed competition inhibitor	2.0 μM	Inhibits several kinase <i>in vitro</i>
 Wortmannin 9	Steroidal furanoids	An ATP-competitor that inhibits Plk1 in an <i>in vitro</i> kinase assay	24 nM	Inhibits Plk1, Plk3 and other kinases
 BI 2536 10	Dihydropteridinone derivative	An ATP-competitor that inhibits Plk1 <i>in vitro</i> and <i>in vivo</i>	0.8 nM	Shows at least 10,000-fold selectivity for Plk1 against a panel of tyrosine- and serine/threonine-kinases
 ON01910 11	Undefined	Targets Plk1 at or near the peptide binding site	9-10 nM	Inhibits Plk1; also inhibits PDGFR, ABL and FLT1 at slightly higher concentrations; at 10- to 20- fold higher concentrations, inhibits CDK1, Plk2, SRC and FYN

Table 4.2: Properties of the four best known Plk1 inhibitors¹⁹⁶.

There is one other type of inhibitor which competes for the enzyme substrate binding sites by mimicking the structure of substrates binding to Plk1. ON01910 **11** is a small molecular inhibitor using this mechanism which works through competing with the PBD of Plk1²²². BI 2536 **10** is one of the most promising Plk1 inhibitor for the treatment of cancer.

4.1.5 BI 2536

BI 2536, an ATP-competitive dihydropteridinone derivative that shows inhibitory effects on Plk1 both *in vitro* and *in vivo*, has at least a 10,000-fold level of selectivity for Plk1 against a large panel of other tyrosine and serine/threonine kinases^{196, 223, 224}. BI 2536 inhibits Plk1 with an IC₅₀ value of

0.83 nM in kinase activity assays. It also has an EC_{50} value of 8.3 nM using human colon tumour cell line HCT-116 and 9 nM in human breast cancer cell line MCF-7, as estimated by Alamar BlueTM proliferation assay with 72 hours exposure. Molecular modelling predicted that BI 2536 binds to Plk1 through Leu132 is a unique feature of this inhibitor (Figure 4.6). It could also be the key to inducing conformational changes in the protein pocket which provide selectivity for inhibiting Plk1²²⁵. According to FACS analysis, treatment with BI 2536 arrested HeLa S3 cervix adenocarcinoma cells in the G2/M cell cycle transition over a 24 hour period²²⁴. Apoptosis was also found in HeLa S3 cells 48 hours after treatment with BI 2536. At that time, Western blot was used to detect DNA degradation which provided evidence of induction of apoptosis.

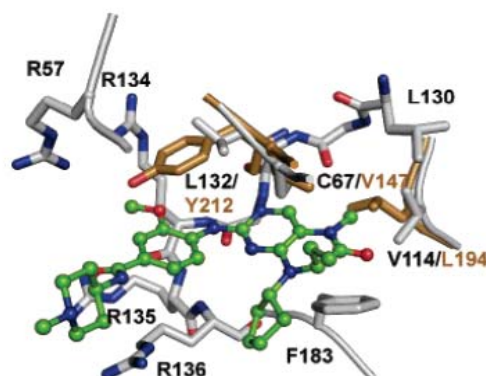


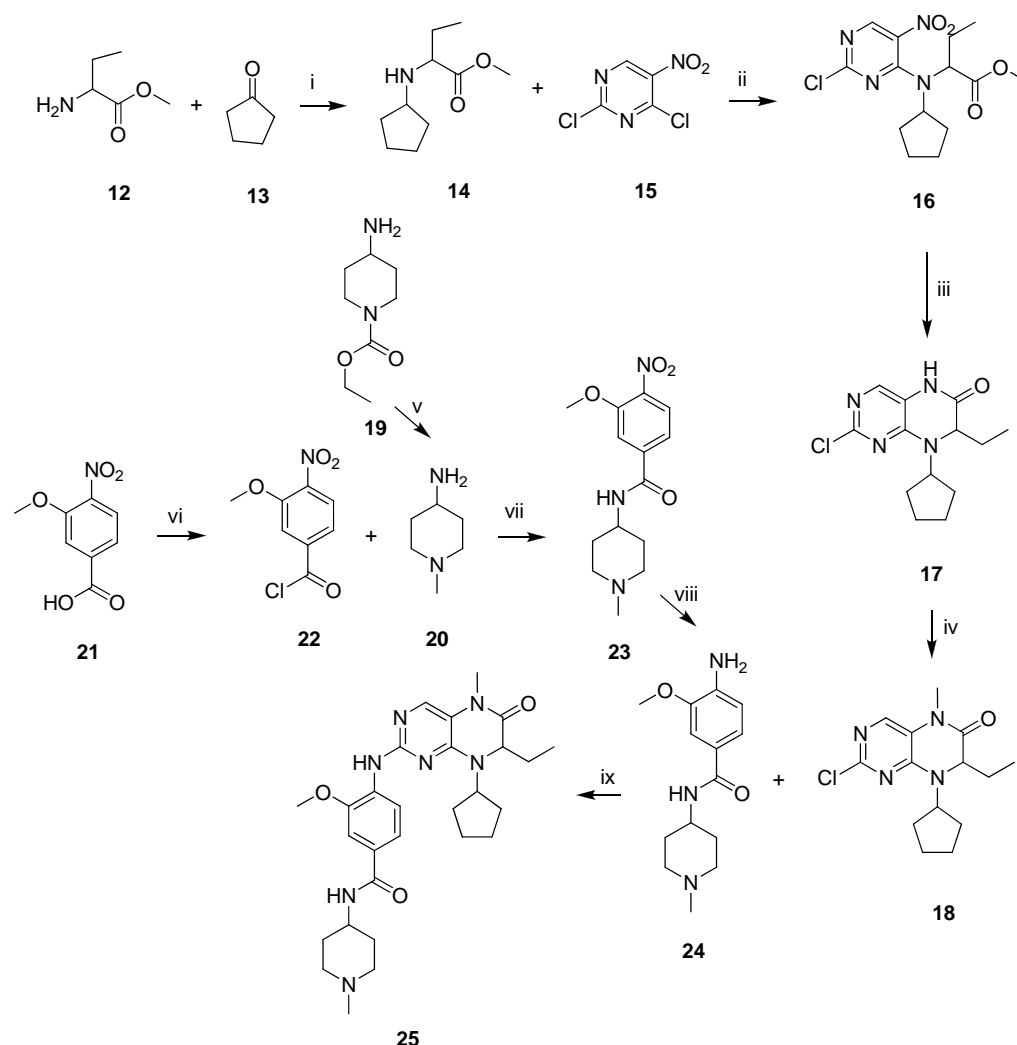
Figure 4.6: Proposed binding model for the selective Plk1 inhibitor BI 2536 in Plk1²²⁵. Computer modelling predicted that BI 2536 (green) would interact with three amino acid residues on the Plk1 protein: L132/Y212, C67/V146 and V114/L194 (brown). These interactions suppress the phosphorylation of Plk1 and possibly provide specificity in inhibiting Plk1 (Adapted from Kothe. *Chemical biology & drug design*. 2007, 70, 540).

From the above *in vitro* biological assay results, BI 2536 is one of the most promising Plk1 inhibitors currently undergoing Phase I clinical trials²²⁶. For this reason, BI 2536 would make an ideal control compound in the development of novel Plk1 inhibitors. Since BI 2536 was not commercially

available, it was proposed to synthesise BI 2536 for use as a positive control in our in-house biological assays.

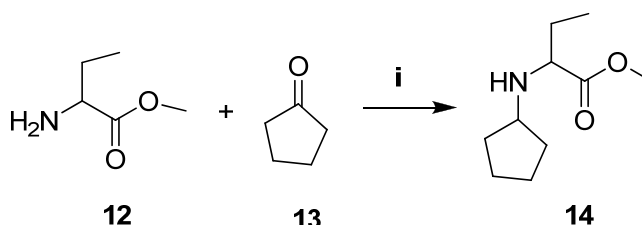
4.2 Synthesis of BI 2536 analogue

Synthesis of BI 2536 is a 9-step process by literature procedures²²⁷. However, the key starting material, D-alanine ethyl ester, is not commercially available at that time. Therefore, a modified synthetic chemistry was developed as shown in Scheme 4.1²²⁷⁻²²⁹.



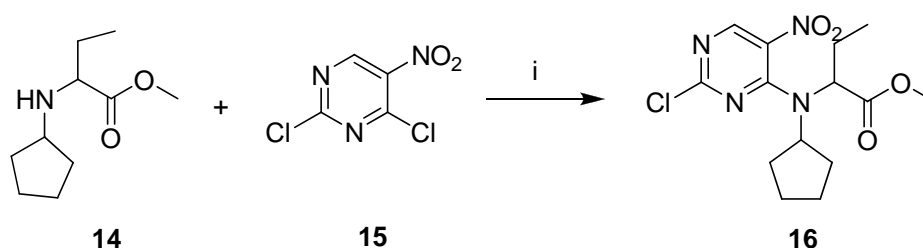
Scheme 4.1: Synthesis of BI 2536 racemate **25**. *Reagents and conditions:* (i) CH_3COONa , $(\text{CH}_3\text{COO})_3\text{BHN}$, DCM, r.t., 12 hrs; (ii) K_2CO_3 , CH_3COCH_3 , r.t., 12 hrs; (iii) Fe, $\text{CH}_3\text{CO}_2\text{H}$, 70°C , 1 h; 100°C , 1.5 hrs; (iv) CH_3I , NaH, DMA, 0°C , 20 min; r.t., 30 min; (v) LiAlH_4 , diethyl ether, reflux, 17 hrs; (vi) SOCl_2 , CHCl_3 , reflux, 3h; (vii) Pyridine, THF, r.t., 2 hrs; reflux, 1.5 hrs; (viii) Pd/C, EtOH, reflux, 1.5 hrs; (ix) 160°C , overnight.

The initial synthesis was focused on the racemic compounds **25** as the low cost of starting material **12** was commercially available. An optical HPLC can then be conveniently used to resolve BI 2536 from the racemates **25**.



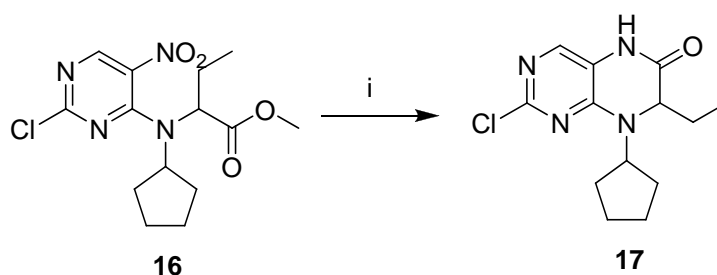
Scheme 4.2: Synthesis of methyl 2-(cyclopentylamino)butanoate. *Reagents and conditions:* (i) CH_3COONa , $(\text{CH}_3\text{COO})_3\text{BHN a}$, DCM, r.t., 12 hrs

DL-alanine ethyl ester hydrochloride **12** was treated with cyclopentanone **13** and dissolved in dichloromethane at 0°C . Sodium acetate and sodium triacetoxyborohydride were added to the reaction mixture which acts as the catalysts of this reaction. After 12 hours at room temperature, 20% aqueous sodium hydrogen carbonate solution was added to the reaction mixture until hydrogen gas no longer evolved, the excessive amount of carbonate reactions with the sodium compounds in the reaction mixture. The product was obtained through extraction of raw reaction mixture with dichloromethane, which was evaporated to give methyl 2-(cyclopentylamino)-butanoate **14** with 100% yield.



Scheme 4.3: Synthesis of the core pyrimidine ring. *Reagents and conditions:* (i) K_2CO_3 , CH_3COCH_3 , r.t., 12 hrs.

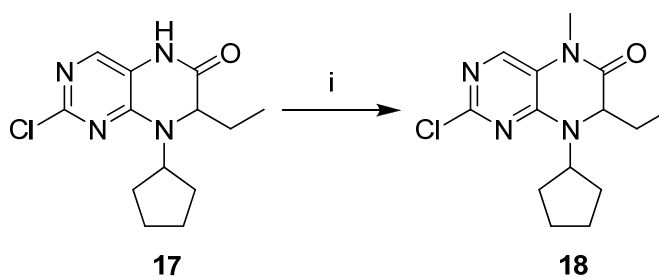
The next step was to obtain the core pyrimidine ring of the inhibitor. To prevent undesired reactions, **14** was suspended in acetone in an ice bath prior the addition of 2,4-dichloro-5-nitropyrimidine **15** and potassium carbonate. Further amounts of 2,4-dichloro-5-nitropyrimidine were added after 12 hours reaction at room temperature. This addition proved to increase the yield of **16** from 10% to 30% after chromatography. The reaction mixture was allowed for further 3 hours at room temperature. The product, in the form of brown oil, was obtained through extraction with ethyl acetate. This brown oil had at least 5 different substances, which was applied to silica gel and purified by chromatography to obtain **16** as yellow crystals.



Scheme 4.4: Cyclisation of **16** to form product with 2 aromatic rings **17**. *Reagents and conditions:* (i) Fe, CH₃CO₂H, 70°C, 1 h; 100°C, 1.5 hrs.

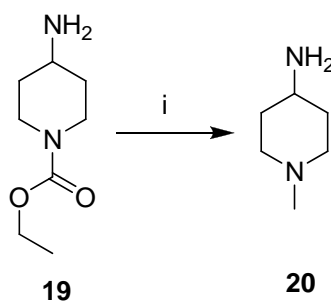
To turn the molecule **16** into a product with two aromatic rings, **16** was dissolved in excess glacial acetic acid at 70°C followed by the addition of iron powder in batch-wise manner, which minimised the undesired reaction driven by this powerful reducing agent. Here, iron was used as a reducing agent and glacial acetic acid provided H⁺ ion for the formation of an amine. The reaction mixture was stirred at 70°C for 1 hour which reduces the nitrogen dioxide to amine, and 100°C for further 1.5 hours to complete the cyclisation. The

reaction mixture was filtered hot through Kieselguhr to remove the iron powder. **17** was obtained with 60% yield.



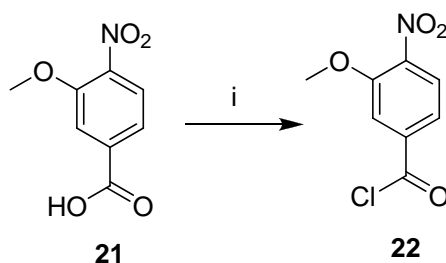
Scheme 4.5: Methylation of amine. *Reagents and conditions:* (i) CH₃I, NaH, DMA, 0°C, 20 min; r.t., 30 min.

The final reaction in preparing the pyrimidine ring was to methylate the amine group. **17** was dissolved in dimethylacetamide (DMA) at -14°C followed by the addition of methyl iodide and sodium hydride in 60% mineral oil suspension; DMA is a strong solvent in dissolving and polarising **17**, sodium hydride acts as a strong base triggering the addition of methyl group to the amine by methyl iodide. The reaction mixture was stirred for 20 minutes at 0°C which dehydrogenated the amine by sodium hydride and 30 minutes at ambient temperature for the addition of a methyl group by methyl iodide. The raw product was applied to silica gel after the removal of the reaction catalysts and solvent, which was then purified by chromatography to obtain **18** as yellow oil with 60% yield.



Scheme 4.6: Synthesis of 1-methylpiperidin-4-amine **20**. *Reagents and conditions:* (i) LiAlH₄, diethyl ether, reflux, 17 hrs.

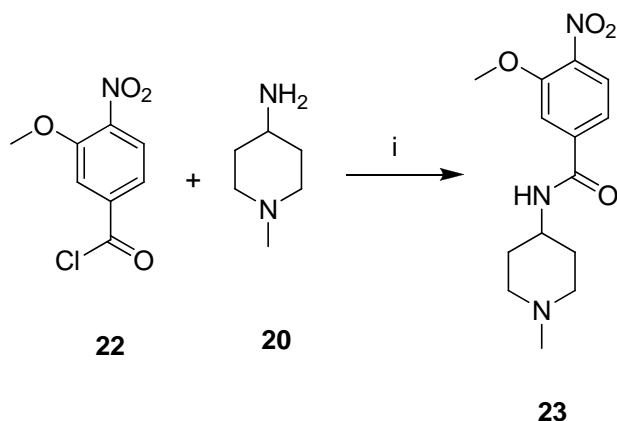
After completing the synthesis of the region which functions as the adenine of ATP, we proceeded to the synthesis of the region which acts as the phosphate tail of ATP in BI 2536. To obtain the piperidine ring required for the synthesis, ethyl 4-aminopiperidine-1-carboxylate **19** was employed as a starting material. Under anhydrous conditions (nitrogen gas), Lithium aluminium hydride (LiAlH_4) was used to reduce **19**, its addition to the reaction mixture was under anhydrous condition (nitrogen gas), which then stirred in an ice-bath for half hour for mixing without initiating the reaction. The reaction mixture was then placed into an oil bath and slowly heated to 44°C to reflux for 17 hours, allowing reduction of **19** by LiAlH_4 to occur. The unreacted LiAlH_4 was quenched by the addition of 10% aqueous NaOH at the end of the reaction. The resulting slurry was filtered under vacuum and the filtrate washed with ether to elute **20**. The combined ether was dried with magnesium sulphate, filtered and evaporated resulting in **20** as yellow oil with 70% yield.



Scheme 4.7: Synthesis of 3-methoxy-4-nitrobenzoyl chloride **22**. Reagents and conditions: (i) SOCl_2 , CHCl_3 , reflux, 3hrs.

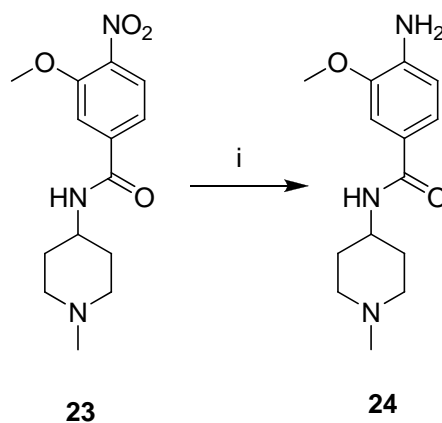
To synthesise the other starting material of the phosphate antagonist region, a suspension of 3-methoxy-4-nitrobenzoic acid **21** was dissolved in chloroform under nitrogen followed by the addition of thionyl chloride. Chloride ion has a higher polarity than hydroxide ion, which attack **21** at the hydroxide group for nucleophilic substitution. The reaction mixture was refluxed for 3 hours until a

clear solution formed under nitrogen, which prevented the reaction to be reversed by the hydroxide ion from moisture. The reaction mixture was evaporated at 60°C to remove the thionyl chloride, **22** was obtained as a yellow solid with 100% yield.



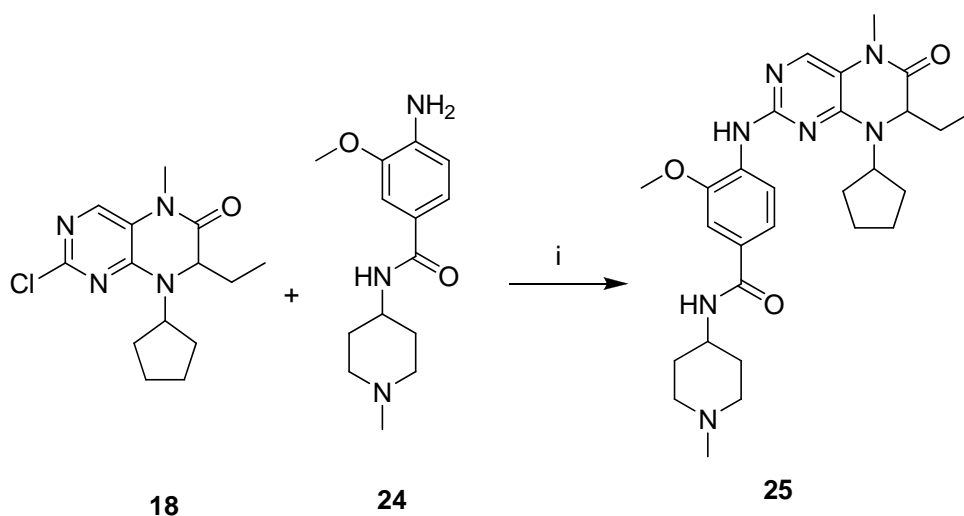
Scheme 4.8: Synthesis of 3-methoxy-*N*-(1-methylpiperidin-4-yl)-4-nitrobenzamide **23**.
Reagents and conditions: (i) Pyridine, THF, r.t., 2 hrs; reflux, 1.5 hrs.

To combine **20** and **22**, **20** was dissolved in tetrahydrofuran (THF) followed by the addition of pyridine. Pyridine acted as a base to allow the substitution of amine on piperidin **20** to chloride on the alanine **22**. Followed by the addition of **22**, the reaction mixture was stirred for 2 hours under nitrogen at ambient temperature, which prevented the conversion of **22** to **21**. 1 hour reflux was followed allowing the completion of the reaction. As **23** is a non-polar molecule, re-crystallisation with ethanol is a better method than column chromatography for the purification of this compound, as a large amount of product would stay in the silica and the use of high polarity solvent may result in contamination by silica. Re-crystallisation precipitated **23** as white solid with 65% yield.



Scheme 4.9: Reduction of 3-methoxy-*N*-(1-methylpiperidin-4-yl)-4-nitrobenzamide **23**.
Reagents and conditions: (i) Pd/C, EtOH, reflux, 1.5 hrs.

Palladium in 10% carbon, which is a powerful agent in reducing large, non-polar molecules²³⁰⁻²³², was used to reduce the nitrogen dioxide on **23** to primary amine. Tin chloride could replace palladium as the reducing agent²³³, but the yield would be reduced. The reaction mixture was stirred at ambient temperature under hydrogen gas, which provided the source of hydrogen for the formation of amine. Kieselguhr was used to filter out the palladium at the end of the reaction. Re-crystallisation with hot ethanol was used again to purify the non-polar product. **24** precipitated as white solid, which was suction filtered out with 90% yield.



Scheme 4.10: Synthesis of BI 2536 racemic **25**. *Reagents and conditions:* (i) 160°C, overnight.

To combine **18** and **24** to form the final compound, both compounds were heated at 160°C overnight without any solvent and base (catalyst) to allow the occurrence of nucleophilic substitution by amine. The completion of the reaction was checked by TLC (100% ethyl acetate, $R_F = 0.22$). The reaction mixture was purified by column chromatography; Purification by recrystallisation was followed, ethyl acetate was added to dissolve the product, followed by the addition of excess hexane until the formation of precipitate. The precipitate was filtered and washed with hexane yielding **25** as a yellow solid in 50% yield. The chemical structure of this compound was confirmed by mass spectrometry (MS) and ^1H nuclear magnetic resonance (NMR).

4.3 Conclusion

Plk1 is a kinase involved in multiple roles within mitosis and cytokinesis. Evidence has shown that over expression of Plk1 is associated with the formation of certain types of cancers. As normal cells were found to survive without the expression of Plk1, targeting Plk1 as an anti-cancer drug has become a favoured topic in cancer research. Since the claims of the first Plk1 inhibitor a decade ago, about a dozen Plk1 inhibitors have entered clinical trials to date. One of these compounds is BI 2536, one of the most potent and selective Plk1 inhibitor reported.

Since BI 2536 is unavailable commercially, we aimed to synthesise this compound for use as a positive control in our project to design novel Plk1 inhibitors. Compound **25** was successfully prepared as the racemates of BI

2536. However, by the time we completed the synthesis, the clinical compound BI 2536 has become available commercially. Therefore, further purification and resolution of compound **25** was not carried out.

Chapter Five

General discussion, conclusion and future work

5.1 General discussion and conclusion

5.1.1 Elucidation of the mechanism of action of a novel CDK9 inhibitor

Our mechanism studies of S-134 have shown that this novel inhibitor induced a nano-molar inhibition across a large range of cell lines using MTT assay with 72 hours exposure. In particular, S-134 was most potent in inhibiting HCT-116 human colon and A2780 human ovarian carcinoma cell lines respectively. S-134 showed a micro-molar growth inhibition on the human malignant glioma cell line SNB19 and human astrocytoma cell line U373; these are actually promising results in comparison to some clinical drugs. Using SNB19 cells as an example, one of the “gold standard” treatments for glioma is a small molecule inhibitor called temozolomide, which has a GI_{50} value of 30.70 μM in this cell line under similar experimental conditions (Personal communication with J.H. Zhang).

The data from kinase assays show S-134 to be most potent in inhibiting the activity of CDK9/cyclin T1, followed by CDK2/cyclin E and CDK7/cyclin H. Comparing these kinase assays with those from other CDK inhibitors in clinical trials, S-134 achieved a better selectivity and potency between these three CDKs than Roscovitine, but not Flavopiridol. More importantly, the kinase assay data could not conclude which of these three compounds achieved the best potency and selectivity on CDK9 in cells. Firstly, there are numerous protein functions in conjunction with CDK9 during cell cycle, which could interfere with the binding between the inhibitors and CDK9. Also, it is not possible to use this type of *in vitro* protein assay to verify whether other kinases and proteins inhibited by the compounds before CDK9, as large number of human kinases and proteins have still not being fully characterised.

In terms of cell cycle, S-134 had no effect at its GI₅₀ concentration but induced a G2/M transition block in HCT-116 cells at 10 times GI₅₀ concentration. This inhibition was also observed with DRB, a known CDK9 inhibitor with the same time points at the equivalent GI₅₀ concentration. Flavopiridol has also been reported to induce this G2/M transition arrest in a number of cell lines²³⁴. In addition, the inhibition of CDK7 could result in this cell cycle accumulation, as the concentration of compounds required for this blockage exceeded the IC₅₀ for CDK7 in the kinase assay: RB activity is another possible candidate contributing to this arrest. The cell cycle arrest induced by Flavopiridol has been found to be more potent in cell lines expressing RB to enhance resistance to apoptosis²³⁴. The same study also pointed out the apoptosis caused by Flavopiridol did not relate to RB activity and this cell cycle arrest.

Assays which aim to demonstrate that S-134 causes cell death include the Annexin-V assay, PARP cleavage by Western blot and the caspase-3 assay. Both Annexin-V and caspase-3 assays used HCT-116 cells. The Annexin-V assay, which measures the percentage of total cell death, showed cell death reached a peak level at 36 hours with 1 μ M S-134. The caspase-3 assay, which only measures apoptotic cell death, showed the peak of caspase-3 activation at 48 hours with 1 μ M S-134. Combining the data from both assays, we can conclude that S-134 induces both apoptosis. Since the Annexin-V assay has shown a higher population of death cells than the other assays used, it is a possible suggestion that S-134 also induces necrotic cell death. In the same cell line, DRB was seen to induce a higher level of cell death than S-134 in the caspase-3 assay, based on their GI_{50} concentrations. In MTT assays, we demonstrate the cytostatic (i.e. growth inhibition) rather than cytotoxic effect (i.e. how effect of compound in killing the cells) of the compounds, hence the equivalent GI_{50} concentration is no reflection on the efficiency of compound in causing cell death. Therefore, the difference in caspase-3 activation by the two compounds is possibly due to the compound concentration (i.e. 1 μ M S-134 compared to 60 μ M DRB). Alternatively, it could be an indication that S-134 is a slower acting compound compared to DRB.

To verify that S-134 targets CDK9 and to clarify its effect on CDK7 in cells, Western blot was used to detect the phosphorylation of RNAP II Ser 2 and Ser 5 using A2780 cells, which indicates that S-134 specifically inhibits CDK9 up to 1 μ M, followed by CDK7. Compared to S-134, DRB appears to be a more specific CDK9 inhibitor as the phosphorylation of Ser 2 is always more severely reduced than Ser 5. Since there is some evidence showing that

phosphorylation of Ser 5 could be related to CDK9 activity¹⁸¹, the reduced phosphorylation states of Ser 5 induced by S-134 could be due to the inhibition of CDK9, rather than an inhibition of CDK7.

The effect of S-134 on anti-apoptotic proteins Mcl-1, Bcl-2 and XIAP was observed by Western blot. The expression of Mcl-1 was reduced by S-134, followed by Bcl-2 and XIAP. At 24 hours, Ser 2 phosphorylation was reduced by 1 μ M S-134, the inhibition of these anti-apoptotic proteins, which started with 1 μ M, was undoubtedly affected by the inhibition of CDK9. This reduction also proved the apoptotic cell death observed by PARP cleavage, which appeared with 2.5 μ M S-134, is a direct result of CDK9 inhibition. The level of reduction of the anti-apoptotic proteins observed by Western blot could be affected by the half-life of the proteins; a shorter protein half-life would reduce the level of protein detected by Western blot, which may explain our observation on XIAP being more profoundly suppressed than Mcl-1 at 24 hours²³⁵.

p53 is an important tumour suppressor which responds to DNA damage and other genomic alterations; its inactivation and activity is closely linked to the development of tumours²³⁶. In A2780 cells, p53 protein levels increased in a dose dependent manner. The increase in p53 level should be caused by the altered transcription in the absence of CDK9⁸⁹. HDM-2, the negative regulator of p53, showed a very low level of reduction at 24 hours with 5 μ M S-134. This indicates that S-134 stabilised, but not necessarily activates p53, at concentrations below 5 μ M at 24 hours, as the negative feedback loop was not inhibited. Flavopiridol has been reported to activate p53 by suppressing CDK9, which inhibited the transcription of HDM-2²³⁷. As S-134 is a CDK9

inhibitor, it should also activate p53. A higher concentration may be required to observe this significantly.

The effect of S-134 on gene transcription was examined by RT-PCR. The mRNA of *Mcl-1*, *Bcl-2*, *XIAP* and *HDM-2* were investigated. In A2780 cells, the transcription all the genes studied were found reduced. The reduced patterns of *Mcl-1*, *Bcl-2* and *XIAP* were similar to those observed in Western blot at the corresponding time point. Comparing the effects of S-134 on these genes and the proteins detected by RT-PCR and Western blots respectively, the effect of the compound on the genes was more profound than on the proteins. Using *HDM-2* as an example, the transcription at 24 hours was reduced from 2.5 μ M S-134, with protein expression reduced with 5 μ M only. This is possibly due to the RNA synthesis being suppressed by S-134, which led to the reduced expression in proteins. Another example is the transcription inhibition of *Bcl-2*, which was much more profound than on protein expression, indicating that Bcl-2 protein might have a long half-life which delays the observation of reduced protein expression on Western blot^{238, 239}.

To summarise the mechanism of action of S-134, it is a novel CDK9 inhibitor with nano-molar activity *in vitro*. It primarily inhibits CDK9 at biochemical and cellular levels as well as affecting CDK7 at higher concentrations. The inhibition of CDK9 leads to the alteration in transcription elongation. The inhibition of CDK9 results in reduction of anti-apoptotic factor, including Mcl-1, Bcl-2 and XIAP, which increases the sensitivity of cells to apoptotic signals. The genomic abnormality in cells enhances the expression of p53, which possibly induces a G2/M transition accumulation in

the cell cycle. Cell-cycle arrest is followed by significant cell death through apoptosis and necrosis.

A therapeutic window of S-134 between tumour and normal cells has been demonstrated in a number of experiments. An approximate eight fold selectivity between HCT-116 and MRC-5 cell lines has been shown in MTT assays. In terms of cell death, Annexin-V assays using MRC-5 cells and the same compound concentration and time points as with HCT-116 cells indicated that no cell death was induced. In addition, Western blot only showed PARP cleavage induced at 24 hours with 5 μ M S-134, double the concentration in A2780 cells. For the effect on CDK9, Westerns blots using MRC-5 cells show a higher concentration of S-134, compare to A2780 cell, is required to affect the phosphorylation of RNAP II Ser 2, hence no effect on the anti-apoptotic proteins, while DRB showed the same phosphorylation pattern of Ser 2 in both A2780 and MRC-5 cells for the inhibition of Ser, resulting in a reduction in Mcl-1 was detected.

The discovery of S-134 is only the beginning of the development of our novel CDK9 inhibitors. From MTT assays, a number of other analogues in our novel CDK9 series modified from S-134 have proved better compounds in terms of potency and selectivity between cancer and normal cells. The Cellomic Array Scan using HCT-116 to observe the effect of compounds on p53 stabilisation indicating a number of analogous performs better than S-134. The continuous biology mechanism studies and compound modification will hopefully produce a potential clinical candidate in the future.

5.1.2 Elucidation of the mechanism of action of ZJU-6

A group of semi-synthetic compounds were screened in MTT assays to estimate their cellular growth inhibition. These compounds were derived from a natural product known as Erianin, a small molecule produced by a plant species *Dendrobium chrysotoxum*¹⁸². The aim of the synthetic modification was to enhance its activity, but all the modified compounds possessed reduced potency, by at least 20 fold compared to Erianin in cellular growth inhibition assays. The most potent compound in this group, ZJU-6, was selected for further study. ZJU-6 was screened using 10 cell lines for estimating its effect on cell growth; its GI₅₀ values in most of the cell lines tested were reduced by at least 20 fold compared to Erianin, with a few exceptions including HCC-2998, a human colon cell line.

The image study showed Erianin and ZJU-6 induced similar physical effect on the cells using four times GI₅₀ concentration of the corresponding compound. Both compounds caused cell death by inhibiting cell division, in which the genetic material in cells failed to condense in order to form chromosomes. As the formation of chromosomes is triggered by the formation of microtubules (i.e. polymerisation of tubulin) during mitotic prophase⁵⁶, this observations confirmed Erianin, as reported from literature¹⁸², and ZJU-6 inhibited the polymerisation of tubulin, hence resulting a cell cycle arrest at G2/M transition, which was proved by FACS.

The mode of cell death induction by Erianin has not been reported. Here, the cell death caused by Erianin and ZJU-6 had been observed by four different

experiments. The significant pre-G1 population from cell cycle analysis showed an early indication that both compounds induce similar level of cell death in MCF-7 cells, under the same equivalent GI_{50} concentration, which was further confirmed by Annexin-V assay. However, Erianin induced significant caspase-3 activation at 10 times GI_{50} concentration, while ZJU-6 activated caspase-3 dose-dependently. PARP cleavage, as detected by Western blot, revealed a similar pattern to caspase-3 assays for both compounds. The data confirmed that both compounds induced cell death, possibly with different modes of cell death induction. Erianin induced cell death possibly by caspase-3 dependent and independent apoptosis, in addition to non-apoptotic cell death, such as necrosis, which has been reported¹⁸²; while ZJU-6 induced specific caspase-3 dependent apoptosis. As mention previously, Erianin has been reported to induce heavy toxicity to patients during clinical trials (S. Wang personal communication); the various mode of cell death employed by Erianin could be a possible factor responsible for this issue.

The transcription of *Bcl-2* has been found reduced by Erianin¹⁸⁴, which responsible for cell death. Therefore, ZJU-6 could possibly reduce the expression of *Bcl-2*. The effect of compounds on Bcl-2 and Mcl-1 protein was examined by Western blot in MCF-7 cells. No change on Mcl-1 expression was detected, while an extra band of protein was induced with treatment of Erianin and ZJU-6, but not with DMSO vehicle control, on the Western blot. This means both compounds affect Bcl-2 in the same manner. Although the reduction of Bcl-2 is well linked to apoptosis (see section 1.3), however, from our observation, it does not necessarily apply to Erianin and ZJU-6. If there is another possible mechanism that Erianin and ZJU-6 affect Bcl-2 other than a

simple reduction, one suggestion is that the compounds affect the phosphorylation status of Bcl-2, another suggestion is that both compounds alter the transcription machinery which then increases the length of the amino acid chain of Bcl-2¹⁸⁸.

The effect of compounds on transcription was examined by RT-PCR using the same time points and doses as in Western blot. Both compounds reduced the transcription levels of *Mcl-1* and *Bcl-2*. Erianin inhibited *Bcl-2* transcription to a greater extent, while ZJU-6 was more effective in inhibiting *Mcl-1* transcription. The results from Western blot and RT-PCR showed the compounds affected the transcription machinery of the anti-apoptotic proteins rather than having direct interaction with the proteins. For *Mcl-1*, the observable changes detected in transcription did not result in changes in protein level may be due to the longer half-life of these proteins than their RNAs²³⁸⁻²⁴⁰. This transcription inhibition of *Mcl-1* by ZJU-6 could be one of the many possibilities triggering apoptotic cell death.

There was no information about the effect of Erianin on p53 in the literature. As Erianin inhibits the polymerisation of tubulin, which resulting in cell abnormality, this could trigger an increase in p53 protein in an attempt to repair the abnormality²⁴¹. Here, we proved both Erianin and ZJU-6 increase the level of p53 in MCF-7 cells by Western blot (section 3.7). However, there is no reduction in HDM-2 protein or mRNA, proved by Western blot and RT-PCR respectively, by either compound; hence, the p53 protein may not be fully active on its functions.

Erianin clearly inhibited tubulin polymerisation, as reported in the literature¹⁸². ZJU-6 should also have this property as indicated by the imaging

study. A biochemical assay was used to confirm the effects of the compounds on tubulin polymerisation, which proved ZJU-6 was more effective than Erianin. The concentration used was above the GI_{50} of Erianin and below that of ZJU-6. Although it was a non-cellular detection, it is sensible to suggest that ZJU-6 may primarily function by inhibiting tubulin polymerisation, while Erianin may initially target other factors which lead to this inhibition.

Erianin has already been proved to have anti-angiogenic effects by using an assay similar to our *ex vivo* chick embryo chorioallantoic membrane (CAM) assay¹⁸². The CAM assay here indicated that ZJU-6 was more effective in suppressing angiogenesis than Erianin. The use of GI_{50} concentration in MCF-7 for this experiment was aim to achieve an observable result without killing the embryo, which minimised the possible problem of ZJU-6 entering into cells. However, if this assumption was not correct and same concentrations of both compounds were used, we might not be able to conclude that ZJU-6 was more effective at anti-angiogenesis than Erianin.

The aim of introducing a free radical into ZJU-6 was to introduce an anti-oxidant property for cancer prevention. Biochemical assays using DPPH and cellular assays with H_2DCFDA analysed by FACS were used to examine the anti-oxidant properties of Erianin and ZJU-6. Erianin has not been classified as anti-oxidant. However, in the biochemical assays, Erianin was found to be a more potent anti-oxidant than ZJU-6. In cellular assays, both compounds failed to reduce the oxidative state of cells and were unable to protect the cells against attack by oxygen radicals from hydrogen peroxide. In chapter one, the anti-oxidant effect of EGCG (a polyphenol in green tea) was mentioned. However, a high dose of EGCG would be required for it to be observed in cells

and tissues¹⁴³. Biochemically, Erianin and ZJU-6 have anti-oxidant properties, but they were weaker than EGCG. The concentrations of Erianin and ZJU-6 used in assays determining their anti-oxidant properties were high enough to induce significant cell death. Hence, unlike EGCG, it was not possible to examine the anti-oxidant effects of Erianin and ZJU-6 at high-doses. Therefore, Erianin and ZJU-6 would not be suitable compounds for the use as anti-oxidants in cancer prevention.

A natural product and its derivatives should target a number of molecular targets. However, based on the data collected from our study and from the available literature^{182, 184}, we could only conclude the following: Erianin is a natural product with nano-molar activity in tumour cells. It induces cell cycle arrest at the G2/M transition through inhibiting the formation of microtubules and induces cell death. Erianin also inhibits the transcription of *Bcl-2*; it also has anti-angiogenic and anti-oxidant properties. ZJU-6 is a micro-molar activity small molecule derived from Erianin, created with the intention of enhancing the activity of the molecule. The addition of an extra structure may have reduced its effect on cellular growth inhibition and its ability to enter cells. ZJU-6 evokes a similar cell cycle effects as Erianin. However, unlike Erianin, the main pathway of cell death induced by ZJU-6 is apoptosis. Its tubulin polymerisation inhibition, which is believed to be the primary mode of action of ZJU-6, and its anti-angiogenic properties were enhanced. However, *Bcl-2* suppression and the anti-oxidant property of the molecule were reduced. Both Erianin and ZJU-6 stabilise p53 though inhibiting the polymerisation of tubulin. Neither compound would be a suitable anti-oxidant.

Throughout the mechanism studies on Erianin and ZJU-6, the ability of ZJU-6 to enter cells has been emphasised as the reason contributing to the reduced GI₅₀ value. Alternatively, the origins of Erianin and ZJU-6 could be used to form an alternative hypothesis to explain this difference. Erianin is a natural product, which evolved together with the plant species; therefore Erianin should be more cytostatic and less cytotoxic. ZJU-6 is a synthetic natural product derivative which aims to enhance the activity of Erianin; hence it is more cytotoxic and less cytostatic. Accordingly, MTT assays indicated that Erianin performed better as a cytostatic agent, whereas ZJU-6 is a more cytotoxic agent as demonstrated in caspase-3 assays.

5.1.3 Synthesis of BI 2536 racemate

BI 2536 is one of the most selective and potent small molecule inhibitors of Plk1. An alternative synthetic route was carried out which achieved synthesis of a racemic BI 2536; this route could potentially lead to synthesis BI 2536 itself. The synthetic routes used to synthesise the aromatic pyrimidine ring **18** were similar to that described in the patent of BI 2536²²⁴. The synthetic route for alanine **24** was a combination of routes used for synthesis of similar molecules.

The racemate had been tested for cellular growth inhibition (data not shown), which was ~600 times less effective in cell growth compare to the literature data of BI 2536. This difference in cellular growth inhibition suggested the possibility of impurities. Although ¹H NMR and mass spectrometry data did not indicate the presence of impurities, but there are some exceptions of impurities which could not be detected by these analytical

methods. This possible impurity was probably the main reason for the reduction in potency of our racemate, with the loss of stereo chemistry being a further reason²⁴². The interaction between the racemates itself is also an possibility, but less likely.

5.2 Future work

According to the biological assay results with S-134, we proved this molecule to be a potent and selective CDK9 inhibitor *in vitro*. To fully study the cytotoxicity of the molecule across a large number of human cell lines from other origins, S-134 could be sent for screening against the NCI 60 cell panel. To test the selectivity of the molecule against other members of human CDKs, kinase assay screening against CDK1, 3, 4, 5, 6 and 8 should be done. Although a highly unlikely possibility, the effect of S-134 could vary between cell lines and cell cycle analysis should be done in a range of cell lines to investigate the possibility. Although we have done a range of assays to test the effect of S-134 on cell death, further experiments could be done to interrogate cell death pathways, such as the caspase-7 activation assay. In addition to the proteins and genes we screened in Western blot and RT-PCR, respectively, there are still a number of proteins affected by CDK9 inhibition, such as BAG-1²⁴³. Individual compound screening is an extremely time consuming process. The long term aim of the project is to obtain a potential drug candidate from large number of compounds; high-throughput screening (HTS) should be used to replace western blots and RT-PCR, which could generate data on the effect of a compound series with respect to a large number of molecular targets in a short period of time. The most common HTS is the microarray technology

which screens the effects of compounds on hundreds of genes at the RNA level and could predict the effect of compounds on proteins. For those genes whose transcription is significantly altered, the effect of compounds on protein expression could then be investigated using traditional technology such as Western blot. The limitation of Western blot is the number of samples that can be tested at one time. The Cellomic Array Scan used in p53 stabilisation screening could represent a way forward to increase the number of samples per assay, hence increasing the number of concentration points and compounds screened.

From our data, S-134 seems to be a slow acting compound compared to other CDK9 inhibitors; other *in vitro* assays, such as time lapse cell imaging and diffusion assay studies, could be done. In addition, further characterisation including stability studies and PK determination, should also be carried out. For *in vivo* animal studies, S-134 should be tested in mouse xenografts; as our data proved that the molecule is a promising inhibitor of cancer growth. Studies on the effect of S-134 on leukaemia cell death and HIV replication could also be done in the future. After all these studies with S-134 and other promising analogues selected from SAR, compounds with promising *in vitro* and *in vivo* data will be obtained.

In our study of natural products, the chemical modification of Erianin to ZJU-6 reduced the potency of the molecule; one of the hypotheses is the reduced transportation into cells. A diffusion assay such as the lipophilicity test could be used; a more lipophilic molecule would have increased affinity to diffuse across the cell membrane. Furthermore, imaging studies using labelled compounds could observe transportation/diffusion efficiency²⁴⁴. In terms of

further direction for *in vitro* assays, growth inhibition assays could be done in additional tumour cell lines. Cell cycle analysis could be done in these cell lines, expanding time points and concentrations to further elucidate the cell cycle perturbation effects of Erianin compounds. Other assays could also be done to consolidate the evidence on cell death induction, such as the red green staining in conjunction with cell imaging. The effects on tubulin polymerisation could be researched using cellular assays such as the collagen gel migration assay. For angiogenic assays, the CAM assay could be repeated using the same concentration with all compounds; this was not carried out as it was a time consuming assay with a potentially low success rate. Alternatively, Western blot and PCR could be used to test for proteins involved in angiogenesis, such as VEGF. Erianin has been reported to inhibit endothelial tube formation, migration and adhesion using HUVECs cell, which indicated Erianin may work in more than one step in the process of angiogenesis. This assay can be performed to prove the anti-angiogenic property of ZJU-6.

Although natural products are a good source from which to search for potential drug candidates, it is hard to predict and verify primary targets. Therefore, modern technology such as microarray could be a quick method in the search for these target proteins. However, availability of compounds is a fundamental limitation in these suggestions; the yield after modification to ZJU-6 was low, restricting the number of experiments that could be done. High yield and ease of synthesis are fundamental aims of semi-synthetic compounds. Further detailed studies in the mechanism of action of Erianin are also necessary to guide synthesis of more promising compounds.

Chapter Six

Materials and Methods

6.1 Suppliers of reagents

Amersham Pharmacia Biotech (Little Chalfont, Buckinghamshire, UK)

ECLTM Western blotting detection kit, HyperfilmTM ECL

Beckman Coulter (London, UK)

COULTER CLENZ[®] Cleaning Agent, IsoFlowTM Sheath Fluid

Bioline (London, UK)

Oligo (dT)₁₈ Primers

Bio-Rad Laboratories (Hertfordshire, UK)

Bio-Rad DC protein assay kit, bovine serum albumin (BSA) standard solution, polyvinylidene difluoride (PVDF) membrane

Calbiochem (Nottingham, UK)

Seliciclib, 5,6-dichloro-1-β-d-ribofuranosylbenzimidazole (DRB)

Cell Signalling Inc. (Beverly, MA, USA)

Rabbit anti-Mcl-1 monoclonal antibody, rabbit anti-XIAP monoclonal antibody, rabbit anti-PARP polyclonal antibody

Champion Photochemistry International Limited (CPIL) (Brentwood, UK)

X-ray films processing solutions (Developers and Fixers)

Covance Research Products (Berkeley, CA, USA)

Mouse anti-RNAP II monoclonal antibody (clone 8WG16), mouse anti-RNAP II Ser 2 monoclonal antibody (clone H2), mouse anti-RNAP II Ser 5 monoclonal antibody (clone H5)

Cytoskeleton Inc (Denver, Colorado, USA)

Microtubules/tubulin Biochem KitTM, HTS tubulin

Dako (Glostrup, Denmark)

Mouse anti-Bcl-2 monoclonal antibody, mouse anti-p53 monoclonal antibody, goat anti-mouse IgG-HPR conjugated antibody, swine anti-rabbit IgG-HPR conjugated antibody

Fisher Scientific (Loughborough, Leicestershire, UK)

Acetone (analytical reagent grade), Acetonitrile (HPLC grade), chloroform, concentrated HCl (analytical reagent grade), denatured ethanol (IMS), dichloromethane, ethanol, ether, ethidium bromide (EtBr) solution, ethyl acetate, glacial acetic acid (analytical reagent grade), hexane, magnesium sulphate, methanol (analytical reagent grade), potassium carbonate (K₂CO₃), pyridine, silica, sodium chloride (NaCl), sodium hydroxide (NaOH), sodium hydrogen carbonate (NaHCO₃), tetrahydrofuran (THF)

Invitrogen Ltd (Paisley, UK)

High resolution agarose

Joice and Hill Poultry Ltd (Peterborough, UK)

Fertilised chicken eggs

Millipore Corporation (Billerica, MA, USA)

CDK9/cyclin T1, ATP, PDK

MWG-Biotech AG (Ebersberg, Germany)

Forward and reverse primers for β -Actin

Oxoid limited (Hampshire, UK)

Phosphate buffer saline (PBS) tablet

Perkin Elmer (Massachusetts, USA)

Easy-lite reagent

Qiagen Ltd (Crawley, West Sussex, UK)

RNeasy mini kit

Roche Diagnostics (Lewes, East Sussex, UK)

Reverse transcriptase, nucleotide mix (dNTP), Taq DNA polymerase, protease inhibitor cocktail tablet

Santa Cruz Biotechnology Inc. (Santa Cruz, CA, USA)

Annexin V-FITC kit

Severn Biotech Ltd, (Worcestershire, UK)

30% acrylamide solution

Sigma-Aldrich (St Louis, MO, USA)

Acetyl-Asp-Glu-Val-Asp-7-amido-4-methylcoumarin (Ac-DEVD-AMC), 4-aminopiperidine-1-carboxylate, ammonium persulfate (AMPS), aprotinin, boric acid, bovine serum albumin (BSA), brij-35, bromocresol Blue, calcium chloride (CaCl₂), caspase-3 fluorimetric assay kit, 2, 4-dichloro-5-nitropyrimidine, 3-[(3-Cholamidopropyl)dimethylammonio]-1-

propanesulfonate (CHAPS), ColorBrustTM electrophoresis markers, DL-Alanine ethyl ester hydrochloride, D-2-aminobutyric acid, 2',7'-dichlorodihydrofluorescein diacetate (H₂DCFDA), 3-(4,5-dimethylthiazol-2-yl)-2,5-diphenyltetrazolium bromide (MTT), cyclopentanone, 1,1-diphenyl-2-picrylhydrazyl (DPPH), dimethylacetamide (DMA), dimethylsulphoxide (DMSO), dithiothreitol (DTT), Direct loadTM PCR 100bp low ladder, ethylenediamine tetra-acetic acid (EDTA), ethyl 4-aminopiperidine-1-carboxylate, ethylene glycol-bis(β-aminoethylether)-*N,N,N',N'*-tetra-acetic acid (EGTA), fetal bovine serum (FBS), forward and reverse primers for Mcl-1, Bcl-2, XIAP and HDM-2, gel loading solution (for nucleic acid product), L-glutamine, glycerol, glycerol-2-phosphate, β-glycerophosphate, *N*-[2-hydroxyethyl]piperazine-*N'*-[2-ethanesulfonic acid] (HEPES), hydrogen peroxide (H₂O₂), iron powder, Kieselguhr, leupeptin, lithium aluminium hydride (LiAlH₄), magnesium chloride (MgCl₂), β-mercaptoethanol, 3-methoxy-4-nitrobenzoic acid, methyl iodide, minimum essential medium, molecular grade H₂O, MOPS-NaOH, mouse anti-MDM2 monoclonal antibody, mouse anti-β-actin monoclonal antibody, non-essential amino acids, palladium in 10% carbon, penicillin, phenylmethylsulfonyl fluoride, polyoxyethylenesorbitan monolaureate (Tween 20), potassium chloride (KCl), propidium iodide (PI), ribonuclease A, RPMI-1640 liquid medium (with L-glutamine and sodium bicarbonate), sodium acetate, sodium bicarbonate, sodium citrate, sodium deoxycholate, sodium dodecyl sulphate (SDS), sodium hydride (NaH), sodium orthovanadate (Na₃VO₄), sodium triacetoxyborohydrate, sucrose, *N,N,N',N'*-Tetramethylethylenediamine (TEMED), tert-butyl-methyl-ether, thionyl chloride, thymidine, Trizma® base [Tris(hydroxymethyl)aminomethane], Trizma® hydrochloride (Tris.Cl) [Tris(hydroxymethyl)aminomethane hydrochloride], triton X-100, trypsin/EDTA solution, water (molecular biology grade)

6.2 General cell culture

A2780 and WI38 cells were purchased from European Collection of Cell Cultures (ECACC, UK). All other cell lines were obtained from the cell bank at Centre for Biomolecular Sciences (Division of Medicinal Chemistry and Structural Biology, School of Pharmacy, University of Nottingham). MRC-5 and WI38 cells were cultured in minimum essential medium with 10% fetal bovine serum (FBS), 1% 7.5% Sodium bicarbonate, 1% 0.1 mM non-essential amino acids, 1% 1 M Hepes, 1% 200 mM L-glutamine and 1% penicillin. All other cell lines were maintained in RPMI-1640 with 10% FBS.

6.3 *In vitro* biological assays

6.3.1 Preparation of sample compounds

The novel CDK9 inhibitors tested in this thesis were synthesised by Mr S. Shi (University of Nottingham, UK), while the nature product derivatives were

synthesised by Dr H. Mao (Zhejiang University, China). All solid compounds were weighted in mini gram scales; the compounds were dissolved in DMSO to make up a 10 mM concentration stock solution and stored at -20°C.

6.3.2 MTT cell viability assay

Dependent on the cell line, cells were seeded at $1.5-3 \times 10^3$ per well in a 96 well plate. The volume of each well was made up to 180 μ l with cell culture media and incubated at 37°C in a 5% carbon dioxide (CO₂) atmosphere overnight. Before the addition of compounds, the T₀ plate was treated with 50 μ l MTT (3-(4,5-dimethylthiazol-2-yl)-2,5-diphenyltetrazolium bromide) solution (2 mg/ml in phosphate buffered saline) per well and incubated for further 2-6 hours at 37°C in a 5% CO₂ atmosphere. Light absorbencies were read at 550 nm on an Anthos Labtec Systems plate reader after the removal of media and MTT mixture, addition of 150 μ l DMSO per well was followed. Data was automatically transferred to a computer with software Deltasoft 3™. Chemical inhibitor(s) from a 10 mM stock were added to the cells in a concentration range between 0.1 nM - 100 μ M and incubated for further 72 hours at 37°C with 5% CO₂. All plates were treated and analysed in the same manner from the addition of MTT after 72 hours. All data was transferred to Microsoft Excel, which was used to analyse the data and used to calculate the GI₅₀ value of each compound.

6.3.3 Kinase assay

This assay was carried out both internal and externally. For the internal assay, inhibitor(s) were diluted in a concentration range of 0.11 nM to 250 nM in 10% DMSO. To carry out this assay, a white 96 well plate was used and 5 μ l of inhibitor were added per well, followed by 5 μ l CDK9/Cyclin T1 [40 ng in dilution buffer (20 mM MOPS-NaOH at pH 7.4, 0.1 mM EGTA, 150 mM Sodium chloride, 270 mM Sucrose, 0.03% Brij-35, 0.07% β -mercaptoethanol) 1:10] and 5 μ l reaction buffer (20 mM MOPS-NaOH at pH 7.4, 25 mM Glycerol-2-phosphate, 5 mM EGTA, 1 mM DTT). The reaction was started by the addition of 5 μ l 75 mM MgCl₂, 100 nM ATP and 5 μ l PDK (5 μ M). The reaction was preceded at room temperature for 1 hour and consequently stopped by the addition of 25 μ l Easy-lite reagent (PerkinElmer). The plate was incubated for 1 minute at room temperature with gentle shaking and was read on Victor 2™ plate reader for luminescence detection. All data was transferred to Microsoft Excel, which was used to analyse the data. The external assays were performed by Millipore (Billerica, MA, USA).

6.3.4 Cell cycle analysis

Cells were seeded at a density of 3×10^5 and incubated at 37°C in a 5% CO₂ atmosphere overnight. Cells were treated with compounds at the appropriate concentrations and harvested with the medium at appropriate time points,

washed with PBS (Phosphate Buffered Saline) and transferred into FACS tube. All samples were centrifuged at 1200 rpm for 5 minutes at 4°C and the supernatants were discarded. Following the disregard of the supernatant, 300 µl fluorochrome solution (50 µg/ml propidium iodide, 0.1 mg/ml ribonuclease A, 0.1% sodium citrate, 0.1% triton X-100) were added to each samples. Cells were suspended, protected from light and stored at 4°C overnight. Cell cycle status was analysed using flow cytometer (Beckman Counter FACS).

For synchronisation assays, cells were seeded at a density of 5×10^5 and incubated at 37°C in a 5% CO₂ atmosphere overnight. Thymidine was added to the medium at a final concentration of 2 mM followed by 18 hours incubation at 37°C 5% CO₂ atmosphere. Thymidine containing media was removed and the cells washed with PBS. Following this wash, medium without thymidine was added and the cells incubated for a further 8 hours at 37°C with 5% CO₂ atmosphere. Thymidine was added after this incubation period to the media at a final concentration of 2 mM followed by 16 hours incubation at 37°C in a 5% CO₂ atmosphere. After the second incubation with thymidine, cells were used to start the experiment by removing the thymidine containing medium and replaced with the medium with appropriate compound. Post-processed were carried out as previously described.

6.3.5 Annexin-V assay

Cells were seeded at a density of 3×10^5 and were treated with compounds after overnight culture. Cells were collected, together with the media at an appropriate length of time, washed with PBS, placed in a FACS tube and centrifuged at 1200 rpm for 5 minutes at room temperature. The supernatants were discarded and suspended with 1 ml fresh medium. For each sample, the cell number was counted using a haemocytometer and 1×10^5 cells were transferred into a fresh FACS tube with 1 ml PBS, and centrifuged at 1200 rpm for 5 minutes at room temperature. Supernatants were again discarded followed by the addition of 100 µl Annexin V binding buffer [0.01 M Hepes (pH 7.4), 0.14 M NaCl, 2.5 mM CaCl₂] and 5 µl Annexin V-FITC. After 15 minutes incubation in the dark at room temperature, there was the addition of 400 µl Annexin V buffer and 10 µl propidium iodide in PBS (50 µg/ml). Samples were placed in ice and dark for a further 10 minutes and analysed using FACS within 1 hour.

6.3.6 Caspase-3 assay

Caspase-3 activity was determined using the caspase-3 fluorimetric assay kit (cat no. CASP3F) and used under manufacturer instruction. Briefly, cells were seeded at 2×10^4 cells per well in a 96 well plate and incubated at 37°C and 5% CO₂ atmosphere for a further 48 hours. Compounds were added to cells and incubated for the appropriate length of time. Cell culture media was removed after the incubation period, and placed on ice. 25 µl lysis buffer (50 mM HEPES (pH 7.4), 5 mM CHAPS, and 5 mM DTT) were added per well followed by a further 15-20 minutes incubation on ice. 200 µl assay buffer [20

mM HEPES (pH 7.4), with 0.1% CHAPS, 5 mM DTT, 2 mM EDTA, and 0.66 mM Acetyl-Asp-Glu-Val-Asp-7-amido-4-methylcoumarin (Ac-DEVD-AMC)] were added per sample. 200 μ l from each sample was transferred into 96 well fluorimeter plates. Fluorescence was measured at 460 nm in a kinetic mode every 10 minutes for 60 minutes at room temperature using EnVision multilabel plate reader (PerkinElmer). The data was calculated in comparison to the AMC standard curve according to manufacturer recommendation.

6.3.7 Western blot analysis

Cells were seeded at a density of 3×10^5 on a 10 cm tissue culture plate and were treated with compounds after 2 days culture at 37°C with 5% CO₂ atmosphere. Cells were collected at appropriate time points and lysed in buffer [25 mM Hepes (pH 7.5), 300 mM NaCl, 1.5 mM MgCl₂, 0.5% sodium deoxycholate, 20 mM β -glycerophosphate, 1% Triton X-100, 0.1% sodium dodecyl sulphate, 0.2 mM EDTA (pH 8), 0.5 mM DTT, 1 mM sodium orthovanadate (pH 10), 1 mM phenylmethylsulfonyl fluoride, 20 μ g/ml aprotinin, 20 μ g/ml leupeptin].

Protein content in the lysates was determined using the Bio-Rad DC protein assay kit operated according to the manufacturer's instructions (Bio-Rad, Hercules, CA).

Dependant on the size of the protein of interest, the percentage of acrylamide used in the gels varies between 7-15%. Acrylamide solution was mixed with 25% resolving gel buffer solution (1.5 M Tris.Cl, pH 8.8, 0.4% SDS) and water. After the addition of AMPS, polymerisation initiated with the addition of TEMED in a gel cassette. After the resolving gel had polymerised, stacking gel (for 5 ml: 0.67 ml 30% acrylamide, 0.63 ml stacking gel buffer (1 M Tris.Cl, pH 6.8, 0.8% SDS), and 3.70 ml H₂O) was added after the addition of AMPS and TEMED. A comb for the sample wells was added immediately.

Each cell lysate sample (250 μ g protein) with loading buffer (three times) [For 10 ml: 2.4 ml 1 M Tris.Cl (pH 6.8), 3ml Glycerol, 3 ml 20% SDS, 1.6 ml β -Mercaptoethanol, 0.006 g Bromoplectol Blue) were denatured at 95°C for 5 minutes and separated by SDS-polyacrylamide gel electrophoresis at a voltage between 70-150V. At the end of electrophoresis, the gel was removed from the cassette and transferred for post-processing as required.

Separated cell lysates were electrotransferred onto a PVDF membrane (Bio-Rad, Hercules, CA). Dependant on the primary antibody, the membrane was blocked in TBST (Tris buffered saline with 0.1% Tween 20) with either 5-10% BSA or 10% non-fat dry milk for a minimum of 1 hour, followed by incubation with primary antibodies solutions overnight at 4°C. Incubation of appropriate secondary antibodies conjugated to horseradish peroxidase for a minimum of 1 hour were followed and washes with TBST at an appropriate length of time. Antibodies for Mcl-1, PARP, XIAP were purchased from Cell signalling technology. Antibodies for Bcl-2 and p53 were obtained from Dako (Dako Denmark A/S). Antibodies for total RNA (8WG16), phosphorylated CTD at Ser 2 (H5) or Ser 5 (H14) were purchased from Covance research Products (Berkeley, CA). Antibody for HDM-2 and β -actin were purchased from Sigma (Sigma-Aldrich, USA). Both anti-mouse and anti-rabbit Immunoglobulin G

(IgG) horseradish peroxidase-conjugated antibodies were obtained from Dako (Dako Denmark A/S).

All blots were visualised using enhanced chemiluminescence according to the manufacturer's instruction (Amersham plc, GE healthcare) and exposed to X-ray films (Amersham plc, GE healthcare) at an appropriate length of time. The X-ray films were processed by developers and fixers solutions (CPIL).

For membrane stripping, blots were washed three times with TBST for 10 minutes each. Stripping buffer (To prepare 100 ml, mix 0.76 g Trizma® base, 2 g SDS and 700µl β-mercaptoethanol. Bring to 100ml with dH₂O and adjust pH to 6.8 with HCl) were incubated with blots for 30 minutes at 50°C. Blots were washed three times with TBST for 10 minutes each and membranes were used as fresh for appropriate applications.

6.3.8 Reverse transcription polymerase chain reaction (RT-PCR)

Cells were seeded at a density of 3×10^5 on 10 cm tissue culture plate and were treated with compounds after 2 days culture at 37°C with 5% CO₂ atmosphere. Cells were collected at appropriate time points following the removal of culture medium. RNA was extracted using Qiagen RNeasy® mini kit (Qiagen) and used under manufacturer's instruction.

The concentration of RNA samples were estimated by NanoDrop® ND-1000 Spectrophotometer (Thermo Fisher Scientific, USA), which was used under manufacturer's instruction. Resultant RNA content was calculated at ng per µl by software provided by the manufacturer.

To obtain a cDNA template from the RNA samples, 4 µg of RNA for each individual sample were mixed with 10 µM oligo (dT)₁₈ primers (Bioline) and diluted with H₂O (Sigma) to a final volume of 13 µl. Addition of 0.5 µl transcriptor reverse transcriptase (20 U/µl) (Roche) and 4 µl transcriptor RT reaction buffer (5x) (Roche) was followed with the final addition of 20 mM PCR grade nucleotide mix (Roche) and 7.5 µl of H₂O (Sigma). Samples were incubated at 25°C for 10 minutes followed by 30 minutes at 55°C in thermal cycler (PTC-100™, MJ Research INC). Reactions were stopped by heating at 85°C for 10 minutes and cooled down at 4°C. For long term storage, the cDNAs were kept at -20°C.

To quantify the mRNA product, 100 ng cDNA from each individual sample was mixed with 25 µM forward and reverse primers, followed with the addition of 10 mM PCR grade nucleotide mix (Roche). Addition of 0.25 µl Taq DNA polymerase (5 U/µl) (Roche) and 5 µl PCR reaction buffer (10x) (Roche), H₂O was added to make up the final volume of 50 µl. The PCR reactions were heated in thermal cycler at 94°C for 2 minutes and 30 cycles of denaturation annealing elongation (94°C for 30 seconds, 55°C for 60 s, and 72°C for 3 minutes). The final elongation for 7 minutes at 72°C and cooled down at 4°C. The PCR products were stored at -20°C.

The primers for amplifying β-Actin were purchased from MGW Biotech AG (Ebersberg, Germany), other primers were custom designed by Dr Scott Roberts and produced by Sigma. The sequences of these primers were listed below (Table 6.1).

Oligo	Forward primer	Reverse primer
Mcl-1	5' GAAGGCGCTGGAGACCTTAC 3'	5' CATTCTGATGCCACCTCT 3'
Mcl-1 LT	5' TAAGGACAAAACGGGACTGG 3'	5' GCTCCTACTCCAGCAACACC 3'
Bcl-2	5' ATGTGTGTGGAGAGCGTCAA 3'	5' GCCGTACAGTTCCACAAAGG 3'
XIAP (1)	5' TCACTTGAGGTTCTGGTTGC 3'	5' CGCCTTAGCTGCTCTTCAGT 3'
XIAP (2)	5' TCACTTGAGGTTCTGGTTGC 3'	5' TGCAAAGCTTCTCCTCTTGC 3'
HDM-2	5' TGGTGCTGTAACCACCTACA 3'	5' TTTTGTGCACCAACAGACTTT 3'

Table 6.1: Sequences of custom designed PCR primers

The PCR products were analysed using agarose gel electrophoresis. The agarose gel was prepared at a concentration of 2.5% agarose with TBE buffer (0.89 M Trizma® base, 0.89 M Boric acid, 0.02 M EDTA). Reaction mixture was heated in microwave to dissolve the agarose. The clear mixture was cooled down to room temperature and ethidium bromide (EtBr) was added to make up the concentration of 0.2 µg/ml. The mixture was poured into the gel container with the combs added. After the gel was set, combs were removed and load with 5 µl PCR product with 1 µl gel loading solution (Sigma) per samples. Samples were separated with TBE buffer at 100 V for 30 minutes.

Gel with separated PCR products were visualised under UV light. Images were recorded digitally and to estimate the relative effect on nucleic acids between samples, intensity of bands was measured using software Image J™.

6.3.9 Cellomics Array Scan protein expression assay

Cellomics Array Scan protein expression assay was used to determine the stabilisation of p53 protein by compounds. Samples were prepared by Dr Carol Midgley (Open University, Cambridge, UK). Plates were read in the University of Nottingham using ImageXpress Micro (Molecular Devices) available in the institute of cell signalling. Images were analysis by software MetaXpress™ (Molecular Devices) to give the statistical data.

6.3.10 Cell imaging studies

Cells were seeded at a density of 1×10^5 in 6 well tissue culture plates and were treated with compounds after overnight culture at 37°C with 5% CO₂ atmosphere. At the time point required, images were observed under light microscope (Olympus) at 40 times magnification and recorded by digital camera (Nikon).

6.3.11 Biochemical tubulin polymerisation assay

HTS-Tubulin Polymerisation Assay Kit (Cytoskeleton, Inc.) was used to determine the effect of drug on tubulin polymerisation and the kit was used under manufacturer's instruction. Briefly, compounds were diluted into desired concentration with General tubulin buffer (PEM) supplied [80 mM Na-PIPES (pH 6.9), 1 mM MgCl₂ and 1 mM EGTA]. HTS-Tubulin was diluted with PEM to give a final concentration of 4mg/ml. Compounds were added to each well of the 96 well plate followed by the addition of PEM buffer with 1mM GTP. The assay starts following the addition of tubulin solution. The reaction occurred at 37°C for 1 hour. The optical density was measured every minute at the absorbance wavelength of 340 nm in a spectrophotometer.

6.3.12 *Ex vivo* angiogenesis assay

Chorioallantoic Membrane (CAM) Assay is the *ex vivo* assay to determine the anti-angiogenic effect of compounds. Appointed on the arrival of fertilised chicken eggs (Henry Stuart, Joice and Hill Poultry Ltd, Peterborough, UK), eggs were placed horizontally and incubated at 37°C for 4 days. After the incubation period, eggs were placed under a detectable light source to check the blood vessels formations that have occurred around the embryo. The position of the embryo was marked by pencil on the shell of eggs. Eggs were placed horizontally at all times. A sterile 19 g needle and 10 ml syringes (BD, USA) were inserted into the egg at the "9 o'clock" position of the embryo to remove 6-10 mls of albumin. The puncture hole was sealed by sterile masking tape after removal of needle. An approximate 1x1.5 cm² window was cut by a band-saw with shells removed. Viability of the embryo was checked before addition of compounds. Compounds were soaked in sterile filter paper with size 2x3 mm² and placed at a site of vasulisation approximate 1-2 cm away from the embryo. The "window" was sealed with sterile masking tape after the addition of compounds and egg were incubated at 37°C for a further 6 days. Eggs were removed from incubator after 6 days incubation followed by additional shells removed from the "window". Stereomicroscope (Lecia, model no. MZ16F) was used to capture the images of embryos. Retrieved specimens were disposed according to ethical guidelines.

6.3.13 DPPH assay

The mixture containing 20 µL of sample solution (different concentrations) and 180 µL of DPPH (1,1-diphenyl-2-picrylhydrazyl, 150 µM) **7** was taken in a 96 well plate and incubated at 37°C for 30 minutes. The absorbance was measured at 517 nm by a microplate reader. Radical scavenging activity was calculated by the following equation:

$$I (\%) = 100 \times (A_{\text{blank}} - A_{\text{sample}}) / A_{\text{blank}}$$

Where A_{blank} is the absorbance of the control mixture excluding the test compounds, and A_{sample} is the absorbance of the mixture with the tested

compounds. IC_{50} values represent concentration of compounds to scavenge 50% of DPPH radicals.

6.3.14 *In vitro* oxidation states analysis with FACS

Cells were seeded at a density of 3×10^5 and were treated with compounds at 37°C with 5% CO_2 atmosphere after overnight culture. Cells were treated with $5 \mu\text{M}$ hydrogen peroxide as required 1 hour before the collation of samples. 30 minutes prior to the end of the experiment, $5 \mu\text{M}$ 2',7'-dichlorofluorescein diacetate (H_2DCFDA) were added to the cells. Cells were collected together with the media at appropriate length of time, washed with PBS, placed in FACS tube and centrifuged at 1200 rpm for 5 minutes at room temperature. Supernatants were discarded and suspended in FACS tube with $300 \mu\text{l}$ PBS containing $50 \mu\text{g/ml}$ propidium iodide. All samples were analysed using FACS within 1 hour.

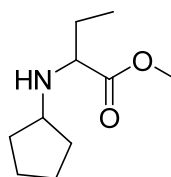
6.3.15 Statistical analysis

GraphPad Online Software (GraphPad Software, Inc.) was used for calculation of p values. Microsoft Excel was used in generate statistical data, such as mean values and standard deviations, from all data set demonstrated. It was also used in calculating all graphic related statistics.

6.4 Compound synthesis

General. $^1\text{H-NMR}$ spectra were obtained using a Bruker-400 spectrometer. Chemical shifts are reported in parts per million relative to internal tetramethylsilane standard. Coupling constants (J) are quoted to the nearest 0.1 Hz. The following abbreviations are used: s, singlet; d, doublet; t, triplet; q, quartet; qu, quintuplet; m, multiplet and br, broad. Mass spectra were obtained using a Waters 2795 single quadrupole mass spectrometer with electrospray ionization (ESI). Microwave assisted chemistry was carried out using CEM Discovery model (Biotage Ltd. UK). TLC (thin-layer chromatography) was performed using alumina plates coated with silica gel G60. Developed plates were air dried and analysed under a UV lamp (254 / 365 nm). Silica gel (EM Kieselgel 60, 0.040-0.063 mm, Merck) or ISOLUTE pre-packed columns was used for flash chromatography.

Methyl 2-(cyclopentylamino)butanoate **14**

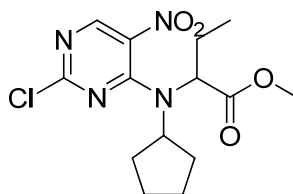


DL-alanine ethyl ester hydrochloride **12** and 1 equivalent of cyclopentanone **13** were dissolved with dichloromethane (10 equivalents) at 0°C. 1 equivalent of sodium acetate and 1.5 equivalents of sodium triacetoxyborohydrate were added and the reaction mixture was stirred for 12 hours. 20% aqueous sodium hydrogen carbonate solution was added to the reaction mixture until hydrogen gas was no longer generated. The reaction mixture was extracted into dichloromethane twice and the combined organic phase collected, washed with water and dried over magnesium sulphate. The organic phase was evaporated to give [**14**, colourless oil].

¹H NMR (400 MHz, DMSO-*d*₆) δ 3.63 (s, 3H), 3.12-3.08 (m, 1H), 2.90-2.88 (m, 1H), 1.90 (s, 1H), 1.60-1.43 (m, 8H), 1.29-1.22 (m, 2H), 0.86-0.81 (t, J=8.4Hz, 3H)

(MS-ES) m/z 186.14 (MH⁺, C₁₀H₁₉NO₂ requires m/z 186.26)

Methyl 2-((2-chloro-5-nitropyrimidin-4-yl)(cyclopentyl)amino)butanoate **16**

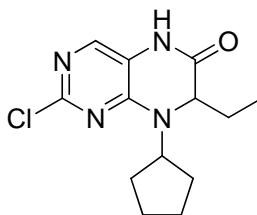


While cooling on ice, 1 equivalent of **14** was suspended in acetone (30 equivalents). 1 equivalent of 2,4-dichloro-5-nitropyrimidine **15** was added into the reaction mixture followed by the addition of potassium carbonate (1.1 equivalents). The reaction mixture was returned to room temperature and stirred for a further 12 hours. 0.1 equivalents of 2,4-dichloro-5-nitropyrimidine were added after 12 hours and the reaction mixture was stirred for further 3 hours. The reaction mixture was evaporated down, taken up in ethyl acetate and water (4:3) and the aqueous was extracted with ethyl acetate. The combined organic phase was washed with water, dried with magnesium sulphate and evaporated down. The product in the form of brown oil was applied to silica gel and purified by chromatography to obtain [**16**, yellow crystal].

¹H NMR (400 MHz, DMSO-*d*₆) δ 8.84 (s, 1H), 2.08 (s, 3H), 1.92-1.64 (m, 9H), 1.42-1.35 (m, 1H), 0.96-0.92 (t, J=7.4Hz, 3H), 0.89-0.80 (m, 2H)

(MS-ES) m/z 343.12 (MH⁺, C₁₄H₁₉ClN₄O₄ requires m/z 343.78)

2-chloro-8-cyclopentyl-7-ethyl-7,8-dihydropteridin-6(5H)-one **17**

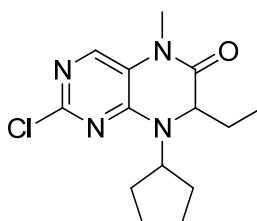


5 equivalents of **16** was dissolved in excess glacial acetic acid at 70°C, 1 equivalent of iron powder was added batch-wise. The reaction mixture was

stirred at 70°C for 1 hour and 100°C for further 1.5 hours. The reaction mixture was filtered hot through Kieselguhr. The reaction mixture was evaporated resulted in brown oil. [**17**, brown oil].

¹H NMR (400 MHz, DMSO-*d*₆) δ 7.56 (s, 1H), 2.08 (s, 1H), 1.99 (s, 1H), 1.94-1.54 (m, 9H), 1.19-1.16 (m, 2H), 0.81-0.76 (t, J=9.4Hz, 3H)
(MS-ES) m/z 281.12 (MH⁺, C₁₃H₁₇ClN₄O requires m/z 281.75)

2-chloro-8-cyclopentyl-7-ethyl-5-methyl-7,8-dihydropteridin-6(5H)-one **18**

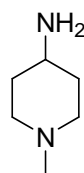


1 equivalent of **17** was dissolved in dimethylacetamide at -14°C. After 1 equivalent of methyl iodide and 1 equivalent of sodium hydride in 60% mineral oil suspension were added, the reaction mixture was stirred for 20 minutes in 0°C and 30 minutes at ambient temperature. To stop the reaction, ice was added and the reaction mixture was evaporated down. The reaction mixture was diluted with water and suction filtered after the formation of precipitate. The precipitate was re-dissolved in dichloromethane, applied to the silica gel and purified with chromatography to obtain **18**. [**18**, yellow oil].

¹H NMR (400 MHz, DMSO-*d*₆) δ 7.87 (s, 1H), 4.36-4.34 (q, J=3.5, 1H), 4.18-4.14 (t, J=8.2Hz, 1H), 4.05-4.00 (q, J=7.1Hz, 1H), 1.99 (s, 3H), 1.94-1.77 (m, 8H), 1.73-1.67 (m, 1H), 1.56-1.53 (m, 2H), 1.19-1.15 (t, J=7Hz, 3H), 0.75-0.71 (t, J=7.6Hz, 3H)

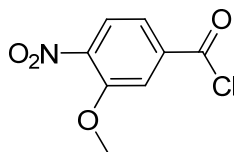
(MS-ES) m/z 295.12 (MH⁺, C₁₄H₁₉ClN₄O requires m/z 295.78)

1-methylpiperidin-4-amine **20**



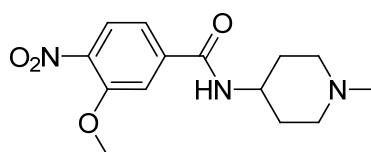
1 equivalent of ethyl 4-aminopiperidine-1-carboxylate **19** was dissolved in dry ether and cooled in ice bath. Under anhydrous conditions (nitrogen gas), 2.5 equivalents of lithium aluminium hydride (LiAlH₄) was added and the reaction mixture was stirred in an ice-bath for another half hour. The reaction mixture was placed into oil bath after 30 minutes and slowly heated up to 44°C to allow reflux for 17 hours. To stop the reaction, the reaction mixture was cooled in ice and the unreacted LiAlH₄ was quenched by the addition of 10% aqueous NaOH until the effervescence subsided. The resulting slurry was filtered under vacuum and the filtrate washed with ether. The combined ether was dried with magnesium sulphate, filtered and evaporated. [**20**, yellow oil].

3-methoxy-4-nitrobenzoyl chloride **22**



A suspension of 3-methoxy-4-nitrobenzoic acid **21** (1 equivalent) was dissolved in chloroform under nitrogen. Thionyl chloride (3 equivalents) was subsequently added and the reaction mixture was reflux for 3 hours under nitrogen until a clear solution formed and then concentrated to dryness at 60°C. [**22**, yellow solid].

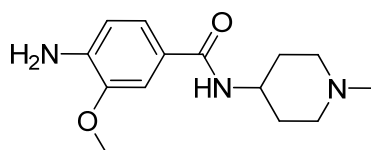
3-methoxy-*N*-(1-methylpiperidin-4-yl)-4-nitrobenzamide **23**



1 equivalent of **20** was dissolved in Tetrahydrofuran (THF) and 1.5 equivalents of pyridine were added. The reaction mixture was added to the 1 equivalent of **22** and stirred for 2 hours under nitrogen at ambient temperature, followed by 1 hour reflux. The reaction mixture was cooled down and evaporated. The resulting solid was re-dissolved in hot ethanol. After the formation of precipitate, the reaction mixture was suction filtered and participate collected. [**23**, white solid].

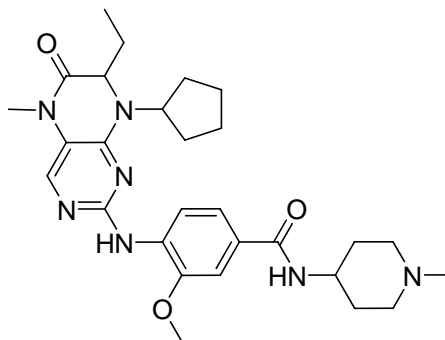
^1H NMR (400 MHz, DMSO- d_6) δ 8.92-8.91 (d, $J=6.8$ Hz, 1H), 7.97-7.95 (d, $J=8.4$, 1H), 7.79, (s, 1H), 7.62-7.60 (d, $J=8.0$ Hz, 1H), 4.01 (s, 1H), 3.43-3.36 (t, $J=15.4$ Hz, 4H), 3.10 (s, 2H), 2.71 (s, 3H), 1.99 (s, 4H)
(MS-ES) m/z 294.13 (MH^+ , $\text{C}_{14}\text{H}_{19}\text{N}_3\text{O}_4$ requires m/z 294.32)

4-amino-3-methoxy-*N*-(1-methylpiperidin-4-yl)benzamide **24**



23 (10 equivalents) was dissolved in excess ethanol followed by the addition of palladium in 10% carbon (1 equivalent). The reaction mixture was stirred at ambient temperature under hydrogen gas. After 4 hours, the reaction mixture was filtered through Kieselguhr. The reaction mixture was evaporated and re-dissolved in hot ethanol. After the formation of precipitate, the reaction mixture was suction filtered, and participate were collected. [**24**, white solid]

^1H NMR (400 MHz, DMSO- d_6) δ 8.15-8.13 (d, $J=7.2$ Hz, 1H), 7.36-7.34 (q, $J=2.1$, 2H), 6.62-6.60 (d, $J=8.8$ Hz, 1H), 5.28 (s, 2H), 4.02-3.99 (m, 1H), 3.81 (s, 3H), 3.38-3.35 (d, $J=12.0$ Hz, 2H), 3.06 (s, 2H), 2.68 (s, 3H), 1.95-1.94 (d, $J=2.8$ H)
(MS-ES) m/z 264.17 (MH^+ , $\text{C}_{14}\text{H}_{21}\text{N}_3\text{O}_2$ requires m/z 264.34)

4-(8-cyclopentyl-7-ethyl-5-methyl-6-oxo-5,6,7,8-tetrahydropteridin-2-ylamino)-3-methoxy-N-(1-methylpiperidin-4-yl)benzamide 25

1.1 equivalents of **18** and 1 equivalent of **24** were heated at 160°C overnight without any solvent and base. After the reaction completed (checked by TLC, 100% ethyl acetate, RF = 0.22), the reaction mixture was dissolved in methanol and applied to silica for column chromatography, the fraction with product was evaporated down, and a small amount of ethyl acetate added followed by the addition of excess hexane until the formation of precipitate. The precipitate **25** was filtered and washed with hexane. [**25**, yellow solid].

¹H NMR (400 MHz, DMSO-*d*₆) δ 7.82-7.80 (t, J=4.0Hz, 1H), 7.72 (s, 1H), 7.29-7.27 (m, 2H), 6.60-6.57 (m, 1H), 5.22-5.18 (d, J=16.0Hz, 2H), 4.56-4.53 (d, J=13.6, 2H) 4.56-4.00 (m, 6H), 3.80-3.75 (m, 2H), 3.19 (s, 3H), 2.94-2.91 (t, J=6.0Hz, 3H), 1.99-1.78 (m, 6H), 1.77-1.72 (m, 6H) 1.62-1.33 (m, 9H), 1.23-1.15 (m, 5H), 0.85-0.73 (m, 5H)

(MS-ES) m/z 522.00 (MH⁺, C₁₄H₂₁N₃O₂ requires m/z 522.65)

References

1. Kufe, D.W. & Holland, J.F.C.m. *Cancer medicine* 6, Edn. 6th ed. (Decker, Hamilton, Ont. ; London; 2003).
2. Box, F. & Htmf, F.F.H. Report sees 7.6 million cancer deaths worldwide in 2007. *Chinese Medical Journal* **121**, 26-26 (2008).
3. American Cancer, S. Cancer facts and figures 2007. (2007).
4. Ferlay, J. *et al.* Estimates of the cancer incidence and mortality in Europe in 2006. *Annals of Oncology* **18**, 581 (2007).
5. Lewin, B. *Genes VIII*, Edn. Instructor's ed. (Pearson Prentice Hall, Upper Saddle River, N.J.; 2004).
6. Powell, S.N. & Kachnic, L.A. Roles of BRCA1 and BRCA2 in homologous recombination, DNA replication fidelity and the cellular response to ionizing radiation. *Oncogene* **22**, 5784-5791 (2003).
7. Alberts, B. *Molecular biology of the cell*, Edn. 4th ed / Bruce Alberts ... [et al.]. (Garland Science, New York; 2002).
8. Bertino, J.R. *Encyclopedia of cancer*. (Academic Press, San Diego ; London; 1996).
9. Nagao, M. & Sugimura, T. *Food borne carcinogens : heterocyclic amines*. (Wiley, Chichester; 2000).
10. Tannock, I. *The basic science of oncology*, Edn. 4th ed. (McGraw-Hill Medical, New York; 2005).
11. Vineis, P. *et al.*, Vol. 96 99-106 (© Oxford University Press, 2004).
12. Ikeda, K. *et al.* A multivariate analysis of risk factors for hepatocellular carcinogenesis: a prospective observation of 795 patients with viral and alcoholic cirrhosis. *Hepatology* **18** (1993).
13. Ananthaswamy, H.N. & Pierceall, W.E. Molecular mechanisms of ultraviolet radiation carcinogenesis. *Photochemistry and photobiology* **52**, 1119-1136 (1990).
14. Little, J.B. Radiation carcinogenesis. *Carcinogenesis* **21**, 397 (2000).

15. Butel, J.S. Viral carcinogenesis: revelation of molecular mechanisms and etiology of human disease. *Carcinogenesis* **21**, 405 (2000).
16. Okabe, H. *et al.*, Vol. 61 2129-2137 (AACR, 2001).
17. Watanabe, T., Tada, M., Nagai, H., Sasaki, S. & Nakao, M. Helicobacter pylori infection induces gastric cancer in Mongolian gerbils. *Gastroenterology* **115**, 642-648 (1998).
18. Nandi, S., Guzman, R.C. & Yang, J. Hormones and mammary carcinogenesis in mice, rats, and humans: a unifying hypothesis. *Proceedings of the National Academy of Sciences* **92**, 3650-3657 (1995).
19. Whitby, D. *et al.* Detection of Kaposi sarcoma associated herpesvirus in peripheral blood of HIV-infected individuals and progression to Kaposi's sarcoma. *Lancet* **346**, 799 (1995).
20. Walboomers, J.M.M. *et al.* Human papillomavirus is a necessary cause of invasive cervical cancer worldwide. *The Journal of pathology* **189** (1999).
21. Ford, D., Easton, D.F., Bishop, D.T., Narod, S.A. & Goldgar, D.E. Risks of cancer in BRCA1-mutation carriers. Breast Cancer Linkage Consortium. *Lancet* **343**, 692 (1994).
22. Miki, Y. *et al.* A strong candidate for the breast and ovarian cancer susceptibility gene BRCA1. *Science (New York, N.Y)* **266**, 66-71 (1994).
23. Kramer, E.R., Scheuringer, N., Podtelejnikov, A.V., Mann, M. & Peters, J.M. Mitotic regulation of the APC activator proteins CDC20 and CDH1. *Molecular biology of the cell* **11**, 1555-1569 (2000).
24. Fulda, S. Hereditary Tumors in Children. *Hereditary Tumors: From Genes to Clinical Consequences* (2009).
25. Gonzalez, C.A. & Riboli, E. Diet and cancer prevention: where we are, where we are going. *Nutrition and cancer* **56**, 225-231 (2006).
26. Calle, E.E., Rodriguez, C., Walker-Thurmond, K. & Thun, M.J., Vol. 348 1625-1638(2003).
27. Block, G., Patterson, B. & Subar, A. Fruit, vegetables, and cancer prevention: a review of the epidemiological evidence. *Nutrition and cancer* **18**, 1-29 (1992).
28. Sinha, R. *et al.*, Vol. 59 4320-4324 (AACR, 1999).
29. Zheng, W. *et al.* Well-done meat intake and the risk of breast cancer. *J Natl Cancer I* **90**, 1724-1729 (1998).

30. Skowronski, R.J., Peehl, D.M. & Feldman, D. Vitamin D and prostate cancer: 1, 25 dihydroxyvitamin D₃ receptors and actions in human prostate cancer cell lines. *Endocrinology* **132**, 1952-1960 (1993).
31. Powles, T. *et al.* Interim analysis of the incidence of breast cancer in the Royal Marsden Hospital tamoxifen randomised chemoprevention trial. *Lancet* **352**, 98-101 (1998).
32. Tachibana, H. Molecular basis for cancer chemoprevention by green tea polyphenol EGCG. *Forum of nutrition* **61**, 156-169 (2009).
33. Jang, M. *et al.* Cancer chemopreventive activity of resveratrol, a natural product derived from grapes. *Science (New York, N.Y)* **275**, 218 (1997).
34. Schrag, D., Kuntz, K.M., Garber, J.E. & Weeks, J.C., Vol. 283 617-624 (Am Med Assoc, 2000).
35. Netea, M.G. *et al.* The role of toll-like receptor (TLR) 2 and TLR4 in the host defense against disseminated candidiasis. *The Journal of infectious diseases* **185**, 1483-1489 (2002).
36. Crosbie, E.J. & Kitchener, H.C. Cervarix™-a bivalent L1 virus-like particle vaccine for prevention of human papillomavirus type 16-and 18-associated cervical cancer. *Expert Opin. Biol. Ther.* **7**, 391-396 (2007).
37. Lee, M.S. *et al.* Hepatitis B vaccination and reduced risk of primary liver cancer among male adults: a cohort study in Korea. *International journal of epidemiology* **27**, 316-319 (1998).
38. Bergman, P.J. *et al.* Development of a xenogeneic DNA vaccine program for canine malignant melanoma at the Animal Medical Center. *Vaccine* **24**, 4582-4585 (2006).
39. Pazdur, R. *Cancer management: a multidisciplinary approach : medical, surgical & radiation oncology*, Edn. 5th ed. (PRR Melville, New York; 2001).
40. Illidge, T. *Treatment of cancer*, Edn. 5th ed. / edited by Tim Illidge. (Hodder Arnold, London; 2008).
41. Goldenberg, D.M. Targeted therapy of cancer with radiolabeled antibodies. *Journal of Nuclear Medicine* **43**, 693-713 (2002).
42. Rosenberg, S.A., Spiess, P. & Lafreniere, R. A new approach to the adoptive immunotherapy of cancer with tumor-infiltrating lymphocytes. *Science (New York, N.Y)* **233**, 1318-1321 (1986).
43. Byar, D.P. & Corle, D.K. Hormone therapy for prostate cancer: results of the Veterans Administration Cooperative Urological Research Group studies. *NCI monographs: a publication of the National Cancer Institute*, 165 (1988).

44. Deininger, M.W. & Druker, B.J. Specific targeted therapy of chronic myelogenous leukemia with imatinib. *Pharmacological reviews* **55**, 401-423 (2003).
45. Johnson, L.N., Noble, M.E. & Owen, D.J. Active and inactive protein kinases: structural basis for regulation. *Cell* **85**, 149-158 (1996).
46. Manning, G., Whyte, D.B., Martinez, R., Hunter, T. & Sudarsanam, S. The protein kinase complement of the human genome. *Science (New York, N.Y)* **298**, 1912-1934 (2002).
47. de Carcer, G., Perez de Castro, I. & Malumbres, M. Targeting cell cycle kinases for cancer therapy. *Current medicinal chemistry* **14**, 969-985 (2007).
48. Lee, M.G. & Nurse, P. Complementation used to clone a human homologue of the fission yeast cell cycle control gene *cdc2*. *Nature* **327**, 31-35 (1987).
49. Spurr, N.K., Gough, A.C. & Lee, M.G. Cloning of the mouse homologue of the yeast cell cycle control gene *cdc2*. *DNA Seq* **1**, 49-54 (1990).
50. Knockaert, M., Greengard, P. & Meijer, L. Pharmacological inhibitors of cyclin-dependent kinases. *Trends in pharmacological sciences* **23**, 417-425 (2002).
51. Ferrari, S. Protein kinases controlling the onset of mitosis. *Cell Mol Life Sci* **63**, 781-795 (2006).
52. Fisher, R.P. & Morgan, D.O. A novel cyclin associates with MO15/CDK7 to form the CDK-activating kinase. *Cell* **78**, 713-724 (1994).
53. Lolli, G. & Johnson, L.N. CAK-Cyclin-dependent Activating Kinase: a key kinase in cell cycle control and a target for drugs? *Cell cycle (Georgetown, Tex)* **4**, 572-577 (2005).
54. Chen, J., Larochelle, S., Li, X. & Suter, B. Xpd/Ercc2 regulates CAK activity and mitotic progression. *Nature* **424**, 228-232 (2003).
55. Kyprianou, N., English, H.F., Davidson, N.E. & Isaacs, J.T. Programmed cell death during regression of the MCF-7 human breast cancer following estrogen ablation. *Cancer research* **51**, 162-166 (1991).
56. Wilson, J.H. & Hunt, T. *Molecular biology of the cell, 4th ed. A problems approach*. (Garland, New York ; London; 2002).
57. Nigg, E.A. Mitotic kinases as regulators of cell division and its checkpoints. *Nature reviews* **2**, 21-32 (2001).

58. Orlando, D.A. *et al.* Global control of cell-cycle transcription by coupled CDK and network oscillators. *Nature* **453**, 944-947 (2008).
59. Li, J.J. & Li, S.A. Mitotic kinases: the key to duplication, segregation, and cytokinesis errors, chromosomal instability, and oncogenesis. *Pharmacology & therapeutics* **111**, 974-984 (2006).
60. Malumbres, M. & Barbacid, M. Cell cycle, CDKs and cancer: a changing paradigm. *Nat Rev Cancer* **9**, 153-166 (2009).
61. Wolfel, T. *et al.* A p16INK4a-insensitive CDK4 mutant targeted by cytolytic T lymphocytes in a human melanoma. *Science (New York, N.Y)* **269**, 1281-1284 (1995).
62. Vermeulen, K., Van Bockstaele, D.R. & Berneman, Z.N. The cell cycle: a review of regulation, deregulation and therapeutic targets in cancer. *Cell proliferation* **36**, 131-149 (2003).
63. Lazarov, M. *et al.* CDK4 coexpression with Ras generates malignant human epidermal tumorigenesis. *Nature medicine* **8**, 1105-1114 (2002).
64. Motokura, T. *et al.* A novel cyclin encoded by a bcl1-linked candidate oncogene. *Nature* **350**, 512-515 (1991).
65. Inaba, T. *et al.* Genomic organization, chromosomal localization, and independent expression of human cyclin D genes. *Genomics* **13**, 565-574 (1992).
66. Oelgeschlager, T. Regulation of RNA polymerase II activity by CTD phosphorylation and cell cycle control. *Journal of cellular physiology* **190**, 160-169 (2002).
67. Kato, J.Y., Matsuoka, M., Strom, D.K. & Sherr, C.J. Regulation of cyclin D-dependent kinase 4 (cdk4) by cdk4-activating kinase. *Molecular and cellular biology* **14**, 2713-2721 (1994).
68. Kaldis, P. The cdk-activating kinase (CAK): from yeast to mammals. *Cell Mol Life Sci* **55**, 284-296 (1999).
69. Meyerson, M. *et al.* A family of human cdc2-related protein kinases. *The EMBO journal* **11**, 2909-2917 (1992).
70. Meyerson, M. & Harlow, E. Identification of G1 kinase activity for cdk6, a novel cyclin D partner. *Molecular and cellular biology* **14**, 2077-2086 (1994).
71. Guan, K.L. *et al.* Growth suppression by p18, a p16INK4/MTS1- and p14INK4B/MTS2-related CDK6 inhibitor, correlates with wild-type pRb function. *Genes & development* **8**, 2939-2952 (1994).
72. Harbour, J.W., Luo, R.X., Dei Santi, A., Postigo, A.A. & Dean, D.C. Cdk phosphorylation triggers sequential intramolecular interactions that

- progressively block Rb functions as cells move through G1. *Cell* **98**, 859-869 (1999).
73. Ninomiya-Tsuji, J., Nomoto, S., Yasuda, H., Reed, S.I. & Matsumoto, K. Cloning of a human cDNA encoding a CDC2-related kinase by complementation of a budding yeast *cdc28* mutation. *Proceedings of the National Academy of Sciences of the United States of America* **88**, 9006-9010 (1991).
74. Hinchcliffe, E.H., Li, C., Thompson, E.A., Maller, J.L. & Sluder, G. Requirement of Cdk2-cyclin E activity for repeated centrosome reproduction in *Xenopus* egg extracts. *Science (New York, N.Y)* **283**, 851-854 (1999).
75. Morisaki, H. *et al.* Cell cycle-dependent phosphorylation of p27 cyclin-dependent kinase (Cdk) inhibitor by cyclin E/Cdk2. *Biochemical and biophysical research communications* **240**, 386-390 (1997).
76. Arellano, M. & Moreno, S. Regulation of CDK/cyclin complexes during the cell cycle. *The international journal of biochemistry & cell biology* **29**, 559-573 (1997).
77. Frouin, I. *et al.* Cell cycle-dependent dynamic association of cyclin/Cdk complexes with human DNA replication proteins. *The EMBO journal* **21**, 2485-2495 (2002).
78. Technology, C.S. (Cell Signaling Technology, 2002).
79. Liu, F., Stanton, J.J., Wu, Z. & Piwnicka-Worms, H. The human Myt1 kinase preferentially phosphorylates Cdc2 on threonine 14 and localizes to the endoplasmic reticulum and Golgi complex. *Molecular and cellular biology* **17**, 571-583 (1997).
80. Mitra, J. & Enders, G.H. Cyclin A/Cdk2 complexes regulate activation of Cdk1 and Cdc25 phosphatases in human cells. *Oncogene* **23**, 3361-3367 (2004).
81. Pines, J. & Hunter, T. Isolation of a human cyclin cDNA: evidence for cyclin mRNA and protein regulation in the cell cycle and for interaction with p34cdc2. *Cell* **58**, 833-846 (1989).
82. Carazo-Salas, R.E. *et al.* Generation of GTP-bound Ran by RCC1 is required for chromatin-induced mitotic spindle formation. *Nature* **400**, 178-181 (1999).
83. Taylor, S.S., Ha, E. & McKeon, F. The human homologue of Bub3 is required for kinetochore localization of Bub1 and a Mad3/Bub1-related protein kinase. *The Journal of cell biology* **142**, 1-11 (1998).
84. Luo, X., Tang, Z., Rizo, J. & Yu, H. The Mad2 spindle checkpoint protein undergoes similar major conformational changes upon binding to either Mad1 or Cdc20. *Molecular cell* **9**, 59-71 (2002).

85. Yu, H. Regulation of APC–Cdc20 by the spindle checkpoint. *Current opinion in cell biology* **14**, 706-714 (2002).
86. Nevins, J.R. The Rb/E2F pathway and cancer. *Human molecular genetics* **10**, 699-703 (2001).
87. Gallie, B.L., Ellsworth, R.M., Abramson, D.H. & Phillips, R.A. Retinoma: spontaneous regression of retinoblastoma or benign manifestation of the mutation? *British journal of cancer* **45**, 513-521 (1982).
88. Ortega, S., Malumbres, M. & Barbacid, M. Cyclin D-dependent kinases, INK4 inhibitors and cancer. *Biochimica et biophysica acta* **1602**, 73-87 (2002).
89. An, W., Kim, J. & Roeder, R.G. Ordered cooperative functions of PRMT1, p300, and CARM1 in transcriptional activation by p53. *Cell* **117**, 735-748 (2004).
90. Honda, R., Tanaka, H. & Yasuda, H. Oncoprotein MDM2 is a ubiquitin ligase E3 for tumor suppressor p53. *FEBS letters* **420**, 25-27 (1997).
91. Wang, X.Q., Redpath, J.L., Fan, S.T. & Stanbridge, E.J. ATR dependent activation of Chk2. *Journal of cellular physiology* **208**, 613-619 (2006).
92. Banin, S. *et al.* Enhanced phosphorylation of p53 by ATM in response to DNA damage. *Science (New York, N.Y)* **281**, 1674-1677 (1998).
93. Chehab, N.H., Malikzay, A., Stavridi, E.S. & Halazonetis, T.D. Phosphorylation of Ser-20 mediates stabilization of human p53 in response to DNA damage. *Proceedings of the National Academy of Sciences of the United States of America* **96**, 13777-13782 (1999).
94. Shieh, S.Y., Taya, Y. & Prives, C. DNA damage-inducible phosphorylation of p53 at N-terminal sites including a novel site, Ser20, requires tetramerization. *The EMBO journal* **18**, 1815-1823 (1999).
95. Hirao, A. *et al.* DNA damage-induced activation of p53 by the checkpoint kinase Chk2. *Science (New York, N.Y)* **287**, 1824-1827 (2000).
96. Ito, A. *et al.* p300/CBP-mediated p53 acetylation is commonly induced by p53-activating agents and inhibited by MDM2. *The EMBO journal* **20**, 1331-1340 (2001).
97. Sakaguchi, K. *et al.* DNA damage activates p53 through a phosphorylation-acetylation cascade. *Genes & development* **12**, 2831-2841 (1998).

98. Solomon, J.M. *et al.* Inhibition of SIRT1 catalytic activity increases p53 acetylation but does not alter cell survival following DNA damage. *Molecular and cellular biology* **26**, 28-38 (2006).
99. Haupt, S., Berger, M., Goldberg, Z. & Haupt, Y. Apoptosis - the p53 network. *Journal of cell science* **116**, 4077-4085 (2003).
100. Oda, K. *et al.* p53AIP1, a potential mediator of p53-dependent apoptosis, and its regulation by Ser-46-phosphorylated p53. *Cell* **102**, 849-862 (2000).
101. Agarwal, M.L., Taylor, W.R., Chernov, M.V., Chernova, O.B. & Stark, G.R. The p53 network. *The Journal of biological chemistry* **273**, 1-4 (1998).
102. Fulda, S. & Debatin, K.M. Extrinsic versus intrinsic apoptosis pathways in anticancer chemotherapy. *Oncogene* **25**, 4798-4811 (2006).
103. Li, H., Zhu, H., Xu, C.J. & Yuan, J. Cleavage of BID by caspase 8 mediates the mitochondrial damage in the Fas pathway of apoptosis. *Cell* **94**, 491-501 (1998).
104. Yang, J. *et al.* Prevention of apoptosis by Bcl-2: release of cytochrome c from mitochondria blocked. *Science (New York, N.Y)* **275**, 1129 (1997).
105. Adrain, C. & Martin, S.J. The mitochondrial apoptosome: a killer unleashed by the cytochrome seas. *Trends in Biochemical Sciences* **26**, 390-397 (2001).
106. Chen, R. *et al.* Mechanism of action of SNS-032, a novel cyclin-dependent kinase inhibitor, in chronic lymphocytic leukemia. *Blood* **113**, 4637-4645 (2009).
107. Kozopas, K.M., Yang, T., Buchan, H.L., Zhou, P. & Craig, R.W. MCL1, a gene expressed in programmed myeloid cell differentiation, has sequence similarity to BCL2. *Proceedings of the National Academy of Sciences of the United States of America* **90**, 3516-3520 (1993).
108. Mott, J.L., Kobayashi, S., Bronk, S.F. & Gores, G.J. mir-29 regulates Mcl-1 protein expression and apoptosis. *Oncogene* **26**, 6133-6140 (2007).
109. Yang, T., Kozopas, K.M. & Craig, R.W. The intracellular distribution and pattern of expression of Mcl-1 overlap with, but are not identical to, those of Bcl-2. *The Journal of cell biology* **128**, 1173-1184 (1995).
110. Germain, M., Milburn, J. & Duronio, V. MCL-1 inhibits BAX in the absence of MCL-1/BAX Interaction. *The Journal of biological chemistry* **283**, 6384-6392 (2008).

111. Leu, J.I., Dumont, P., Hafey, M., Murphy, M.E. & George, D.L. Mitochondrial p53 activates Bak and causes disruption of a Bak-Mcl1 complex. *Nature cell biology* **6**, 443-450 (2004).
112. Tsujimoto, Y., Finger, L.R., Yunis, J., Nowell, P.C. & Croce, C.M. Cloning of the chromosome breakpoint of neoplastic B cells with the t(14;18) chromosome translocation. *Science (New York, N.Y)* **226**, 1097-1099 (1984).
113. Wang, H.G., Rapp, U.R. & Reed, J.C. Bcl-2 targets the protein kinase Raf-1 to mitochondria. *Cell* **87**, 629-638 (1996).
114. Migheli, A., Cavalla, P., Piva, R., Giordana, M.T. & Schiffer, D. bcl-2 protein expression in aged brain and neurodegenerative diseases. *Neuroreport* **5**, 1906-1908 (1994).
115. Tsujimoto, Y. Overexpression of the human BCL-2 gene product results in growth enhancement of Epstein-Barr virus-immortalized B cells. *Proceedings of the National Academy of Sciences of the United States of America* **86**, 1958-1962 (1989).
116. Strasser, A., Harris, A.W. & Cory, S. bcl-2 transgene inhibits T cell death and perturbs thymic self-censorship. *Cell* **67**, 889-899 (1991).
117. Youle, R.J. & Strasser, A. The BCL-2 protein family: opposing activities that mediate cell death. *Nature reviews* **9**, 47-59 (2008).
118. Rajcan-Separovic, E., Liston, P., Lefebvre, C. & Korneluk, R.G. Assignment of human inhibitor of apoptosis protein (IAP) genes xiap, hiap-1, and hiap-2 to chromosomes Xq25 and 11q22-q23 by fluorescence in situ hybridization. *Genomics* **37**, 404-406 (1996).
119. Deveraux, Q.L., Takahashi, R., Salvesen, G.S. & Reed, J.C. X-linked IAP is a direct inhibitor of cell-death proteases. *Nature* **388**, 300-304 (1997).
120. Srinivasula, S.M. *et al.* A conserved XIAP-interaction motif in caspase-9 and Smac/DIABLO regulates caspase activity and apoptosis. *Nature* **410**, 112-116 (2001).
121. Tang, G. *et al.* Inhibition of JNK activation through NF-kappaB target genes. *Nature* **414**, 313-317 (2001).
122. Zhang, H.G., Wang, J., Yang, X., Hsu, H.C. & Mountz, J.D. Regulation of apoptosis proteins in cancer cells by ubiquitin. *Oncogene* **23**, 2009-2015 (2004).
123. Dohi, T., Xia, F. & Altieri, D.C. Compartmentalized phosphorylation of IAP by protein kinase A regulates cytoprotection. *Molecular cell* **27**, 17-28 (2007).

124. Blackwell, T.K. & Walker, A.K. Transcription mechanisms. *WormBook*, 1–16 (2006).
125. Dubois, M.F. *et al.* Heat-shock inactivation of the TFIIH-associated kinase and change in the phosphorylation sites on the C-terminal domain of RNA polymerase II. *Nucleic acids research* **25**, 694-700 (1997).
126. Latchman, D.S. *Gene regulation : a eukaryotic perspective*, Edn. 4th ed. (Nelson Thornes, Cheltenham; 2002).
127. Panning, B. & Taatjes, D.J. Transcriptional regulation: it takes a village. *Molecular cell* **31**, 622-629 (2008).
128. Bensaude, O. *et al.* Regulated phosphorylation of the RNA polymerase II C-terminal domain (CTD). *Biochemistry and cell biology = Biochimie et biologie cellulaire* **77**, 249-255 (1999).
129. Tassan, J.P., Jaquenoud, M., Leopold, P., Schultz, S.J. & Nigg, E.A. Identification of human cyclin-dependent kinase 8, a putative protein kinase partner for cyclin C. *Proceedings of the National Academy of Sciences of the United States of America* **92**, 8871-8875 (1995).
130. Akoulitchev, S., Chuikov, S. & Reinberg, D. TFIIH is negatively regulated by cdk8-containing mediator complexes. *Nature* **407**, 102-106 (2000).
131. Yamaguchi, Y. *et al.* NELF, a multisubunit complex containing RD, cooperates with DSIF to repress RNA polymerase II elongation. *Cell* **97**, 41-51 (1999).
132. Hu, D., Mayeda, A., Trembley, J.H., Lahti, J.M. & Kidd, V.J. CDK11 complexes promote pre-mRNA splicing. *The Journal of biological chemistry* **278**, 8623-8629 (2003).
133. Cragg, G.M., Newman, D.J. & Snader, K.M. Natural products in drug discovery and development. *Phytochemicals in Human Health Protection, Nutrition, and Plant Defense*, 1 (1999).
134. Newman, D.J., Cragg, G.M. & Snader, K.M. The influence of natural products upon drug discovery. *Natural product reports* **17**, 215-234 (2000).
135. Ligon, B.L., Vol. 15 52-57 (Elsevier, 2004).
136. Gerwick, W.H. *et al.* Structure of Curacin A, a novel antimetabolic, antiproliferative and brine shrimp toxic natural product from the marine cyanobacterium *Lyngbya majuscula*. *The Journal of organic chemistry* **59**, 1243-1245 (1994).
137. Tan, P.T.J., Khan, A.M. & Brusic, V. Bioinformatics for venom and toxin sciences. *Briefings in bioinformatics* **4**, 53-62 (2003).

138. Altmann, K.H. & Gertsch, J. Anticancer drugs from nature--natural products as a unique source of new microtubule-stabilizing agents. *Natural product reports* **24**, 327-357 (2007).
139. Navashin, S.M. & Navashin, P.S. [Semisynthetic penicillins: their importance in the current antibiotic therapy of infections. Penicillinase-resistant penicillins with predominantly antistaphylococcal action]. *Antibiotiki i khimioterapiia = Antibiotics and chemotherapy [sic] / Ministerstvo meditsinskoi i mikrobiologicheskoi promyshlennosti SSSR* **38**, 21-28 (1993).
140. Ng, T.B., Liu, F. & Wang, Z.T. Antioxidative activity of natural products from plants. *Life sciences* **66**, 709-723 (2000).
141. Williamson, M.P., McCormick, T.G., Nance, C.L. & Shearer, W.T. Epigallocatechin gallate, the main polyphenol in green tea, binds to the T-cell receptor, CD4: Potential for HIV-1 therapy. *The Journal of allergy and clinical immunology* **118**, 1369-1374 (2006).
142. Valko, M., Izakovic, M., Mazur, M., Rhodes, C.J. & Telser, J. Role of oxygen radicals in DNA damage and cancer incidence. *Molecular and cellular biochemistry* **266**, 37-56 (2004).
143. Nance, C.L., Siwak, E.B. & Shearer, W.T. Preclinical development of the green tea catechin, epigallocatechin gallate, as an HIV-1 therapy. *The Journal of allergy and clinical immunology* **123**, 459-465 (2009).
144. Grana, X. *et al.* PITALRE, a nuclear CDC2-related protein kinase that phosphorylates the retinoblastoma protein in vitro. *Proceedings of the National Academy of Sciences of the United States of America* **91**, 3834-3838 (1994).
145. Marshall, R.M. & Grana, X. Mechanisms controlling CDK9 activity. *Front Biosci* **11**, 2598-2613 (2006).
146. de Falco, G. & Giordano, A. CDK9 (PITALRE): a multifunctional cdc2-related kinase. *Journal of cellular physiology* **177**, 501-506 (1998).
147. Baumli, S. *et al.* The structure of P-TEFb (CDK9/cyclin T1), its complex with flavopiridol and regulation by phosphorylation. *The EMBO journal* **27**, 1907-1918 (2008).
148. Yang, Z. *et al.* Recruitment of P-TEFb for stimulation of transcriptional elongation by the bromodomain protein Brd4. *Molecular cell* **19**, 535-545 (2005).
149. Hirose, Y. & Ohkuma, Y. Phosphorylation of the C-terminal domain of RNA polymerase II plays central roles in the integrated events of eucaryotic gene expression. *Journal of biochemistry* **141**, 601-608 (2007).

150. Kohoutek, J., Blazek, D. & Peterlin, B.M. Hexim1 sequesters positive transcription elongation factor b from the class II transactivator on MHC class II promoters. *Proceedings of the National Academy of Sciences of the United States of America* **103**, 17349-17354 (2006).
151. Wang, S. & Fischer, P.M. Cyclin-dependent kinase 9: a key transcriptional regulator and potential drug target in oncology, virology and cardiology. *Trends in pharmacological sciences* **29**, 302-313 (2008).
152. Fong, Y.W. & Zhou, Q. Stimulatory effect of splicing factors on transcriptional elongation. *Nature* **414**, 929-933 (2001).
153. Sano, M. & Schneider, M.D. Cyclins that don't cycle--cyclin T/cyclin-dependent kinase-9 determines cardiac muscle cell size. *Cell cycle (Georgetown, Tex)* **2**, 99-104 (2003).
154. Sano, M. *et al.* Activation of cardiac Cdk9 represses PGC-1 and confers a predisposition to heart failure. *The EMBO journal* **23**, 3559-3569 (2004).
155. Sano, M. & Schneider, M.D. Cyclin-dependent kinase-9: an RNAPII kinase at the nexus of cardiac growth and death cascades. *Circulation research* **95**, 867-876 (2004).
156. Giacinti, C., Bagella, L., Puri, P.L., Giordano, A. & Simone, C. MyoD recruits the cdk9/cyclin T2 complex on myogenic-genes regulatory regions. *Journal of cellular physiology* **206**, 807-813 (2006).
157. Nojima, M., Huang, Y., Tyagi, M., Kao, H.Y. & Fujinaga, K. The positive transcription elongation factor b is an essential cofactor for the activation of transcription by myocyte enhancer factor 2. *Journal of molecular biology* **382**, 275-287 (2008).
158. Strasser, A., Jost, P.J. & Nagata, S. The many roles of FAS receptor signaling in the immune system. *Immunity* **30**, 180-192 (2009).
159. Huang, Y. & Sheikh, M.S. TRAIL death receptors and cancer therapeutics. *Toxicology and applied pharmacology* **224**, 284-289 (2007).
160. Hu, X. Proteolytic signaling by TNFalpha: caspase activation and IkkappaB degradation. *Cytokine* **21**, 286-294 (2003).
161. Ambrosini, G., Adida, C. & Altieri, D.C. A novel anti-apoptosis gene, survivin, expressed in cancer and lymphoma. *Nature medicine* **3**, 917-921 (1997).
162. Koumenis, C. & Giaccia, A. Transformed cells require continuous activity of RNA polymerase II to resist oncogene-induced apoptosis. *Molecular and cellular biology* **17**, 7306-7316 (1997).

163. Wesche-Soldato, D.E., Swan, R.Z., Chung, C.S. & Ayala, A. The apoptotic pathway as a therapeutic target in sepsis. *Current drug targets* **8**, 493-500 (2007).
164. Wang, S. *et al.* 2-Anilino-4-(thiazol-5-yl)pyrimidine CDK inhibitors: synthesis, SAR analysis, X-ray crystallography, and biological activity. *Journal of medicinal chemistry* **47**, 1662-1675 (2004).
165. Hirai, H., Kawanishi, N. & Iwasawa, Y. Recent advances in the development of selective small molecule inhibitors for cyclin-dependent kinases. *Current topics in medicinal chemistry* **5**, 167-179 (2005).
166. Canduri, F., Perez, P.C., Caceres, R.A. & de Azevedo, W.F., Jr. CDK9 a potential target for drug development. *Medicinal chemistry (Sharīqah (United Arab Emirates))* **4**, 210-218 (2008).
167. Gojo, I., Zhang, B. & Fenton, R.G. The cyclin-dependent kinase inhibitor flavopiridol induces apoptosis in multiple myeloma cells through transcriptional repression and down-regulation of Mcl-1. *Clinical cancer research* **8**, 3527 (2002).
168. Marciniak, R.A. & Sharp, P.A. HIV-1 Tat protein promotes formation of more-processive elongation complexes. *The EMBO journal* **10**, 4189 (1991).
169. Jager, W. *et al.* Metabolism of the anticancer drug flavopiridol, a new inhibitor of cyclin dependent kinases, in rat liver. *Life sciences* **62**, 1861-1873 (1998).
170. Chao, S.H. & Price, D.H. Flavopiridol inactivates P-TEFb and blocks most RNA polymerase II transcription in vivo. *Journal of Biological Chemistry* **276**, 31793 (2001).
171. Brown, J.R. Chronic lymphocytic leukemia: a niche for flavopiridol? *Clin Cancer Res* **11**, 3971-3973 (2005).
172. Byrd, J.C. *et al.* Flavopiridol administered using a pharmacologically derived schedule is associated with marked clinical efficacy in refractory, genetically high-risk chronic lymphocytic leukemia. *Blood* **109**, 399 (2007).
173. Senderowicz, A.M. & Sausville, E.A. Preclinical and clinical development of cyclin-dependent kinase modulators. *Journal of the National Cancer Institute* **92**, 376-387 (2000).
174. Blagosklonny, M.V. Flavopiridol, an inhibitor of transcription: implications, problems and solutions. *Cell cycle (Georgetown, Tex)* **3**, 1537-1542 (2004).
175. Bible, K.C. & Kaufmann, S.H. Cytotoxic synergy between flavopiridol (NSC 649890, L86-8275) and various antineoplastic agents: the

- importance of sequence of administration. *Cancer research* **57**, 3375-3380 (1997).
176. Meijer, L. & Raymond, E. Roscovitine and other purines as kinase inhibitors. From starfish oocytes to clinical trials. *Accounts of chemical research* **36**, 417-425 (2003).
177. Bregman, D.B., Pestell, R.G. & Kidd, V.J. Cell cycle regulation and RNA polymerase II. *Front Biosci* **5**, D244-257 (2000).
178. Satoh, M.S. & Lindahl, T. Role of poly(ADP-ribose) formation in DNA repair. *Nature* **356**, 356-358 (1992).
179. Nicholson, D.W. *et al.* Identification and inhibition of the ICE/CED-3 protease necessary for mammalian apoptosis. *Nature* **376**, 37-43 (1995).
180. Oliver, F.J. *et al.* Importance of poly(ADP-ribose) polymerase and its cleavage in apoptosis. Lesson from an uncleavable mutant. *The Journal of biological chemistry* **273**, 33533-33539 (1998).
181. Zhou, M. *et al.* Tat modifies the activity of CDK9 to phosphorylate serine 5 of the RNA polymerase II carboxyl-terminal domain during human immunodeficiency virus type 1 transcription. *Molecular and cellular biology* **20**, 5077-5086 (2000).
182. Gong, Y.Q. *et al.* In vivo and in vitro evaluation of erianin, a novel anti-angiogenic agent. *Eur J Cancer* **40**, 1554-1565 (2004).
183. Gong, Y. *et al.* Erianin induces a JNK/SAPK-dependent metabolic inhibition in human umbilical vein endothelial cells. *In vivo (Athens, Greece)* **18**, 223-228 (2004).
184. Li, Y.M., Wang, H.Y. & Liu, G.Q. Erianin induces apoptosis in human leukemia HL-60 cells. *Acta pharmacologica Sinica* **22**, 1018-1022 (2001).
185. Dekkers, J.C., van Doornen, L.J. & Kemper, H.C. The role of antioxidant vitamins and enzymes in the prevention of exercise-induced muscle damage. *Sports medicine (Auckland, N.Z)* **21**, 213-238 (1996).
186. Kelter, G., Schierholz, J.M., Fischer, I.U. & Fiebig, H.H. Cytotoxic activity and absence of tumor growth stimulation of standardized mistletoe extracts in human tumor models in vitro. *Anticancer research* **27**, 223-233 (2007).
187. Liang, Y., Yan, C. & Schor, N.F. Apoptosis in the absence of caspase 3. *Oncogene(Basingstoke)* **20**, 6570-6578 (2001).
188. Seto, M. *et al.* Alternative promoters and exons, somatic mutation and deregulation of the Bcl-2-Ig fusion gene in lymphoma. *The EMBO journal* **7**, 123 (1988).

189. Kruse, L.I. *et al.* Synthesis, tubulin binding, antineoplastic evaluation, and structure-activity relationship of oncodazole analogues. *Journal of medicinal chemistry* **32**, 409-417 (1989).
190. Snijman, P.W. *et al.* Antioxidant Activity of the Dihydrochalcones Aspalathin and Nothofagin and Their Corresponding Flavones in Relation to Other Rooibos (*Aspalathus linearis*) Flavonoids, Epigallocatechin Gallate, and Trolox. *Journal of Agricultural and Food Chemistry*, 376-412.
191. Llamazares, S. *et al.* polo encodes a protein kinase homolog required for mitosis in *Drosophila*. *Genes & development* **5**, 2153-2165 (1991).
192. Lowery, D.M., Lim, D. & Yaffe, M.B. Structure and function of Polo-like kinases. *Oncogene* **24**, 248-259 (2005).
193. Mundt, K.E., Golsteyn, R.M., Lane, H.A. & Nigg, E.A. On the regulation and function of human polo-like kinase 1 (PLK1): effects of overexpression on cell cycle progression. *Biochemical and biophysical research communications* **239**, 377-385 (1997).
194. Barr, F.A., Sillje, H.H. & Nigg, E.A. Polo-like kinases and the orchestration of cell division. *Nature reviews* **5**, 429-440 (2004).
195. Johnson, E.F., Stewart, K.D., Woods, K.W., Giranda, V.L. & Luo, Y. Pharmacological and functional comparison of the polo-like kinase family: insight into inhibitor and substrate specificity. *Biochemistry* **46**, 9551-9563 (2007).
196. Strebhardt, K. & Ullrich, A. Targeting polo-like kinase 1 for cancer therapy. *Nat Rev Cancer* **6**, 321-330 (2006).
197. Li, B. *et al.* Prk, a cytokine-inducible human protein serine/threonine kinase whose expression appears to be down-regulated in lung carcinomas. *The Journal of biological chemistry* **271**, 19402-19408 (1996).
198. Ko, M.A. *et al.* Plk4 haploinsufficiency causes mitotic infidelity and carcinogenesis. *Nature genetics* **37**, 883-888 (2005).
199. Kleylein-Sohn, J. *et al.* Plk4-induced centriole biogenesis in human cells. *Developmental cell* **13**, 190-202 (2007).
200. Dai, W. Polo-like kinases, an introduction. *Oncogene* **24**, 214-216 (2005).
201. Kothe, M. *et al.* Structure of the catalytic domain of human polo-like kinase 1. *Biochemistry* **46**, 5960-5971 (2007).
202. Elia, A.E. *et al.* The molecular basis for phosphodependent substrate targeting and regulation of Plks by the Polo-box domain. *Cell* **115**, 83-95 (2003).

203. Garcia-Alvarez, B., de Carcer, G., Ibanez, S., Bragado-Nilsson, E. & Montoya, G. Molecular and structural basis of polo-like kinase 1 substrate recognition: Implications in centrosomal localization. *Proceedings of the National Academy of Sciences of the United States of America* **104**, 3107-3112 (2007).
204. Jang, Y.J., Ma, S., Terada, Y. & Erikson, R.L. Phosphorylation of threonine 210 and the role of serine 137 in the regulation of mammalian polo-like kinase. *The Journal of biological chemistry* **277**, 44115-44120 (2002).
205. van de Weerd, B.C. *et al.* Uncoupling anaphase-promoting complex/cyclosome activity from spindle assembly checkpoint control by deregulating polo-like kinase 1. *Molecular and cellular biology* **25**, 2031-2044 (2005).
206. Petronczki, M., Lenart, P. & Peters, J.M. Polo on the Rise-from Mitotic Entry to Cytokinesis with Plk1. *Developmental cell* **14**, 646-659 (2008).
207. Tsvetkov, L. Polo-like kinases and Chk2 at the interface of DNA damage checkpoint pathways and mitotic regulation. *IUBMB life* **56**, 449-456 (2004).
208. Brennan, I.M., Peters, U., Kapoor, T.M. & Straight, A.F. Polo-like kinase controls vertebrate spindle elongation and cytokinesis. *PLoS ONE* **2**, e409 (2007).
209. Golsteyn, R.M., Mundt, K.E., Fry, A.M. & Nigg, E.A. Cell cycle regulation of the activity and subcellular localization of Plk1, a human protein kinase implicated in mitotic spindle function. *The Journal of cell biology* **129**, 1617-1628 (1995).
210. Lane, H.A. & Nigg, E.A. Antibody microinjection reveals an essential role for human polo-like kinase 1 (Plk1) in the functional maturation of mitotic centrosomes. *The Journal of cell biology* **135**, 1701-1713 (1996).
211. Casenghi, M. *et al.* Polo-like kinase 1 regulates Nlp, a centrosome protein involved in microtubule nucleation. *Developmental cell* **5**, 113-125 (2003).
212. Warner, S.L., Gray, P.J. & Von Hoff, D.D. Tubulin-associated drug targets: Aurora kinases, Polo-like kinases, and others. *Seminars in oncology* **33**, 436-448 (2006).
213. Neef, R. *et al.* Phosphorylation of mitotic kinesin-like protein 2 by polo-like kinase 1 is required for cytokinesis. *The Journal of cell biology* **162**, 863-875 (2003).
214. Petronczki, M., Glotzer, M., Kraut, N. & Peters, J.M. Polo-like kinase 1 triggers the initiation of cytokinesis in human cells by promoting

- recruitment of the RhoGEF Ect2 to the central spindle. *Developmental cell* **12**, 713-725 (2007).
215. Smith, M.R. *et al.* Malignant transformation of mammalian cells initiated by constitutive expression of the polo-like kinase. *Biochemical and biophysical research communications* **234**, 397-405 (1997).
216. Knecht, R. *et al.* Prognostic significance of polo-like kinase (PLK) expression in squamous cell carcinomas of the head and neck. *Cancer research* **59**, 2794-2797 (1999).
217. Elez, R. *et al.* Tumor regression by combination antisense therapy against Plk1 and Bcl-2. *Oncogene* **22**, 69-80 (2003).
218. Johansson, M. & Persson, J.L. Cancer therapy: targeting cell cycle regulators. *Anti-cancer agents in medicinal chemistry* **8**, 723-731 (2008).
219. Plyte, S. & Musacchio, A. PLK1 inhibitors: setting the mitotic death trap. *Curr Biol* **17**, R280-283 (2007).
220. Schmidt, M. *et al.* Molecular alterations after Polo-like kinase 1 mRNA suppression versus pharmacologic inhibition in cancer cells. *Molecular cancer therapeutics* **5**, 809-817 (2006).
221. Cheng, K.Y., Lowe, E.D., Sinclair, J., Nigg, E.A. & Johnson, L.N. The crystal structure of the human polo-like kinase-1 polo box domain and its phospho-peptide complex. *The EMBO journal* **22**, 5757-5768 (2003).
222. Gumireddy, K. *et al.* ON01910, a non-ATP-competitive small molecule inhibitor of Plk1, is a potent anticancer agent. *Cancer cell* **7**, 275-286 (2005).
223. Lenart, P. *et al.* The small-molecule inhibitor BI 2536 reveals novel insights into mitotic roles of polo-like kinase 1. *Curr Biol* **17**, 304-315 (2007).
224. Steegmaier, M. *et al.* BI 2536, a potent and selective inhibitor of polo-like kinase 1, inhibits tumor growth in vivo. *Curr Biol* **17**, 316-322 (2007).
225. Kothe, M. *et al.* Selectivity-determining residues in Plk1. *Chemical biology & drug design* **70**, 540-546 (2007).
226. Rudolph, D. *et al.* BI 6727, A Polo-like Kinase Inhibitor with Improved Pharmacokinetic Profile and Broad Antitumor Activity. *Clinical Cancer Research* **15**, 3094 (2009).
227. Linz, G., Kraemer, G.F., Gutschera, L. & Asche, G. METHOD FOR THE PRODUCTION OF DIHYDROPTERIDINONES. (2006).

228. Stambuli, J.P., Kuwano, R. & Hartwig, J.F. Unparalleled rates for the activation of aryl chlorides and bromides: coupling with amines and boronic acids in minutes at room temperature. *Angewandte Chemie (International ed)* **41**, 4746-4748 (2002).
229. Zim, D. & Buchwald, S.L. An air and thermally stable one- component catalyst for the amination of aryl chlorides. *Organic letters* **5**, 2413-2415 (2003).
230. Chen, G., Lam, W.H., Fok, W.S., Lee, H.W. & Kwong, F.Y. Easily accessible benzamide-derived P₂O ligands (Bphos) for palladium-catalyzed carbon-nitrogen bond-forming reactions. *Chemistry, an Asian journal* **2**, 306-313 (2007).
231. Ackermann, L., Spatz, J.H., Gschrei, C.J., Born, R. & Althammer, A. A diaminochlorophosphine for palladium-catalyzed arylations of amines and ketones. *Angewandte Chemie (International ed)* **45**, 7627-7630 (2006).
232. Charles, M.D., Schultz, P. & Buchwald, S.L. Efficient pd-catalyzed amination of heteroaryl halides. *Organic letters* **7**, 3965-3968 (2005).
233. Ranu, B.C., Dutta, J. & Guchhait, S.K. Indium metal as a reducing agent. Selective reduction of the carbon-carbon double bond in highly activated conjugated alkenes. *Organic letters* **3**, 2603-2605 (2001).
234. Schrupp, D.S., Matthews, W., Chen, G.A., Mixon, A. & Altorki, N.K. Flavopiridol mediates cell cycle arrest and apoptosis in esophageal cancer cells. *Clin Cancer Res* **4**, 2885-2890 (1998).
235. Dohi, T. *et al.* An IAP-IAP complex inhibits apoptosis. *Journal of Biological Chemistry* **279**, 34087-34090 (2004).
236. Sherr, C.J. Cancer cell cycles. *Science (New York, N.Y)* **274**, 1672 (1996).
237. Demidenko, Z.N. & Blagosklonny, M.V. Flavopiridol induces p53 via initial inhibition of Mdm2 and p21 and, independently of p53, sensitizes apoptosis-reluctant cells to tumor necrosis factor. *Cancer research* **64**, 3653 (2004).
238. Morris, M.J. *et al.* Phase I Trial of BCL-2 Antisense Oligonucleotide (G3139) Administered by Continuous Intravenous Infusion in Patients with Advanced Cancer 1. *Clinical Cancer Research* **8**, 679-683 (2002).
239. Merino, R., Ding, L., Veis, D.J., Korsmeyer, S.J. & Nunez, G. Developmental regulation of the Bcl-2 protein and susceptibility to cell death in B lymphocytes. *EMBO JOURNAL* **13**, 683-683 (1994).
240. Nijhawan, D. *et al.* Elimination of Mcl-1 is required for the initiation of apoptosis following ultraviolet irradiation. *Genes & development* **17**, 1475-1486 (2003).

241. Giannakakou, P. *et al.* p53 is associated with cellular microtubules and is transported to the nucleus by dynein. *Nature cell biology* **2**, 709-717 (2000).
242. Chen, J. *et al.* Development of protegrins for the treatment and prevention of oral mucositis: structure-activity relationships of synthetic protegrin analogues. *Biopolymers* **55** (2000).
243. Kelland, L.R. Flavopiridol, the first cyclin-dependent kinase inhibitor to enter the clinic: current status. *oid* **9**, 2903-2911 (2000).
244. Schmidt, T., Schütz, G.J., Baumgartner, W., Gruber, H.J. & Schindler, H. Imaging of single molecule diffusion. *Proceedings of the National Academy of Sciences* **93**, 2926 (1996).

Appendix: Publication

2009 AACR Annual Meeting, poster presentation #2665

April 18-22, 2009, Colorado Convention Center, Denver, CO , USA

Abstract:

ZJU-6, a novel derivative of Erianin – a potent anti-tumour agent showing anti-tubulin polymerisation and anti-angiogenic activities

¹Frankie F.K. Lam, ²Hui Mao, ¹Tracey D. Bradshaw, ¹Scott Roberts, ²Yuanjiang Pan and ¹Shudong Wang

¹School of Pharmacy and Centre for Biomolecular Sciences, University of Nottingham, NG7 2RD, United Kingdom

²Department of Chemistry, Zhejiang University, Hangzhou 310027, P. R. China

It is now a well established fact that natural products can provide compounds having either immediate drug potential or which provide inspiration for synthetic drug discovery. It is estimated that over 60 percent of the current anticancer drugs are derived from natural sources. Erianin, a known natural product of *Dendrobium chrysotoxum*, possesses potent anti-tumour activity and is currently in clinical development for the treatment of haematological malignancies in China. Erianin has been shown to disrupt endothelial tube formation and to inhibit the polymerised both F-actin and β -tubulin. In this study, we report that ZJU-6, a novel semi-synthetic derivative of Erianin, demonstrated excellent anti-proliferative and anti-angiogenic activities. The anti-proliferative activity of ZJU-6 was evaluated against several human tumour cell lines by 72 hrs MTT assay which gave low to sub- μ M GI₅₀ values. The cellular mode of action was further investigated. FACS analyses revealed that treatment of MCF-7 cells with 5 μ M ZJU-6 for 48 hrs resulted in G2/M phase cell cycle block. Microtubule polymerisation assays showed that ZJU-6 inhibits polymerisation of tubulin more effectively than Erianin. Furthermore, when MCF-7 cells are treated with 5 μ M ZJU-6 for 24hrs, Western blots showed that Bcl-2 protein expression was significantly inhibited while the level of Mcl-1 was not affected. PARP cleavage indicated the cells undergoing apoptosis in the presence of ZJU-6. The effect of ZJU-6 on angiogenesis was also investigated in the chick embryo chorioallantoic membrane assay. The compound possessed potent anti-angiogenic property, being more effectively than Erianin, by blocking the blood vessel formation during embryonic development. In conclusion, we have identified a novel anti-tumour agent ZJU-6 which inhibited tubulin polymerisation, causing accumulation of cells within G2/M cell cycle phase. The compound was able to suppress the expression of Bcl-2 anti-apoptotic protein and induce apoptosis in cancer cells. Furthermore ZJU-6 has demonstrated potent anti-angiogenic activity. These data suggest that ZJU-6 is a potential drug candidate for cancer therapy.